

Application of a Heat Integrated Post-combustion CO₂ Capture System with Hitachi Advanced Solvent into Existing Coal-Fired Power Plant

Final Technical Report

Reporting Period:
October 1, 2011 to March 31, 2020

Principal Authors:

Kunlei Liu, Heather Nikolic, Jesse Thompson, Reynolds Frimpong, and Lisa Richburg

Contributing Authors (in alphabetical order):
Keemia Abad, Saloni Bhatnagar, Brad Irvin, James Landon, Wei Li, Naser Seyed Matin
Jonathan Pelgen, Andy Placido
University of Kentucky, Lexington, KY

Clay Whitney
Smith Management Group
Lexington, KY

Abhoyjit Bhow and Yang Du
Electric Power Research Institute
Palo Alto, CA

Report Issued
June 30, 2020

Work Performed Under Award Number
DE-FE0007395

SUBMITTED BY
University of Kentucky Research Foundation
109 Kinkead Hall, Lexington, KY 40506-0057

PRINCIPAL INVESTIGATOR
Kunlei Liu
+1-859-257-0293
kunlei.liu@uky.edu

DOE PROGRAM MANAGER
Isaac A. Aurelio
Isaac.Aurelio@netl.doe.gov
(304)285-0244

SUBMITTED TO
U.S. Department of Energy National Energy Technology Laboratory

DISCLAIMER: This report was prepared as an account of work sponsored by an agency of the United States Government. Neither the United States Government nor any agency thereof, nor any of their employees, makes any warranty, express or implied, or assumes any legal liability or responsibility for the accuracy, completeness, or usefulness of any information, apparatus, product, or process disclosed, or represents that its use would not infringe privately owned rights. Reference herein to any specific commercial product, process, or service by trade name, trademark, manufacturer, or otherwise does not necessarily constitute or imply its endorsement, recommendation, or favoring by the United States Government or any agency thereof. The views and opinions of authors expressed herein do not necessarily state or reflect those of the United States Government or any agency thereof.

ACKNOWLEDGEMENT: UK CAER is grateful to the U.S Department of Energy National Energy Technology Laboratory for the support of this project. UK CAER is also grateful to Electric & Kentucky Utilities, Duke Energy, Electric Power Research Institute, Inc., Kentucky Power and the Kentucky Department for Energy Development and Independence for support and partnership.

The project team is grateful to everyone at the Kentucky Utilities E.W. Brown Generating Station for serving as the host site and for their support of the project. Specifically, the assistance of the following people is recognized.

Aron Patrick	Jake Jude	Mahyar Ghorbanian
Brad Pabian	Jeff Frailey	Michael Manahan
David Link	Joe Beverly	
Donnie Duncan	John Moffett	

The project team is also grateful to the many UK CAER research personnel for assistance with the project, as listed below.

Keemia Abad	Nick Holubowitch	Roger Perrone
John Adams	Sarah Honchul	Andy Placido
Saloni Bhatnagar	Quanzhen Huang	Joseph Remias
Jacob Blake	Brad Irvin	Guojie Qi
Jonny Bryant	Don Johnson	Henry Richburg
Darby Campbell	Neal Koebcke	Lisa Richburg
Payal Chandan	Levi Lampe	Keith Ruh
Liangyong Chen	James Landon	Moushumi Sarma
Bethany Clontz	Xiaobing Li	Steve Summers
Megan Combs	Wei Wi	Ye Sun
Richard Curls	Cameron Lippert	Nandini Suresh
Wenfeng Dong	Kun Liu	Jesse Thompson
Zhen Fan	Kunlei Liu	Ti Wang
Allan Flath	Marshall Marcum	Amanda Warriner
Rafael Franca	Chase Martin	Charles Whitenack
Reynolds Frimpong	Naser Matin	Leland Widger
Ishan Fursule	John Moffett	Evan Williams
James Fussinger	James Neathery	Yi Zhang
Len Goodpaster	Chin Ng	Liangfu Zheng
Brandon Harris	Heather Nikolic	Ye Zhou
Emily Harrison	Femke Onneweer	Wenchen Zou
Otto Hoffmann	Logan Owens	
Brian Hogston	Jonathan Pelgen	

ABSTRACT: The goal of this final project report is to comprehensively summarize the work conducted on project DE-FE0007395. In accordance with the Project Management Plan (PMP), Revision F dated 5/10/2019, and Statement of Project Objectives (SOPO) within, the University of Kentucky (UK) Center for Applied Energy Research (CAER) (Recipient) has successfully demonstrated a unique, versatile CO₂ capture system (CCS) using a heat integrated process combined with two-stage stripping for process intensification, heat recovery and demineralized (DM) water generation. This project involved the design, fabrication, installation, testing of and data analysis from the UK CAER 0.7 MWe small pilot scale CO₂ capture process installed at Kentucky Utilities (KU) E.W. Brown Generating Station in Harrodsburg, KY. During each of the four project Budget Periods (BPs), UK CAER met all project deliverables, all project milestones, with National Energy Technology Laboratory (NETL) approved adjustments made to the campaign long-term hours during BP4.

The CCS was constructed in modular skids. Two solvent campaigns were initially conducted; the first with a 30 wt% monoethanolamine (MEA) as a baseline, and the second with the Hitachi H3-1 advanced solvent. Additional tests were performed with two advanced solvents including CAER and Proprietary Solvent C. Short-period testing with a higher concentration of 40 wt% MEA was conducted to evaluate the potential saving with high alkalinity. From the various solvent campaigns, unique aspects of the UK CAER CCS technology, as well as its flexibility and versatility were experimentally validated and demonstrated. With respect to solvent evaluation efforts in identifying candidates with significant operational and capital cost savings potential, performance of solvents were evaluated to determine the energy requirements for regeneration; environmental impacts from secondary emissions and degradation products; degradation rates, solvent make-up rates and stability. The assessments were done from parametric tests that determined optimum operating conditions for the individual solvents to maximize process efficiency and minimize the parasitic load of the power plant, and from long term campaigns (1000 hours for 30 wt% MEA and 1000 hours for H3-1) which collectively informed the techno-economic analyses (TEA) of the process. The long term campaigns included corrosion studies which used three types of metal coupons in different sections of the process: (absorber, primary stripper, lean carbon-loaded and rich carbon loaded flow streams in process) to mimic heat and flow dynamics process equipment were exposed to. The estimated corrosion rates were used to elucidate corrosion mechanisms and to further guide process material selection for potential capital cost savings.

The scope of the technology evaluation was broadened towards the end of the project by the addition of two major components: (i) a pre-concentrating membrane separation unit and (ii) a solid-assisted solvent recovery system. The membrane was used to increase the CO₂ content in the stream fed to the bottom of the absorber for enhanced rich carbon loading by pre-concentrating the incoming flue gas. The solvent recovery system involved a novel concept of addition of activated carbon as nucleation site to recover entrained solvent that could have been lost as aerosols emissions. Tests were performed to evaluate the effectiveness of the membrane-absorption hybrid process on solvent performance for CO₂ capture and the solvent recovery system for reducing solvent emissions from the top of the absorber.

Among the various innovative aspects of the process and studies performed, some of the key findings are:

- (i) The effectiveness of the secondary air stripper in the additional stripping, with the resultant leaner solvents it provided to the absorber for enhanced CO₂ absorption.
- (ii) The impact of the secondary air stripper to oxidative degradation of solvents shown to be negligible.
- (iii) The performance of MEA and H3-1 shown to validate TEA projected energy of regeneration. The energy savings attainable with H3-1 as an advanced solvent as well as ~70% lower solvent degradation in comparison with MEA was also demonstrated.
- (iv) Process temperatures and solvent carbon loadings affected extent of corrosion in different parts of the process. Notably, the corrosion in the absorber and CO₂-lean amine piping sections were negligible compared to the significant corosions detected in the stripper and CO₂-rich amine piping sections. The presence of chemical additives in H3-1 resulted in significantly reduced corrosion compared to MEA with no inhibitors.
- (v) Use of effective corrosion inhibitors to avert corrosion concerns with higher amine concentration would promote assessing associated energy savings of ~20% observed with 40 wt% MEA tests relative to 30 wt% MEA.
- (vi) Addition of the solvent recovery system significantly reduced amine losses entrained with gas exiting from the top of the absorber with the amine concentration being less than 1ppm.
- (vii) The net efficiency of the UK CAER integrated pulverized coal (PC) power plant with CO₂ capture changes from 26.2% for the Reference Case (RC) 10 plant in 2010 revised U.S. Department of Energy (DOE)/NETL baseline report to 27.6% for MEA and 29.1% when utilizing the Hitachi advanced solvent. The CAER Process + Hitachi case also produces an extra 60.9 MW more than DOE RC 10. Levelized Cost of Electricity (LCOE) (\$/MWh) values are \$157.65/MWh considered in comparison to \$189.59/MWh in January 2012 dollar for RC 10.
- (viii) The pre-concentrating membrane could result in high carbon loading but the effectiveness of high gas CO₂ in the incoming stream was observed to have close relationship with solvent temperature exiting the packing bottom.

Other findings and lessons learned during the various stages of the project are highlighted together with recommendations for the advancement of the post-combustion CO₂ capture technology. Overall, the successful demonstration of the UK CAER CCS shows that this process can be scaled up to help pave the way to achieve the DOE CO₂ capture performance and cost targets, as indicated in the project TEA.

Table of Contents

1)	EXECUTIVE SUMMARY.....	8
1.1	Overview.....	8
1.2	Key Results	10
2)	BACKGROUND AND TECHNOLOGY DESCRIPTION.....	20
2.1	Project Objective and Background	20
2.2	Process Description.....	21
3)	PROCESS SPECIFICATION AND DESIGN.....	24
3.1	CO ₂ Capture Process Design	24
3.2	Foundation Design	40
3.3	Tie-in Piping Systems Design.....	40
3.4	Electrical Systems Design.....	41
4)	ON-SITE ERECTION AND INSTALLATION.....	41
4.1	Contractor Selection.....	41
4.2	Excavation.....	42
4.3	Foundation	42
4.4	Module Installation	44
4.5	Module-to-module Tie-ins and Loose Shipped Equipment Installation.....	45
4.6	Tie-in Piping	46
4.7	Electrical Engineering.....	47
4.8	Mobile Control Room and Laboratory	48
4.9	Balance of Plant Instrumentation and Controls	48
4.10	Post-Modifications (Membrane and Water Wash Systems).....	50
5)	START UP AND SHAKEDOWN.....	53
5.1	Safety Policies and Procedures and Standard Operating Procedures (SOPs).....	53
5.2	Leak Check, Wash and Process Start Up.....	55
6)	MEA CAMPAIGN.....	55
6.1	Process Stability and Solvent Concentration	56
6.2	CO ₂ Capture Efficiency and Solvent Regeneration Energy	58
6.3	Corrosion.....	60
6.4	Degradation.....	70
6.5	Emissions	77
6.6	MEA Concentration (~ 40 wt% vs. 30 wt%)	83
7)	H3-1 CAMPAIGN	87

7.1	Process Stability and Solvent Concentration	88
7.2	CO ₂ Capture Efficiency and Solvent Regeneration Energy	92
7.3	Corrosion.....	96
7.4	Degradation.....	100
7.5	Emissions	102
8)	CAER SOLVENT CAMPAIGN.....	107
8.1	Parametric Impacts on Solvent Regeneration Energy	107
8.2	Multi-Parametric Impact on Regeneration Energy and Loading	110
8.3	Varying CO ₂ Capture Efficiency and Impacts on Regeneration Energy	112
8.4	Degradation.....	113
8.5	Emissions	117
9)	POST MODIFICATION – PROPRIETARY SOLVENT C CAMPAIGN	125
9.1	Membrane Performance.....	125
9.2	Proprietary Solvent C Tests with Hybrid Process.....	127
9.3	Emissions and Solvent Recovery with Water Wash System	132
10)	RECLAIMING AND MASS BALANCE	137
11)	CONSTRUCTION AND DESIGN CHALLENGES	140
12)	STATE POINT DATA TABLE AND SYSTEM OPERATING CONDITIONS	141
13)	SUMMARY OF TEA	142
13.1	TEA Methodology	142
13.2	TEA Findings.....	143
14)	SUMMARY OF EH&S ASSESSMENT	144
15)	PROJECT MILESTONES AND LESSONS LEARED	148
16)	LESSONS LEARNED	152
17)	TECHNOLOGY BENEFITS AND SHORTCOMINGS.....	154
18)	RECOMMENDATIONS FOR FUTURE R&D ADDRESSING SHORTCOMINGS	155
19)	LIST OF EXHIBITS	157
20)	REFERENCES.....	164
21)	LIST OF ACRONYMS AND ABBREVIATIONS.....	168

1) EXECUTIVE SUMMARY

1.1 Overview

Project Description

During the course of the execution of this project, a 0.7 MWe small pilot scale post-combustion CCS was designed, fabricated, installed, operated, tested, and analyzed. The UK CAER innovate CCS utilizes a heat integrated cooling tower system, two-stage stripping, and advanced solvent including the Hitachi H3-1 solvent. It is located at the KU E.W. Brown Generating Station in Harrodsburg, KY. The design, start-up, and baseline campaign was performed with a generic 30 wt% MEA solvent to obtain data for direct comparison with the NETL RC 10. A second solvent campaign was conducted with the proprietary Hitachi H3-1 solvent. In BP4, two additional advanced solvent campaigns were added. Each campaign consisted of an initial parametric test campaign and long term continuous verification test. Concurrent with the continuous verification runs, corrosion evaluation, solvent degradation (liquid and gaseous emissions) and solvent emission studies were conducted. Additionally, a system transient dynamic study was conducted to quantify the ability of the carbon capture system to follow load demand, flue gas conditions and individual component operation. The heat integration effectiveness, solvent and water management, and CO₂ capture system stability and operability were evaluated.

Project Goals

The objective of this project was to test and experimentally validate a novel heat integration scheme utilizing waste heat from the CCS to improve both the plant and CCS efficiencies, which paves the way to meet the DOE performance and cost targets of 90% CO₂ capture, 95% CO₂ purity and an increase in the cost of electricity of no more than 35%. This is accomplished with the capture system using a two-stage stripper configuration where the second stage is designed as an air stripper to lower the carbon loading in the lean solvent with exhaust CO₂-laden air feeding into the boiler as combustion air and an optimized two-stage cooling tower concept to reduce the condenser temperature, thereby improving the turbine efficiency. The project involved determining the performance of 30 wt% monoethanolamine (MEA), Hitachi H3-1, the CAER solvent and Proprietary Solvent C in the unique UK CAER CCS, and identification of appropriate materials of construction and solvent pollution control technologies necessary for a 550 MW commercial-scale carbon capture plant. The successful execution of this project demonstrated the UK CAER CCS two stage stripping potential and capability of the CCS internal heat integration scheme to improve the overall power generation plant efficiency. Operational information and experimental data were collected and analyzed in order to complete and finalize both a TEA and Environmental, Health and Safety (EH&S) Assessment based on a 550 MWe commercial scale CCS.

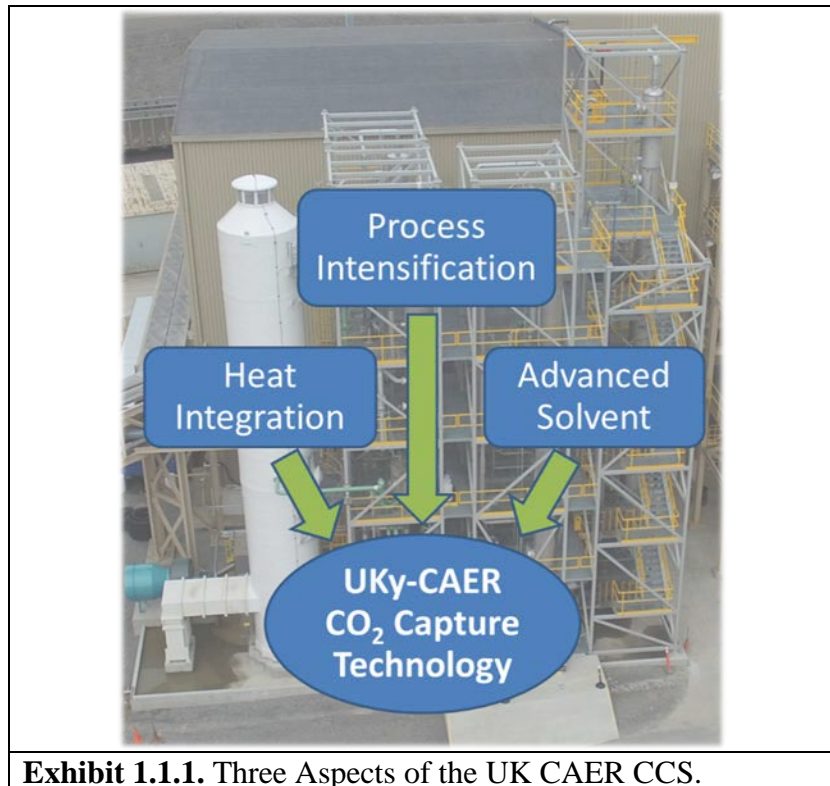
Overview of the UK CAER CCS Technology

The **first key aspect** of the UK CAER CCS is process intensification including a two-stage stripping process for solvent regeneration powered by heat rejected from the CO₂ compressor intercooling. This innovative approach includes the addition of a second stage air stripper, which is located between a conventional lean-rich crossover heat exchanger and a lean solution temperature polishing heat exchanger. This water-saturated air-swept stripper is used to reduce the carbon loading to very low level prior to returning the lean solution to the absorber and while the CO₂ enriched overhead stream generated is recycled back to the power generation boiler to boost CO₂ concentration at absorber inlet. The water-saturated air used for the stripping gas in this secondary stripper comes from regeneration of the water-rich liquid desiccant stream, as described in the second key aspect.

The **second key aspect** of the proposed process is a heat-integrated cooling tower system which recovers heat rejected from the primary stripper overhead condenser and additionally, from the boiler flue gas sensible heat. In this system, the conventional cooling tower is redesigned to include two sections. The top section, with 100% cooling water collection, provides the conventional evaporative cooling function. In the bottom section, a liquid desiccant stream is used to remove moisture from an ambient air stream before it passes to the top section. The working principle is that removing moisture will reduce the cooling air wet bulb temperature which results in additional water cooling to be achieved in the top section, thereby lowering the cooling water supply temperature to the turbine condenser and dropping the steam turbine back pressure for overall efficiency improvement. The water-rich liquid desiccant is then regenerated with recovered heat for circulation.

The **third key aspect** of the 0.7 MWe small pilot scale UK CAER CCS project is the use of the Hitachi H3-1 or other advanced solvents, with a lower regeneration energy, higher CO₂ absorption capacity, and lower degradation rate when compared to the reference case solvent, 30 wt% MEA.

These three aspects work together to improve the overall power generation efficiency to 29.1% when integrated with CCS and Hitachi's H3-1 advanced solvent and can be utilized with new construction or retrofitted into existing coal-fired power plants (Bhown, 2020). Knowledge gained from this project with respect to many aspects of CCS, such as equipment scalability, process simplification/optimization, system compatibility and operability, solvent degradation and secondary environmental impacts, water management, CO₂ absorber temperature profile management, and potential heat integration can be applied to future commercial applications to achieve the current DOE goals for post-combustion CO₂ capture.



1.2 Key Results

The successful completion of this project resulted in many expected results and several additional results. As expected, the UK CAER CCS experimental data validated the performance predicted by the TEA.

Expected Results:

- CO₂ capture efficiency: To be consistent with the Office of Fossil Energy target (U.S. DOE, 2015), a 90% CO₂ capture efficiency was achieved at all parametric and long term process operating conditions, during both solvent campaigns.
- Solvent regeneration energy: The range of MEA solvent regeneration energies found during the parametric portion of the campaign was 1000–1600 Btu/lb CO₂ captured, which is in agreement with the TEA predicted MEA regeneration energy of 1340 BTU/lb CO₂ captured (Bhown, 2020). The range of H3-1 solvent regeneration energies found during the parametric portion of the campaign was 900–1500 Btu/lb CO₂ captured, which is in agreement with the TEA predicted H3-1 regeneration energy of 973 BTU/lb CO₂ captured (Bhown, 2020).
- Emissions: The overall solvent emissions were comparable to the results of other published pilot studies using MEA and it is probably that aerosols are the greatest contributor during this MEA testing campaign. Solvent losses during the H3-1 campaign were found to be ~70% less than during the MEA campaign due to degradation. Nitrosamine emissions were not observed above the low ppbV detection limits calculated during the MEA campaign, but were detected in emissions during the H3-1 campaign.
- Degradation: The overall solvent degradation was comparable to the results of other published pilot studies using MEA under similar coal flue gas conditions and operating hours. Solvent

oxidation in the form of heat stable salts (HSS) and amine polymeric compounds were also comparable to published results showing that the impact of the secondary air stripper on solvent oxidative degradation appears to be negligible.

- Corrosion: During the MEA campaign, low corrosion was found in the absorber and CO₂-lean amine piping sections on all materials tested, including bare carbon steel. Significant corrosion occurred with all material tested except stainless steel in the stripper and CO₂-rich amine piping sections where operating conditions were harsher. During the H3-1 campaign, low corrosion was found for all materials tested in all process areas. The H3-1 solvent is \geq 90% less corrosive than 30 wt% MEA with no inhibitors added.
- Higher MEA concentration: Energy savings of ~20% could be realized with a 40 wt% MEA concentration compared to 30 wt% MEA, and shows advantage could be harnessed with a higher amine concentration used with appropriate corrosion inhibitors to eliminate associated corrosive concerns, but the high viscosity of solvent reduced the heat transfer performance in Lean/Rich (L/R) amine heat exchanger (HXER).
- Advanced solvent campaigns: Additional tests with advanced solvents such as CAER, Proprietary Solvent C demonstrate versatility of the UK-CAER CCS process in achieving varying extent of energy savings relative to MEA, from tuning solvent-specific process parameters.
- Solvent recovery: The solvent recovery system that involved sending treated gas from the top of the absorber through a water wash system further reduced loss of entrained solvent to below instrument detection limit, 1ppm.

Additional Knowledge Gained:

- When developing the process simulation model using the proprietary H3-1 solvent, a viable method to simulate any proprietary solvent, given only the molar concentration, was explored and learned.
- The L/R HXER performance effect on solvent regeneration energy via the sensible heat to stripper and thermal compression benefits are realized only when the L/R HXER approach temperature < 20 °F.
- 90% CO₂ capture and low solvent regeneration energies are achieved with a range of advanced solvent concentrations.
- The UK CAER CCS secondary air stripper performs as expected with partial CO₂ recycling of $> 20\%$ of CO₂ captured being demonstrated to enhance gaseous CO₂ pressure at the absorber inlet.
- Because of the UK CAER CCS heat integrated liquid desiccant loop and two-stage cooling tower, recirculating cooling water is 3-9 °F cooler when compared to a conventional cooling tower at the same ambient conditions.
- In addition to being effective for removing degradation products, thermal reclaiming is also effective for removing heavy metals from the solvent and frequent or continual reclaiming can be used to keep the working solvent classified as nonhazardous.
- The pre-concentrating membrane used to concentrate CO₂ in the flue gas to a higher CO₂ concentration for enhanced absorption did not result in significant energy savings for the solvent as the projected enhancement in permeate CO₂ concentration was not achieved, and the limitation of existing cooling flow to the absorber inter-stage cooler to achieve same rich stream exiting temperature from absorber as prior to modification. A 10-15 °F increase was observed during the parametric and continuous operation.

Tasks 1, 5, 10 and 17 - Project Management and Planning

UK CAER has successfully managed and directed the project in accordance with the PMP, Revision F and SOPO within. UK CAER managed, coordinated and reported on the technical scope, budget and schedule consistent with the project tasks, ensuring that the all work was effectively accomplished, decisions made during the course of the project were appropriately documented and ensuring that the project reporting and briefing requirements were satisfied.

Task 2 - Preliminary Technical and Economic Feasibility Study

The project team completed the preliminary TEA and submitted to DOE NETL in the form of a Topical Report in December 2012 (Bhown, 2012). In the preliminary TEA, four cases utilizing the UK CAER CCS are compared, using different approach temperatures and solvents, against the DOE/NETL RC 10. Detailed results are shown comparing the energy demand for post-combustion CO₂ capture and the net higher heating value (HHV) efficiency of the power plant integrated with the post-combustion capture (PCC) plant. A LCOE assessment was performed showing the costs of the options presented in the study. The results from the preliminary TEA fulfilled the SOPO quantitative success criteria and showed that the proposed technology could be investigated further as a viable alternative to conventional CO₂ capture technology.

The key factors contributing to the reduction of LCOE were identified as CO₂ partial pressure increase at the flue gas inlet, thermal integration of the process, and performance of the Hitachi H3-1 solvent. The net efficiency of the UK CAER CCS integrated with a subcritical PC power plant changes from 26.2% for the RC 10 plant in 2010 revised NETL baseline report to 27.2% for the MEA options considered, and 28.7% for the options utilizing the Hitachi H3-1 advanced solvent. The UK CAER Process + Hitachi case also produces an extra 30.5 MW of generation compared to the UK CAER Process + MEA case and total 52.9 MW more than DOE RC 10. LCOE (\$/MWh) values are \$174.60/MWh for the MEA option and \$164.33/MWh for the Hitachi H3-1 solvent cases considered in comparison to \$189.59/MWh in January 2012 dollar for the RC 10.

The UK CAER CCS process MEA case lowers energy consumption for CO₂ capture to 1340 Btu/lb-CO₂ captured as compared to 1540 Btu/lb-CO₂ in the RC 10. The UK CAER CCS process with H3-1 case further lowers energy consumption for CO₂ capture to 973 Btu/lb-CO₂ captured, for an advantage of 36.8% less energy consumption than RC 10. The study also shows 38.1% less heat rejection associated with the carbon capture system from 3398 MBtu/hr (RC 10) to 2104 MBtu/hr for the UK CAER CCS + MEA system. Heat rejection is reduced to 2464 MBtu/hr in the UK CAER CCS + H3-1 case, for a 27.5 % decrease compared to RC 10.

Modeling outputs show that in the UK CAER process, cooling water 2-5 °C cooler than conventional cooling tower water can be achieved for ambient conditions common to the midwest and other regions.

Task 3 - Initial EH&S Assessment

The project team completed the initial EH&S Assessment and submitted to DOE NETL in the form of a Topical Report in November 2012 (Smith Management Group, 2012). The purpose of the EH&S Assessment was to determine if there were any unacceptable environmental, health or safety concerns that may prevent implementation or environmental permitting of the pilot scale plant. The assessment included review of preliminary process flow diagrams, preliminary input and output flow rates for primary materials, emissions calculations, and Safety Data Sheets (SDSs). The evaluation included identification of risks related to hazardous chemicals, air emissions, wastewater discharges, solid wastes generated and employee hazards.

Potential EH&S issues identified are commonly found and successfully managed at large industrial facilities. No environmental, health or safety risks were identified that could not be successfully managed or likely to prevent implementation or environmental permitting of the pilot scale plant.

The National Environmental Policy Act (NEPA) questionnaire was also completed and submitted to DOE NETL on 2/10/2012.

The environmental group at E.W. Brown Station reviewed the existing environmental permits for air, water and solids. It was determined that a modification to the existing permits was not required. An official notification was made by E.W. Brown Station personnel to the Kentucky Department of Air Quality.

Task 4 - Basic Process Specification and Design

The project team completed the Design Basis Report and submitted to DOE NETL in the form of a Topical Report in November 2012 (Placido and Nikolic, 2012). The details and results of the conceptual process design and the basic process specification and design of the proposed 0.7 MWe small pilot scale, heat integrated post-combustion CO₂ capture slipstream facility attached to an existing coal-fired power plant were presented. There were three phases of design for the entire project: (1) the conceptual process design, (2) the basic process specification and design, and (3) the detailed finalized engineering process specification design. The first two phases occurred during the project budget period 1 and the third during project BP 2. The conceptual process design was performed by UK and the basic process engineering design and specification was performed by Koch Modular Process Systems (KMPS). The Design Basis Report provides details of conceptual process design, the basic process specification and design, and the transition from the first to the second.

The equipment specification list from the basic process engineering design and specification included a system of six columns, 12 heat exchangers, four liquid make-up tanks, two liquid holding tanks, 12 pumps, three blowers, one in-line filter system and appropriate control loops and necessary instruments. According to both UK CAER Aspen Plus® modeling and KMPS's modeling using internal proprietary software, the design conditions of 90% CO₂ capture and 95% CO₂ purity could be met.

Task 6 – Slipstream Site Survey

UK CAER, KMPS and E.W. Brown Generating Station representatives determined the site of the CO₂ capture process based on space available, proximity to the flue gas duct, availability of electrical and other utilities, operations and maintenance safety and minimizing the impact on the host site. The flue gas supply and return tie in locations were identified along with the steam supply, condensate return, instrument air, service air, service water, potable water, and 240 V and 120 V electrical tie in feed locations were identified. Finally, flue gas composition and coal quality data were collected to ascertain the degree of clean up required. The complete details were submitted to DOE NETL in the Q2FY13 project quarterly report on 4/8/2013.

Task 7 - Finalized Engineering Specification and Design

In this task, using the basic process specification and design developed in Task 4, and considering the information collected in Task 6, KMPS used its proprietary in-house model to finalize the technical and engineering specifications including the mass and energy balance around all equipment, size determination and material selection, as well as EH&S requirements identified in Task 3. Measures to prevent health and safety risks were incorporated in the engineering design. The KMPS design scope was increased to include one additional gas analyzer and a steam desuperheating system in order to reduce the pressure and temperature to 100 psi and 5-10 °F above saturated steam conditions from the source identified. KMPS quoted a firm price in August 2013 after this final scope change was made. Finally, WorleyParsons provided a piping and instrumentation diagram (P&ID) review and cost verification of the KMPS process design package, determining that the costs was reasonable.

Task 8 – Test Condition Selection and Test Plan

The project team completed the Sampling and Test Plan and submitted to DOE NETL in the form of a Topical Report in April 2013. Details included sample point process locations, the completed process condition test matrix along with continuous gas composition and liquid composition sampling plan, long term verification solvent degradation and contamination test plan, solvent emissions study plan, and long term verification corrosion study plan for the slipstream test campaign. Details were also provided on the gas and liquid analysis methods and instrumentation, quality assurance/quality control (QA/QC) protocols, and sample handling protocols.

Task 9 - System Engineering Update and Model Refinements

Refinement of the Aspen Plus® model (Aspen, 2015) for the UK CAER CCS with MEA as the solvent was completed to reflect the detailed engineering design and the recommendations listed in the preliminary TEA. Updating the Aspen Plus® model indicated that the process integration adopted during the detailed engineering design could result in a 43 MMBtu/hr energy savings, which equates to approximately 3.2 MWe extra electricity production.

It was also determined that H3-1 solvent kinetic data collection and data regression would be needed to conduct a rate-based Aspen Plus® process simulation by Electric Power Research Institute (EPRI). This scope was added to the SOPO as Task 9B.

Task 9B – Aspen Kinetic Modeling and Preliminary TEA Update

H3-1 solvent kinetic data collection and regression was completed at UK CAER, then applied to the Aspen Plus® model by EPRI. The results were submitted to DOE NETL as a Topical Report in March 2015 (Bhown, 2015), detailing the improvements made to the previous approach using vapor-liquid equilibrium (VLE) data and reaction kinetic data measured for the H3-1 solvent to better model the CO₂ capture process. Property data for H3-1—such as VLE data and mass transfer coefficient—needed by the model were measured at and provided by UK CAER, provided by Mitsubishi Hitachi Power Systems (MHPS), or in some cases estimated using standard correlations often built into Aspen Plus®.

The results of the simulations conducted under this effort showed that the energy needed to regenerate the H3-1 solvent is approximately 1126 Btu/lb CO₂ (2.62 GJ/tCO₂), 16% larger than the 973 Btu/lb CO₂ (2.26 GJ/tCO₂) estimated in the December 2012 report. At the same time, the operating pressure of the stripper increased to 75 psia, compared to 27.3 psia used previously. This results in a reduced compression work load, so that the net plant efficiency for H3-1 changes from 28.7% in the previous report to 28.9% on an HHV basis. This change is small, and hence the economic assessment provided in the December 2012 report still holds.

Additionally, while going through this process a viable method to simulate a proprietary solvent, given only the molar concentration, was developed.

Task 11 - Preliminary Operational Procedure and Safety Protocol

This task allowed for revision of the EH&S Assessment to include preliminary operational procedures and safety protocols, and training for researchers and operators of the CCS. After review, it was determined that the initial EH&S Assessment did not require revision. The training program, operating procedures and safety protocol were first developed as part of this Task. They have been continually updated throughout the project and have grown to include more than 40 SOPs plus many other safety protocols.

Task 12 - Site Preparation

After finalization of the slipstream pilot unit footprint and process utility specifications from the Finalized Engineering Specification and Design (Task 7), the process module foundation was designed by Brown + Kubican (B+K) with full spill containment and to minimize the impact on the E.W. Brown Generating Station. Working within all University of Kentucky regulations, a contract was to be established with B+K, a site preparation work Request for Proposal (RFP) was published, pre-proposal contractor conferences were held, contractor bids were received, the contractor was selected, and site preparation work started in May 2014. The site preparation work included excavation, drilling piers, inspecting the rock strata, pouring piers, installing the grounding ring and connectors, framing the foundation, tying reinforcement steel, pouring the foundation, completing the concrete inspections.

Installation of the power plant tie in root valves (flue gas supply and return, steam supply, condensate return, instrument air supply, service air supply, service water supply, and potable water supply) was completed by E.W. Brown Generating Station personnel, with materials purchased under the project. Pipe specification used by E.W. Brown Generation station were compared with those developed by KMPS to ensure consistency. These root valves remain owned and operated by E.W. Brown Station.

Task 13 – Procurement and Fabrication of Process Modules

The system designed in Task 7 included a pre-treatment tower for SO₂ removal, a packed column scrubber with solvent recovery column (Absorber), two packed-bed strippers with one reboiler and reclaimer, balance of plant (BOP), heat exchangers, pumps, and a filtration device to remove precipitates from the pretreatment tower.

In this task, all necessary materials for the fabrication of specialty vessels and heat exchangers were procured for fabrication in accordance with American Society of Mechanical Engineers (ASME) and industry standards. In addition, all commercially available materials and components needed for the slipstream facility balance of plant were procured to begin fabrication of the slipstream facility. The CO₂ capture facility, in 5 tubular steel frames, was pre-assembled in modular structures at KMPS's assembly shop, CVIP, in Emmaus, PA. The frames house the columns, tanks, blowers, pumps and heat exchangers, leaving enough room for piping, instruments, maintenance access and future design flexibility. The footprint of each module is 14 ft. by 11.5 ft. Operating platforms with grating, hand rails and toe plates are spaced 12 ft. apart and there are 7 levels total. 3 modules are 67 ft. tall, 1 is 56 ft. tall, and 1 (module 1, housing the absorber column) is 77 ft. tall. All piping, heat trace, electrical wiring, signal and control wiring, within the module boundary limits were routed and preinstalled by KMPS.

The Technical Proposal from KMPS to UK was carefully reviewed and revised many times prior to issuing the Purchase Order (PO). Special attention was paid to the sections pertaining to, inspection and performance acceptance guarantees, KMPS and purchaser supplied services, and payment terms. Deliverables were outlined at 8, 12, 20 and 32 weeks after receipt of the PO and payments were scheduled after 9 predefined milestones. Negotiation of the Terms and Conditions for the Purchase Order from the UK to KMPS for the process modules was carefully done and involved legal teams from both parties. Special attention was paid to the sections pertaining to intellectual property, general warranties, transportation and delivery, limitation of liability, and the price warranty. During the module fabrication, weekly progress meetings were held with KMPS and a site visit/inspection was conducted to the CVIP Assembly Shop, Emmaus, PA to verify anchor bolt dimensions and check on assembly progress. Representatives from UK CAER, Louisville Gas & Electric and Kentucky Utilities (LG&E and KU,) U.S. DOE NETL, KMPS were all present at the assembly shop visit. KMPS also sent monthly fabrication inspection and progress reports, including pictures.

As part of the design, KMPS created a three-dimensional (3-D) model. A thorough review of this model allowed for verification of ease of access to all instruments, manually operated valves, liquid, gas and corrosion coupon sample points. Several issues were identified and corrected before assembly.

After installation at E.W. Brown Station, several additional module assembly issues were resolved, including column belly band support replacement, cross-over grating replacement and securing and toe plate addition.

Task 14 - Procurement and Installation of Control Room/Field Lab Section

A stand-alone portable trailer was installed adjacent to the CO₂ capture facility. The trailer is divided into a control room, laboratory and break area. The control room is equipped with two controlling computers and the Continuous Emissions Monitoring System (CEMS) necessary for continuous or on-site monitoring and evaluation. The laboratory is fully functioning with a hood, deionized (DI) water maker, and an automatic liquid sample analysis instrument that allows for quick process liquid sample analysis of C-loading, pH and density. Other capabilities in the on-site laboratory include pH, conductivity of other liquid samples. The building is equipped with CO/fire detectors/alarms, fire extinguishers, a safety shower/eye wash (SS/EW) station, a direct 120 V feed, potable water, a restroom, and a heating, ventilation, air conditioning (HVAC) unit.

Task 15 – Fabrication of Corrosion Coupons

As part of this task, the coupon retention racks (within the columns and within the piping) were designed, and fabricated, and the coupons were fabricated using the UK CAER developed metal coating formulations, including extensive QA/QC measures. Finally, coupon installation and removal procedures were developed.

Task 16 – Slipstream Facility Erection, Start-up, Commissioning and Shakedown

After assembly of equipment within the process modules off-site, KMPS delivered them to E.W. Brown Station. A thorough shipping route survey was completed from door to the installation site and several obstacles were identified for extra caution to be taken. Coordination of the shipping and erection between, KMPS, the shipping company, E.W. Brown Station, and the general contractor had to occur in order to minimize the cost of the shipping trucks and cranes required for erection. The modules arrived, a visual inspection for shipping damage was conducted, and erection occurred during the next 2 days.

The design of the tie-in systems (piping and electrical) between E.W. Brown Station and the CO₂ capture facility was also completed. A design consultant was hired for this purpose and to manage installation by the general contractor and final inspections.

Instrumentation and controls hardware within the modules were pre-wired by KMPS, however connections to the control system from the site trailer to each of the module remote connections were performed by UK CAER. During this work, each instrument was physically checked for continuity at the remote panels within the modules and then were checked again via the DeltaV control system interface on the operating computer. The remaining instrumentation installation and controls wiring (cooling tower trim and other off module equipment) was also completed by UK CAER, during the control system installation and testing work. Individual equipment was started and tested including pumps, blowers and the chiller unit. All instrumentation was checked

and calibrated, as appropriate, including resistance temperature devices (RTDs), pressure sensors, and flow meters. In addition, the control system computer network was setup by UK CAER. Through completion of this control work, UK CAER developed a thorough understanding of the control network that continues to aid in troubleshooting.

Hydro testing and pressure testing, where appropriate, of the entire CO₂ capture system and tie in piping was completed with all leaks being corrected. The CEMS analyzer was installed, commissioned, and integrated into the control network. The entire CO₂ capture system was flushed with water and a dilute soda ash solution was circulated in the amine loop for commissioning, with CO₂ capture being proven.

Task 18 – Test Campaign

Two solvent campaigns, 30 wt% MEA and Hitachi H3-1, were initially conducted, each divided into a parametric and long-term verification portion. During the parametric portion, operating conditions were deliberately changed to establish the limits of the CCS and roughly optimize the best performance parameters in terms of CO₂ capture efficiency and required solvent regeneration energy. The long-term verification portions were each about 1000 operation hours allowing for solvent emission, degradation, reclaiming, coupon material corrosion, and operational trends to be established and observed. Additionally, dynamic load-following studies were conducted. Other parametric campaigns with higher MEA concentration (40 wt%), CAER solvent and Proprietary Solvent C were also performed.

In this task, as part of the data QA/QC, EPRI conducted independent, 3rd party instrument verification and process evaluations during each solvent campaign. Both manual and continuous sampling were done by CB&I, which was subcontracted by EPRI. Verification of the absorber inlet and outlet gas stream flows and compositions, primary stripper gas outlet (CO₂ product) flow and composition, secondary air stripper outlet gas flow and composition was done.

The performance of the UK CAER CCS in terms of CO₂ capture efficiency and solvent regeneration energy was established for direct comparison with the DOE Reference Case 10. The process performance in terms of the effectiveness of the secondary air stripper and heat integrated liquid desiccant loop were also established. The solvent performance in terms of degradation, emissions, corrosion and reclamation were also established. Guidelines for scale up of the UK CAER CCS to the commercial scale were developed. Methods to improve the absorber performance and minimize the solvent regeneration energy were developed.

Task 19 - Final Update of the Technical and Economic Analysis

The TEA performed in Task 2 was updated after completion of both solvent test campaigns. The Aspen Plus[®] models, with 30 wt% MEA and the Hitachi H3-1 solvents, were validated with experimental data. The net efficiency of the UK CAER integrated PC power plant with CO₂ capture changes from 26.2% for the RC 10 plant in 2010 revised DOE/NETL baseline report to 27.6% for the MEA options considered, and 29.1% for the options utilizing the Hitachi advanced solvent. The UK CAER Process + Hitachi case also produces an extra 30.9 MW of generation compared to the UK CAER Process + MEA case and total 60.9 MW more than DOE RC 10.

LCOE (\$/MWh) values are \$172.08/MWh for the MEA option and \$157.65/MWh for the Hitachi H3-1 solvent cases considered in comparison to \$189.59/MWh in January 2012 dollars for the RC 10. A summary of the key advantages of the CAER Process + H3-1 case for LCOE and other economic factors compared to the DOE RC 10 is as follows:

- A lower variable operating cost by \$1.56/MWh (\$1.08MWh less than UK CAER Process + MEA case), a 11.7% reduction compared to the DOE RC 10
- A lower COE by \$25.32MWh (\$13.94/MWh lower than UK CAER Process + MEA case), a 16.9% reduction compared to the DOE RC 10
- A lower LCOE by \$31.94/MWh (\$17.51/MWh lower than UK CAER Process + MEA case), a 16.9% reduction compared to the DOE RC 10
- A lower cost of CO₂ captured by \$18.65/tonne CO₂ (\$9.44/tonne CO₂ lower than UK CAER Process + MEA case), a 30.4% reduction compared to the DOE RC 10
- A lower cost of CO₂ avoided by \$34.95/tonne CO₂ (\$18.53 tonne CO₂ lower than UK CAER Process + MEA case), a 38.7% reduction compared to the DOE RC 10

Task 20 - Final EH&S Assessment

The EH&S assessment completed in Task 11 was reviewed after both solvent campaigns and updated. Data collected during Task 18, solvent emissions and degradation, was incorporated into the final EH&S. Analytical results were obtained from several sources during operation. CB&I Environmental & Infrastructure, Inc. performed system exhaust stack testing on two separate occasions, once each during the MEA and H3-1 solvent testing campaigns. The results for the MEA testing represent results for samples collected between September 29 and October 2, 2015, while the results for the second testing represented results from the H3-1 campaign collected between June 5 and 7, 2016. Additional analytical results, including gas phase emissions, solvent degradation, nitrosamines assessment and waste characterization for MEA and H3-1 testing campaigns were provided by UK CAER. MHPSC provided nitrosamine data for the H3-1 testing campaign.

Task 21 – Design, Procurement, Construction, Start Up and Commissioning

This task involved the modification of the process to include a membrane separation unit (MSU) and a water wash system (WWS). KMPS and Membrane Technology and Research, Inc. (MTR) initially designed the process and priced their respective portions of the scope of the modification. The design specifications including mass and energy balances around all equipment, sizing and material selection was completed by KMPS. KMPS was responsible for the water wash system, absorber design modifications, structural modifications, additional electrical requirements, updated P&IDs (with line sizes, electrical, structural and layout drawings) and the incorporation of the membrane system from MTR. MTR also handled the vacuum pump system, the inline washing system and all the associated instrumentation and controls for the membrane separation unit (MSU). The construction was completed by Blau Mechanical after which various components of the two new systems (MSU and WWS) were started and commissioned per start-up/shut down procedures developed for each system.

2) BACKGROUND AND TECHNOLOGY DESCRIPTION

2.1 Project Objective and Background

UKy-CAER 0.7 MWe Small Pilot Scale CCS Project	
Goal	
	<ul style="list-style-type: none">– Develop a pathway to achieve the US DOE NETL post-combustion CCS target of 90% CO₂ capture with a cost increase (LCOE) of less than 35% (\$40/tonne CO₂ captured)
	Objectives
	<ul style="list-style-type: none">– To demonstrate a heat-integrated post-combustion CO₂ capture system with an advanced solvent– To collect corrosion data leading to appropriate materials of construction for a 550 MWe commercial-scale carbon capture plant– To gather data on solvent degradation, water management, system dynamic control and other information during the long-term verification campaigns– To provide data and design information for larger-scale pilot plant followed by a commercial-scale project
Exhibit 2.1.1. Project Goal and Objectives.	

As illustrated in **Exhibit 2.1.1**, the objective of this project was to pilot test a novel heat integration scheme utilizing waste heat from the CCS to improve the plant and CCS system efficiency, which will develop a path to meet the DOE performance and cost targets of 90% CO₂ capture, 95% CO₂ purity and an increase in the cost of electricity of no more than 35%. This is accomplished with the UK CAER unique CCS. First a two-stage stripper configuration is used where the second stage is designed as a continuous air-swept column to further lower the carbon loading in the lean solvent, and with the exiting overhead CO₂ laden air feeding into the boiler as combustion air. Second, an optimized two-stage cooling tower concept is used to reduce the condenser temperature, thereby improving the power generation turbine efficiency. The project involved the assessment of the performance of baseline 30 wt% MEA solvent and other advanced solvents including Hitachi H3-1, CAER, and Proprietary Solvent C in the proposed CO₂ capture system, identifying appropriate materials of construction and solvent pollution control technologies necessary for a 550 MW commercial-scale carbon capture plant, demonstrating the capability of integrating waste heat from the CO₂ capture platform with the BOP to improve the overall power generation plant efficiency. Additionally, experimental information/data was collected and used to provide a full and comprehensive TEA (Bhown, 2020) and EH&S assessment was collected (Smith Management Group, 2020).

2.2 Process Description



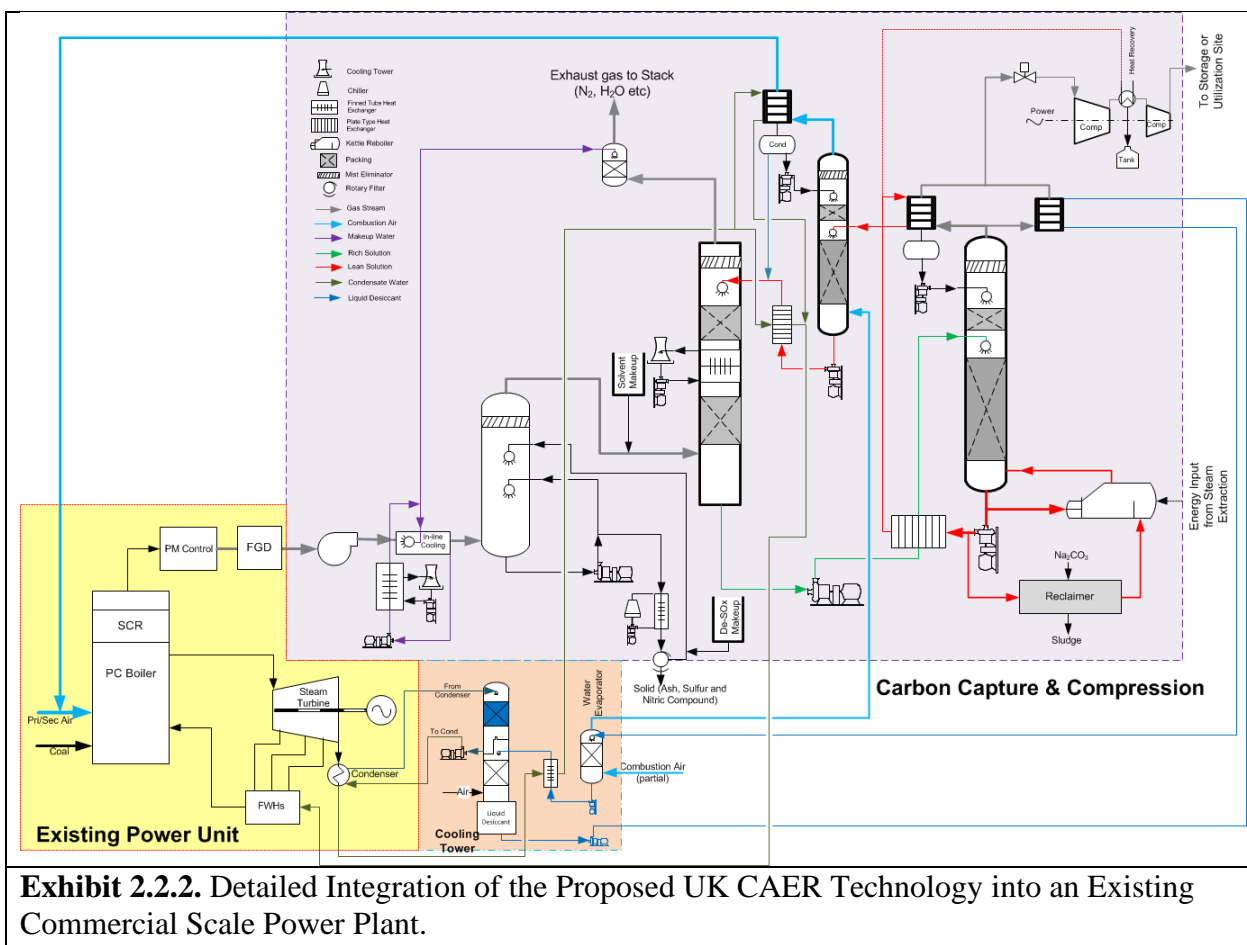
Exhibit 2.2.1. UK CAER 0.7 MWe Post-Combustion CO₂ Capture System at E.W. Brown Generating Station, Harrodsburg, KY.

The UK CAER post-combustion CCS for a coal-fired power plant is building on the traditional aqueous carbon capture technology with advanced heat integrations and three additional unique features. It is completely configured with the same type of components as DOE RC 10 (U.S. DOE NETL, 2013) such as columns, heat exchangers (shell-tube and plate-frame), pumps, blowers, and balance of plant. The key differences from the conventional CCS configuration (one CO₂ absorber column and one stripping column), is the UK CAER technology utilizes an additional air-stripping column, and auxiliary components to recover heat that is typically rejected to the environment in all conventional CCS technology, via an integrated liquid desiccant loop. The UK CAER 0.7 MWe small pilot scale CCS installed at E.W. Brown Generating Station in Harrodsburg, KY is shown in **Exhibit 2.2.1**.

The first important aspect of the proposed process is a two-stage stripping unit for solvent regeneration. This innovative approach includes the addition of an air-based second stage stripping process inserted between a conventional rich-lean crossover heat exchanger and a lean solution temperature polishing heat exchanger. The secondary stripper is powered by heat rejected from the conventional steam-heated (primary) stripper. The secondary stripper outlet stream is used as boiler secondary combustion air, consequently enriching the flue gas with CO₂ resulting in lower energy penalty required by the carbon capture system. The second important aspect is a heat-integrated cooling tower system, which recovers waste energy from the CCS such as compressor

inter-stage coolers. In this process, the cooling tower will be redesigned to include two sections – the top section with 100% cooling water collection for the conventional cooling function; the bottom section to remove moisture from cooling air using a liquid desiccant prior to entering the top section for cooling recirculating water from steam turbine condenser. The working principle is that reducing the relative humidity of the cooling air will lower the turbine condenser cooling water temperature and thereby reduce the steam turbine back-pressure for power generation efficiency improvement. Similarly, a liquid desiccant loop can be deployed to remove moisture from the flue gas prior to the CO₂ absorber for a favorable temperature profile along the column resulting in better performance.

The detailed integration of the proposed UK CAER technology with an existing commercial-scale power plant (Reference Base Plant in the DOE/NETL-2007/1281 Report) (U.S. DOE NETL, 2013) is illustrated in **Exhibit 2.2.2** and summarized as follows:



1. The post-combustion CO₂ capture and compression block includes a direct contact flue gas cooler (DCC), a pre-treatment tower, a packed absorber column with solvent recovery column, two packed-bed strippers with a reboiler and reclaimer, heat exchangers, pumps, and BOP equipment.
2. After the SO₂ scrubber installed with the boiler, flue gas enters a direct contact cooler with a booster fan to overcome pressure drop and to reduce the caustic chemicals consumed in the downstream pre-treatment tower. At this point, the flue gas is saturated with water at a temperature of approximately 55 °C, water content of 17 vol%, and CO₂ concentration of 15-17 vol% of the total wet gas stream (note: vs. 13.5% in DOE RC 10 (U.S. DOE NETL, 2013)).
3. The flue gas then enters a counter-flow pre-treatment tower using dilute caustic solution for further SO₂ polishing and removal of other flue gas contaminants to minimize solvent degradation and lower the steam required for solvent reclaiming. At this point, the flue gas SO₂ concentration is less than 10 ppm. The flue gas temperature will be in the range of 25-40 °C depending on the quantity of heat rejected by the installed in-line heat exchanger.
4. The SO₂-polished flue gas then enters the counter current flow CO₂ scrubber with an intercooling heat exchanger, and bottom pump around section (pump around not shown in **Exhibit 2.2.2.**) to react with the lean aqueous amine solvent.
5. CO₂-depleted flue gas then will be treated in the top section of the absorber column using flue gas condensate from the direct water contactor and make-up water to remove any residual solvent (vapor and aerosol). At this point, the flue gas is water saturated at approximately 42 °C.
6. After gaseous CO₂ is converted into aqueous carbon species, the carbon-rich solution exits the scrubber bottom, is pressurized, and is sent to a heat recovery unit cooling the gaseous stream exiting from the secondary stripper and the CO₂ compressor intercooler for heat recovery (e.g. Heat Pump Loop I), and is then fed to the rich-lean crossover heat exchanger for energy recovery from carbon-lean solvent.
7. After the crossover heat exchanger, the rich solution is sent to the pressurized, packed, conventional (primary) stripper for solvent regeneration. This stage will require an external energy source to drive the steam reboiler. At the primary stripper exit, the gas stream primarily consists of CO₂ (70-75 vol%) and water vapor (25-30 vol%) at a pressure of approximately 3-5 bar and temperature of approximately 100-115 °C.
8. After exiting the heat recovery units cooled by the liquid desiccant from the cooling tower (e.g. Heat Pump Loop II) and steam turbine condensate, the CO₂ enriched gas stream will be pressurized to about 135 bar and intercooled for downstream utilization or sequestration.
9. The carbon-lean solution exiting the primary stripper is sent to the crossover heat exchanger, where the heat will be recovered with the carbon rich solution, then sent to the top of an ambient pressure air-sweeping, packed column secondary stripper to further reduce the carbon loading in the lean solution. Finally, it will be cooled to approximately 40 °C by the liquid desiccant from the cooling tower and recirculating cooling water, and recycled to the scrubber. The water-saturated air used here comes from a liquid desiccant water evaporator (see step 11, below).
10. The CO₂ enriched, secondary stripper outlet, with approximately 3-4 vol% CO₂ content will be fed to an air preheater and used as boiler combustion air.
11. In the cooling tower air path, ambient air enters the integrated cooling tower from the bottom section where it contacts a liquid desiccant reducing the water content of the air.

The dried air will enter the top section to cool the recirculating water through evaporation as in a conventional process. The water-rich liquid desiccant will be collected at the bottom tank and preheated in the primary stripper condenser and heat recovered from power plant, before being sent to an air-blown evaporator for regeneration. The water-lean desiccant will be cooled by steam turbine condensate or recirculating cooling water and a chiller prior to the next cycle. The high-temperature saturated air from the evaporator will be fed to the secondary stripper for CO₂ removal, as indicated in step 9, above.

3) PROCESS SPECIFICATION AND DESIGN

The complete process design was divided as shown in **Exhibit 3.0.1**. While KMPS was responsible for the modular portion of the process, local engineering firms were responsible for the balance of plant design, including the foundation, tie-in piping systems, and electrical systems.

Exhibit 3.0.1. Division of the Design Scope of Work.	
Design Task:	Performed By:
CO ₂ Capture Process	UK CAER
Inside Boundary Limits (ISBL) CO ₂ Capture Process Equipment and Modular Structure Design	KMPS
CEMS	KMPS Spectrum Systems, Inc.
Delta V Controls System	KMPS
Site Preparation and Foundation	B+K
Outside Boundary Limits (OSBL) Tie-in Piping Systems	CMTA Engineers Black & Veatch (B&V)
OSBL Electrical Systems	CMTA Engineers

3.1 CO₂ Capture Process Design

There were three phases of CO₂ capture process design for the entire project: 1) the conceptual process design, 2) the basic process engineering specification and design, and 3) the detailed finalized process design. The first two phases occurred during project budget period 1 (Task 4) and the third during budget period 2 (Task 7). The conceptual process design was performed by UK CAER and the basic process engineering specification and design was performed by KMPS.

Major accomplishments pertaining to the CO₂ capture process design:

- Conceptual design finalized, June 2012
- Conceptual design Aspen Plus® model output shared with project partners, KMPS and EPRI, June 2012
- RFP issued to KMPS, June 2012
- Preliminary Technical Proposal received from KMPS, November 2012
- Preliminary Process Design Package (PDP) received from KMPS, June 2013
- Final Technical Proposal received from KMPS, October 2013
- Purchase Order issued to KMPS, November 2013

- Final PDP received from KMPS, November 2013

Within the scope of the conceptual process design, UK improved an Aspen Plus® model of the process (Aspen, 2012), which was finished in June 2012. All results depicted in the following sections that reference the conceptual process design, originate from this Aspen Plus® model. The conceptual process design Aspen Plus® model allowed for estimating the major equipment sizes, heat/mass balances around the major equipment and the process as a whole, and capture efficiency. The output from this conceptual Aspen Plus® model was distributed to the project partners as a basis to perform their tasks and as a foundation to incorporate into their proprietary models.

UK issued a single RFP in June 2012 to KMPS for completion of (1) Task 7, the finalized engineering process specification and design; (2) Task 13, procurement and fabrication of slipstream modules; and (3) Task 16, slipstream facility erection, start-up, commissioning and shakedown.

The basic process specification and design, done by KMPS, expanded upon the conceptual process design model, for a functional slipstream CO₂ capture facility that meets all the requirements set forth by UK CAER (two-stage stripping, cooling tower integration, heat exchanger placement, etc.). The results from the KMPS model are presented later in this document as the completed basic process specification and design, which includes process flow diagrams, sizing and material of construction for major pieces of equipment. KMPS's experience with modular pilot plant design and construction, as well as similar experience with CO₂ capture systems made them an appropriate and preferred vendor for this service. The basic process specification and design includes liquid make-up systems, solid removal systems, in-line filter systems and control loops. KMPS has also verified using their proprietary software package that the design conditions of at least 90% CO₂ capture with a 95% CO₂ purity, based on the 30 wt% MEA case can be met. UK CAER was satisfied with the finalized basic engineering design provided by KMPS. It incorporated all the important features from the conceptual design combined with the proprietary model outputs and the extensive knowledge of the KMPS team to deliver a complete system as set forth in the proposal.

It is this final version of the basic process specification and design that is presented here. The following were the design basis conditions imposed on KMPS, who offered a **CO₂ Capture Guarantee** of a minimum of 90% CO₂ capture from the inlet flue gas using 30 wt% MEA as the absorption solvent.

Process Design Basis

Inlet Flue Gas Stream Conditions:

Pressure = 14.7 psia

Temperature = 131 °F (55 °C)

Flow Rate, maximum = 2400 scmh

Composition (mol fraction) = 17 mol% H₂O, 16 mol % CO₂, 6 mol% O₂, 60-70 ppm SO₂, balance N₂

Other Design Guidelines:

The gas stream exiting the top of the pretreatment tower must be <10 ppm SO₂ and T= 86–95 °F (30–35 °C).

The absorber intercooler must drop the solvent temperature by 15-20 °F.

The maximum temperature of the lean solvent stream entering the absorber must be $T_{max} = 104^{\circ}\text{F}$ (40°C).

The gas stream being returned to the plant stack must have $T = 104^{\circ}\text{F}$ (40°C), $P = 14.7$ psia.

The pressure at the top of the stripper must be $P = 20\text{--}25$ psia.

The minimum temperature of the solvent stream entering the secondary air stripper must be $T_{min} = 200^{\circ}\text{F}$.

The following were the design basis conditions imposed on KMPS, who offered a **Cooling Tower Performance Guarantee** that the cooling water return temperature, as verified by TI-C106-02, will be $\leq 70^{\circ}\text{F}$ if the supply temperature is $\leq 90^{\circ}\text{F}$, or 20 degrees less than the supply temperature if the supply temperature is $\geq 90^{\circ}\text{F}$ at the cooling water supply flow rate of 206 gpm, as verified by FI-C106-01.

Ambient Air Conditions:

$P = 14.7$ psia

$T_{max} = 86^{\circ}\text{F}$ (30°C)

Flow Rate = 123,500 lb/hr

Relative Humidity = 60%

Dehydration Tower Exit Air Conditions:

$T_{max} = 87^{\circ}\text{F}$ (30.5°C)

Flow Rate = 122,822 lb/hr

Relative Humidity = 0.105 wt% water

Design Scope of Work

The KMPS final detailed design scope of work within the CCS was divided into five timeframes after receipt of the PO. This allowed the BOP design, construction bid package preparation, and contractor selection to be completed concurrently, saving time with (1) complete, comprehensive information necessary to complete the foundation design; (2) information necessary to complete the contractor bid package for other work required to erect and install the modules and peripheral equipment and complete the piping design to connect the modules to the power plant; (3) information and drawings necessary to finalize the contractor's scope of work for all other work required to erect and install the modules and peripheral equipment and complete the piping design to connect the modules to the power plant; (4) information sufficient for plant hydro-testing of the piping per KMPS start-up manual and instructions sufficient to begin training of operators and personnel and to complete a process safety analysis; and (5) final documentation including:

- as built process flow diagrams (PFDs), P&ID's, Equipment Specifications (see Section U: Documentation)
- as built Complete Detailed Engineering Package (see Section U: Documentation)
- Startup & Shutdown instructions
- Operating Manual
- Modular system with equipment, piping, instruments, electrical
- Installation instructions, lifting plan, and foundation loadings
- The final, as-built cost breakdown into the following categories, as previously supplied:

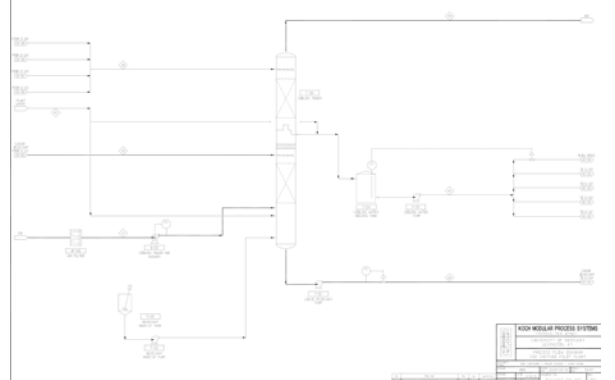
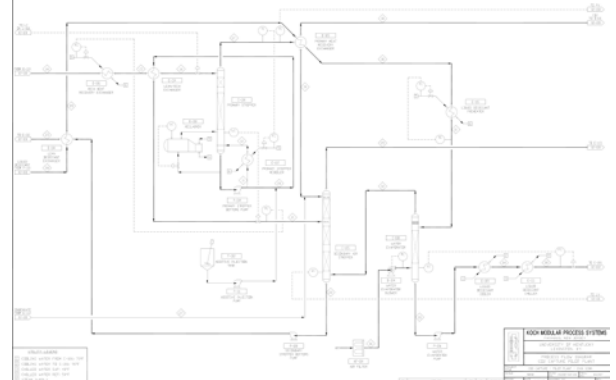
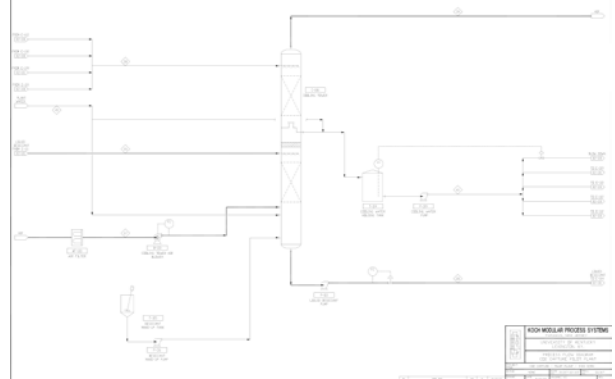
1. Equipment (including columns, vessels, packing, distributors, heat exchanger, tanks, pumps, blowers, filters & chiller and including installation and inspection of the column internals at the vessel shop or field and inspection, quality testing and code testing of the fabricated columns and vessels), as a category
2. Field instruments & control system hardware including the instrumentation hardware, all of the control system hardware including the control panels, instrument panels, and power panels
3. Engineering (process electrical, mechanical and structural), drafting, purchasing, quality control and control system programming, design and detailed drawings of the structural steel, and piping design.
4. Steel structure with tubular frame stair module, including both the materials and the labor to fabricate and assemble each module and the stair tower including the grating, handrails, cross-over bracing etc.
5. Module assembly (piping materials and labor, electrical materials and labor, electrical tracing, insulation, lighting, painting, equipment installation, control panels, and testing) Module assembly also includes:
6. Miscellaneous (travel costs, internal freight, 3rd party quality control inspections, bookkeeping, administration activities)

Drawings

KMPS supplied sets of design drawings for the process, the general arrangement, the piping, the major equipment, electrical system, and the module structure.

Process Drawings (PFDs and P&IDs):

Using in-house proprietary software, KMPS modeled the UK CAER CCS, producing the stream tables and PFDs, shown in **Exhibits 3.3.1 through 3.1.3**. Heat and mass balances associated with all major equipment including reaction columns, rotary devices, and heat exchangers was determined.

	
Exhibit 3.1.1. Pretreatment Tower Block PFD.	Exhibit 3.1.2. Absorber and Stripping Columns Block PFD.
	
Exhibit 3.1.3. Cooling Tower Block PFD.	

In addition to the PFDs, P&IDs were developed with a greater level of detail including pipe sizing, specifications and unique identification, heat trace and insulation specifications, valve locations, types and unique identification, instrumentation location and unique identification, control loops, sample point locations, ISBL definition with identification of each tie in with the power generation plant, equipment sizing and unique identification, and location of basic column internals. As an example **Exhibit 3.1.4** shows the P&ID of the flue gas pretreatment step. Flue gas is drawn into the CCS with a blower (B-101) after passing through a knock-out vessel to remove condensate. The blower flow can be controlled. A column with open packing (C-102) accompanied with a caustic preparation and feeding system (P-101 and P-102) is installed to polish the SO₂ concentration in the flue gas to <10 ppm in order to minimize the heat stable salt formation in the downstream amine loop. The pretreatment tower is level controlled with a blowdown line that is returned to the wet flue gas desulfurization (WFGD) unit. The quality of the soda ash solution is controlled by pH with the addition of a concentrated solution. In order to flexibly control the absorber temperature profile, a heat exchanger (E-102) is installed in the soda ash loop to adjust the flue gas stream temperature.

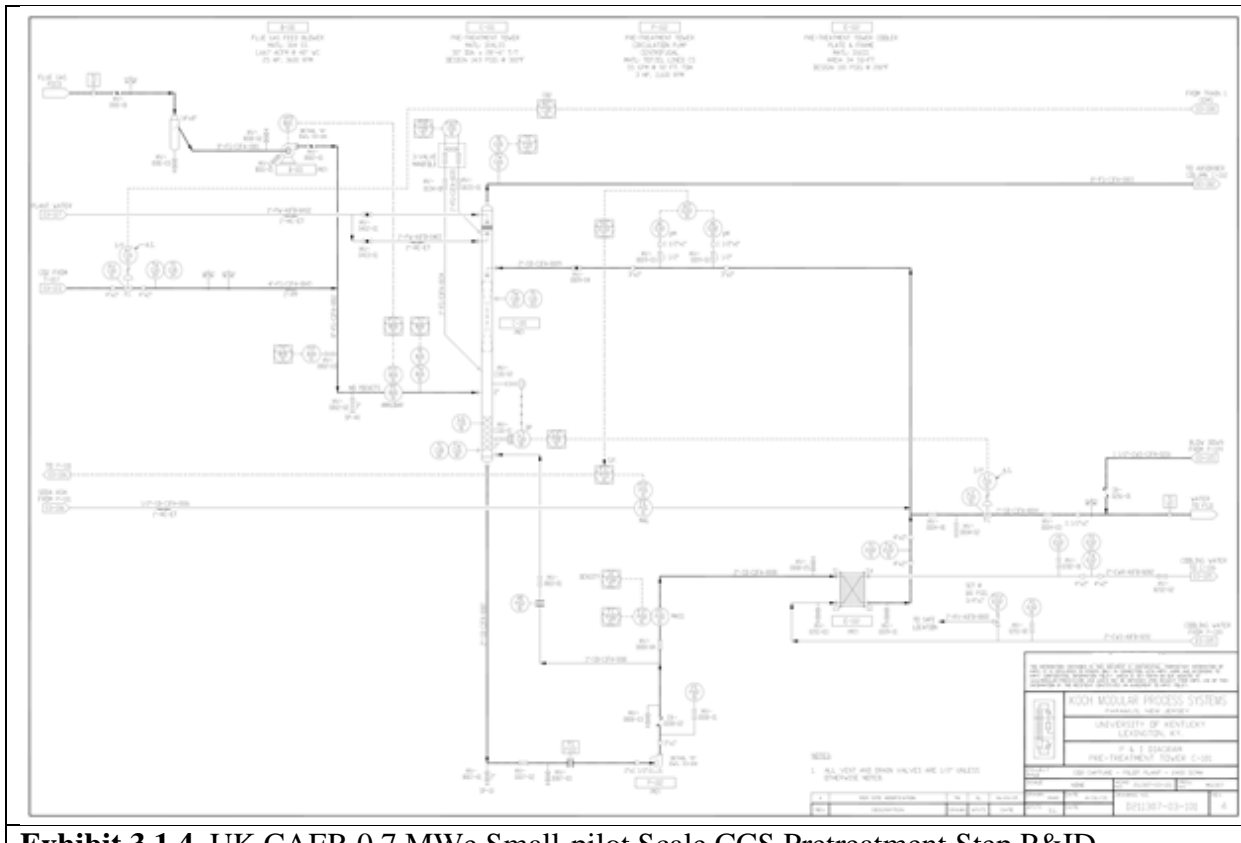


Exhibit 3.1.4. UK CAER 0.7 MWe Small-pilot Scale CCS Pretreatment Step P&ID.

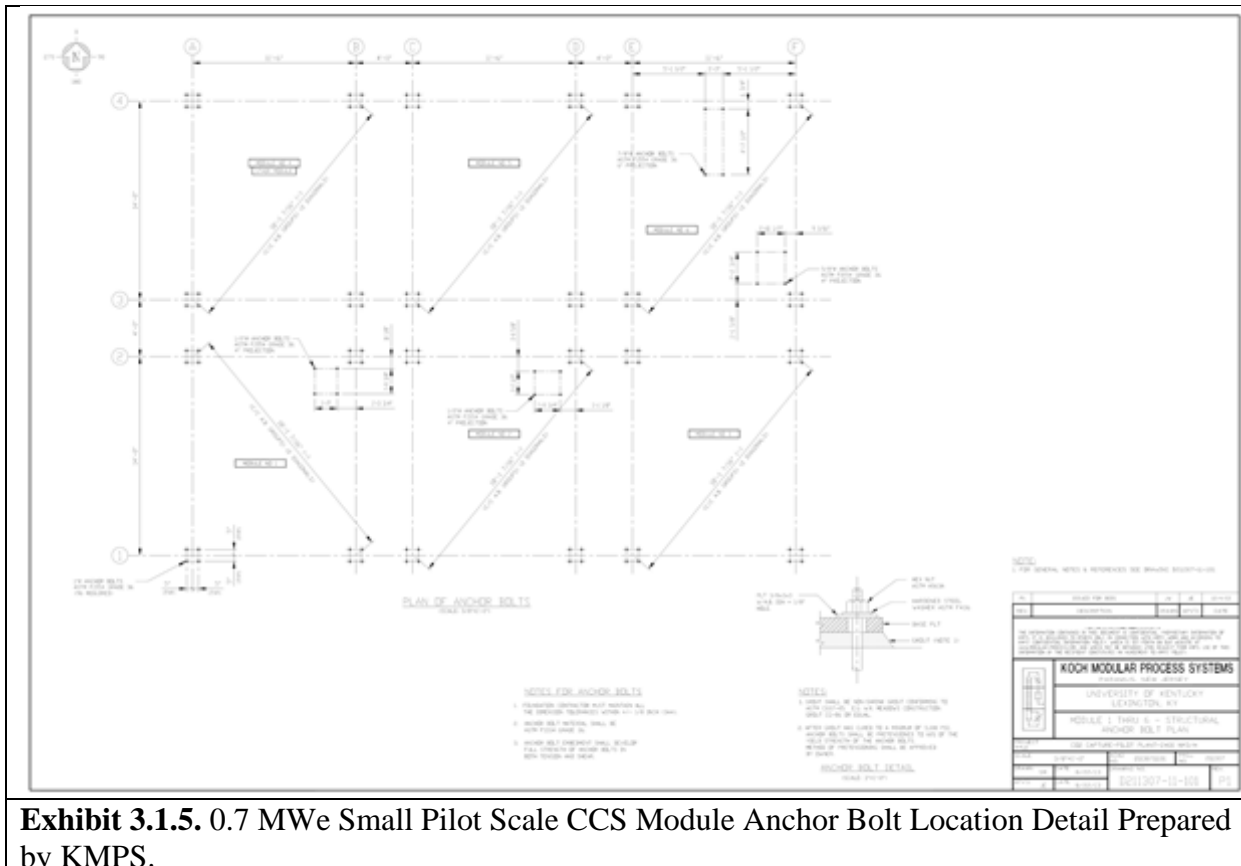
A complete set of general arrangement drawings (GAs) was also supplied by KMPS showing the equipment within the modules and the off module location within the foundation. Platform, process equipment, control panels, walkways, tie-ins, ladders and stairs are shown with north-south dimensions and elevations. Equipment access areas are clearly shown.

Pipe sizing, routing, support and specification within the modules was part of the KMPS design. A complete set of piping isometric, plan, and support drawings along with the specification for each service were also supplied. The isometric drawings detail the size, connection type, location, elevation, of each pipe section, valve, instrument, and fitting, along with complete specification of each gasket, bolt, nut and washer. Pipe support locations are also included in the isometric drawings. The plan drawing show how the piping system fits in with the equipment and module general arrangement. The support details are included in the set of pipe support drawing for spring hangers, U bolt guides, and off module pipe supports.

The ISBL electrical design drawings included the load schedule, electrical installation (control system, the instrument stands, conduit connections motor and receptacle details, and other details), lighting installation, power junction box layouts, instrument locations and conduit plans, the main control panel schematic, remote input/output (I/O) panel schematics, the motor control panel schematic, shop drawings, the cooling tower blower variable frequency drive (VFD), drawing, heat trace drawings.

Detailed equipment drawings were also supplied for agitators, blowers, filters, the chiller, columns, heat exchangers, pumps, vessels and tanks, showing the internal configurations, gasket and bolt details, nozzle and level gauge locations, and support details.

Structural drawings supplied by KMPS include steel and shop drawing. The steel drawings include the module anchor bolt plan, the structural foundation load schedule, module structural plans, elevations and details. The dry equipment weights, point loads, and anchor bolt locations necessary to complete the foundation design. The dry equipment weights were also needed to estimate the lifting requirements and as contributing information for the detailed construction cost estimate. As an example, **Exhibit 3.1.5** shows the module anchor bolt pattern needed to complete the foundation design. The shop drawings include erection drawings, loose handrail and gate details and tie grating details.



Lists

In the course of the design, many lists were created by KMPS including major equipment, instrumentation, piping lines, tie-ins, ship loose equipment and temporary bracing. To accompany the P&IDs, KMPS developed a tie in list, shown in **Exhibit 3.1.6**, for completion of the BOP design.

Exhibit 3.1.6. UK CAER 0.7 MWe Small-pilot Scale CCS Piping Tie In List Prepared by KMPS.

Tie-in Number	Description	P&ID	Flow	Temperature (°F)	Pressure (psig)	Comments
TI-01	Flue Gas Feed	03-101	6,871 lb/h	131	ATM	
TI-02	Plant Water	03-107	7.5 GPM	56-70	60-90	Continuous - Based on T-104, C-102, & Blowdown Flows
TI-02	Plant Water	03-107	50 GPM for 2 mins to T-101	56-70	60-90	Intermittent ~ every 40 hours
TI-03	Soda Ash Waste Stream	03-101	1,385 lb/h	76	ATM	
TI-04	Superheated Steam	03-107	3118 lb/h	500-600	150-650	Based on Desuperheater sizing, Note 1
TI-06	Flue Gas to Stack	03-102	11,268 lb/h	123.3	ATM	
TI-07	Instrument Air	03-107	100 SCFM	AMB	62-120	
TI-08	Steam Condensate	03-107	3,600 lb/h	280	30-40	Pressure based on control valve sizing, FV-E107-01. Estimated 4-5 wt% flashing, FV-E107-01
TI-09	Plant Air	03-107	Normally No Flow	-	-	
n/a	Flue Gas Condensate to OSBL Drum	03-102	Normally No Flow	-	-	

The equipment selection and sizing is shown in **Exhibit 3.1.7.**, where stainless steel (SS), carbon steel (CS), fiber reinforced plastic (FRP) and polytetrafluoroethylene (PTFE) are some materials of construction. The process includes 3 blowers, 6 columns, 14 heat exchangers, 5 filters, 14 pumps, and 5 tanks. The equipment list also contains final sizing information, operating and design conditions, the fabricator, materials of construction, insulation, gasket, and paint details.

Exhibit 3.1.7. 0.7 MWe Small Pilot Scale CCS Equipment List Prepared by KMPS.

Tag	Description	P&ID	Material of Construction	Design Conditions	Operating Condition	Insulation	Gasketing	Fabricator	Painting
B-101	Flue Gas Feed Blower	211307-03-101	304SS	NYB MODEL 2508S25	N/A	NONE	MFG STD	NEW YORK BLOWER	MFG STD
C-101	Pretreatment Tower	211307-03-101	304LSS	ASME SECT VIII, DIV1 CODE, 14.9 PSIG @ 300°F, NOT STAMPED	2 PSIG @ 110°F	NONE	GYLON 3500	DUSENBERY	NONE
P-102	Pretreatment Tower Circulation Pump	211307-03-101	TEFZEL LINED CS	MAKE / MODEL: INNOMAG TB-MAG MODEL A1, 1.5 X 1-6	N/A	NONE	MFG STD	PROCESSFLO	MFG STD
E-102	Pretreatment Tower Cooler	211307-03-101	316SS	ASME SECT VIII, DIV1 CODE, 100 PSIG @ 200°F	54 PSIG @ 110°F	NONE	EPDM	ALFA-LAVAL	MFG STD
P-112	Absorber Cooler Pump	211307-03-102	TEFZEL LINED CS	MAKE / MODEL: INNOMAG TB-MAG MODEL A1, 1.5 X 1-6	N/A	NONE	MFG STD	PROCESSFLO	MFG STD
E-112	Absorber Cooler	211307-03-102	304SS	ASME SECT VIII, DIV1 CODE, 100 PSIG @ 200°F	54 PSIG @ 137°F	NONE	EPDM	ALFA-LAVAL	MFG STD
C-102	CO ₂ Absorber	211307-03-102	304LSS	ASME SECT VIII, DIV1 CODE, 14.9 PSIG @ 200°F, NOT STAMPED	2 PSIG @ 120°F	NONE	GYLON 3500	DUSENBERY	NONE
P-103	Rich Amine Pump	211307-03-102	316SS	MAKE / MODEL: SUNFLO MODEL P25-BDU-60-F	N/A	NONE	MFG STD	PROCESSFLO	MFG STD
F-103	Carbon Filter	211307-03-102	304LSS	ASME SECT VIII, DIV1 CODE, 210 PSIG & FV @ 250°F	30 PSIG @ 110°F	NONE	GYLON 3500	DUSENBERY	NONE
F-104	Cartridge Filter	211307-03-102	304LSS	Model S4GL04-001-3-1.5F-210, 210 PSIG @ 250°F	175 PSIG @ 117°F	NONE	EPDM	FABER / FIL-TREK	NONE
F-102	Rich Amine Strainer	211307-03-102	WCB BODY/316SS BASKET	Model 72-39FHS-150-6, MAWP 230PSIG @ 100°F	187 PSIG @ 117°F	NONE	PTFE	KRASSL	MFG STD
E-110	Absorber Polishing Exchanger	211307-03-102	304SS	ASME SECT VIII, DIV1 CODE, 100 PSIG @ 200°F	85 PSIG @ 100°F	NONE	EPDM	ALFA-LAVAL	MFG STD
E-113	Secondary Heat Recovery Exchanger	211307-03-102	304LSS BOTH S & T	ASME SECT VIII, DIV1 CODE, SHELL: 200 PSIG @ 300°F / TUBE:50 PSIG @ 300°F	SHELL: 160 PSIG @ 162°F TUBE: 15 PSIG @ 178°F	2"-HC SHELL & HEADS	GYLON 3500	WARD TANK	NONE
P-115	Condensate Pump	211307-03-102	Cast Iron	MAKE / MODEL: GRUNDFOS CXR1S-3-A-FGJ-A-E-HQQE	N/A	1" PP - SOFT REMOVABLE	MFG STD	PROCESSFLO	MFG STD
P-104	Primary Stripper Bottoms Pump	211307-03-103	316SS	MAKE/MODEL: HMD-KONTRON GSA 3X1.5-6H-CA3A1	N/A	2" HC - SOFT REMOVABLE	MFG STD	PROCESSFLO	MFG STD
E-104	Lean Desiccant Exchanger	211307-03-103	TITANIUM	ASME SECT VIII, DIV1 CODE, 100 PSIG @ 200°F	85 PSIG @ 152°F	1" PP - SOFT REMOVABLE	EPDM	ALFA-LAVAL	MFG STD
E-106	Rich Heat Recovery Exchanger	211307-03-103	304SS	ASME SECT VIII, DIV1 CODE, 212 PSIG @ 356°F	150 PSIG @ 323°F	2" HC - SOFT REMOVABLE	EPDM	ALFA-LAVAL	MFG STD

E-107	Primary Stripper Reboiler	211307-03-103	SHELL: CS, TUBE: 304LSS	ASME SECT VIII, DIV1 CODE, SHELL: 150PSIG @ 400°F / TUBE:100PSIG @ 300°F	SHELL: 100 PSIG @ 328°F TUBE: 25 PSIG @ 250°F	3" - HC SHELL 2.5" - HC HEADS	GYLON 3500	WARD TANK	PS-2 SHELL
C-104	Primary Stripper	211307-03-103	304LSS	ASME SECT VIII, DIV1 CODE, 100 PSIG & FV @ 350°F	25 PSIG @ 250°F	3" HC	GYLON 3500	DUSENBERY	NONE
E-108	Reclaimer	211307-03-103	304LSS BOTH S & T	ASME SECT VIII, DIV1 CODE, SHELL: 100PSIG @ 350°F / TUBE:150PSIG @ 400°F	SHELL: 25 PSIG @ 287°F TUBE: 100 PSIG @ 328°F	3" - HC SHELL & HEADS	GYLON 3500	WARD TANK	NONE
E-105	Primary Heat Recovery Exchanger	211307-03-103	TITANIUM	ASME SECT VIII, DIV1 CODE, 100 PSIG @ 300°F	65 PSIG @ 200°F	2" HC - SOFT REMOVABLE	EPDM	ALFA-LAVAL	MFG STD
E-114	Lean / Rich Exchanger	211307-03-103	316SS	ASME SECT VIII, DIV1 CODE, 220 PSIG @ 300°F	150 PSIG @ 244°F	2" HC - SOFT REMOVABLE	EPDM	ALFA-LAVAL	MFG STD
P-117	Desuperheater Pump	211307-03-103	316SS	MAKE/MODEL: GREEN PUMP MODEL GPA 1500	N/A	1"-PP	MFG STD	PROCESSFLO	MFG STD
T-107	Condensate Pot	211307-03-103	304L SS	ASME SECT VIII, DIV1 CODE, 100 PSIG & FV @ 300°F	65 PSIG @ 200°F	1"-PP	GYLON 3500	DUSENBERY	NONE
E-115	Liquid Desiccant Preheater	211307-03-104	TITANIUM	ASME SECT VIII, DIV1 CODE, 150 PSIG @ 356°F	75 PSIG @ 323°F	2" HC - SOFT REMOVABLE	EPDM	ALFA-LAVAL	MFG STD
E-109	Liquid Desiccant Cooler	211307-03-104	TITANIUM	ASME SECT VIII, DIV1 CODE, 100 PSIG @ 200°F	65 PSIG @ 130°F	NONE	EPDM	ALFA-LAVAL	MFG STD
E-111	Liquid Desiccant Chiller	211307-03-104	TITANIUM	ASME SECT VIII, DIV1 CODE, 100 PSIG @ 150°F	65 PSIG @ 130°F	2" CC - SOFT REMOVABLE	EPDM	ALFA-LAVAL	MFG STD
Af-104	Air Filter	211307-03-104	CS	N/A	N/A	NONE	MFG STD	NEW YORK BLOWER	MFG STD
B-104	Water Evaporator Air Blower	211307-03-104	CS	NYB MODEL 28504S20	N/A	NONE	MFG STD	NEW YORK BLOWER	MFG STD
P-108	Secondary Stripper Bottoms Pump	211307-03-104	TEFZEL LINED CS	MAKE / MODEL: INNOMAG TB-MAG MODEL A1, 1.5 X 1-8	N/A	NONE	MFG STD	PROCESSFLO	NONE
P-106	Water Evaporator Bottoms Pump	211307-03-104	TEFZEL LINED CS	MAKE / MODEL: INNOMAG TB-MAG MODEL A1, 1.5 X 1-6	N/A	NONE	MFG STD	PROCESSFLO	MFG STD
C-105	Secondary Air Stripper	211307-03-104	304LSS	ASME SECT VIII, DIV1 CODE, 14.9 PSIG @ 300°F, NOT STAMPED	2 PSIG @ 200°F	2" HC	GYLON 3500	DUSENBERY	NONE
C-108	Water Evaporator	211307-03-104	FRP	ASME RTP-1-2011, 2 PSIG @ 180°F	0.5 PSIG @ 154°F	2.5" HC	GORETEX	AUGUSTA FIBERGLASS	TBD
Af-103	Air Filter	211307-03-105	CS	ENDUSTRA MODEL TKZR401-4-E045777	N/A	NONE	MFG STD	NEW YORK BLOWER	MFG STD
B-103	Cooling Tower Air Blower	211307-03-105	CS	NYB MODEL 445 AF	N/A	NONE	MFG STD	NEW YORK BLOWER	MFG STD
C-106	Cooling Tower	211307-03-105	FRP	ASME RTP-1-2011, 2 PSIG @ 150°F	0 PSIG @ 90°F	NONE	GORETEX	AUGUSTA FIBERGLASS	TBD

P-110	Liquid Desiccant Pump	211307-03-105	TEFZEL LINED CS	MAKE / MODEL: INNOMAG TB-MAG MODEL A1, 1.5 X 1-6	N/A	NONE	MFG STD	PROCESSFLO	MFG STD
T-104	Cooling Water Holding Tank	211307-03-105	304LSS	ASME SECT VIII, DIV1 CODE, 0 PSIG @ 110°F, NOT STAMPED	0 PSIG @ 70°F	NONE	TBD	DUSENBERY	NONE
P-109	Cooling Water Pump	211307-03-105	DI	MAKE/MODEL: GRISWOLD MODEL 811 4X3-13	N/A	NONE	MFG STD	PROCESSFLO	MFG STD
T-101	Soda Ash Make-Up Tank	211307-03-106	304LSS	ASME SECT VIII, DIV1 CODE, ATM @ 250°F, NOT STAMPED	ATM @ 100°F	1.5"- HC	TBD	DUSENBERY	NONE
A-101	Soda Ash Make-Up Tank Agitator	211307-03-106	316SS	MODEL FRH-3C	N/A	N/A	MFG STD	CLEVELAND MIXER	MFG STD
P-101	Soda Ash Make-Up Pump	211307-03-106	PTFE/316SS	MAKE / MODEL: NEPTUNE SERIES 560	N/A	1" HC - SOFT REMOVABLE	MFG STD	PROCESSFLO	MFG STD
T-103	Amine Make-Up Tank	211307-03-106	304LSS	ASME SECT VIII, DIV1 CODE, ATM @ 250°F, NOT STAMPED	ATM @ 100°F	1.5"- HC	TBD	DUSENBERY	NONE
P-113	Amine Make-Up Pump	211307-03-106	TEFZEL LINED CS	MAKE / MODEL: INNOMAG TB-MAG MODEL A1, 1.5 X 1-6	N/A	1" HC - SOFT REMOVABLE	MFG STD	PROCESSFLO	MFG STD
T-102	Additive Injection Tank	211307-03-106	304LSS	ASME SECT VIII, DIV1 CODE, ATM @ 250°F, NOT STAMPED	ATM @ 100°F	1.5"- HC	TBD	DUSENBERY	NONE
A-102	Additive Injection Tank Agitator	211307-03-106	316SS	MODEL FRH-2C	N/A	N/A	MFG STD	CLEVELAND MIXER	MFG STD
P-111	Additive Injection Pump	211307-03-106	PTFE/304LSS	MAKE / MODEL: NEPTUNE SERIES 560	N/A	1" HC - SOFT REMOVABLE	MFG STD	PROCESSFLO	MFG STD
T-105	Desiccant Make-Up Tank	211307-03-106	304LSS	ASME SECT VIII, DIV1 CODE, ATM @ 250°F, NOT STAMPED	ATM @ AMBIENT	1.5"- HC	TBD	DUSENBERY	NONE
A-105	Desiccant Make-Up Tank Agitator	211307-03-106	316SS	MODEL FRG-2C	N/A	N/A	MFG STD	CLEVELAND MIXER	MFG STD
P-116	Desiccant Make-Up Pump	211307-03-106	TEFZEL LINED CS	MAKE / MODEL: INNOMAG TB-MAG MODEL A1, 1.5 X 1-6	N/A	1" HC - SOFT REMOVABLE	MFG STD	PROCESSFLO	MFG STD
De-101	Steam Desuperheater	211307-03-107	CS BODY w SS NOZZLE	GRAHAM MODEL 2-SV1 DOUBLE VENTURI	N/A	3" - HT	MFG STD	GRAHAM	MFG STD
Ch-101	Chiller System	211307-03-107	316SS	40°F LCT @42.5 GPM/75 FT TDH	N/A	N/A	N/A	FILTRINE MFG	MFG STD

KMPS also prepared the system liquid volumes, shown in **Exhibit 3.1.8**, which were also utilized for the complete, comprehensive, EH&S assessment and to budget materials costs.

Exhibit 3.1.8. UK CAER 0.7 MWe Small Pilot Scale CCS System Volumes Prepared by KMPS.	
Solution	Volume (gallons)
Amine	1,600
Liquid Desiccant	4800
Soda ash	330
Ethylene Glycol	100

Specifications

Finally, KMPS supplied design specifications for equipment, instruments, insulation, paint, piping, and the structure. Equipment specification sheets were provided for agitators, blowers, the chiller, the desuperheater, filters, heat exchangers, and pumps.

The piping specifications are often consulted and detail the exact type of pipe, valves, gaskets, nuts, bolts, and all possible fittings appropriate for use based on the service and size of the pipe. The insulation specifications detail what piping, fittings, and equipment require insulation along with the insulation and jacketing material, thickness, and fastening hardware appropriate for use. The paint specifications detail what piping, fittings, and equipment require paint, the type of paint and primer, and the application methods appropriate for use.

Manuals and Instructions

KMPS provided an installation manual, a maintenance manual and a separate list of installation activities. The installation manual details the required activities for site preparation, initial module site inspection, module interim storage (which was not done), module placement, shipped equipment, piping, instrumentation/electrical, temporary support removal, and final preparations to be made. The maintenance manual provides manufacturer supplied data sheets, drawings, manuals, and spare parts lists for each type of instrument, and equipment. KMPS also supplied specific installation instructions pertaining to the cooling tower blower, the cooling tower packing and other internals, the cooling tower, and the chiller unit.

3-D Model

KMPS created a 3-D model using Navisworks® Freedom. **Exhibits 3.1.9 and 3.1.10** illustrate the usefulness of this model. A review of this model was conducted with KMPS and UK CAER in early March 2014. We were able to view the process, go inside, turn in any direction, and virtually navigate our way through it. The 3-D Process Model review was extremely beneficial. This was an opportunity to consider and visualize process operations and procedures, before it was too late to make changes. Because of this exercise, several short-comings were found and corrected. Examples of these include difficult reclamer operations, flue gas supply and return condensate removal, proper condensate flow to the absorber water wash section, a cooling water additives addition mechanism, and identification of potential freeze points and possible ways to avoid

problems. Several sample points and process line connection points were moved to eliminate the use of ladders.

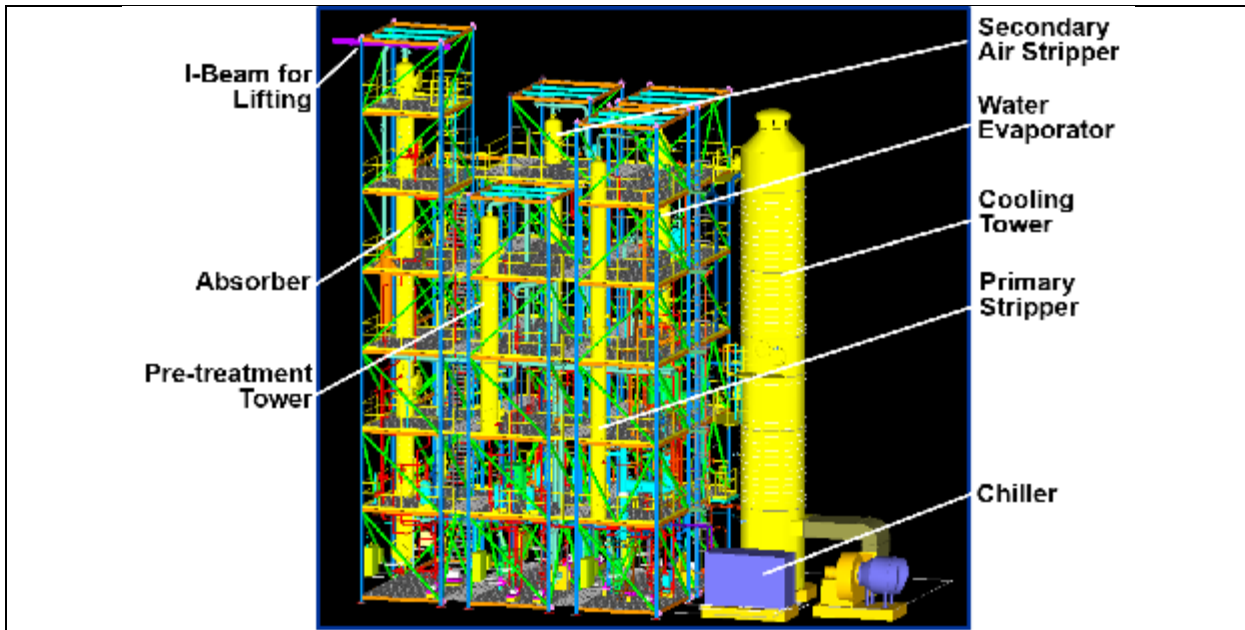


Exhibit 3.1.9. Navisworks® Freedom 3-D Model of the Entire 0.7 MWe Small Pilot Scale CCS Created by KMPS.

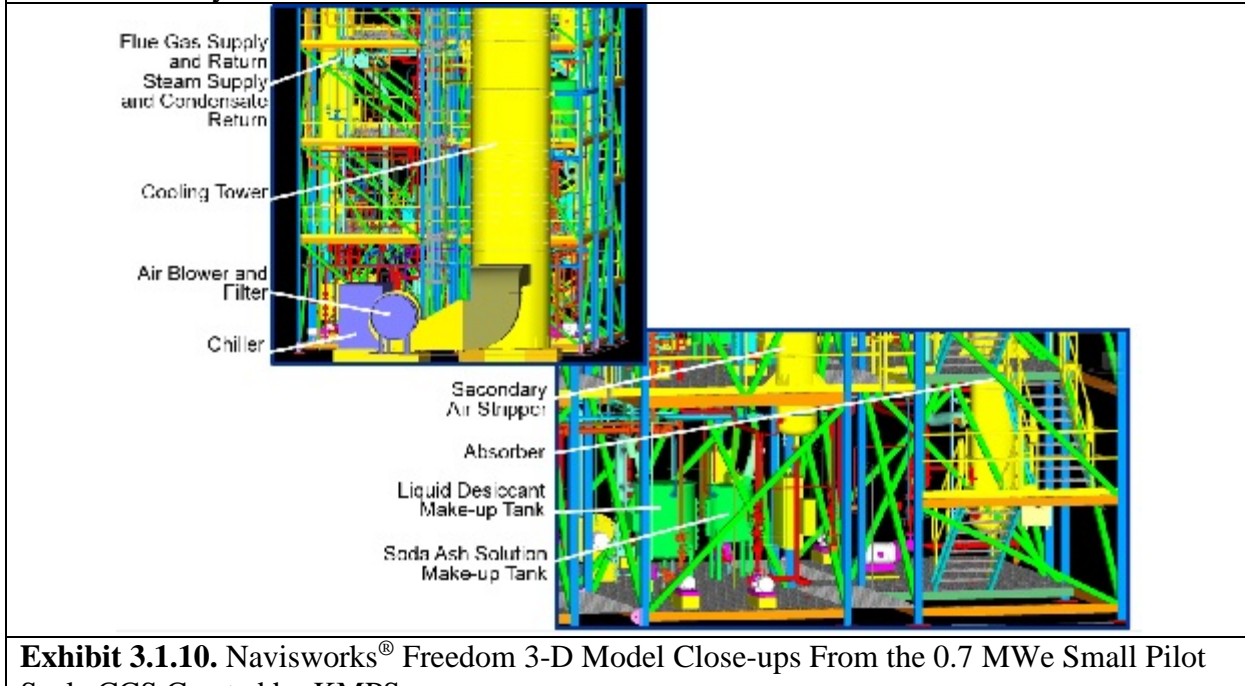
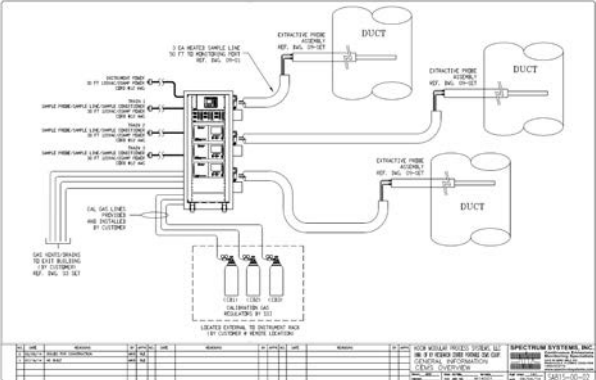


Exhibit 3.1.10. Navisworks® Freedom 3-D Model Close-ups From the 0.7 MWe Small Pilot Scale CCS Created by KMPS.

CEMS:

KMPS facilitated the design of the CEMS unit. It consists of 3 separate sample trains to monitor gas composition, as shown in **Exhibit 3.1.11 and 3.1.12**. Trains 1 and 2 are installed in the absorber gas inlet and outlet lines, respectively, and monitors/records SO₂, CO₂, CO, O₂, NO₂ and NO concentrations. Train 2 is installed in the absorber gas outlet line and monitors/records CO₂ and O₂. Train 3 is installed in the secondary air stripper gas outlet line and monitors/records CO₂ and O₂. Each train includes a separate sample probe, conditioning system, and control panel. Train 1 also includes a heated sample line.

	
Exhibit 3.1.11. Spectrum Systems, Inc. CEMS.	Exhibit 3.1.12. Spectrum Systems, Inc. CEMS.

DeltaV Control System:

Design and creation of the process controls system was also handled by KMPS. Emerson Delta V was the software used (Fisher Rosemount, 1994-2012). 223 separate instruments and control loops were incorporated into the program. Control schemes were configured to help run the process via user-friendly interfaces that offered state-of the-art graphics, real-time and historical trending capabilities as well as single-click access to graphics, directories, and P&IDs and other applications. Process limits were set for various equipment with alarms and interlocks set to trigger when set limits were exceeded. The historical capabilities within software was used to extract process data for analysis and to troubleshoot the system.



Exhibit 3.1.13. The Controlling Computers with Delta V Supplied by KMPS.

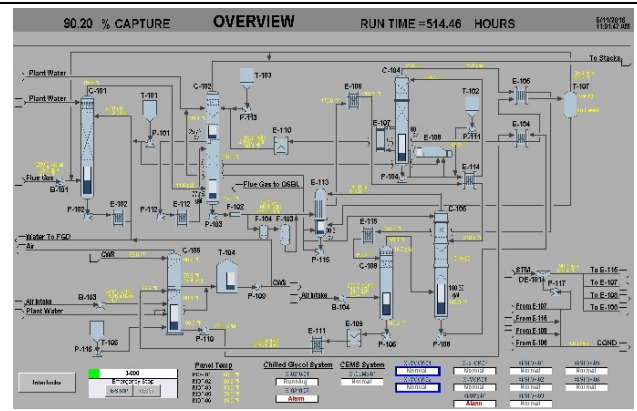


Exhibit 3.1.14. Delta V Control System Operations Screenshot.

Module and Other Equipment Shipping and Delivery



Exhibit 3.1.15. Shipping Modules Required a Crane to Lift the Back when Going Around this Corner, Very Near E.W. Brown Generating Station, 8/20/2014.



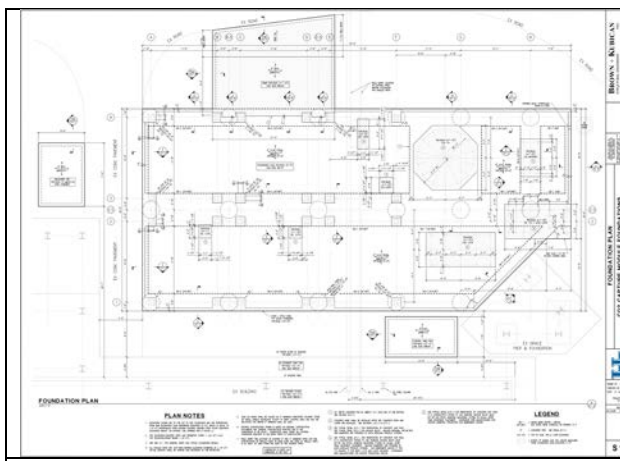
Exhibit 3.1.16. Another Tight Corner Very Near E.W. Brown Generating Station, 8/20/2014.

	
<p>Exhibit 3.1.17. Modules Stages Along the E.W. Brown Generating Station Entrance for Organized Placement the Following Day, 8/20/2014.</p>	<p>Exhibit 3.1.18. Moving Modules into Place for Erection at Process Site, 8/21/2014.</p>

KMPS was also responsible for shipment and delivery of the modules and other loose shipped pieces of equipment. For the delivery of the 6 process modules, a comprehensive shipping survey was done to ensure the trucks could go from the door of the assembly shop to the installation site. The shipping survey included verification of proper bridge underpass clearance, tree and overhead line clearance, corner space, bridge overpass weight capacity. Arrangements for a crane to assist turning two corners, one very near E.W. Brown Generation Station on Hogue Lane and the second to get around the limestone slurry tanks just adjacent to the erection site, as shown in **Exhibit 3.1.15 and 3.1.18**. Careful coordination between the shipping company and the general contractor had to occur to minimize costs associated with both the shipping trucks and the erection crane. The module were shipped in two stages with modules 1-3 arriving on site on 8/20/2014 and being installed on 8/21/2014, and modules 4-6 arriving on site and being installed on 8/28 and 8/29/2014. All erections were completed during the following 2 days. Additionally, many pieces of equipment were shipped separately including the chiller unit, the cooling tower, the cooling tower blower (B-103) and VFD, the cooling tower blower air filter (AF-103), cooling tower internals (packing, mist eliminators, packing supports), 54 module-to-module pipe sections, 16 off-module pipe sections, 9 off-module pipe supports, flue gas inlet blower (B-101) with inlet and outlet flexible connectors, secondary air stripper blower (B-104) with inlet and outlet flexible connectors, the absorber bottoms pump (P-103), the cooling water circulation pump (P-109), three tank agitators (A-101, A-102, and A-105), rupture discs, pH probes, amine cartridge filter (F-104), 9 instruments, heat trace components, lighting components, the hoist monorail, all the cross over grating and hardware, handrails and hardware, module-to-module structural ties, secondary egress ladder and safety gates, cooling tower ladders and platforms, 3 electrical panels (motor control panel (MCP), motor controller central panel (MCCP), power panel (PP)), the CEMS and the CEMS sample umbilical line.

3.2 Foundation Design

B+K was selected for the foundation design in April 2014. After system loads and dimensions were finalized by KMPS, details were passed onto B+K for foundation design. It was designed for structural support of the process modules and off module equipment with 150% spill containment curbs, as shown in **Exhibit 3.2.1**. B+K was also responsible for excavation, pier, reinforcement steel placement and concrete inspections. Mounting bolts for several pieces of rotating equipment along with the process modules were embedded into the foundation at the exact locations, then concrete was poured. The cooling tower also required an elevated pad, but the anchor bolts for it were added after the column was positioned.

	
Exhibit 3.2.1. Process Foundation Design by B+K.	Exhibit 3.2.2. Reinforcing Steel Inspection by B+K During the Construction Phase.

3.3 Tie-in Piping Systems Design

CMTA Consulting Engineers was selected for the design of the BOP tie in piping systems and electrical systems. Nine tie in piping systems were required; the flue gas supply and return, steam supply and condensate return, instrument air, service air, service water, potable water, and the soda ash waste stream line. Design of the piping systems was subcontracted to B&V, including route selection, sizing, thermal expansion considerations, material selection, supports, steam trap specification, derating the steam pressure from the source. As an example, a portion of the B&V design is shown in **Exhibit 3.3.1**. CMTA was responsible for interfacing between UK CAER and B&V, management of contractor installation, and final inspections.

To save on cost, chlorinated polyvinyl chloride (CPVC) was chosen as the material of construction for all horizontal sections of flue gas supply and return piping. It was painted with an ultraviolet (UV) resistant paint to extend the life. Stainless steel was used for the vertical sections of flue gas piping. CPVC has a higher coefficient of thermal expansion than stainless steel and this had to be taken into consideration, but as of writing this report, the CPVC is still performing well and its use resulted in cost savings.

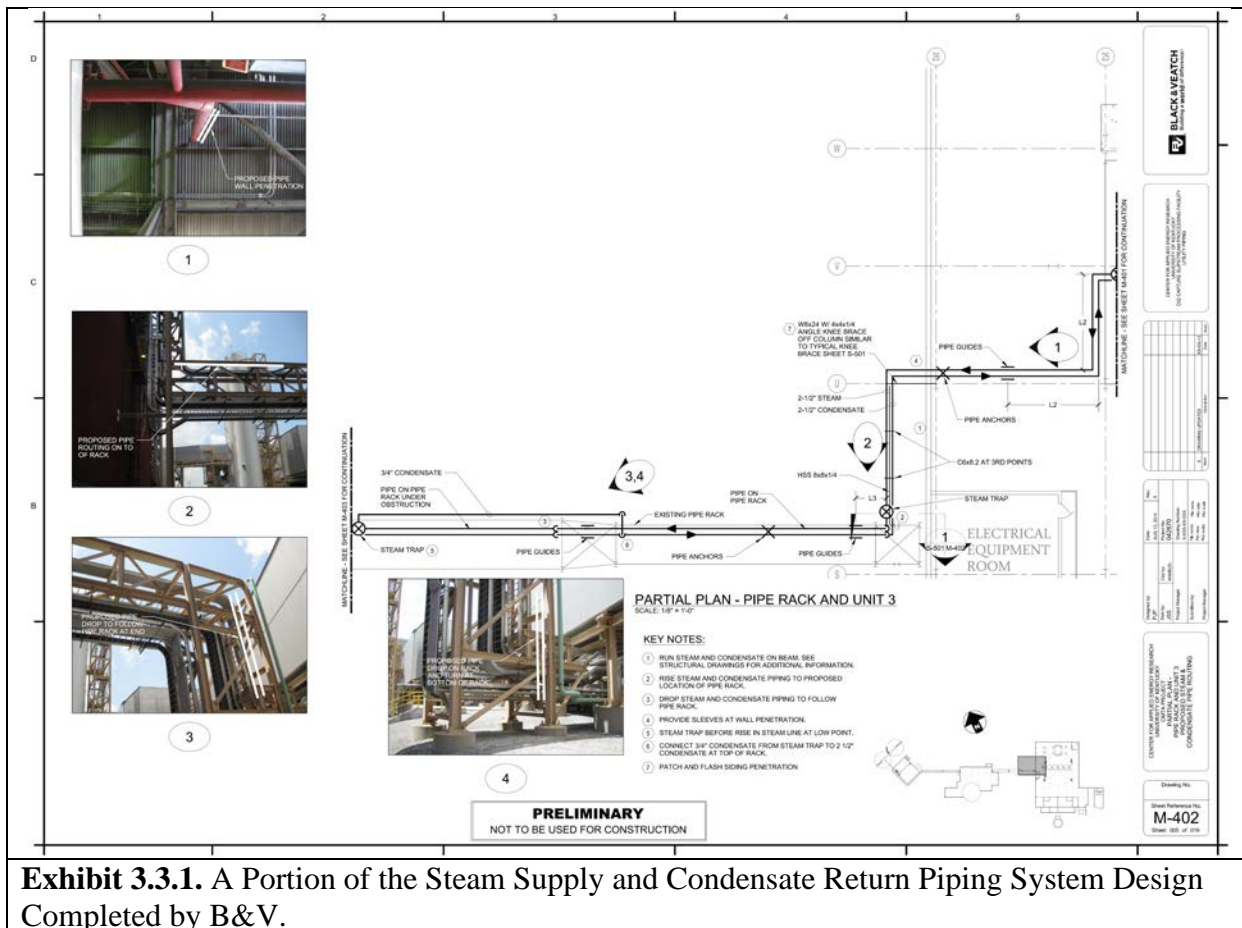


Exhibit 3.3.1. A Portion of the Steam Supply and Condensate Return Piping System Design Completed by B&V.

3.4 Electrical Systems Design

CMTA Consulting Engineers completed the BOP electrical systems design. This included the 480 V and 120 V feed tie ins, routing of the feed lines to the electrical shed, location of the electrical panels within the shed, routing of the lines from the process motors to the shed, routing of the lines from the shed to the mobile control room.

4) ON-SITE ERECTION AND INSTALLATION

4.1 Contractor Selection

After a formal bid process conducted in coordination with the UK Purchasing Department, the contractor for foundation construction and module erection site preparation work was selected in May 2014.

To save time, the construction scope was divided as listed in **Exhibit 4.1.1**.

Exhibit 4.1.1. Division of Construction.		
Construction Task:	Performed By:	Managed By:
Site Preparation & Excavation	Hall Contracting of Kentucky	B + K UK CAER
Foundation Construction	Hall Contracting of Kentucky	B + K UK CAER
Process Module and Off Module Equipment Placement	Hall Contracting of Kentucky	UK CAER
Process Intra-modular Tie Ins	Hall Contracting of Kentucky	UK CAER
Tie in Piping Systems	Hall Contracting of Kentucky	CMTA Engineers
Tie in Electrical Systems	Hall Contracting of Kentucky	CMTA Engineers
Flue Gas Line Expansion Joints	Evans Construction	CMTA Engineers

	
Exhibit 4.2.1. Removed Existing Electrical Duct Bank, 6/2/2014.	Exhibit 4.2.2. Drilling Foundation Pier A, 4, 6/13/2014.

4.2 Excavation

As per B+K specifications, the following tasks were performed. The site was excavated, piers were drilled along with a test hole at the bottom. The strata inside the pier excavation was inspected for structural integrity, reinforcement steel was added to the pier and concrete was poured and tested. The top elevations of the piers were determined by survey. B+K reviewed and approved all test results.

4.3 Foundation

As per B+K specifications, the following task were performed. The grade beams were formed and reinforcing steel was tied in place. The concrete casing was constructed. Anchor bolts were placed and dimensions between anchor points were verified. The concrete was poured for the main slab,

the concrete was inspected, sloped and smoothed. The spill containment curb, and other raised pedestals were poured second and the concrete was inspected. Finally, the cast was removed.

 A photograph showing the slab reinforcement for a large concrete structure. The reinforcement consists of a dense grid of black steel bars. Several workers in high-visibility vests and hard hats are visible, working on the reinforcement. The structure is supported by wooden formwork and yellow safety railings.	 A photograph showing a worker in a high-visibility vest and hard hat standing on a wooden platform, using a long yellow tape measure to check the dimensions of a modular structure. The structure is supported by a grid of black steel reinforcement bars. The background shows an industrial building with various equipment and structures.
Exhibit 4.3.1. Slab reinforcement, 07/17/2014.	Exhibit 4.3.2. Modular Structure Anchor Bolt Dimension Check, 7/17/2014.
 A photograph showing the main slab concrete pour. A large area of smooth, grey concrete is visible, supported by a wooden formwork. Several workers in high-visibility vests and hard hats are standing around the perimeter of the pour, monitoring the process. The background shows an industrial building with various equipment and structures.	 A photograph showing the main slab with completed anchor bolt pedestals. The slab is a large, flat, light-colored surface. Numerous small, rectangular pedestals are evenly spaced across the surface, each supporting a large anchor bolt. Workers are visible in the background, and the structure is supported by wooden formwork and yellow safety railings.
Exhibit 4.3.3. Main Slab Concrete Pour, 7/22/2014.	Exhibit 4.3.4. Main Slab with Completed Anchor Bolt Pedestals, 8/8/2014.

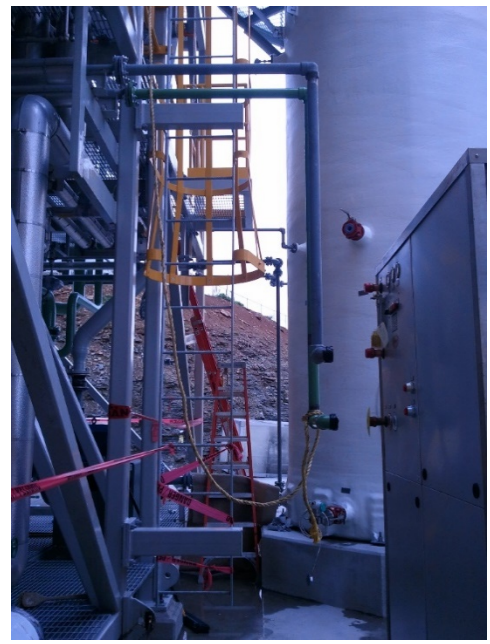
4.4 Module Installation

Coordination of module shipment was made to all for sufficient foundation drying time and minimize the truck and crane rental time. Modules 1, 2 and 3 were shipped together and installed in one day and modules 4, 5 and 6 were shipped together a week later and again installed in one day. Off module equipment, such as the cooling tower, the chiller package, blowers and pumps were installed subsequently.

	
Exhibit 4.4.1. Erection of Module 2, 8/21/2014.	Exhibit 4.4.2. Erection of Module 6, 8/29/2014.
	
Exhibit 4.4.3. Erection of Cooling Tower, 9/17/2014.	Exhibit 4.4.4. Cooling Tower Blower (B-103) is Set, 10/15/2014.

4.5 Module-to-module Tie-ins and Loose Shipped Equipment Installation

Three truckloads of loose shipped equipment were received, inventoried and installed. This included module-to-module piping and grating, off module pipe sections, module handrails and hardware, the secondary egress ladder, the monorail, loose lighting components, the cooling tower internal equipment and external landings, tanks agitators, several pumps and blowers, and electrical panels. Each piece was installed per KMPS specifications.

	
Exhibit 4.5.1. Off-module Piping Installation, 10/15/2014.	Exhibit 4.5.2. Secondary Egress Ladder Installation, 10/15/2014.

4.6 Tie-in Piping

Tie-in piping included the flue gas supply line, the flue gas return line, the steam supply line, the condensate return line, the soda ash waste return line, and utility supply lines including plant air, instrument air, plant water, potable water.

	
Exhibit 4.6.1. Flue Gas Supply Lines Installed at Top of Stack Duct, 4/7/2015.	Exhibit 4.6.2. Vertical Sections of Flue Gas Supply and Return Lines, 4/7/2015.
	
Exhibit 4.6.3. Construction of the Steam Supply Line, 12/3/2014.	Exhibit 4.6.4. Steam Supply and Condensate Return Lines Installed on Pipe Roller Support, 12/3/2014.

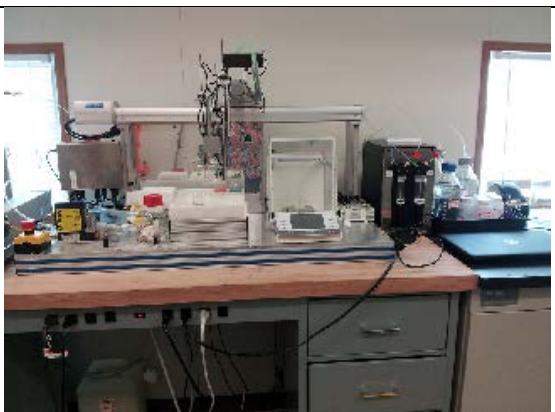
	
Exhibit 4.7.1. Process Grounding Ring Trench, 6/25/2014.	Exhibit 4.7.2. Electrical Shed Set, 10/8/2014.

4.7 Electrical Engineering

The electrical scope included installation of a grounding ring around and under the foundation, installation and connection of all electrical panels inside the electrical shed, installation of grounding cables on the process modules and cooling tower, and running the 480V and 240V feed cables and trays.

4.8 Mobile Control Room and Laboratory

The mobile control room and laboratory was specified, permitted, and set into place. Then the electrical and water connections were made. The laboratory equipment and apparatuses were set up and tested. The controlling computers and CEMS were set up and tested.

	
Exhibit 4.8.1. Mobile Control Room and Field Laboratory is Set, 11/13/2014.	Exhibit 4.8.2. Automatic Liquid Sample Analysis Instrument, 5/6/2015.
	<p>0.7 MWe Pilot Scale CO₂ Capture Project KU E.W. Brown Generating Station</p> <p>Sponsored by: U.S. Department of Energy Office of Fossil Energy National Energy Technology Laboratory Kentucky Department of Energy Development and Independence Carbon Management Research Group University of Kentucky</p> <p>Center for Applied Energy Research ICE KU U.S. DEPARTMENT OF ENERGY Office of Fossil Energy NETL MITSUBISHI HITACHI POWER SYSTEMS DUKE ENERGY EPRI DEPI AEP KENTUCKY POWER A NEW PARTNERSHIP FOR ENERGY</p> <p>Copyright © 2016 Battelle Energy Alliance, LLC</p>
Exhibit 4.8.3. Field Laboratory, 5/6/2015.	Exhibit 4.8.4. Mobile Control Room Identification Sign, 4/8/2016.

4.9 Balance of Plant Instrumentation and Controls

KMPS designed the control system using DeltaV charms which minimized site installation of controls and instrumentation wiring. The charms layout provided I/O terminals within the modules allowing the BOP instrumentation and controls wiring to be performed by UK CAER personnel. While most of the instrumentation was pre-wired to the appropriate field boxes by KMPS for all instrumentation within the modules, all off-modules instrumentation and equipment had to be wired to the appropriate field termination location. Since most of the off-module instrumentation was located around the cooling tower, a significant portion of the balance of plant instrumentation and controls were wired to the closest I/O panel (Module 6) based on the design from KMPS. However, it should be noted that some items such as the soda ash pH probes were pre-wired by KMPS but the probe itself was installed by UK CAER just before startup in order to protect the probe during transport and also to keep them from drying out. Before wiring of the instrumentation

could occur, installation of the probes and their associated transmitters were physically installed to their proper location. Once installed, appropriate control cables were run from the instrument to the field panel, and then terminated on both sides. After connecting the cables, each instrumentation/control loop was checked for continuity. An example of off-module BOP controls/instrumentation wiring performed by UK CAER can be seen in **Exhibits 4.9.1 and 4.9.2**.

In addition to the off-module BOP controls/instrumentation, there were several loose shipped pieces of equipment that had to be field installed and required on-site controls integration. Loose shipped items that required UK CAER controls/instrumentation wiring included, all pumps and all blowers, as well as the CEMS unit and electrical shed components (motor control cabinet and electrical shed controls cabinet). Work on the electrical shed components by UK CAER personnel also required programming of the VFD's, setting of the overload protection devices and installing power monitors. UK CAER also designed and fabricated ports for gas and liquid sample collection for installation along the columns, shown in **Figure 4.9.3**.

The final portion of the UK CAER site installation work on the controls and instrumentation consisted of wiring the 6 remote panels (modules 1, 2, 3, 5 and 6 as well as electrical shed panel) to the main control room in the site trailer. Once each remote panel was connected to the control system, the control computer was started up and every instrument/connection was checked for continuity again. After successfully checking continuity, each instrument was calibrated and commissioned for service. An example of the controls wiring performed by UK CAER is shown in **Exhibit 4.9.4**.

	
Exhibit 4.9.1. Cooling Tower Level Gauge (LT-C106-01), 5/7/2015.	Exhibit 4.9.2. Soda Ash Loop pH Probes, 1/23/2015.
	
Exhibit 4.9.3. Column Liquid/Gas Sample Collection Port.	Exhibit 4.9.4. Controls Wiring Installed by UK CAER, 2/11/2015.

4.10 Post-Modifications (Membrane and Water Wash Systems)

In UK CAER's continued effort to improve its CCS and demonstrate the readiness of various technology aspects proven at laboratory and bench scales, two major process additions, (1) Membrane Separation Unit and (2) Water Wash System were subsequently incorporated with equipment, electricals and controls system fully in place in May 2019. The major phases for the post-modification are as highlighted:

- KMPS and MTR finalized detailed design and specifications after an initial process specification and design was used to determine feasibility and define equipment location. KMPS subsequently completed P&IDs with line sizes, electrical, layout drawings and structural drawings which incorporated structural modifications needed for the installation of the new equipment. A final 3-D model of the system including the location of new equipment which included the membrane unit, vacuum pump system, knock-out pot, blower (B200), circulation pump (P200), heat exchanger (E200), water wash column (C200), filter (F200) is shown in **Exhibit 4.10.1**.

- All equipment was delivered on site by end of November 2018. MTR provided the membrane and ordered the vacuum pump system. KMPS provided and ordered new equipment associated with the water wash system and required instrumentation and controls for motors and process.
- UK CAER closed the bidding process for mechanical construction on 12/18/2018, reviewed bids and selected Blau Mechanical. Per terms of established contract and host-site relations, construction began on 2/25/19 and was completed in May 2019. Ready Electric completed required major electrical installations and UK CAER performed control wiring. **Exhibits 4.10.2 – 4.10.5** show the installed vacuum system, water wash column, MSU with blower, and heat exchanger.

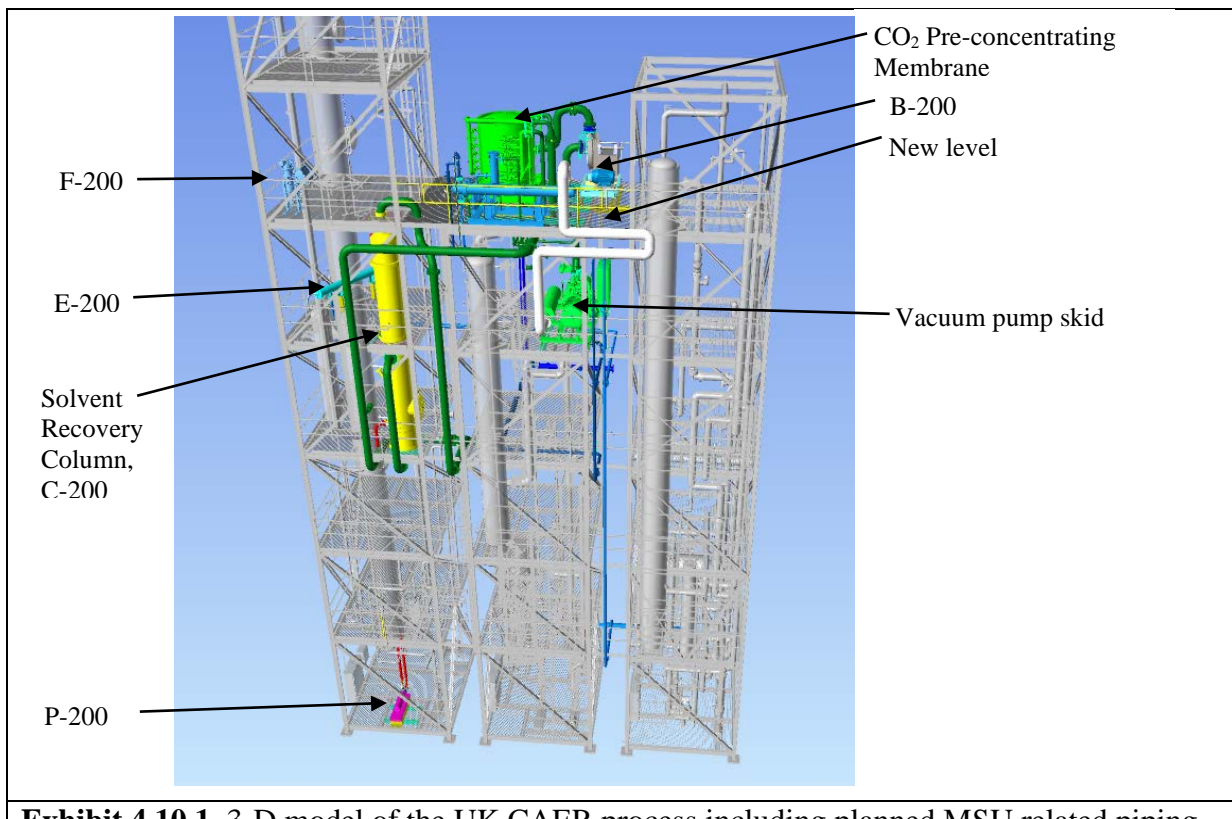


Exhibit 4.10.1. 3-D model of the UK CAER process including planned MSU related piping.



Exhibit 4.10.2. The vacuum pump installed within Module 2.



Exhibit 4.10.3. The solvent recovery column (C-200) installed within Module 1.



Exhibit 4.10.4. The MSU and B-200 blower installed on the newly constructed floor atop Module 2.



Exhibit 4.10.5. Heat exchanger (E-200) installation within Module 1.

5) START UP AND SHAKEDOWN

5.1 Safety Policies and Procedures and Standard Operating Procedures (SOPs)

At the University of Kentucky, the highest priority is placed on the health and safety of people and the environment, and they are managed like any key resource – by integrating every process with good management and leadership techniques. In order to meet our objectives, every employee is committed to working in a safe, environmentally conscientious manner. All employees are expected to take personal responsibility for their own safety, to be conscious of the safety of others, and to help identify potential hazards so they can be corrected. Moreover, continuous evaluations of our processes occur, looking for ways to minimize our impact on the environment by reducing and recycling waste. For work on the UK CAER small pilot scale CCS (and subsequently the large pilot scale CCS project discussed in this report), the following safety training classes are mandatory.

Training Programs:

LG&E and KU's Passport Training
Ammonia Awareness Training
Occupational Safety and Health Administration (OSHA) 10- and 30- hour Training
National Safety Council (NSC) First Aid and Cardiopulmonary Resuscitation (CPR) Training
Blood Borne Pathogens
Lock Out/Tag Out (LO/TO) Training, developed specifically for this project
Ladder Safety Training
Respirator Use Training
Hazardous Waste Specific Training
Chemical Hygiene Training
Fire Extinguisher Training
Lab Specific Training

Safety Protocols:

Emergency Action Plan, developed specifically for this project
Chemical Hygiene Plan, developed specifically for this project
Chemical Inventory Program
Drug Screening Program, developed specifically for this project
Contractor Management Program
Spill Prevention, Control and Countermeasure Plan
Daily Job Safety Analysis and Attendance, developed specifically for this project
Equipment Preventative Maintenance Program, developed specifically for this project
Laboratory and Hood Inspections
Fire Extinguisher Inspections
Respirator Fit Testing

Select Standard Operating Procedures, all developed specifically for this project:

Process Start up, based on weather conditions
Process Shutdown, based on weather conditions

Normal Operations
Winter Operations
Instrument Calibrations
Mechanical Repairs
Waste and Material Handling

LG&E and KU Tools Safety Program:

As part of their contractor management program and covered in the Passport Training program LG&E and KU has developed a set of Tools, which are comprehensive safety analyses to be completed before each job. Tool 2 covers equipment (hand tools, platforms, vehicles, barricades and grounding), hazardous substances (chemicals, blood borne pathogens, waste, radiation, SDSs, personal protective equipment (PPE) (electrical, welding, natural gas, eye protection, fall protection, hearing protection, foot and hand protection, respiratory protection, hard hats, and traffic vests), specific respirator hazards(dust, asbestos, lead, hexavalent chromium, SO₂, etc.), safety procedures (compressed gas cylinders, confined spaces, bulk chemical unloading, excavation, fire protection, explosion hazards, scaffolding, etc.), permits (hot work, asbestos, building, etc.), and lighting. Tool 3 is an aid to specify all details associated with the hazards and controls identified in Tool 2. Tool 4 is a monitoring checklist to be completed by a 3rd party while the job is being performed and includes housekeeping (trip hazards, trash and debris, barricades, etc.), equipment (proper guards and grounding, proper use, proper safety features), hazardous substances (compliance with procedures, SDSs available), PPE (proper use), specific work requirements (person on site qualified in CPR, proper vehicle licenses, employee qualifications, permits, lighting, equipment inspections, etc.). Prior to taking control of the process, after construction was complete, UK CAER identified 19 separate commissioning and startup tasks, and completed the appropriate Tools for each. (Tool 1 is an LG&E and Brown Station maintained list of contractors.)

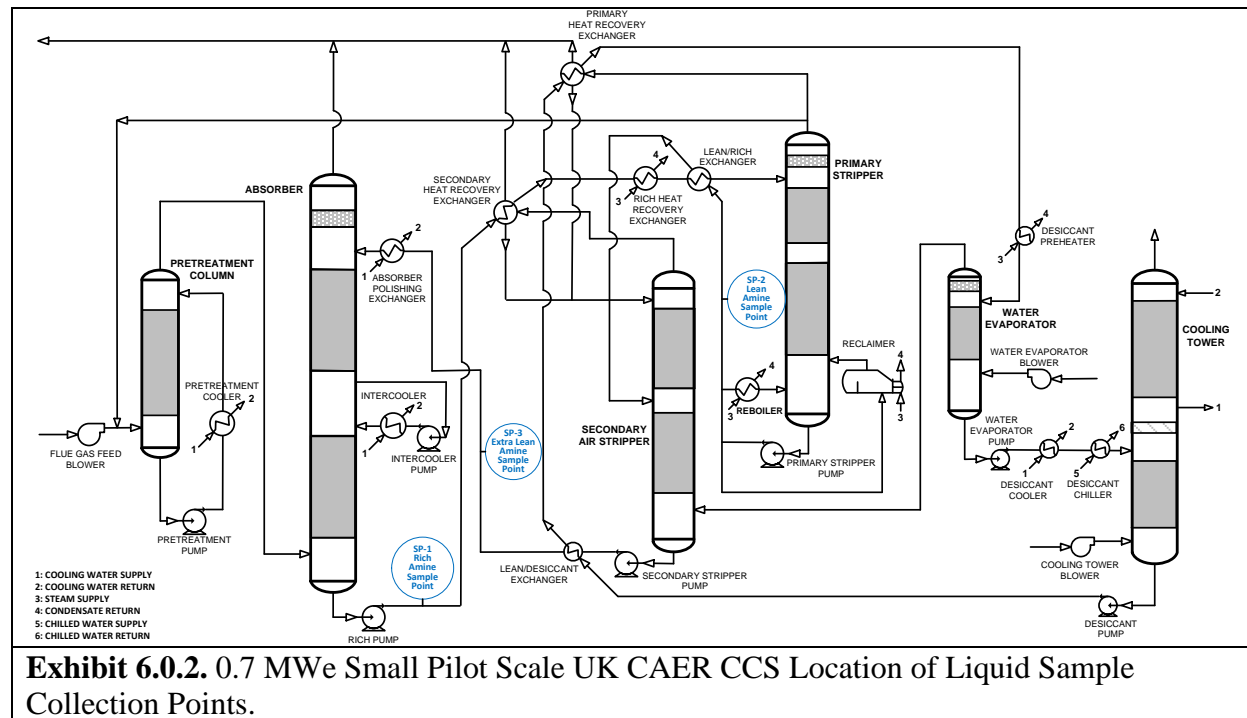
5.2 Leak Check, Wash and Process Start Up

Piping systems and equipment were filled with compressed air to a pressure of about 10 psig. Process connections such as flanges or threaded connections were all visually tested for leaks using a soap solution and a pressure gauge was monitored to ensure that isolated sections of piping and equipment would maintain pressure. After the air leak test, service water was added to each process loop and circulated. Again process connections such as flanges or threaded connections were all visually tested for leaks. A soda ash and water solution was added to the amine loop for initial testing. Flue gas was brought through the system and CO₂ capture with the soda ash solution was observed with the CEMS.

6) MEA CAMPAIGN

Exhibit 6.0.1. MEA Parametric Campaign Operating Conditions.

Absorber Liquid/Gas Flow Rate Ratio, L/G (kg/kg)	Primary Stripper Pressure (psia)	Inlet CO ₂ Concentration (vol%)
3.5, 4 and 5	30, 36 and 51	12, 14 and 16



The first solvent to be run in this system was 30 wt% MEA without any additional additives from 7/19/2015 to 1/15/2016, with 1217 operational hours being accumulated. A parametric campaign was conducted first, where operating conditions were deliberately varied in order to establish trends and a set of conditions resulting in a low solvent regeneration energy. During the MEA parametric campaign 27 different conditions were evaluated by varying the process conditions as listed in **Exhibit 6.0.1**. The absorber inlet gas flow was held constant at 1400 ACFM. The lean

solvent inlet flow rate to the absorber was set and controlled to obtain different L/G ratios. The primary stripper pressure was set and controlled with the outlet gas (CO₂ product) flow rate (PV-E105-02) after heat recovery in the primary heat recovery exchanger (E-105) and condensate removal (T-107). After these three process parameters were set, the steam flow to the primary stripper reboiler was set at a minimum value, while still achieving 90% CO₂ capture.

For each parametric condition, after steady state was achieved and maintained for approximately 30 minutes, a set of liquid samples were collected from the SP-1, SP-2 and SP-3 sample points shown in **Exhibit 6.0.2**. The key process parameters were evaluated and averaged near to the liquid sample collection time and used to evaluate the process performance (CO₂ capture efficiency and the solvent regeneration energy) associated with the conditions and to analyze trends.

Nearly 200 parameters (temperatures, pressures, flow rates, gas compositions, pH, etc.) are measured and recorded with the Delta V process control software. The most relevant operating temperatures, pressures, gas stream CO₂ contents, absorber gas velocity, and L/G ratio, were taken directly from, or calculated from, the Delta V data export files. Solvent carbon loadings are measured from liquid samples collected during steady state times and solvent working capacity is calculated from the measured carbon loadings. Solvent make up rates are known directly from the solvent addition log.

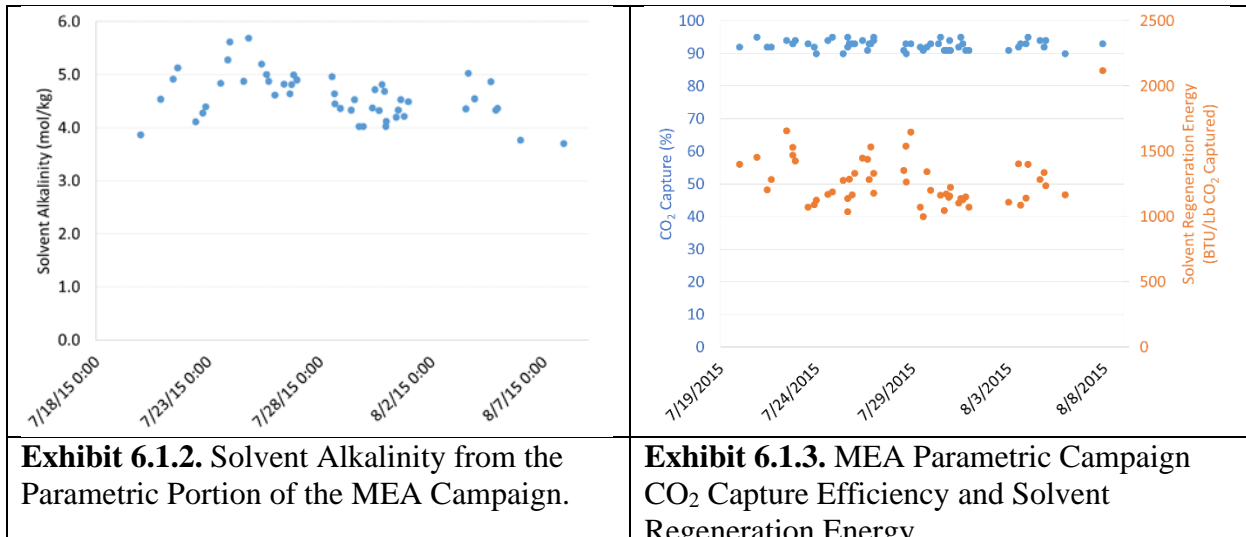
6.1 Process Stability and Solvent Concentration

Exhibit 6.1.1 lists the values and variation of most pertinent operating parameters affecting CO₂ capture and solvent regeneration energy during one steady state time during the MEA campaign, and illustrates the process stability of the UK CAER CCS. These parameters all had small variations during steady state. The temperatures all varied by $\leq \pm 2.2\%$ with the exception of the lean/rich heat exchanger hot end approach temperature, which varied by $\leq \pm 5.7\%$. The variation of the primary stripper pressure was $\leq \pm 1.1\%$ and this parameter is controlled by the overhead flow (CO₂ product flow). Consequently, this was the flow rate with the most variation of $\leq \pm 13.1\%$, while the other flow rates all varied by $\leq \pm 2\%$. The gas CO₂ concentrations varied by $\leq \pm 3.0\%$ at the absorber inlet, $\leq \pm 11.0\%$ at the absorber outlet and $\leq \pm 5.9\%$ at the secondary air stripper outlet. The solvent loading were measured from one sample collected from the middle of the steady state period. Two analyses are conducted from each liquid solvent sample with the results being accepted from the first if the second differs by $\leq \pm 5\%$.

Exhibit 6.1.1. Most Pertinent Process Parameters from One Steady State Condition from the MEA Campaign: 9/30/2015 from 21:15 to 23:15.				
Description	Instrument Tag	Units	Average Value	Process Variation
Temperatures				
Absorber Gas Inlet Temperature	TI-C101-01	°F	81.2	$\leq \pm 0.4\%$
Absorber Lean Solvent Inlet Temperature	TI-E110-02	°F	101.5	$\leq \pm 2.2\%$
Absorber Solvent Outlet Temperature, Bottom of Column	TI-C102-04	°F	107.1	$\leq \pm 0.6\%$

Primary Stripper Rich Solvent Inlet Temperature	TI-C104-01	°F	219.1	≤± 0.9%
Primary Stripper Lean Solvent Outlet Temperature	TI-C104-04	°F	258.6	≤± 0.2%
Lean/Rich Exchanger Hot End Approach Temperature	Calculated	°F	39.5	≤± 5.7%
Secondary Air Stripper Lean Solvent Inlet Temperature	TIC-E114-01	°F	196.3	≤± 1.8%
Pressures				
Primary Stripper Operating Pressure	PIC-E105-02	psia	36.0	≤± 1.1%
Flow Rates				
Absorber Gas Inlet Flow	FIC-B101-01	ACFM	1400.0	≤± 1.0%
Absorber Solvent Inlet Flow	FIC-C102-01	lb/hr	29010.7	≤± 1.1%
Primary Stripper Gas Outlet Flow, CO ₂ Product Flow	FI-E105-01	ACFM	98.6	≤± 13.1%
Steam Flow to Primary Stripper Reboiler	FIC-E107-01	lb/hr	2145.1	≤± 1.8%
Air Flow to Secondary Air Stripper	FIC-B104-01	ACFM	399.9	≤± 0.8%
Gas Compositions				
Absorber Inlet CO ₂ Concentration	AI-C101-01	Dry, vol%	15.0	≤± 3.0%
Absorber Outlet CO ₂ Concentration	AI-C102-01	Dry, vol%	1.8	≤± 11.0%
Secondary Air Stripper Outlet CO ₂ Concentration	AI-C105-01	Dry, vol%	2.0	≤± 5.9%
Solvent Loadings and Difference Between Repeated Analysis				
Rich Solvent C-loading	SP-1	mol/kg	1.86	≤± 5%
Lean Solvent C-loading	SP-2	mol/kg	1.14	≤± 5%
Extra-lean Solvent C-loading	SP-3	mol/kg	1.10	≤± 5%
Solvent Cyclic Capacity	Calculated	mol/kg	0.76	≤± 5%
Other Parameters				
Absorber Liquid to Gas Flow Ratio, L/G	Calculated	mass/mass	4.5	
Absorber Gas Velocity	Calculated	ft/min	250.9	
Solvent Loss Rate due to Solvent degradation	Calculated	lb/ ton CO ₂ captured	8.6	
System Performance				
Capture Efficiency	Calculated	%	90	
Solvent Regeneration Energy	Calculated	BTU/lb-CO ₂ captured	1472	

The solvent alkalinity from the parametric portion of the MEA campaign is shown in **Exhibit 6.1.2**, with variation from 3.7 to 5.7 mol/kg.



6.2 CO₂ Capture Efficiency and Solvent Regeneration Energy

To remain consistent with NETL RC 10, a 90% CO₂ capture efficiency was targeted for all parametric and long term conditions.

The CO₂ capture efficiency was calculated and monitored during both the parametric and long-term portions of the MEA solvent campaign. While running, the CO₂ and O₂ concentrations in the flue gas, before and after the absorber, were continuously monitored and recorded. The CO₂ capture efficiency was calculated from **Equation 6.2.1**.

$$CO_2 \text{ Capture Efficiency} = \frac{\left(Q_{CO_2 \text{ inlet}} - Q_{CO_2 \text{ outlet}} * \left[\frac{\left(\frac{1-Q_{CO_2 \text{ inlet}}}{100} \right)}{\left(\frac{1-Q_{CO_2 \text{ outlet}}}{100} \right)} \right] \right)}{Q_{CO_2 \text{ inlet}}} \quad \text{Equation 6.2.1.}$$

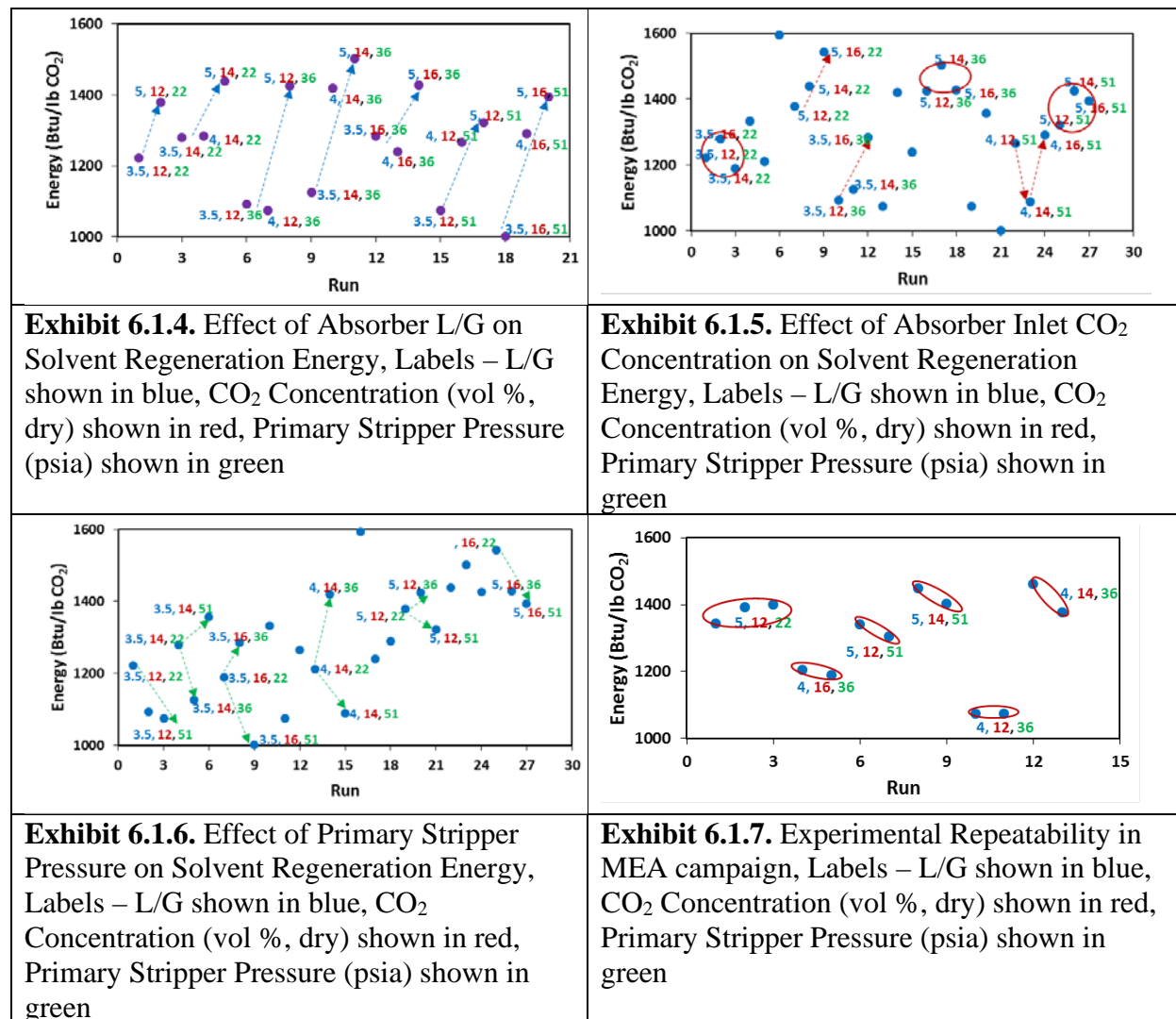
At this pilot scale, the inlet CO₂ concentration is controlled with a slipstream of the CO₂ product gas exiting the primary stripper. This demonstrates higher inlet CO₂ concentrations expected at a commercial scale due to the secondary air stripper outlet gas being recycled to the boiler as combustion air.

The solvent regeneration energy is calculated with **Equation 6.2.2**.

$Solvent \text{ Regeneration \ Energy} \\ = (H_{reboiler,steam \ in} - H_{reboiler,steam \ out}) * \dot{m}_{reboiler,steam \ in}$	Equation 6.2.2.
---	------------------------

The CO₂ capture efficiency and solvent regeneration energy from the parametric portion of the MEA campaign are shown in **Exhibit 6.1.3**. The CO₂ capture efficiency ranged from 90 to 95% and the solvent energy of regeneration ranged from 1000–1600 Btu/ lb CO₂ captured, which is in agreement with the TEA predicted MEA regeneration energy of 1340 BTU/lb CO₂ captured (Bhown, 2012).

A more detailed analysis was done to learn how the key process parameters listed in **Exhibit 6.1.1** affected the solvent regeneration energy. As shown in **Exhibit 6.1.4**, at the target 90% capture, increased L/G resulted in an increase in the energy of regeneration. Since the operating conditions were such that no fixed lean loading to the absorber was used, sensible heat input mainly contributed to the energy increase from the increased liquid circulation. In **Exhibits 6.1.5 and 6.1.6**, however, the trends changed for varying inlet CO₂ concentration and stripper pressure respectively as highlighted by the different directions of the arrows and circles. Good repeatability of the experiments is demonstrated by the narrow deviation as highlighted by the circles in **Exhibit 6.1.7** for the few repeat runs.

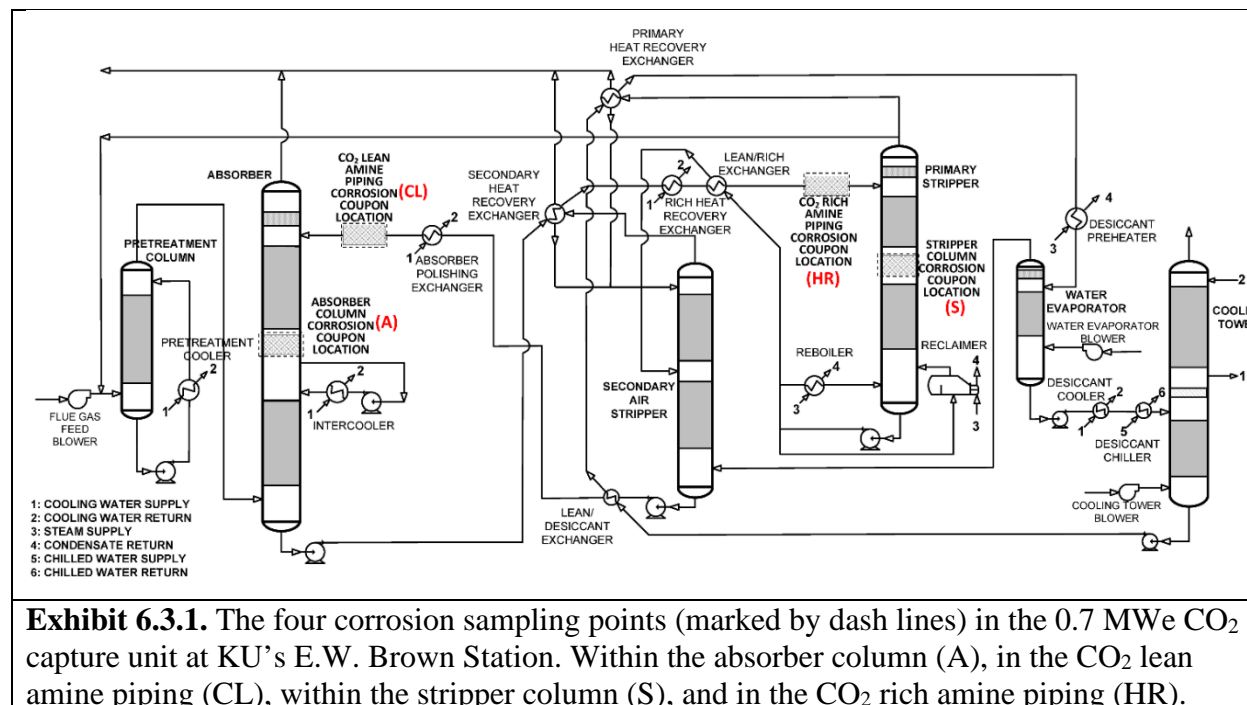


Summary

90% CO₂ capture was achieved at all MEA parametric conditions studied and during the long term campaign, and the solvent energy of regeneration ranged from 1000–1600 Btu/ lb CO₂. Overall, the experience gained with the progress of this first campaign with MEA was used to fine tune settings of operational parameters and how the process was run and controlled to ensure consistency in data acquired and establishing of trends in subsequent campaigns.

6.3 Corrosion

Exhibit 6.3.1 shows a generalized schematic of the process with the corrosion coupon sampling locations clearly shown.



Two corrosion sampling locations were chosen within the two primary process columns: the absorber (A) and the primary stripper (S); while two additional corrosion sampling locations were chosen within the process piping: the CO₂ lean amine stream (CL) after the polishing heat exchanger and just prior to entering the absorber, and the CO₂ rich amine stream (HR) after the crossover heat exchanger and just before entering the stripper. These four locations represented varied process conditions such as flow, temperature, and pressure, which were chosen to gain a more comprehensive understanding of the corrosion behavior in the CO₂ capture process. The stripper and hot rich amine piping were expected to have more corrosion issues, as the temperature and pressure are higher at these locations.

Corrosion Specimens

The specimen types included American Society for Testing and Materials (ASTM) A106 (grade B) carbon steel as a representative carbon steel material, Ni-coated A106 carbon steel, Ni₂Al₃/Al₂O₃-coated A106 carbon steel, and American Iron and Steel Institute (AISI) 304 stainless steel. The nominal chemical composition for carbon steel and stainless steel is listed in **Exhibit 6.3.2**. The purpose of this selection was to determine the viability of using commercially available carbon steel, and two UK CAER developed coatings on carbon steel in a deployed CO₂ capture process, while using stainless steel as a benchmark construction material.

Exhibit 6.3.2. Chemical composition of A106 carbon steel and 304 stainless steel (wt.%).										
Steel type	C	Cr	Ni	Cu	Mn	Mo	P	S	Si	Fe
A106 carbon	0.27	0.12	0.15	0.21	0.86	0.04	0.01	0.02	0.26	Bal.
304 stainless	0.05	18.22	8.04	0.52	1.74	0.30	0.03	0.001	0.30	Bal.

Specimens of all types were cut to rectangular cuboids with dimensions of 3.81 cm x 1.27 cm x 0.16 cm (3/2 in x 1/2 in x 1/16 in). A hole was drilled at one end of the specimen for hanging on a PTFE-covered sample rod on the corrosion rack with non-conductive spacers as shown in **Exhibit 6.3.3**. All of the exposed surface (including the surface of the hole) of the specimen was ground with SiC sand paper from 240, 400, to 600 grit, and then ultrasonically cleaned with deionized (DI) water and acetone.

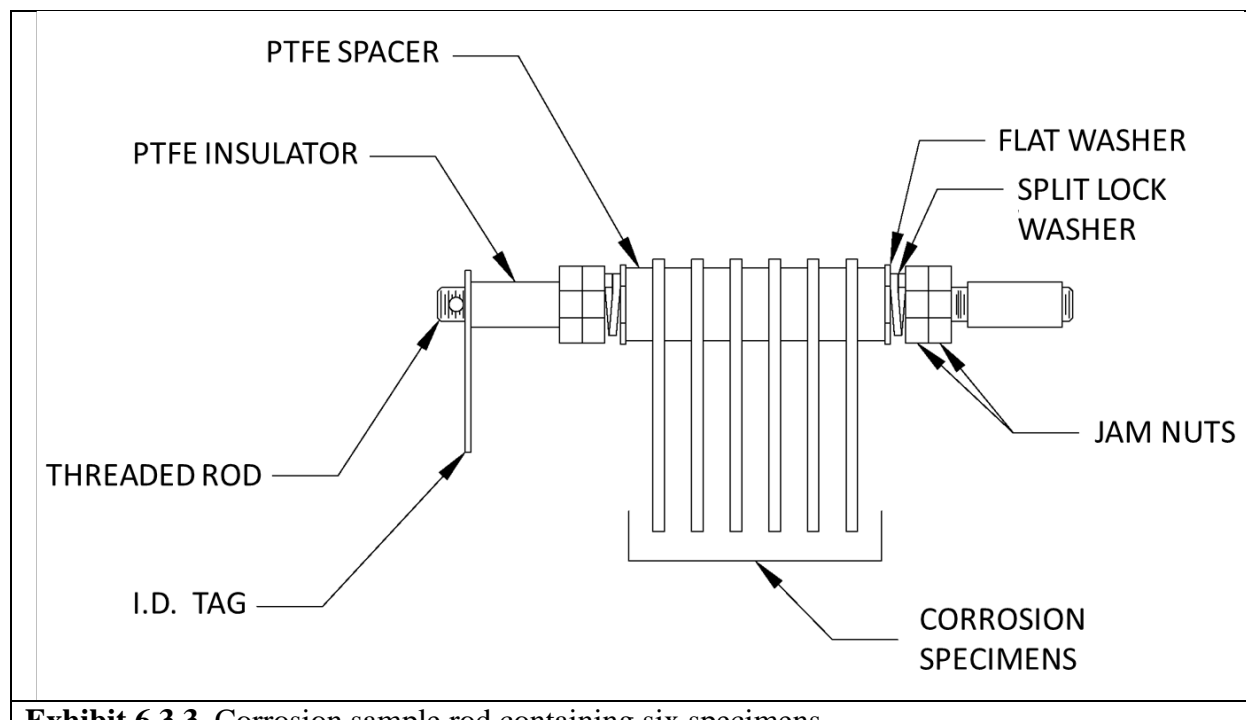


Exhibit 6.3.3. Corrosion sample rod containing six specimens.

After grinding, Ni plating and aluminizing were carried out for the Ni-coated A106 and Ni₂Al₃/Al₂O₃-coated A106 specimens. The Ni coating was electrodeposited by a galvanostatic

method from a conventional Ni-plating bath containing 150 g/L $\text{NiSO}_4 \cdot 6\text{H}_2\text{O}$, 35 g/L H_3BO_3 , 12 g/L NaCl , and 120 g/L $\text{C}_6\text{H}_5\text{Na}_3\text{O}_7 \cdot 2\text{H}_2\text{O}$. After all of the salts were dissolved in DI water, the electrolyte was kept at 80 °C for 2 h. Thereafter, the electrolyte was filtered before use. The current density was set to 2.5 A/dm²; the temperature was 35 °C; the stirring rate was 400 rpm; and the plating time duration chosen was 2.5 h. After plating, specimens were washed with DI water and acetone then stored in a desiccator.

To produce the $\text{Ni}_2\text{Al}_3/\text{Al}_2\text{O}_3$ -coated A106 samples, a mixture of powders consisting of 40 wt% Al (particles size: 74 µm) + 55 wt.% Al_2O_3 (particle size: 74 — 177 µm) + 5 wt% NH_4Cl was used as an aluminizing source. After weighing, all of the powders were put into a mortar and ground with a pestle for approximately 15 minutes. The above mentioned Ni-plated A106 corrosion specimens were placed into a small reactor cell and packed tightly with the prepared powder mixture. The specimens were separated by powder so that every specimen received enough aluminizing source. The reactor cell was then placed into a tube furnace and continuously purged with ultrahigh purity Ar gas at a flow rate of 300 ml/min. After 5 minutes, the furnace temperature was set to 615 °C with a heating rate of 5 °C/min. When the designated furnace temperature was reached, it was held steady for 5 h. After that, the furnace was allowed to cool to room temperature. After the temperature fell below 100 °C, Ar purging was stopped. When the furnace cooled to room temperature, the reactor cell was removed. The specimens were ultrasonically cleaned with DI water. Thereafter, the specimens were cleaned with boiling water for 20 minutes to remove contaminants and any loose particles from the aluminizing powders. The specimens were dried and subjected to a heat treatment at 900 °C for 2 h in air to promote the formation of a corrosion-resistant alumina layer. Finally, they were placed in a vacuum desiccator for storage until installation in the CO_2 capture process.

In total, 384 specimens were produced for this test, 96 specimens each of A106, Ni-coated A106, $\text{Ni}_2\text{Al}_3/\text{Al}_2\text{O}_3$ -coated A106 (denoted hereafter as Ni_2Al_3 -coated A106), and SS304. These specimens were then installed into the four sampling locations of the CO_2 capture process. For each location, 24 specimens of each material type, a total of 96 specimens, were placed in a corrosion rack using 16 corrosion sample rods, as shown in **Exhibit 6.3.3**. Each rod held six specimens, three of each material type.

During corrosion sampling event, two corrosion sample rods for a total of 12 corrosion specimens, three corrosion specimens of each material type, were removed from each location. The removed corrosion specimens were immediately cleaned with DI water and acetone, sequentially. After drying, the specimens were stored in a desiccator and transported to the laboratory for analysis. Two of the three corrosion specimens of each type were used for the corrosion rate calculations and the third specimen was used for surface analyses.

In the laboratory, all of the obtained specimens were cleaned with DI water and acetone again prior to further study. For the mass loss corrosion rate calculation, the carbon steel (with/without coatings) and stainless steel specimens were chemically cleaned for removal of the corrosion product according to the ASTM G1-90 standard. A 1000 mL solution containing 500 mL of hydrochloric acid (HCl, specific gravity 1.19) and 3.5 g of hexamethylene tetramine was used for the carbon steel specimens; while 1000 mL solution containing 100 mL nitric acid (HNO_3 , specific gravity 1.42) was used for the stainless steel specimens. Subsequently, the specimens were flushed

with DI water and weighed after drying with compressed air. The corrosion rate (CR , mm/yr) was calculated using the following equation:

$$CR = \frac{8.76 \times 10^6 \times (m_0 - m_1)}{S \times t \times \rho}$$

Equation 6.3.1.

where m_0 , m_1 , S , t , and ρ are the mass before corrosion (g), mass after removal of corrosion product (g), specimen surface area (mm^2), experiment duration (h), and density of the tested material (g/cm^3), respectively.

A Hitachi (Trade Name) S-4800 field emission SEM was used to characterize the surface morphology of the specimens. A voltage of 15 kV and a current of 15-20 mA were used for SEM characterizations. The chemical composition of the specimens was analyzed by X-ray diffraction (XRD) using a Rigaku (Trade Name) Smartlab 1 kW powder system equipped with a Cu target. The operation voltage and current were 40 kV and 44 mA, respectively. Scan ranges from 20 to 90° were used with a scan rate of 0.5 °/min.

Process Run Time vs. Total Exposure Time

Unlike stable laboratory environments, the pilot-scale CO_2 capture process in the present study was operated intermittently, with repetitive process startups and shutdowns due to the work shifts and operating schedules of the power station, which may result in a high corrosion rate due to thermal cycling. The specimens were exposed to the process environments for the entire experiment as a more representative study of actual commercial processes. To document the results, two time definitions, process run time and total exposure time, were used. Process run time is counted only when the CO_2 capture process was operating while total exposure time is counted from initial installation of the specimens into the process until sampling (removal), regardless of the process operating status.

Exhibit 6.3.4. Typical operating conditions in the pilot-scale CO_2 capture process.	
Process Parameter	Range
Flue gas inlet CO_2 (vol.%)	14 – 16
Flue gas inlet O_2 (vol.%)	6 – 12
Temperature at the absorber column corrosion sampling location (°C)	20 – 80
Temperature at the lean amine piping corrosion sampling location (°C)	10 – 50
Temperature at the rich amine piping corrosion sampling location (°C)	85 – 110
Temperature at the stripper column corrosion sampling location (°C)	85 – 130
Absolute pressure in the stripper (bara)	1.5 – 3.5
Liquid flow velocity at the lean amine piping corrosion sampling location (m/s)	0.3 – 0.6
Liquid flow velocity at the rich amine piping corrosion sampling location (m/s)	0.3 – 0.6
Absorber outlet CO_2 loading (mol CO_2 / mol amine, C/N)	0.37 – 0.65
Primary stripper outlet CO_2 loading (mol CO_2 / mol amine, C/N)	0.20 – 0.41

Note: The absorber column operates at atmospheric pressure.

Operating Conditions at the Pilot Plant

The operating conditions in the pilot plant were constantly monitored during the experiment. Due to frequent process shutdowns, a significant amount of transitional time was observed during the experiment, which significantly affected operating parameters, for example, temperature. The ranges of characteristic operating conditions for the individual process unit locations were identified. **Exhibit 6.3.4** shows typical operating conditions, in order to demonstrate how the conditions vary depending on the location within the process. The absorber column and the cold CO₂ lean amine piping had moderate operating conditions, while the conditions were much harsher within the stripper column and in the hot CO₂ rich amine piping with a significantly higher maximum temperature and pressure observed. Therefore, the latter two locations were more susceptible to internal corrosion problems. In addition, it is noted that the CO₂ loading at the absorber outlet was high (up to 0.65 mol CO₂/mol amine). This is likely because of the large absorber column height allowing for a long solvent residence time.

Corrosion Rates

Exhibit 6.3.5 shows the corrosion rates as measured by the mass loss method for all specimens in the four locations of the process (see **Exhibit 6.3.1**) after approximately 125, 250, 500, 750, 850, and 1000 hours of process run time. The performance of all materials was satisfactory in the CO₂ lean amine piping just prior to entering the absorber and within the absorber column itself with low corrosion rates observed. In fact, measurable corrosion was only noted for Ni-coated carbon steel in the CO₂ lean piping. On the contrary, significant corrosion of carbon steels, with and without coatings, was found in both the CO₂ rich amine piping just prior to entering the stripper as well as within the stripper column.

The bare carbon steel (A106) and Ni-coated carbon steel showed a similar pattern with substantial corrosion (> 5 mm/yr) in each of these locations. The results indicate that Ni-coated carbon steel shows no marked benefit over bare carbon steel in this process. Interestingly, it is also noted that Ni-coated carbon steel suffered more corrosion in the cold lean piping than in the absorber column. Recalling the fact that the operating temperature in the absorber at the corrosion sampling location was much higher than in the CO₂ lean amine piping prior to entering the absorber (**Exhibit 6.3.4**), this suggests that either the flow effect in the piping on corrosion was significant, or the temperature (lower in the CO₂ lean amine piping) played a role in the nickel dissolution process.

Regarding the Ni₂Al₃-coated carbon steel, the relatively low corrosion rates prior to 250 hours suggest that this coating was quite protective, initially. However, the corrosion rate eventually reached the same level as that of other carbon steels, which indicates that the protective Ni₂Al₃ coating (protective due to an Al₂O₃ surface layer) lost its integrity after 250 hours. It is noted that under the harsh conditions in the stripper, all A106 carbon steel-based specimens (A106, Ni-coated A106, Ni₂Al₃-coated A106) were lost after 500 hours, which highlights the need for proper materials of construction in the stripper. To provide a reference, corrosion rates for carbon steels in the stripper after 500 hours were calculated, assuming a final specimen mass of zero (denoted by dash lines in **Exhibit 6.3.5 (c)**). While carbon steels showed substantial corrosion in certain locations, stainless steel (SS304) was found to be stable and corrosion resistant in all of the sampling locations at all sampling events.

To compare the corrosion behavior of all materials, **Exhibit 6.3.6** and **Exhibit 6.3.7** show representative pictures of each specimen at all four sampling locations after approximately 500 and 1000 hours of process run time, respectively. Immediately apparent in **Exhibit 6.3.6** is the substantial loss of specimen thickness/mass for the A106, Ni-coated A106, and Ni₂Al₃-coated A106 carbon steel in the stripper column (S). In addition, substantive thickness loss is seen for all of these carbon steel-based specimens in the CO₂ rich amine piping prior to entering the stripper (HR) while they are stable for the absorber (A) and CO₂ lean amine piping prior to the absorber (CL) process locations. Similar corrosion behavior was observed for specimens after 1000 process run hours (shown in **Exhibit 6.3.7**). In fact, the corrosion rate of all carbon steels in the stripper was so high that specimens were lost at that time. The results suggest that these coatings on carbon steel eventually showed no corrosion benefit at these locations in the process.

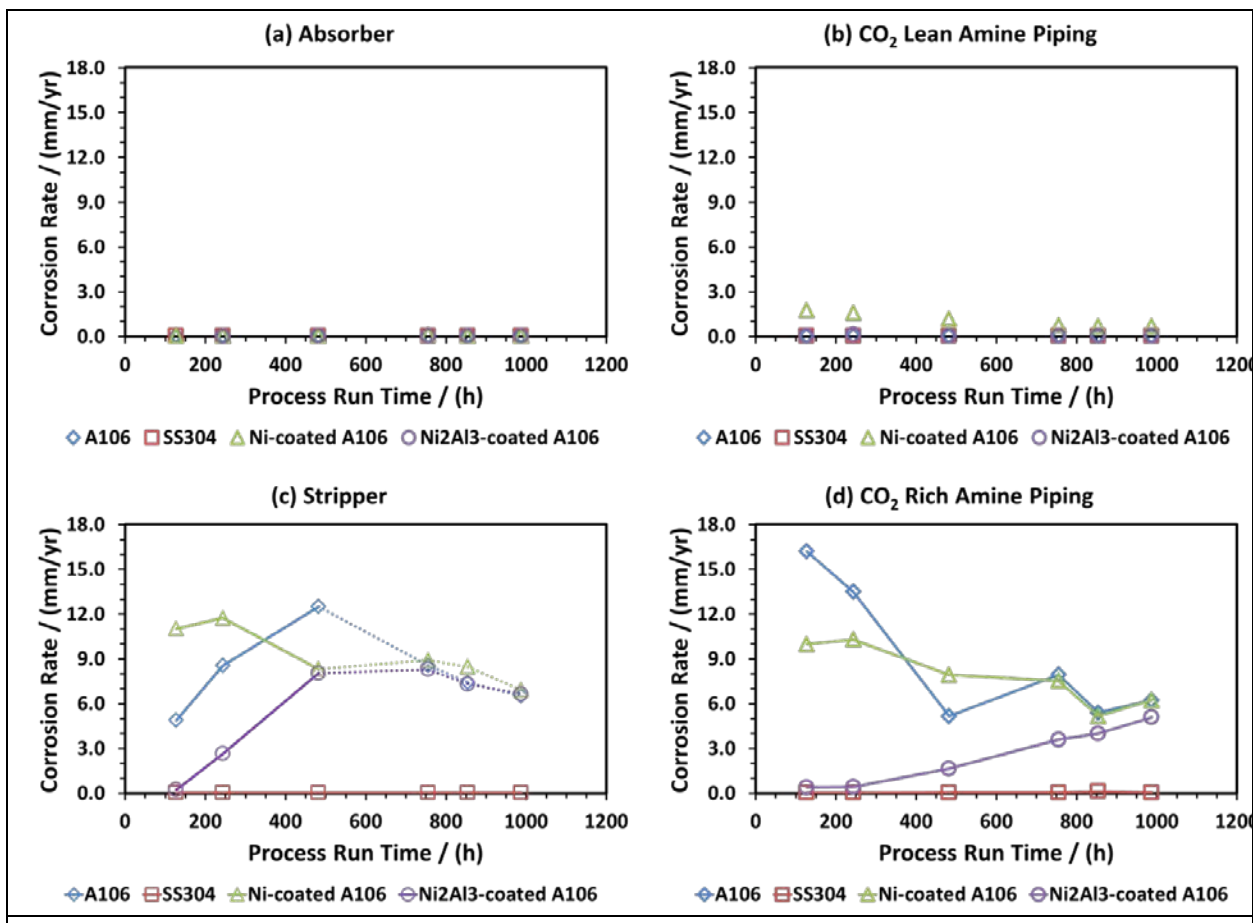


Exhibit 6.3.5. Mass loss corrosion rates in 30 wt.% monoethanolamine based on process run time for A106, Ni-coated A106, Ni₂Al₃-coated A106, and SS304 in the (a) absorber column, (b) CO₂ lean amine piping, (c) stripper column, and (d) CO₂ rich amine piping. For the stripper (c), corrosion rates for carbon steels after 500 process run hours are calculated values (dash lines), assuming a final specimen mass of zero.

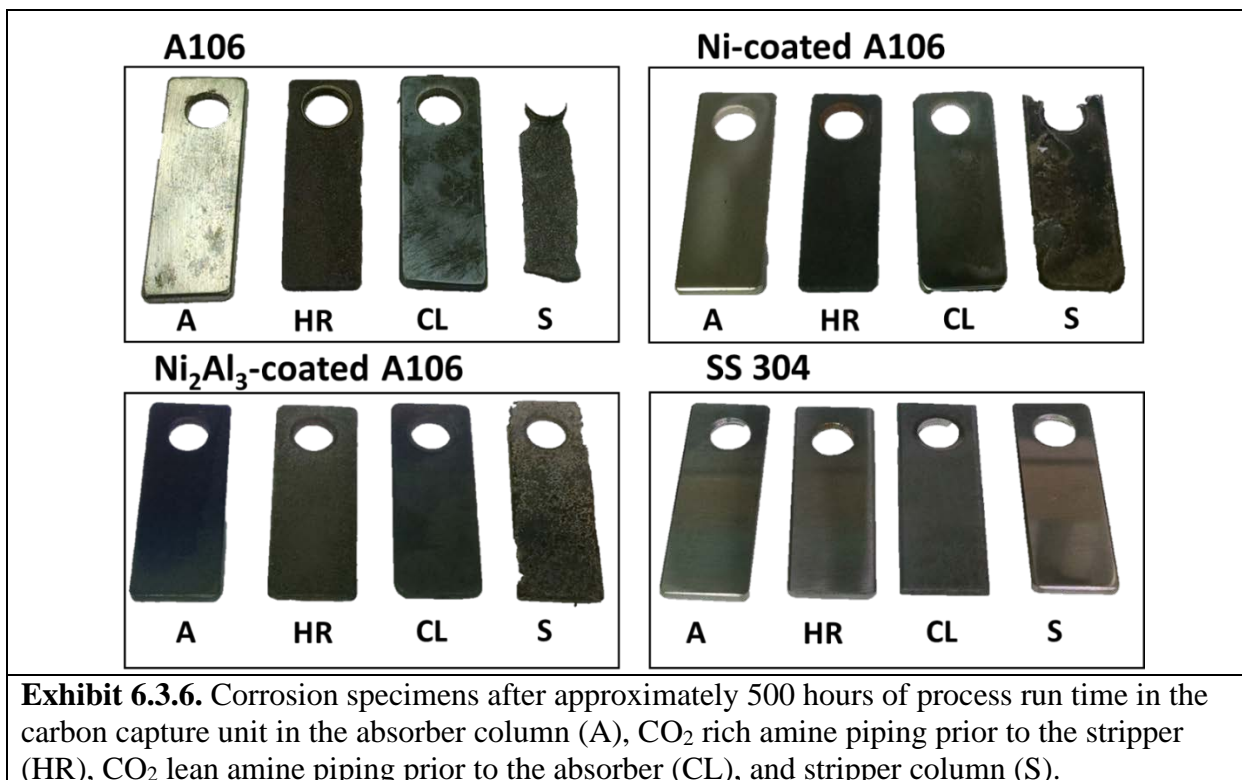


Exhibit 6.3.6. Corrosion specimens after approximately 500 hours of process run time in the carbon capture unit in the absorber column (A), CO₂ rich amine piping prior to the stripper (HR), CO₂ lean amine piping prior to the absorber (CL), and stripper column (S).

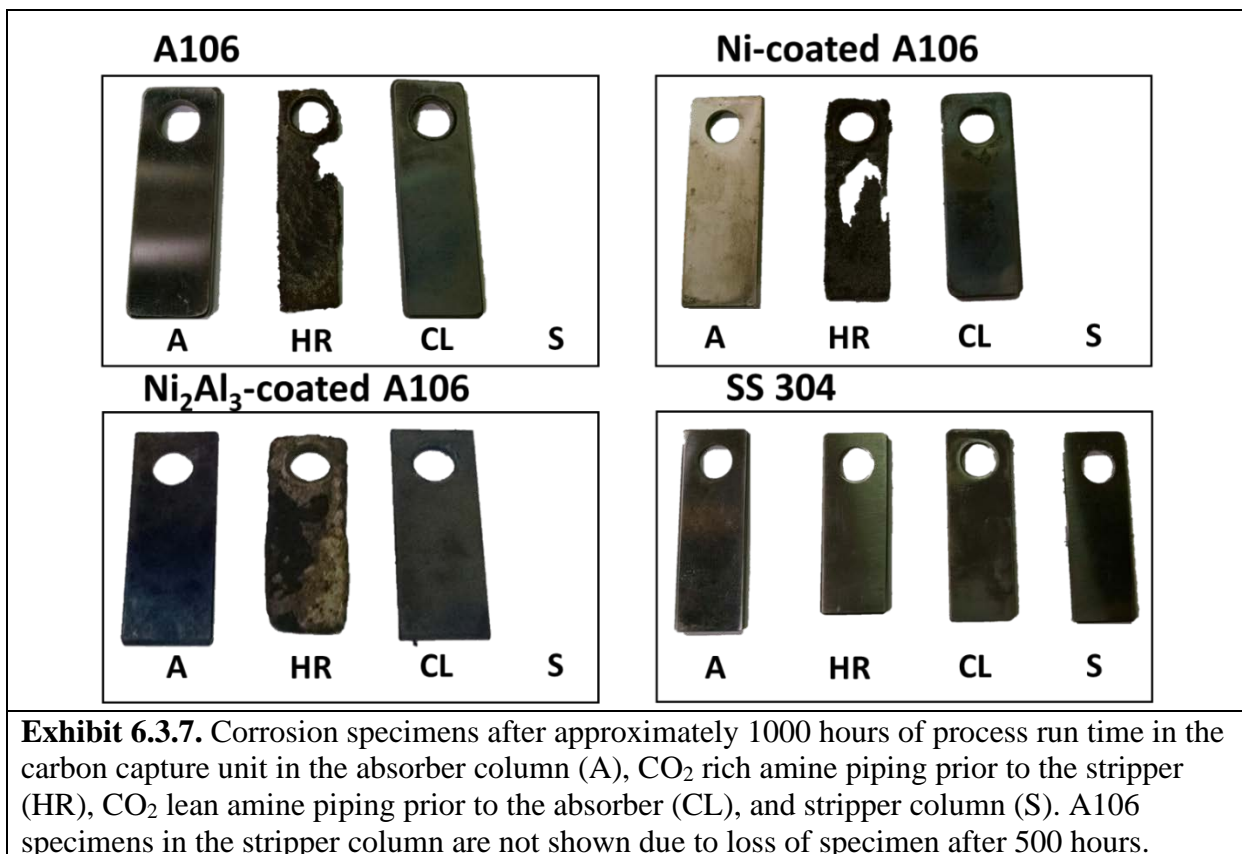


Exhibit 6.3.7. Corrosion specimens after approximately 1000 hours of process run time in the carbon capture unit in the absorber column (A), CO₂ rich amine piping prior to the stripper (HR), CO₂ lean amine piping prior to the absorber (CL), and stripper column (S). A106 specimens in the stripper column are not shown due to loss of specimen after 500 hours.

Surface Characterizations

In addition to examining the corrosion rate, surface analyses were carried out to determine the type of corrosion that occurred. The post-test surface morphology of all specimens was examined through SEM. **Exhibit 6.3.8** shows representative images of all types of materials from the stripper column after 500 hours of process run time, and substantial corrosion of carbon steel is observed. The bare carbon steel **Exhibit 6.3.8 (a)** showed a uniformly-corroded surface, while no appreciable corrosion was observed for stainless steel **Exhibit 6.3.8 (d)**. Local damage and removal of the top layers can be clearly seen for the Ni-coated and Ni₂Al₃-coated carbon steels (see **Exhibit 6.3.8 (b)** and **(c)**).

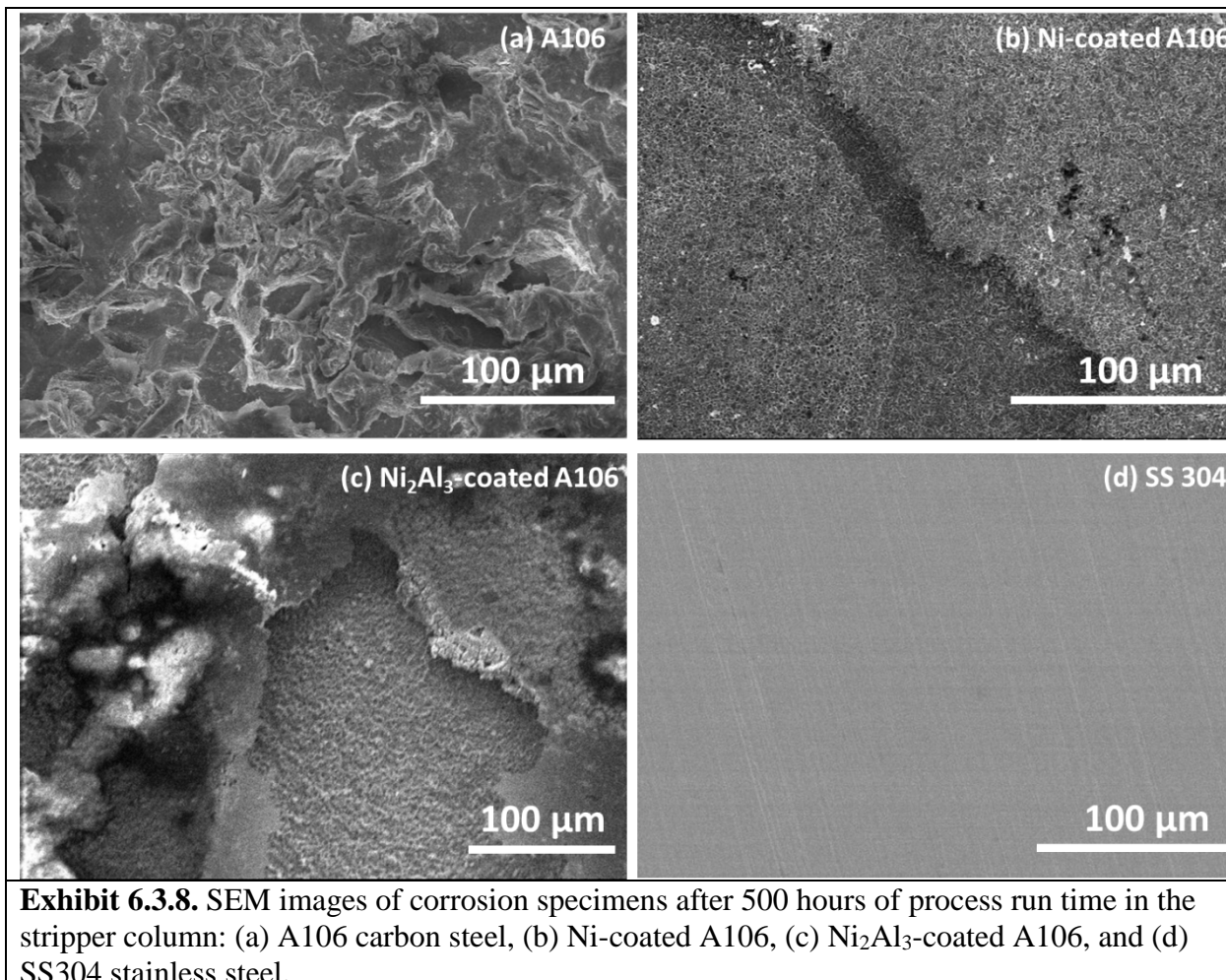
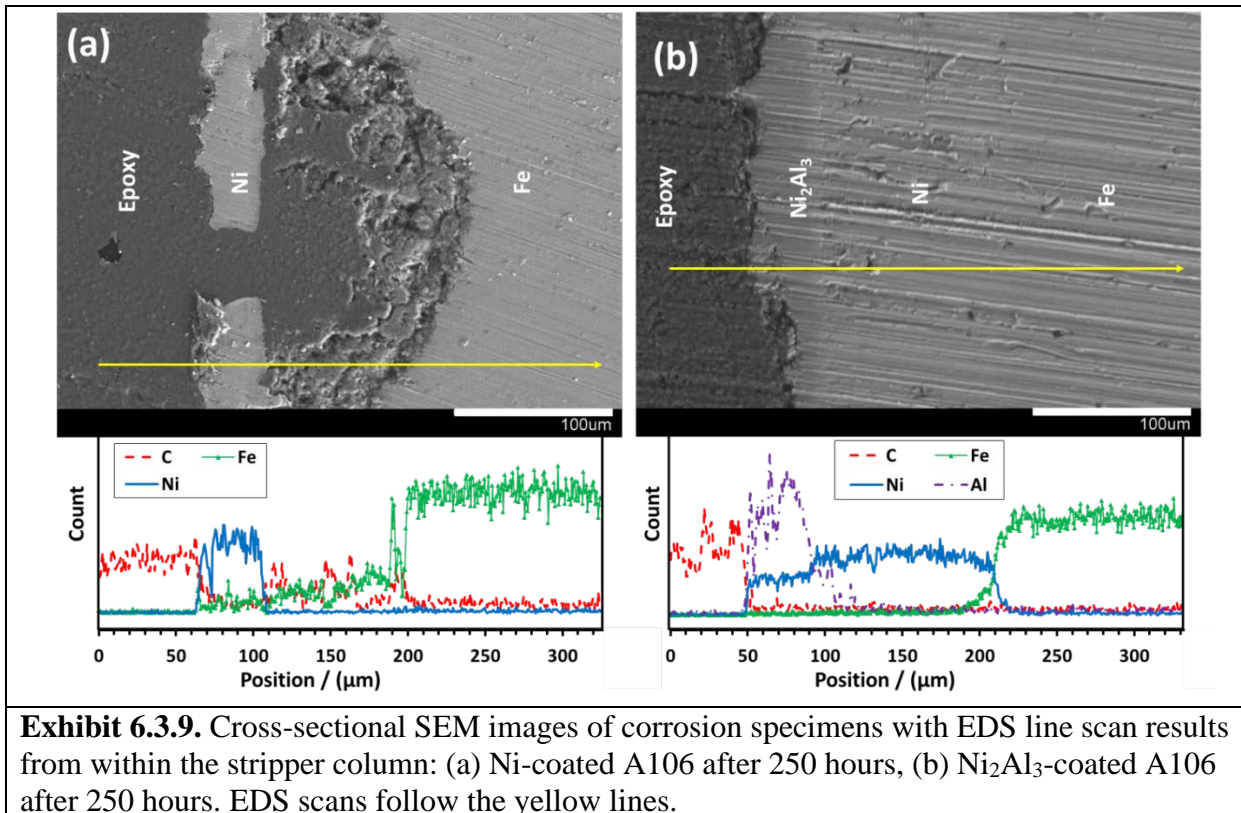


Exhibit 6.3.8. SEM images of corrosion specimens after 500 hours of process run time in the stripper column: (a) A106 carbon steel, (b) Ni-coated A106, (c) Ni₂Al₃-coated A106, and (d) SS304 stainless steel.

To confirm loss of these coatings, cross-sectional samples of the specimens were prepared, and analyzed by scanning electron microscopy (SEM)/energy dispersive X-ray spectroscopy (EDS). For example, the cross sections with EDS line scans of the Ni-coated and Ni₂Al₃-coated specimens in the stripper after 250 hours and 500 hours of process run time are shown in **Exhibit 6.3.9** and **Exhibit 6.3.10**, respectively. Both coatings suffered corrosion damage after 250 hours. Part of the Ni coating was lost, where severe localized corrosion of the underlying steel substrate occurred (see **Exhibit 6.3.9 (a)**). For Ni₂Al₃-coated carbon steel, although a continuous top Ni₂Al₃ layer

(~50 μm) was still visible, local thickness loss of this layer was observed (see **Exhibit 6.3.9 (b)**). This is consistent with the fact that a substantial corrosion rate



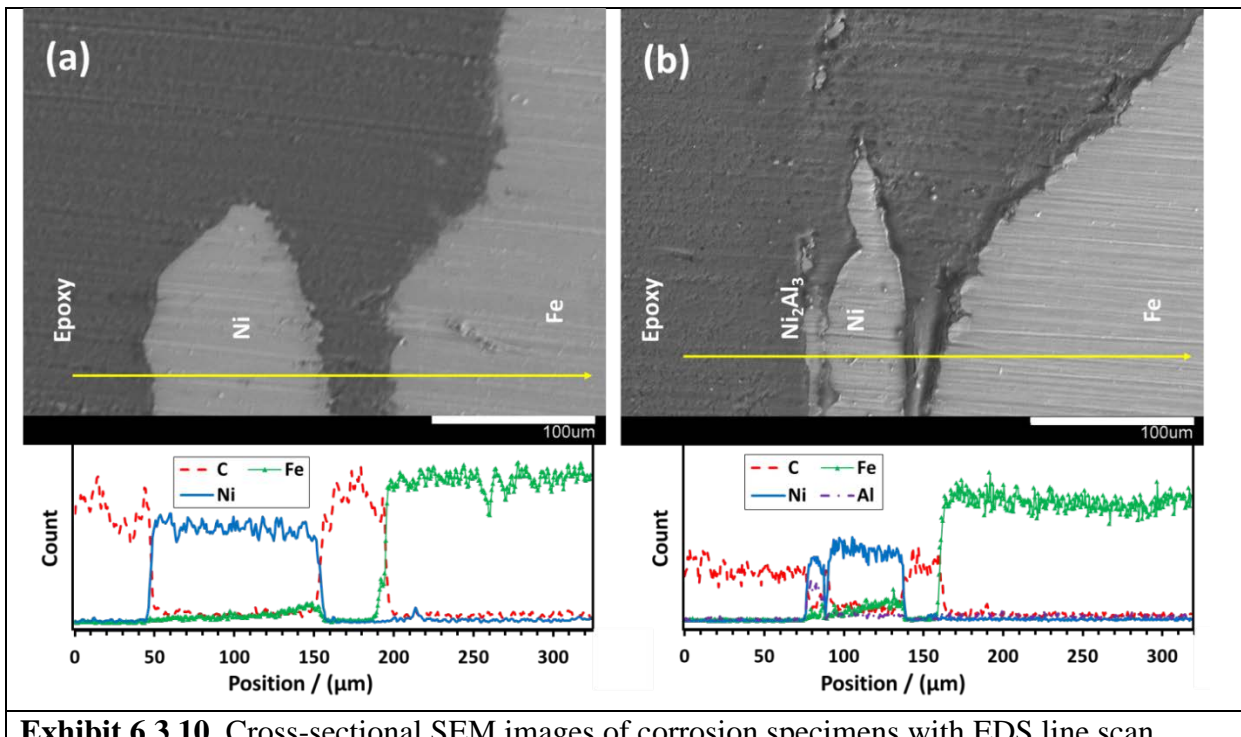


Exhibit 6.3.10. Cross-sectional SEM images of corrosion specimens with EDS line scan results from within the stripper column: (a) Ni-coated A106 after 500 hours, (b) Ni₂Al₃-coated A106 after 500 hours. EDS scans follow the yellow lines.

(~2.5 mm/yr) for Ni₂Al₃-coated carbon steel in the stripper after 250 hours was observed (**Exhibit 6.3.5 (c)**), which may be due to dissolution of the top protective Al₂O₃ thin layer and subsequent corrosion of the underlying Ni₂Al₃ coating and carbon steel. For both specimens after 500 process run hours, the coatings completely lost their integrity and a large surface area of the steel substrate was directly exposed to the corrosive environment, where severe local corrosion damage of the underlying iron substrate was seen (see **Exhibit 6.3.10 (a)** and **(b)**). The results demonstrated that neither of these coatings were stable or protective under the extreme conditions of this process, e.g., the stripper and CO₂ rich amine piping conditions. Moreover, local breakdown of these coatings resulted in severe corrosion damage of the underlying carbon steel substrate.

Through this corrosion study in 30 wt% MEA, the Ni₂Al₃ coating was found to provide short-term protection for certain highly corrosive aqueous environments (such as in contact with spray, as in the stripper column) in a post-combustion CO₂ capture process. The protection most likely is from the top alumina layer of the Ni₂Al₃ coating, and the lack of continuous formation of dense Al₂O₃ layers in the absence of effective oxygen content and favorable temperature limits the effectiveness of this coating. This is consistent with previous findings carried out in a laboratory environment. Once this thin layer (~ 2 μm) was depleted, more significant corrosion took place. Ultimately a very thick as-tested alumina coating would be needed to ensure equipment integrity. Seeking a more stable corrosion coating is therefore still a topic of interest. For example, thick nonmetallic coatings could be an economic option. Research efforts have also been put into promoting the formation of protective iron carbonate layers, a natural corrosion product of carbon steel in certain aqueous CO₂ environments. This could be another direction to pursue for corrosion mitigation.

Seeking stable corrosion inhibitors with less environmental impact is an alternative option. While these inhibitors may be consumed or degraded over time, they are more easily replenished than conventional coatings in process units of CO₂ capture operations. Their potential influence on solvent performance also will need to be considered.

6.4 Degradation

UK CAER tested its heat integrated post combustion CO₂ capture system with two-stage solvent regeneration system using 30 wt% MEA as a baseline solvent. The overall solvent degradation was comparable to the results of other published pilot studies using MEA under similar coal flue gas conditions and operating hours. Heat stable salts and polymeric amine formation showed a linear behavior over time which indicates that these compounds were not involved in competing secondary reactions in the time frame measured. Solvent oxidation in the form of heat stable salts and amine polymeric compounds were also comparable to published results showing that the impact of the secondary air stripper on solvent oxidative degradation appears to be negligible. Nitrosamine were not observed above the detection limits calculated during this MEA testing campaign.

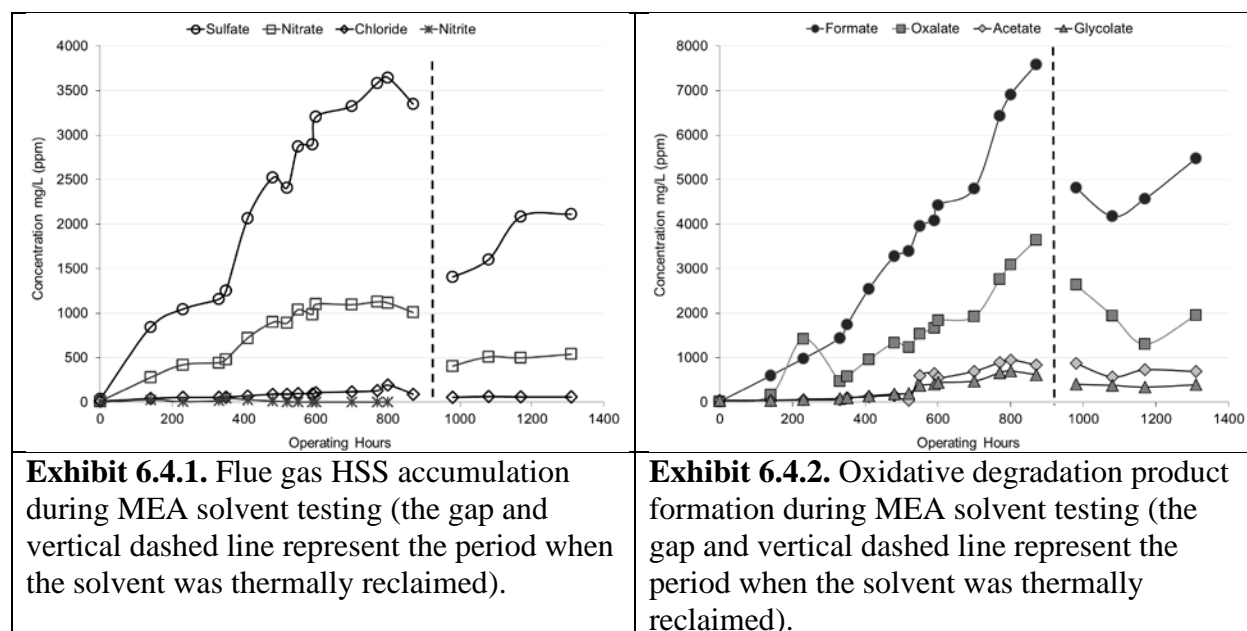
The solvent tested during the MEA campaign was (99%, Univar, Walbridge, OH) diluted and maintained near 5 mol/kg with service water, but without any anti-oxidation or anti-corrosion additives. Service water was provided by the plant and sourced from a nearby lake with minimal pretreatment. Operating hours refer only to periods when flue gas was contacting the solvent and steam was used for regeneration. For the first 880 operating hours, the solvent was not reclaimed. This was followed by a period of approximately 90 hours where the solvent was thermally reclaimed with soda ash caustic (as noted in the figures by a vertical dashed line). After this period, the solvent was neither cleaned nor purified through the end of the testing period (1316 total operating hours).

Degradation analysis was performed on MEA solvent samples collected after the absorber (CO₂ rich) in certified metal and inorganic analyte free HDPE bottles. Detection and quantitation of HSS and several MEA degradation products was performed with a Dionex ICS-3000 Ion Chromatography (IC) system. Solvent samples were analyzed to identify and quantify polymeric MEA degradation products with an Agilent 1260 Infinity High Performance Liquid Chromatography (HPLC) system coupled with an Agilent 6224 Time of Flight Mass Spectrometer (TOF-MS). Aldehydes were analyzed as 2,4-dinitrophenylhydrazine (2,4-DNPH) derivatives in a similar fashion to the methodology described in US Environmental Protection Agency (EPA) Method 8315A (1996). Nitrosamines were isolated and concentrated from the solvent using solid phase extraction (SPE) cartridges and analyzed using an Agilent Technologies 7890A GC with 7693 auto sampler and 5975C EI/MSD. Elemental concentrations in the solvent were examined after acidic microwave digestion using Inductively Coupled Plasma-Optical Emission Spectrometry (ICP-OES, Varian) and ICP Mass Spectrometry (ICP-MS, Agilent).

Results

Heat stable salts (HSS) formed in the solvent and produced from coal flue gas is primarily a function of the flue gas composition, including residual SO₂ and NO_x. The flue gas from KU's Brown Station was treated to NO_x and SO₂ before being supplied to the small pilot CCS. The accumulation of the flue gas derived HSS during this MEA testing campaign is presented in **Exhibit 6.4.1** as concentration in the solvent (ppm) against the tonnes of CO₂ captured.

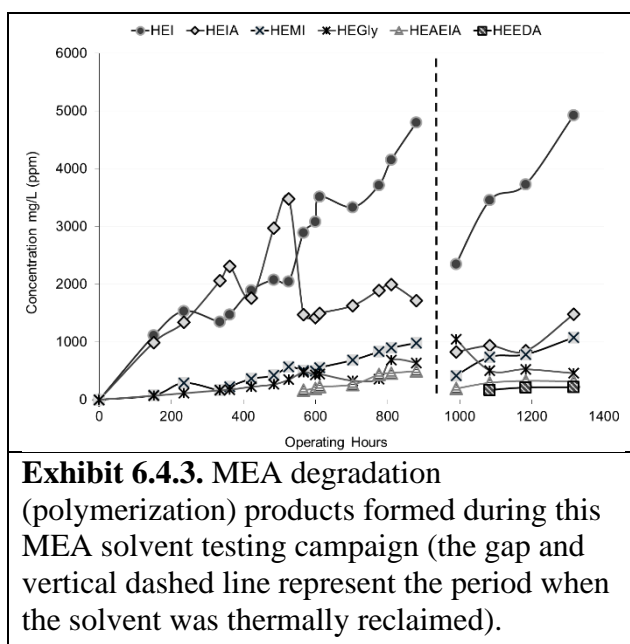
The flue gas SO₂ concentration entering the absorber was normally maintained below 5 ppm by polishing with soda ash in the pretreatment tower of the small pilot scale CCS. As expected and due to the high solubility of SO₂ in MEA, sulfate was the major HSS species observed. Even with the additional SO₂ polishing prior to the absorber, sulfate had a steady accumulation rate of 3.76 ppm/hr and reached a maximum of 3640 ppm prior to solvent reclaiming. Likewise, nitrate and chloride levels also showed steady accumulation rates of 1.13 ppm/hr and 0.09 ppm/hr, respectively, prior to solvent reclaiming. Nitrate reached a maximum of 1115 ppm, while chloride reached a maximum concentration of 193 ppm during the same period. After reclaiming and through the end of the testing campaign, the chloride concentration remained unchanged, while the sulfate and nitrate returned to similar yet slightly lower accumulation rates. Nitrite levels in the solvent were low with an average value of 8 ppm during the initial part of the testing campaign. The nitrite stayed below 5 ppm after 500 operating hours (250 tonnes of CO₂ captured) and was not observed above the detection limit (0.1 ppm) after reclaiming through the end of the testing campaign. Fluoride never exceeded 5 ppm during the entire testing period.

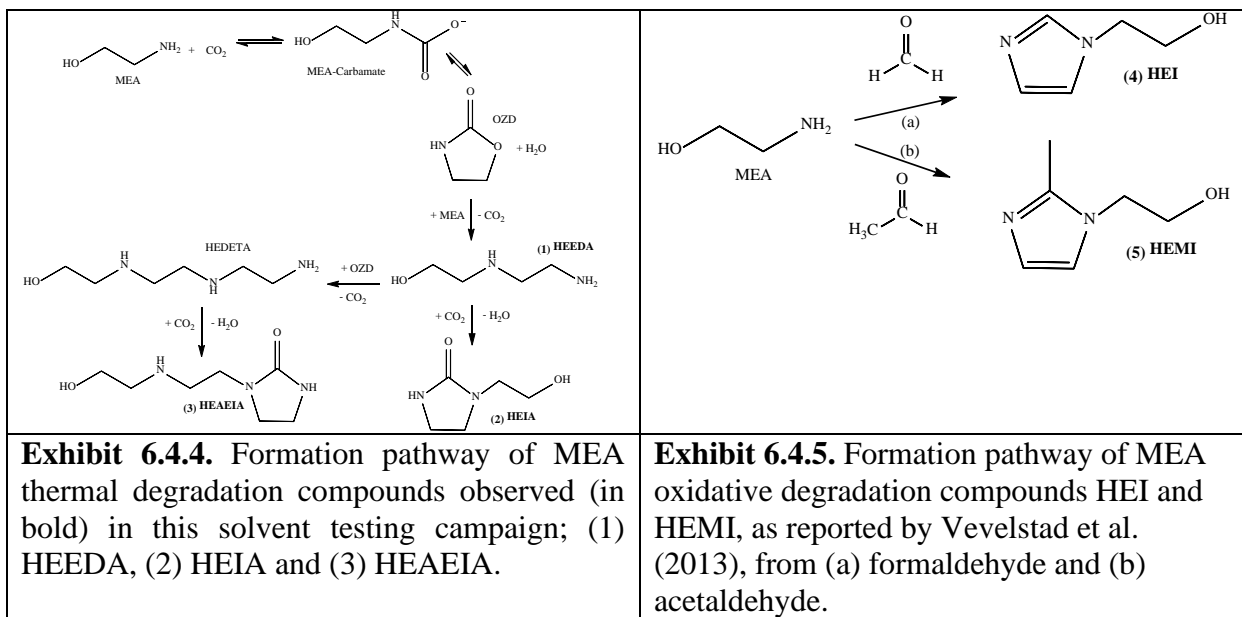


The impact of using a secondary air stripper to further reduce the CO₂ loading in the amine solvent has yet to be fully examined as it relates to amine oxidation. First, the formation of oxidative HSS species from MEA were examined and are shown in **Exhibit 6.4.2**. The major oxidative HSS observed was formate, which was expected and is commonly used as an indication of overall MEA oxidative degradation (Chandan et al., 2014). Formate reached a maximum of 7583 ppm prior to

reclaiming, followed by oxalate at 3643 ppm, acetate at 884 ppm, and finally glycolate at 619 ppm. The oxidative HSS totaled approximately 1.16 wt% prior to solvent reclaiming (at 880 operating hours and 436 tonnes of CO₂ captured). This total is equivalent to a loss of 4.2% of the MEA from the initial solvent charge during this period. The level of amine oxidation in the form of HSS seen in this testing campaign, with the addition of the secondary air stripper, is consistent with other reported MEA solvent campaigns (without anti-oxidation inhibitors).

In addition to yielding HSS, amines can degrade as the result of oxidation and/or thermal decomposition and produce polymeric type compounds. The accumulation rates of the five major polymeric amine degradation compounds identified by TOF-MS are presented in **Exhibit 6.4.3**. The main degradation product identified in this MEA solvent testing campaign was HEI. This compound is a very important molecular marker for oxidative degradation of MEA during pilot testing campaigns (Vevelstad et al., 2013; Reynolds et al., 2015). Previous reports have also shown that the concentration of metals in the solvent can be directly related to increased HEI production through MEA oxidation (Leonard et al., 2014; Chandan et al., 2014).





The second most abundant degradation compound was HEIA, a commonly observed thermal degradation product (Huang et al., 2014). HEMI, HEGly, HEAEIA and HEEDA were also observed in the solvent, although at relatively lower concentrations and at later stages in the testing campaign. The likely pathway for the formation of the three thermal degradation compounds identified in this MEA campaign is shown in **Exhibit 6.4.4**. OZD is usually considered an intermediate in MEA thermal degradation reactions and stays at relatively low concentrations in the solvent, as it tends to be consumed by additional degradation reactions (da Silva et al., 2012). In this study, OZD was not identified above its detection limit of 1 ppm. Another intermediate thermal degradation compound is HEDETA. This compound was also not identified in the solvent above its detection limit of 1 ppm, but was likely formed as it can react with CO₂ and undergo an intramolecular cyclization to form HEAEIA, which was observed in the solvent. The secondary reaction to form HEAEIA may be energetically favored and explain why HEDETA was not observed in the solvent at significant quantities, while HEAEIA accumulated over time. The degradation pathway of the final two main MEA degradation compounds, HEI and HEMI, is presented in **Exhibit 6.4.5**. Both of these degradation compounds have been reported as a product of oxidative degradation and are formed in the presence of an aldehyde, either formaldehyde (HEI) or acetaldehyde (HEMI) (Velvested et al., 2013). Formaldehyde and acetaldehyde have both been reported as MEA oxidative degradation products (Sexton and Rochelle, 2011; da Silva et al. 2012), but their presence in pilot solvent samples has not been routinely reported due to the analytical challenges associated with isolating and analyzing these compounds.

Exhibit 6.4.6. Aldehydes observed in 30% MEA solvent during pilot testing campaign.	
Analyte	Concentration Range (ppm)
Formaldehyde	24.4 – 35.4
Acetaldehyde	< 15.2 ^a - 31.9
Propionaldehyde	< 18.9 ^a

^a Calculated quantitation limits (LOQ)

In this study, the MEA solvent was also analyzed to determine the formaldehyde and acetaldehyde concentrations in the solvent (**Exhibit 6.4.6**) by converting these compounds into their 2,4-DNPH derivative. Formaldehyde and acetaldehyde were both identified in the solvent and were maintained at a fairly constant concentration levels throughout the testing campaign. This suggests that aldehydes were forming from MEA oxidation, but were either partitioning into the gas phase and being emitted from the system in the scrubbed flue gas, or were undergoing secondary reactions and generating additional degradation products, such as HEI and HEMI.

Metals can accumulate in process solvents from coal-combustion flue gas and by corrosion of structural components (Nikolic et al., 2015). Although these elements typically accumulate at relatively low levels compared to amine degradation compounds or acidic flue gas contaminants, they can catalyze and accelerate amine degradation reactions (Moser et al., 2011; Chandan et al., 2014; Huang et al., 2014). Metal accumulation in the solvent, if high enough, could also impact the cost of treating or disposing of spent solvent by exceeding hazardous waste characterization limits. The metal accumulation from coal combustion and corrosion during this MEA solvent testing campaign is presented in **Exhibit 6.4.7**, and plotted as concentration versus tons of CO₂ captured. Eight of the ten elements monitored, the Resource Conservation and Recovery Act (RCRA)-8 (Cr, As, Se, Ba, Pb, Ag, Cd) minus mercury (RCRA 1976) and Fe, Ni, and Cr from steel corrosion (Carter, 2012) were detected in the MEA solvent. Ag and Cd were not found above their detection limits of 625 ppb and 12.5 ppb, respectively. As noted by the vertical gray line, ICP-OES was used to analyze the initial samples. After observing a large variability in the results from ICP-OES analysis, and specifically a large variability in the Se values that appeared to move up and down around its RCRA limit of 1 ppm, it was decided to switch and use ICP-MS to analyze the remaining samples. Se has been recognized as an element of concern from previous coal combustion pilot testing campaigns (Carter, 2012) and therefore getting an accurate concentration of this metal in the solvent was critical. After switching to ICP-MS analysis the levels for Se, and all the other elements analyzed, showed much lower variability between samples.

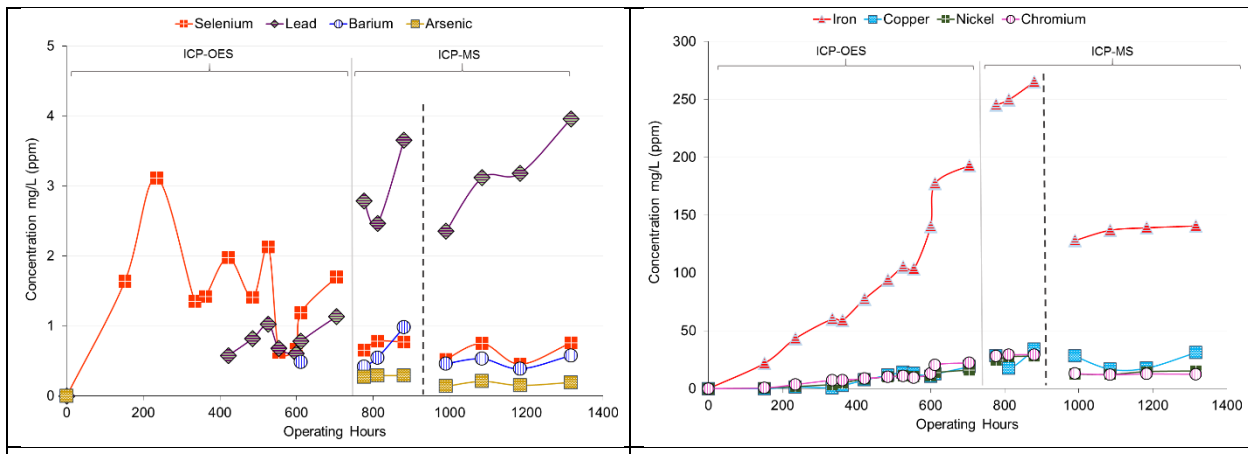


Exhibit 6.4.9. Corroding amine strainer fabricated materials not specified for amine service that was removed after the conclusion of the MEA solvent testing campaign.

Arsenic was first observed in the solvent after switching to ICP-MS and remained relatively stable below 0.3 ppm. Pb reached a maximum of 3.65 ppm, but was below the RCRA hazardous waste allowable limit of 5 ppm. Likewise, the Ba concentration reached 0.98 ppm and stayed well below the RCRA hazardous waste level of 100 ppm. Both Se and As levels remained below the RCRA allowable levels of 5 ppm and 1 ppm for RCRA hazardous waste classification, with final concentrations of 0.77 ppm and 0.29 ppm, respectively. Only Se and Pb reached above one ppm before the solvent was thermally reclaimed. After reclaiming (dashed line), Ba, As and Se concentrations remained stable below 1 ppm, with only Pb showing a notable increase through the end of the campaign.

Metal accumulation from corrosion during the MEA testing campaign is shown in **Exhibit 6.4.8**, with ICP-OES used to analyze samples at the beginning of the campaign before switching to ICP-MS (denoted by the vertical gray line). Fe was overwhelmingly the most abundant metal reaching a maximum of 265 ppm. Cr also rose during the initial period (start-up through reclaiming) to a maximum just below 30 ppm, while Ni reached 28 ppm during the same time period. Elevated corrosion metal concentrations have been observed when MEA is used to commission a newly constructed pilot system (Wheeldon, 2013), similar to the results presented in this study where MEA was also used to commission the newly constructed pilot CO₂ capture system.

The most surprising element observed in the solvent was Cu, reaching a maximum of 33 ppm just prior to reclaiming. Cu, along with Fe, are reported to significantly accelerate amine oxidative degradation (Goff and Rochelle, 2004; Goff and Rochelle, 2006; Sexton and Rochelle, 2011), especially at elevated temperatures such as those found in the stripper/reboiler (Voice and Rochelle, 2013). After the conclusion of this MEA testing campaign, a component in the amine loop was leaking as the result of excessive corrosion. Upon inspection, it was determined that the component was fabricated with materials not specified for amine service, including brass, and is likely, at least in part, the source of the high Fe and Cu in the solvent (**Exhibit 6.4.9**). Thermal reclaiming of the solvent was shown to be effective at the Fe concentration (-52%), but was slightly less effective at reducing the Pb (-36%) and Cu (-17%) concentrations in the solvent. Additional reclaiming in future campaigns may be warranted to limit additional amine oxidative degradation.

Published research into the role of Cu in amine oxidation, while limited because components containing Cu such as brass are usually avoided in the construction of amine CO₂ capture systems, show that Cu can be a very strong amine oxidizer (Goff and Rochelle, 2004; Goff and Rochelle, 2006; Sexton and Rochelle, 2011). The possibility does exist, as shown here, that some brass and/or copper components could be mistakenly used somewhere in the amine loop in newly constructed or retrofitted CO₂ capture systems. Due to this finding, it is recommended that all future amine CO₂ capture systems actively monitor Cu levels in the solvent, regardless of the material(s) specified for construction, to avoid excessive amine oxidation and unplanned solvent losses as a result of Cu induced amine oxidation.

Amines, specifically secondary amines, can react with NO_x to form a class of stable degradation products known as nitrosamines (Chandan et al., 2014). Nitrosamines are a class of carcinogenic compounds previously associated with cigarette smoke, cooked meat and vehicle emissions (Farren et al., 2015), but more recently as a disinfectant byproduct formed during chlorination of wastewater (Venkatsen et al., 2015). The first report of nitrosamines in amine-based carbon

capture was from Strazisar and coworkers (2003), where a total nitrosamine concentration of 2.91 $\mu\text{mol}/\text{mL}$ was identified in a lean MEA solvent. Since then, many other research groups have identified nitrosamines both in amine solvents and water-wash systems. Nitrosamines were isolated from the concentrated MEA solvent in this testing campaign using solid phase extraction and analyzed by mass spectrometry. A total of 7 samples collected throughout the testing campaign were analyzed for twelve distinct nitrosamines; eight were available commercially for direct comparison, and four that could potentially be generated from MEA degradation (secondary amines). In all the MEA solvent samples examined, no nitrosamines were identified above the calculated limits of quantitation (LOQ).

MEA degradation products, especially secondary amines, also have the potential to form nitrosamines. With this in mind, the MEA solvent samples were also screened for additional nitrosamines that could arise from MEA degradation compounds observed during the MEA testing campaign. Again, after an in-depth investigation none of the MEA degradation nitrosamines were positively detected in any of the MEA solvent samples analyzed.

Conclusions

The overall solvent degradation was comparable to the results of other published pilot studies using MEA under similar coal flue gas conditions and operating hours. Heat stable salts and polymeric amine formation showed a linear behavior over time which indicates that these compounds were not involved in competing secondary reactions in the time frame measured. Solvent oxidation in the form of heat stable salts and amine polymeric compounds were also comparable to published results showing that the impact of the secondary air stripper on solvent oxidative degradation appears to be negligible.

6.5 Emissions

UK CAER successfully tested its innovative two-stage solvent regeneration system using MEA as a baseline solvent. The overall solvent emissions were comparable to the results of other published pilot studies using MEA. The magnitude of the MEA emissions is greater than can be explained as vapor emissions, so it is probable that much of the MEA emissions are the result of aerosols. Solvent oxidation in the form of ammonia and aldehyde emissions levels were also comparable to published results showing that the impact of the secondary air stripper on solvent oxidative degradation appears to be negligible. The ammonia emissions were strongly correlated with the accumulated concentrations of dissolved iron and copper in the solvent. Nitrosamine emissions were not observed above the low ppbV detection limits calculated during this MEA testing campaign.

Amine emissions in treated flue gas consist of volatile losses, aerosol losses and entrainment losses. Volatile amine emission should vary with the vapor pressure of amine over the solvent at the top of the absorber. Volatile losses can be managed by appropriate water wash design and operating conditions. Aerosol losses occur from small droplets of solvent (<3 microns) that grow in the absorber and water wash from nuclei such as sulfuric acid (SO_3) and submicron fly ash (Fulk, 2014; Khakharia, 2015). These aerosol are often too small to be collected by packing or mist eliminators, but can constitute a large fraction of total amine emissions. Entrainment losses

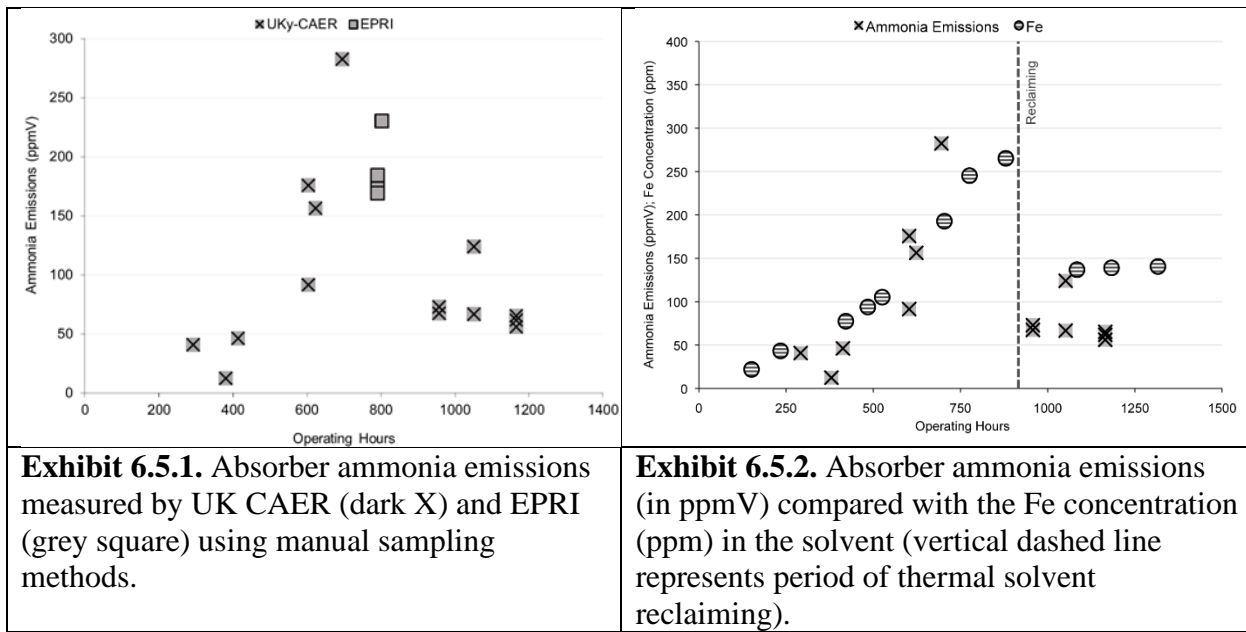
are 1 - 10 micron drops created by fluid mechanics, usually near the top of the contactor, but can be minimized by proper design of the packing and mist eliminators. Aerosol losses are expected to dominate in the absorber, while volatile losses will probably dominate at locations with no aerosol nuclei. Entrainment losses are usually negligible in pilot plant units.

Manual gas sampling ports were located at the absorber exit and the secondary air stripper exit. Samples at the absorber exit were withdrawn through a 3" port using a sampling probe connected to an impinger train. Extractive samples were collected from the secondary stripper exit through a 3/8" port. Gas phase degradation products and MEA emissions were collected using sampling methodology adapted from U.S. EPA Methods 1 and 5, and individual methods including EPA SW-846 Test Method 0011 for aldehydes, and CTM-027 for ammonia. Nitrosamine emission samples were collected with an impinger train containing a dilute sulfamic acid solution (Fraboulet et al., 2016).

Emission sampling was conducted by EPRI and its subcontractor CB&I Environmental and Infrastructure, Inc. (Cincinnati, OH) as third-party verification (QA/QC data check) for a period of one week during the MEA testing campaign (around 790 - 810 operating hours). The procedures outlined in EPA CTM-027 were used to collect samples for ammonia and MEA. Aldehyde and ketone compounds were collected and analyzed using the procedures found in EPA SW 846 Method 0011. The emission data collected by EPRI was used to validate the methodology and emission values obtained separately by UK CAER during a similar testing period.

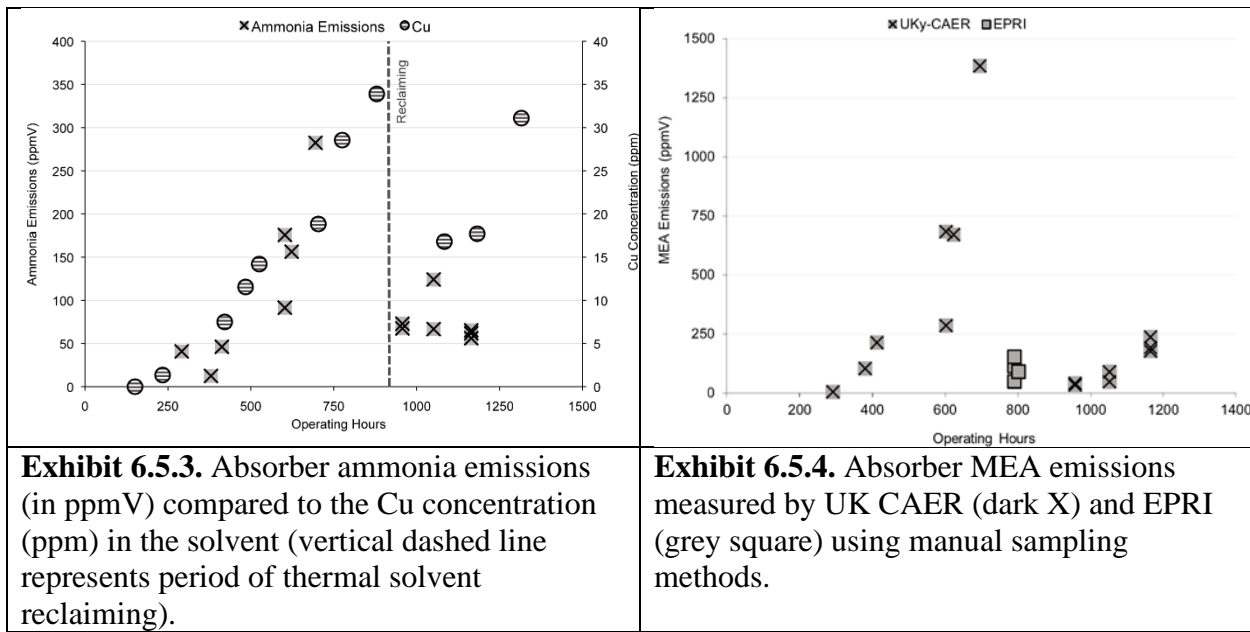
Results

Emission samples were collected in this study during a variety of operation conditions including; (1) unit start-up and commissioning when individual systems were pushed to their design limits, (2) parametric testing conditions where major operating changes were intentionally imposed on the capture system, and (3) daily operating changes during long-term testing when changes were related to power plant load following, local weather conditions, and miscellaneous system testing.



Ammonia emissions from the absorber exit collected by all three sampling teams are presented in **Exhibit 6.5.1** in ppmV units. The observed ammonia emissions values covered a very large range from 12.4 – 282 ppmV (0.046 – 1.123 lbs/hr) over the course of the testing campaign. The samples collected by EPRI during the middle of the MEA testing are very similar to the samples collected by UK CAER during the same time period when system operating parameters were generally similar. The set of results obtained by EPRI serves as a third-party validation of the methodology and data obtained by UK CAER. The ammonia emissions show a clear increase during the first half of the testing campaign. During this time the MEA solvent was not cleaned or reclaimed and started to accumulate several different heavy metal elements from the coal combustion flue gas. Likewise, the solvent also started to degrade through oxidative and thermal degradation routes forming heat stable salts and polymeric MEA compounds.

The impact of dissolved metals, specifically iron and copper, on MEA oxidative degradation has been previously reported. (Goff and Rochelle, 2004; Goff and Rochelle, 2006; Sexton and Rochelle, 2011; Leonard et al., 2014). Fe and Cu in an MEA solvent have been shown to directly increase NH_3 production (Voice and Rochelle, 2013). The ammonia emission levels (in ppmV) versus the Fe concentration in the MEA solvent (in ppm) is shown in **Exhibit 6.5.2**. A clear positive correlation (0.92) between these two parameters can be seen, especially during the first half of the testing campaign before the solvent was reclaimed and the Fe concentration was reduced. This trend is similar to those reported by Mertens (2013) and Khakharia (2015) where ammonia emissions increased along with Fe accumulation in the solvent. After the solvent was reclaimed (as noted by the dashed vertical line) both the Fe concentration and ammonia emission levels remained relatively constant.



A strong positive correlation (0.91) between ammonia emissions and Cu can also be observed in **Exhibit 6.5.3**. The trend of increasing ammonia as the Cu content increases is again very clear during the first 890 hours of operation when the solvent was not cleaned or reclaimed. The exact role of Fe and/or Cu in the ammonia emissions observed from this test cannot be clearly defined as both are present in significant quantities. Thermal reclaiming (as noted by the dashed vertical line) was shown to be effective at reducing both the Fe and Cu content in the solvent by approximately 50%. The drop in metal concentration in the solvent corresponds to a drop in the ammonia emission levels. Additional reclaiming to further reduce the Fe and Cu concentrations in the solvent may further reduce ammonia emissions.

The high Fe levels seen in this MEA solvent testing campaign can likely be traced back to several different factors. Elevated Fe levels have been observed when MEA is used to commission a newly constructed pilot system (Wheeldon, 2013). Additionally, after the conclusion of this MEA testing campaign, a component in the amine loop was found to have excessive corrosion. Upon further inspection it was determined that the component was fabricated with improper materials, including brass, and is likely, at least in part, the source of the high Fe in the solvent. This corroding component was positively identified as the source of Cu in the solvent. Little research has been published investigating the role Cu plays in amine oxidation because components containing Cu, such as brass, are usually avoided in the construction of amine CO₂ capture systems. However, the possibility does exist that some brass or copper components could be mistakenly used somewhere in the amine loop suggesting that active monitoring of Cu in amine systems may be warranted, regardless of the material(s) used for construction, to avoid excessive amine oxidation and unplanned solvent losses.

MEA emissions from the absorber exit are presented in **Exhibit 6.5.4**. MEA emissions ranged greatly from 4.9-1384.6 ppmV (0.065-18.657 lbs/hr) over the course of the entire testing campaign (1316 total operating hours). MEA emissions were highest during parametric testing periods where operating parameters, including temperatures and flow rates, were increased to see their impact on

performance and energy consumption, not necessarily to lower emissions. As such, it was expected that some parametric conditions would lead to high emission levels. The samples collected by EPRI during the middle of the testing campaign are very similar (within 30%) to the samples collected by UK CAER during the second half of the testing campaign. The set of results obtained by EPRI serves as a third-party validation of the methodology and data obtained by UK CAER.

Exhibit 6.5.5. Aldehyde and ketone emissions measured during pilot MEA testing.				
	UK CAER emissions range		EPRI emissions range	
Analyte	lb/hr	ppbV	lb/hr	ppbV
Formaldehyde	2.31 - 4.78 x10 ⁻⁴	35 - 73	2.3 - 3.6 x 10 ⁻⁴	41 - 60
Acetaldehyde	5.78 - 5.82 x10 ⁻³	602 - 606	1.6 - 2.1 x 10 ⁻³	186 - 238
Propionaldehyde	< 2.8 x 10 ⁻⁴	< 217	< 2.6 x10 ⁻⁶	< 2.2
Acetone	1.19 - 1.22 x10 ⁻³	94 - 96		
Acetophenone			< 1.7 x10 ⁻⁶	< 0.068
Isophorone			3.2 - 8.4 x10 ⁻⁵	1.3 - 3.2
Total	7.2 x10 ⁻³ - 7.5 x10 ⁻³	731 - 775	1.8 x10 ⁻³ - 2.5 x10 ⁻³	228 - 301

The primary aldehydes of interest were formaldehyde and acetaldehyde, as these have been reported as MEA oxidative degradation products (Sexton and Rochelle, 2011). Aldehyde and ketone emission samples were collected from the absorber exit by UK CAER during the long-term testing period. Additionally, EPRI collected samples from the absorber exit as third-party verification during the same period in the long-term testing. **Exhibit 6.5.5** shows the ranges (in ppbV and lbs/hr) for the individual aldehydes and ketones observed in the flue gas exiting the absorber by the two sampling teams. Several different aldehydes and ketones were observed including formaldehyde, acetaldehyde, acetone and isophorone. Propionaldehyde was not observed by either team. The total aldehyde and ketone emission levels at the absorber exit were very low ranging from 731 - 775 ppbV (UK CAER) and 228 - 301 ppbV (EPRI).

Acetone emission have been reported by Moser (2011) in post combustion capture systems running an MEA solvent in the low 0.5 to 1.0 mg/Nm³ range. However, acetone was only observed in one set of samples in this study and may be from contamination of the sampling equipment or laboratory, where acetone is a commonly used chemical. Overall, the aldehyde emission levels are very comparable between these two separate sample sets. The aldehyde emission values obtained by both teams during this MEA testing campaign.

Nitrosamine emission samples were collected using a sulfamic acid reagent and analyzed with mass spectrometry to identify and, if present, quantify each individual nitrosamine. The use of the aqueous sulfamic acid reagent in a cold impinger train to trap any nitrosamine emissions, while also inhibiting *in situ* nitrosamine formation, has become a relatively standard sampling method for amine based CO₂ capture systems (Dia et al., 2012; Fraboulet et al., 2016).

Fraboulet (2016) showed that the total nitrosamine analysis method (TONO) can be unreliable and can overestimate the actual amount of nitrosamines in the samples. Fraboulet also showed that nitrosamine gas sample analysis using a variety of MS methods was more reliable regardless of the actual sample preparation method or instrumentation used. In addition, when using nitrosamine emission data to perform EH&S evaluations, information on specific nitrosamines is critical as the

potential health risks may be different for each nitrosamine. Given this, a combined solid phase extraction and GC/MS method was used in this study for nitrosamine analysis.

A total of ten nitrosamine emission samples were collected from the absorber exit. Based on previously published reports from MEA solvent testing campaigns and the availability of authentic standards, eight distinct nitrosamines were examined in detail. In all the collected samples, no nitrosamines were identified above the calculated LOQ. **Exhibit 6.5.6** shows the limit of quantitation ranges in the high parts per trillion (pptV) to low parts per billion (ppbV) for the individual nitrosamines calculated from the combined sampling, sample preparation and analysis procedures.

Exhibit 6.5.6. Calculated nitrosamine emissions LOQ during MEA pilot testing.		
Nitrosamine	CAS	LOQ Range (ppbV)
N-nitrosopiperidine (NPIP)	100-75-4	0.058 - 1.89
N-nitrosodimethylamine (NDMA)	62-75-9	0.066 - 2.87
N-nitrosomethylethylamine (NMEA)	10595-95-6	0.056 - 2.42
N-nitrosodiethylamine (NDEA)	55-18-5	0.048 - 2.08
N-nitrosodipropylamine (NDPA)	621-64-7	0.036 - 1.62
N-nitrosomorpholine (NMOR)	59-89-2	0.211 - 9.16
N-nitrosopyrrolidine (NPY)	930-55-2	0.049 - 2.12
N-nitrosodibutylamine (NDBA)	924-16-3	0.036 - 1.32

MEA degradation products, especially secondary amines, also have the potential to form nitrosamines. With this in mind, the emission samples were also screened for several additional nitrosamines that could arise from polymeric MEA degradation compounds reported during pilot testing campaigns. However, after an in-depth investigation none of the MEA degradation nitrosamines were positively detected in any of the collected emission samples.

The secondary air stripper is also a location where amine losses could occur. The top of the secondary air stripper contains a section of high efficiency packing combined with a spray nozzle where a portion of the condensate from the primary stripper is returned to the amine loop. The exit gas from the secondary air stripper is also routed through a heat recovery exchanger, where the warm gas is used to pre-heat the rich amine solvent exiting the absorber, before it is combined with the scrubbed flue gas and returned to the plant.

Since there should be a low concentration of aerosol nuclei in the ambient air used by the secondary stripper, amine emissions as aerosols from the location should be negligible. The observed amine emissions are probably, at least in part, a consequence of the amine volatility over the warm lean solvent at the top of the air stripper. The condensate spray at the top of this column will remove and recycle some of the vapor emissions, while the heat recovery exchanger on the exhaust will further cool the air and condense more water that will also help capture more of the vapor MEA. Therefore, the total MEA emissions from the air stripper should be much lower than those from the main absorber.

Emission samples collected after the heat exchanger in **Exhibit 6.5.7** show very low levels of MEA slip from this location. The MEA emissions levels from this location ranged from 0.3-32 ppmV

(0.002-0.17 lbs/hr). Since the stripping air will be used as combustion air in a commercial unit, amine emissions at this location will result in an economical loss of the solvent, but will probably not increase system wide emissions. Depending on the economic value of the amine loss, additional emissions controls may or may not be needed at this location.

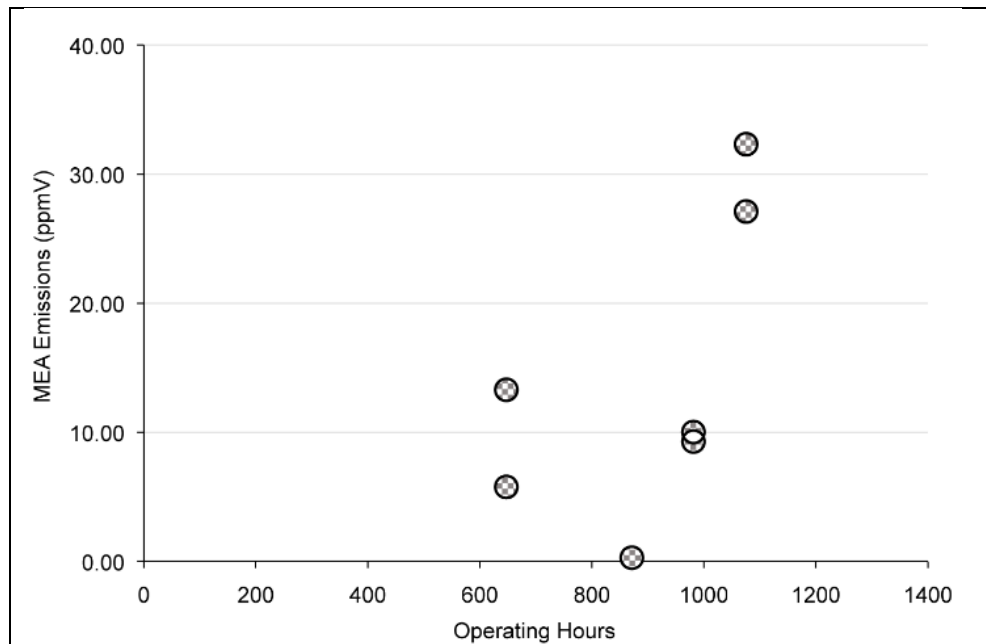


Exhibit 6.5.7. MEA emissions (in ppmV) from the secondary air stripper.

Conclusion

The overall solvent emissions were comparable to the results of other published pilot studies using MEA. The magnitude of the MEA emissions is greater than can be explained as vapor emissions, so it is probable that much of the MEA emissions observed are the result of aerosols. Solvent oxidation in the form of ammonia and aldehyde emissions levels were also comparable to published results showing that the impact of the secondary air stripper on solvent oxidative degradation appears to be negligible. The ammonia emissions were strongly correlated with the accumulated concentrations of dissolved iron and copper in the solvent. Nitrosamine emissions were not observed above the low ppbV detection limits calculated during this MEA testing campaign. Future modification to this unit will likely be necessary to further reduce and manage amine emission including the installation of a water wash column and other emission controls.

6.6 MEA Concentration (~ 40 wt% vs. 30 wt%)

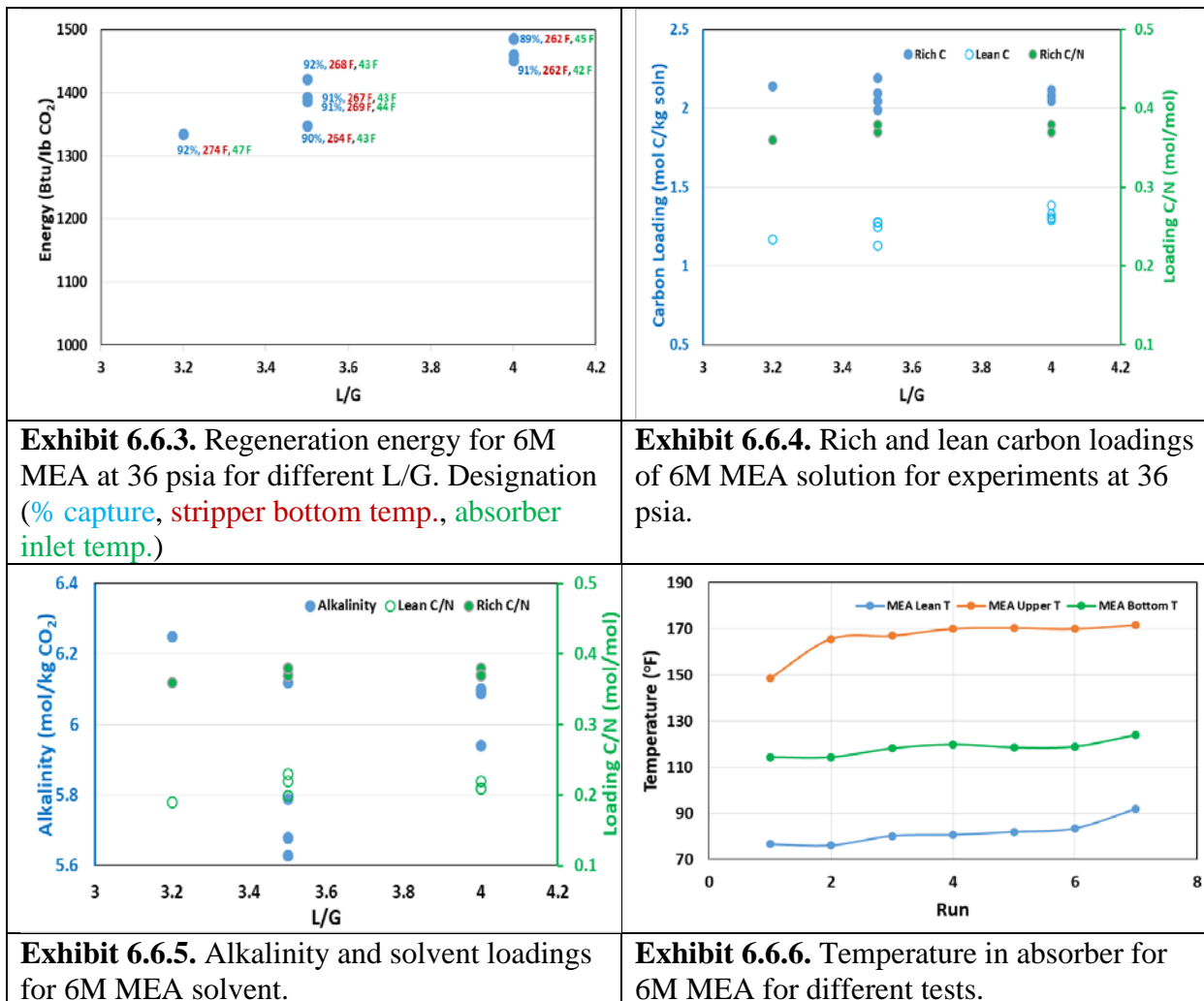
Operating with higher concentration amines can potentially provide energy savings from the lower liquid circulation rates required due to enhanced cyclic carbon capacity in terms of mole/kg solution. However, concerns with solvent viscosity and resultant increase in diffusion resistance to solvent performance, low heat conductivity to lean/rich solvent heat exchanger and increased corrosion are limiting to the usable concentrations for the process. Corrosion inhibitors are particularly important for higher concentration amines test.

Parametric tests were performed with a 6M concentration of MEA at an inlet CO₂ concentration of 14 vol% for different L/G ratios and stripper pressures. Test conditions used are shown in **Exhibits 6.6.1**. The target CO₂ capture was 90% and in the middle of steady state conditions maintained for a 2 hour period, liquid samples for the rich solution (SP1) from the bottom of the absorber, lean sample from the bottom of the primary stripper (SP2) and extra lean from the bottom of the secondary stripper (SP3) were collected. The capture efficiency and energy of regeneration of the solvent were determined, averaged for process conditions over the steady state period. The energy of regeneration ranged between 1300 and 1500 Btu/lb CO₂.

Exhibit 6.6.1. 6M MEA Parametric Test Conditions.		
Absorber Liquid/Gas Flow Rate Ratio, L/G (kg/kg)	Primary Stripper Pressure (psia)	Inlet CO₂ Concentration (vol%)
3.2, 3.5 and 4	22 and 36	14

Exhibits 6.6.2 - 6.6.6 show test conditions and results for experiments at a stripper pressure of 36 psia. Similar to findings from 30 wt% MEA campaign, **Exhibit 6.6.3** shows the energy of regeneration obtained for different L/G. The overall increase in the energy of regeneration as liquid circulation (L/G) is increased is a result of the increase in sensible heat and carbon loading in the solution. Although at the lower liquid circulation rates, a reduction in energy was realized, the temperature at the bottom of the stripper increased to generate leaner solvent as shown in **Exhibit 6.6.2**. To meet the target capture of 90%, the higher stripper bottom temperature was needed but it must be noted that this could contribute to accelerated degradation of the solvent.

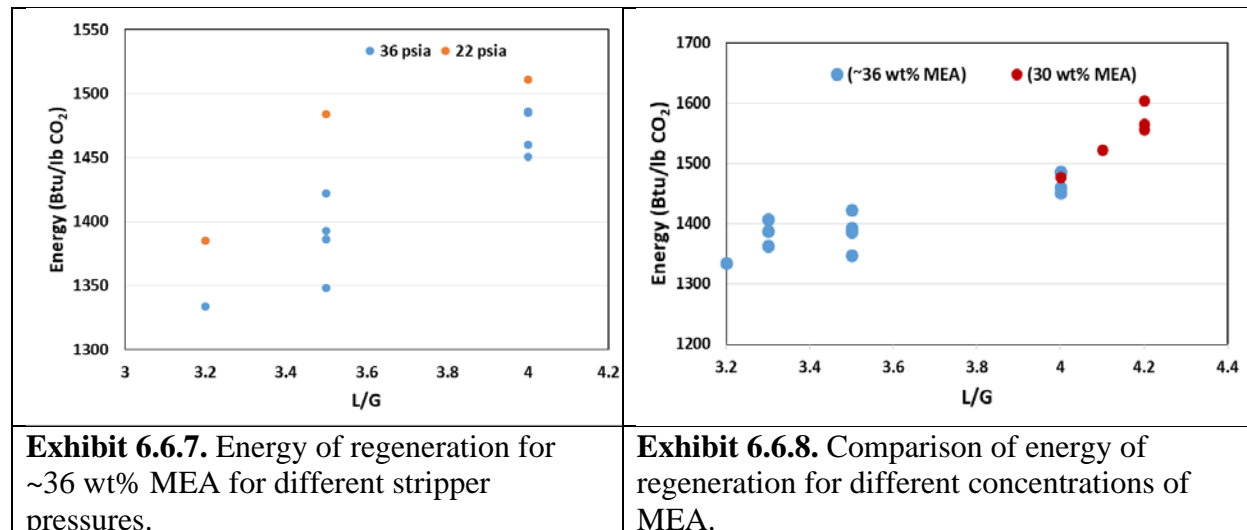
Exhibit 6.6.2. Experimental conditions and results for 6M MEA at 36 psia.							
	L/G	Absorber Inlet Temp. °F	Absorber Bottom Temp. °F	Stripper Overhead Temp. °F	Stripper Bottom Temp. °F	Capture Efficiency %	Regen. Energy Btu/lb CO ₂
1	3.2	82	119	227	274	92	1334
2	3.5	77	114	221	264	90	1348
3	3.5	81	120	225	270	91	1386
4	3.5	80	118	224	267	91	1393
5	3.5	76	114	224	268	92	1422
6	4	79	115	220	262	91	1451
7	4	92	129	221	267	89	1485



The lean alkalinity of the solvent as shown in **Exhibit 6.6.5** indicates the estimated solvent concentration was mostly between 35 – 37 wt% MEA. The typical lean loading under the test conditions was at carbon to nitrogen molar ratio (C/N) ~ 0.21 with the rich loading obtained at ~0.38. The rich loading (C/N) obtained did not significantly vary over the range of liquid to gas mass flow ratios (L/Gs) tested.

Fluctuations in ambient conditions during the experiments were noted to contribute to some of the observed variations in repeat runs for same conditions (e.g., L/G). For instance, the lean temperature to the absorber showed some variation by following the circulating cooling water temperature. This required process adjustments as needed to maintain desired temperatures. The intercooler flow rates, for example, were adjusted during the tests to effect needed heat recovery to maximize the rich loading at the bottom of the absorber. **Exhibit 6.6.6** shows the temperature profile for three sections of the absorber: the lean inlet temperature to the absorber, an upper section temperature (located in top half of the absorber) and the bottom temperature. It is observed that, the temperature difference between the lean return temperature and bottom temperature did not vary significantly due to overall same CO₂ captured. The intercooler provided the necessary heat rejection to lower the solvent temperature as desired.

With concerns over high temperature at the bottom of the stripper potentially accelerating the degradation of the solvent, lower stripper pressure experiments were performed at 22 psia. The temperature at the bottom of the stripper ranged between 246–250 °F; a reduction of about 15-20 °F relative to stripping at 36 psia. The energy of regeneration comparison for the two different stripper pressures is shown in **Exhibit 6.6.7**. At the lower stripper pressure, an increase in the regeneration energy is observed. This can be attributed to higher H₂O/CO₂ needed at the reduced stripper pressure at the top of stripper for similar rich loadings in the absorber. The rich loading (C/N) obtained at 22 psia was ~0.36, and the lean loading (C/N) was ~0.20.



The performance of the solvent at the higher concentration of 6M (~36 wt%) was compared with earlier experiments at 5M (30 wt%). For 5M MEA tests, at the same stripping pressure of 36 psia, the temperature at the bottom of the stripper was 254-257 °F and tests were mainly performed at L/G of 4-4.2. The lean return temperature was lower, ranging from 62-75 °F with corresponding lower temperatures at the bottom of absorber of 100-110 °F. At target capture of 90%, the energy of regeneration is compared for the two concentrations in **Exhibit 6.6.8**. It shows that being able to use reduced liquid circulation rates (lower L/G) with the higher concentration results in energy savings. The cyclic range for the 5M MEA experiments was different due to the solvent viscosity. Here, the lean and rich C/N was typically at ~0.29 and 0.45 respectively, compared to 0.21-0.38 obtained for the higher MEA concentration.

Based on viscosity measurements of a lean (C/N = 0.21) and rich (C/N = 0.36) samples from the 6M MEA at 50 °C (122 °F – close to operating absorber bottom temperature), it was determined that the solvent was about 7 times more viscous than expected from measurements of freshly prepared 6M MEA solutions with close carbon loadings, (lean C/N = 0.22 with viscosity of ~4 cP, and rich loading C/N = 0.44 with viscosity of ~5 cP). It is likely that accumulation of degradation products in the solvent could be a factor to have low rich carbon loading due to high diffusion resistance and possible low wet surface area from high viscosity. A low rich carbon loading result in the much higher stripper bottom temperatures required to achieve the target.

7) H3-1 CAMPAIGN

The second solvent campaign to be conducted was performed with the MHPS H3-1 advanced solvent from 2/18/2016 to 7/14/2016, with 1493 operating hours being accumulated. During the parametric campaign, 35 different steady state experiments were performed by deliberately varying process conditions, as shown in **Exhibit 7.0.1**.

Exhibit 7.0.2. H3-1 Parametric Campaign Operating Conditions.		
Absorber Liquid/Gas Flow Rate Ratio, L/G (kg/kg)	Primary Stripper Pressure (psia)	Inlet CO₂ Concentration (vol%)
3.1, 3.7 and 4	22, 30 and 36	12, 14 and 16

After steady state was achieved (taking approximately 4 hours), it was maintained for about 2 hours before liquid samples were collected from SP-1, SP-2 and SP-3, as shown in **Exhibit 6.0.2**, and conditions were changed again. The key process parameters were averaged during about two hours of steady state time, with liquid sample collection occurring at the midpoint, to evaluate the process performance (CO₂ capture efficiency and solvent regeneration energy) associated with the condition and to analyze trends. During the H3-1 parametric campaign the solvent alkalinity varied from 3.7 to 4.7 mol/L, the capture efficiencies ranged from 91-94%, and energy of regeneration from 900–1500 Btu/lb-CO₂ captured, which is in agreement with an energy consumption for CO₂ capture to 973 Btu/lb-CO₂ captured predicted by the preliminary TEA (Bhown, 2012)

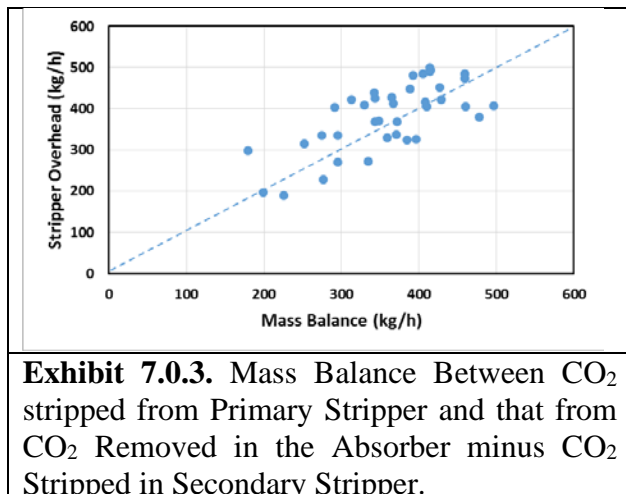


Exhibit 7.0.2 is a parity plot of the measured CO₂ stripped from primary stripper and the calculated mass balance from CO₂ absorbed in the absorber minus CO₂ stripped from secondary stripper, and shows that a good mass balance closure is obtained. During the long-term campaign, process conditions were held constant for much longer periods, often several consecutive days, and liquid samples were collected three times in a 24 hour period. One steady state condition (4/26/2016 from 13:00 to 14:00) was chosen to represent the process performance on a long-term, continual basis.

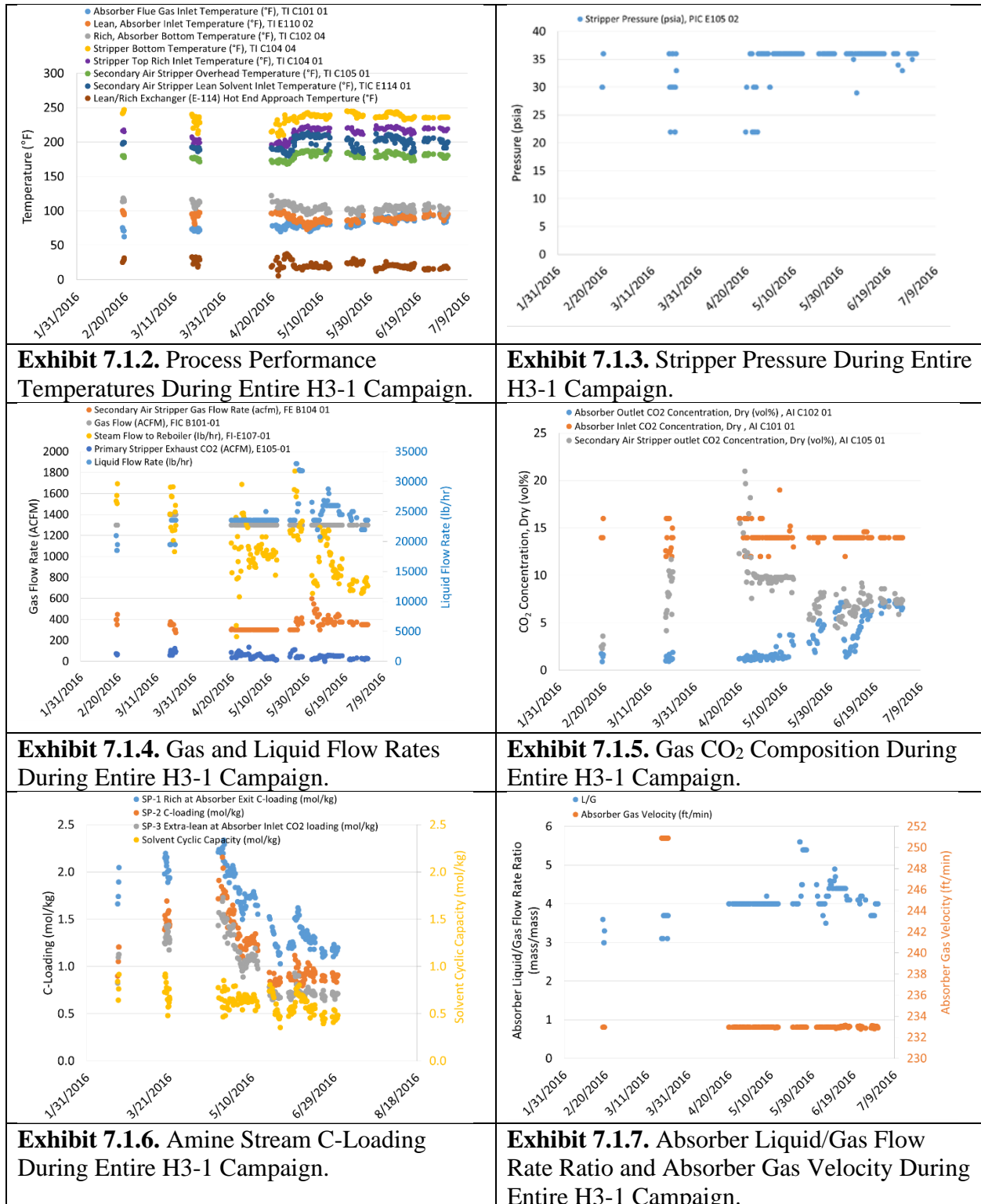
7.1 Process Stability and Solvent Concentration

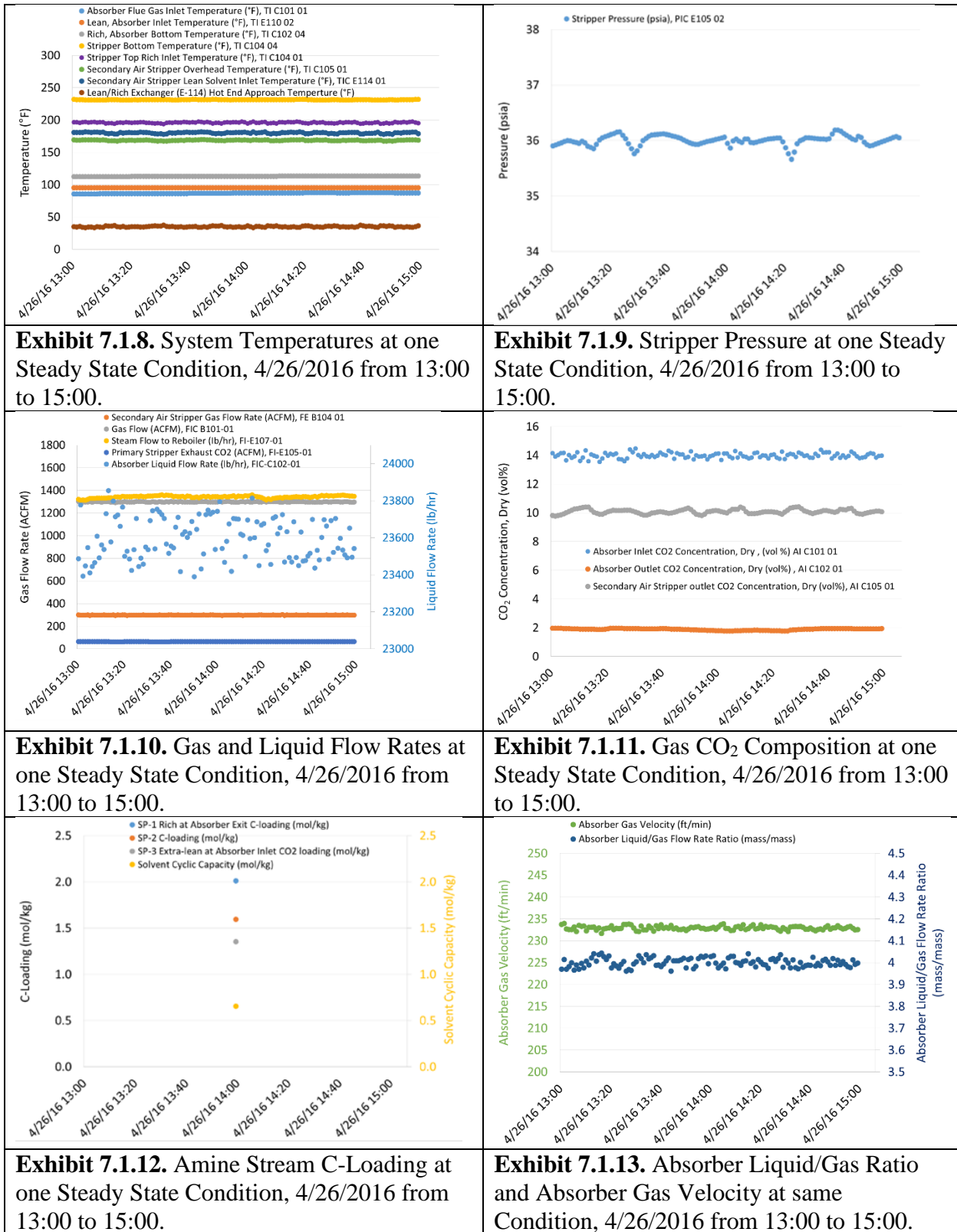
During the H3-1 operational periods, 24-hour per day, 7-day per week operational capability was demonstrated and sustained with downtime being related only to the steam source power generation unit being offline, and for official UK recognized holidays. **Exhibit 7.1.1** lists the values and variation of most pertinent operating parameters affecting CO₂ capture and solvent regeneration energy during one steady state time during the H3-1 campaign, and illustrates the process stability of the UK CAER CCS. These parameters all had small variations during steady state. The temperatures all varied by $\leq \pm 1.5\%$ with the exception of the lean/rich heat exchanger hot end approach temperature, which varied by $\leq + 6.3\% - 4.2\%$. The variation of the primary stripper pressure was $\leq \pm 1.0\%$ and this parameter is controlled by the overhead flow (CO₂ product flow). All flow rates varied by $\leq \pm 2.5\%$. The gas CO₂ concentrations varied by $\leq \pm 3.5\%$ at the absorber inlet, $\leq \pm 6.2\%$ at the absorber outlet and $\leq \pm 3.3\%$ at the secondary air stripper outlet. The solvent loading were measured from one sample collected from the middle of the steady state period. Two analyses are conducted from each liquid solvent sample with the results being accepted from the first if the second differs by $\leq \pm 5\%$.

Exhibit 7.1.1. Most Pertinent Process Parameters from one steady state condition from the H3-1 Campaign: 4/26/2016 from 13:00 to 15:00				
Description	Instrument Tag	Units	Average Value	Process Variation
Temperatures				
Absorber Gas Inlet Temperature	TI-C101-01	°F	87.1	$\leq \pm 1.2\%$
Absorber Lean Solvent Inlet Temperature	TI-E110-02	°F	95.7	$\leq \pm 0.2\%$
Absorber Solvent Outlet Temperature, Bottom of Column	TI-C102-04	°F	113.4	$\leq \pm 0.6\%$
Primary Stripper Rich Solvent Inlet Temperature	TI-C104-01	°F	196.3	$\leq \pm 1.1\%$
Primary Stripper Lean Solvent Outlet Temperature	TI-C104-04	°F	231.7	$\leq \pm 0.3\%$
Lean/Rich Exchanger Hot End Approach Temperature	Calculated	°F	35.4	$+ 6.3\% - 4.2\%$
Secondary Air Stripper Lean Solvent Inlet Temperature	TIC-E114-01	°F	189.5	$\leq \pm 1.2\%$
Pressures				
Primary Stripper Operating Pressure	PIC-E105-02	psia	36.0	$\leq \pm 1.0\%$
Flow Rates				
Absorber Gas Inlet Flow	FIC-B101-01	ACFM	1300.1	$\leq \pm 0.6\%$
Absorber Solvent Inlet Flow	FIC-C102-01	lb/hr	23592.9	$\leq \pm 1.2\%$
Primary Stripper Gas Outlet Flow, CO ₂ Product Flow	FI-E105-01	ACFM	65.6	$\leq \pm 2.2\%$
Steam Flow to Primary Stripper Reboiler	FIC-E107-01	lb/hr	1344.4	$\leq \pm 2.3\%$
Air Flow to Secondary Air Stripper	FIC-B104-01	ACFM	299.9	$\leq \pm 1.4\%$
Gas Compositions				

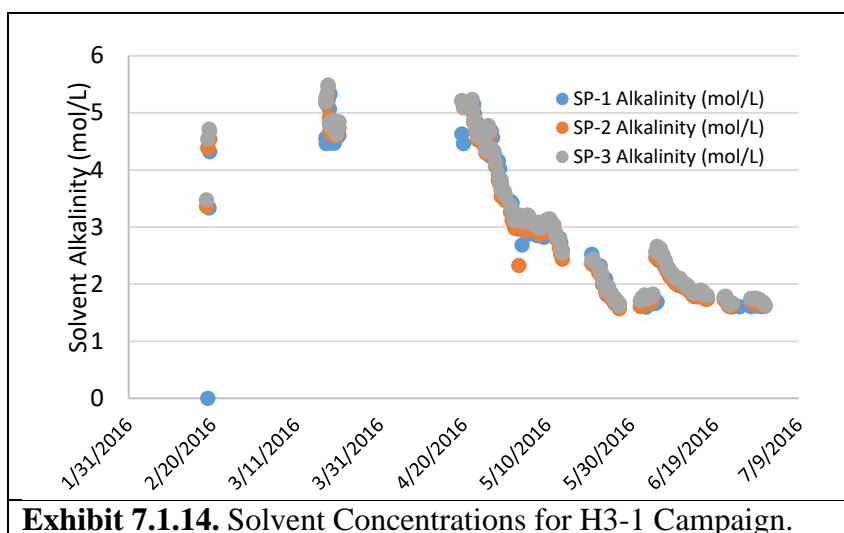
Absorber Inlet CO ₂ Concentration	AI-C101-01	Dry, vol%	14.0	≤± 3.5%
Absorber Outlet CO ₂ Concentration	AI-C102-01	Dry, vol%	1.9	≤± 6.2%
Secondary Air Stripper Outlet CO ₂ Concentration	AI-C105-01	Dry, vol%	10.1	≤± 3.3%
Solvent Loadings and Difference Between Repeated Analyses				
Rich Solvent C-loading	SP-1	mol/kg	2.11	≤± 5%
Lean Solvent C-loading	SP-2	mol/kg	1.60	≤± 5%
Extra-lean Solvent C-loading	SP-3	mol/kg	1.35	≤± 5%
Solvent Cyclic Capacity	Calculated	mol/kg	0.76	≤± 5%
Other Parameters				
Absorber Liquid to Gas Flow Ratio, L/G	Calculated	mass/mass	4.0	
Absorber Gas Velocity	Calculated	ft/min	232.0	
Solvent Loss Rate due to Solvent degradation	Calculated	lb/ ton CO ₂ captured	0.7	
System Performance				
Capture Efficiency	Calculated	%	88	
Solvent Regeneration Energy	Calculated	BTU/lb-CO ₂ captured	1052	

The values of the parameters most pertinent to the process performance, as listed in **Exhibit 7.1.1**, during the entirety of the H3-1 campaign are shown in **Exhibits 7.1.2-7.1.7**, illustrating the variation of the conditions considered. Each point shown in these figures is averaged from about a minimum of 2 hours of steady state data collected. **Exhibits 7.1.8-7.1.13** show each of these process performance parameters during a selected steady state time, early on in the long-term campaign, illustrating the variation of the conditions at steady state.





During the portion of H3-1 long-term operation, in order to understand the impact of amine concentration on solvent emissions (including aerosols), thermal and oxidative degradation, and the limits of the solvent and process while maintaining 90% CO₂ capture and energy consumption associated with CO₂ capture, after 200 hour operation, UK CAER decided to not makeup the solvent until after approximately 800 running hours. As consequence, the solvent was allowed to become dilute during the long term campaign due to amine emissions and water makeup needed for system continuous operation. This experiment resulted in useful knowledge gained: a dilute solvent can have even better performance than at the specified concentration for a facility constructed. 90% CO₂ capture is still easily achievable with a low solvent regeneration energy due to a beneficial change in the solvent physical properties such as lower viscosity, lower surface tension, and better heat transfer. The solvent alkalinity (recommended at 5 mol/L) from the entire H3-1 campaign is shown in **Exhibit 7.1.14**.



7.2 CO₂ Capture Efficiency and Solvent Regeneration Energy

To remain consistent with NETL RC 10, a 90% CO₂ capture efficiency was targeted for all parametric and long term conditions.

Exhibits 7.2.1 and 7.2.2 show the solvent alkalinity along with the process performance results. CO₂ capture efficiency in **Exhibit 7.2.1** and solvent regeneration energy, along with the absorber L/G ratio in **Exhibit 7.2.2**. Generally, a 90% CO₂ capture efficiency was obtained prior to the solvent alkalinity decreasing to about 3 mol/L. Beyond this point 90% CO₂ capture became difficult to achieve, but even as the alkalinity approached 1 mol/L, a capture efficiency of > 50% was still possible. As the solvent alkalinity decreased below about 4 mol/L the solvent regeneration energy increased, at constant absorber L/G ratio, but by increasing the absorber L/G, low solvent regeneration energies, of about 1000 BTU/lb CO₂ captured, were still achievable.

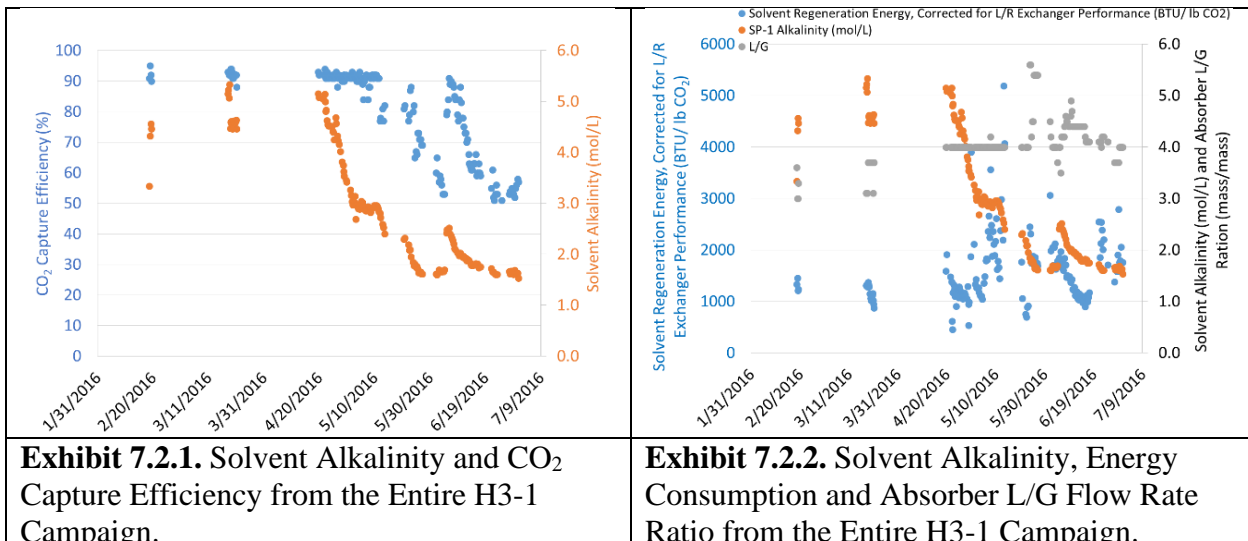


Exhibit 7.2.1. Solvent Alkalinity and CO₂ Capture Efficiency from the Entire H3-1 Campaign.

Exhibit 7.2.2. Solvent Alkalinity, Energy Consumption and Absorber L/G Flow Rate Ratio from the Entire H3-1 Campaign.

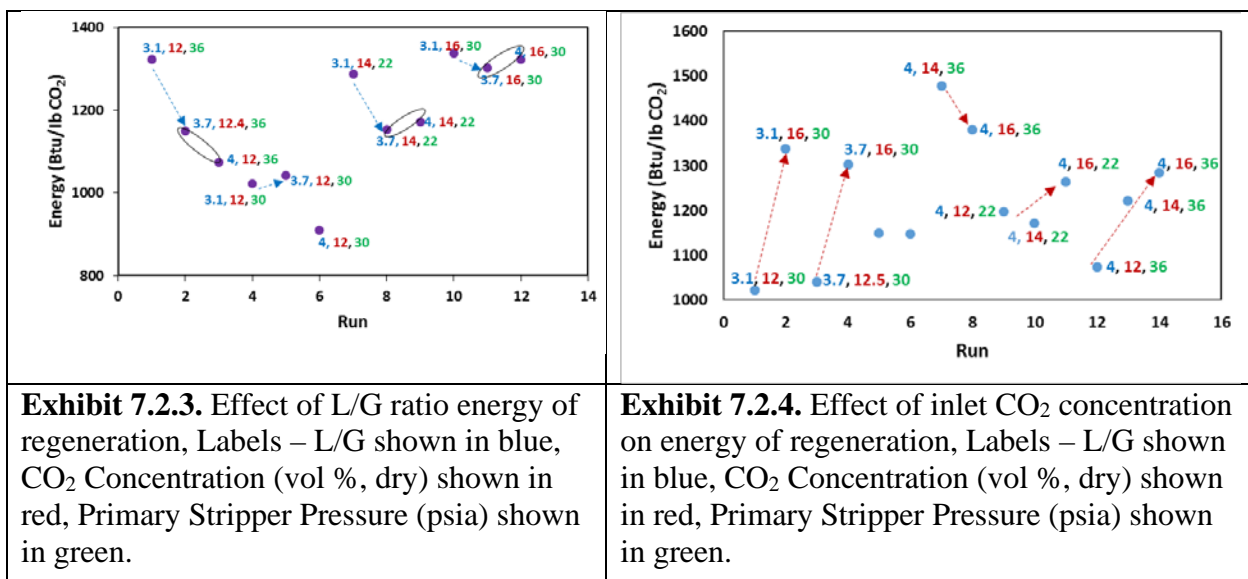


Exhibit 7.2.3. Effect of L/G ratio energy of regeneration, Labels – L/G shown in blue, CO₂ Concentration (vol %, dry) shown in red, Primary Stripper Pressure (psia) shown in green.

Exhibit 7.2.4. Effect of inlet CO₂ concentration on energy of regeneration, Labels – L/G shown in blue, CO₂ Concentration (vol %, dry) shown in red, Primary Stripper Pressure (psia) shown in green.

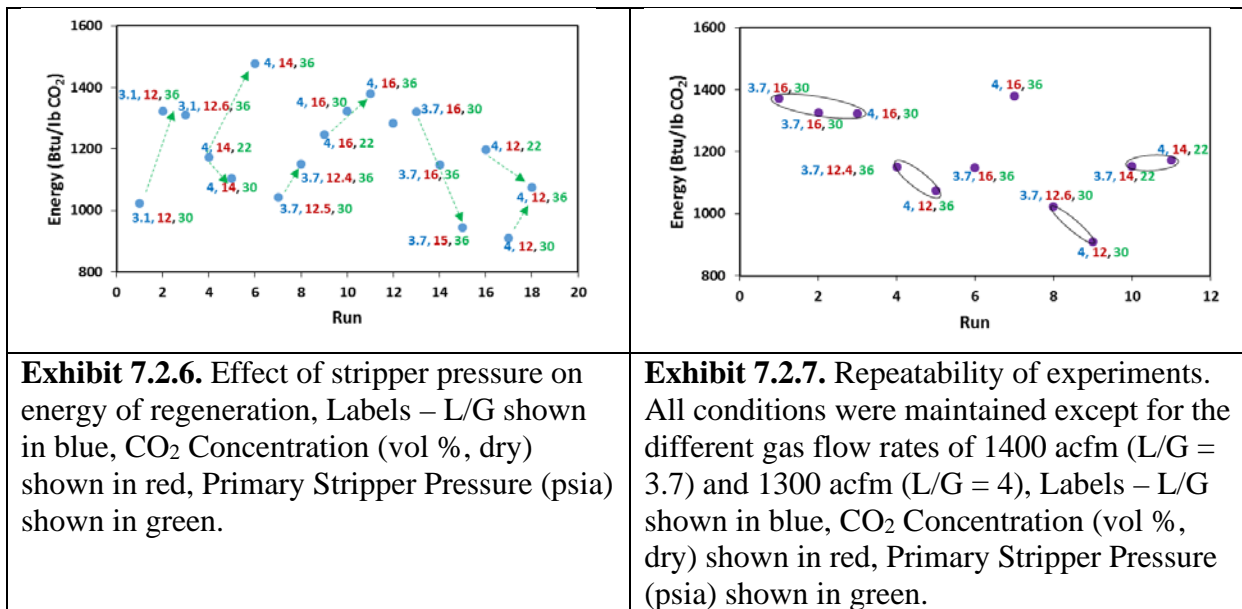
35 steady state conditions were evaluated during the parametric portion of the H3-1 campaign. During this time, the CO₂ capture efficiencies ranged from 91-94% and the solvent energy of regeneration ranged from 900-1500 BTU/lb CO₂ captured. A more detailed analysis was done to learn how the key process parameters listed in **Exhibit 7.1.1** affected the solvent regeneration energy.

As shown in **Exhibit 7.2.3**, when the absorber L/G ratio was increased from 3.1 to 3.7, there was generally a reduction in the energy of regeneration highlighted mostly as shown starting with the downward pointing arrows. Included in **Exhibit 7.2.3** are results for experiments at L/G of 4, which are repeat conditions (done with a gas flow rate of 1300 acfm) for same conditions at L/G = 3.7 (done at a gas flow rate of 1400 acfm). The black circles illustrate the repeatability of some of the runs at the L/G ratios of 3.7 and 4. Generally, the energy consumption was reduced with increase of L/G from 3.1 to 3.7, but bounced back from L/G from 3.7 to 4. However, the trends are varied based upon the stripper operating pressure and CO₂ concentration entering CO₂

absorber. The possible explanation on those findings are the effectiveness of gas-liquid interfacial area and sensible heat of recirculating solvent. As shown in **Exhibit 7.2.4**, the energy of regeneration generally increased with increased inlet CO₂ concentration as shown with the red arrows.

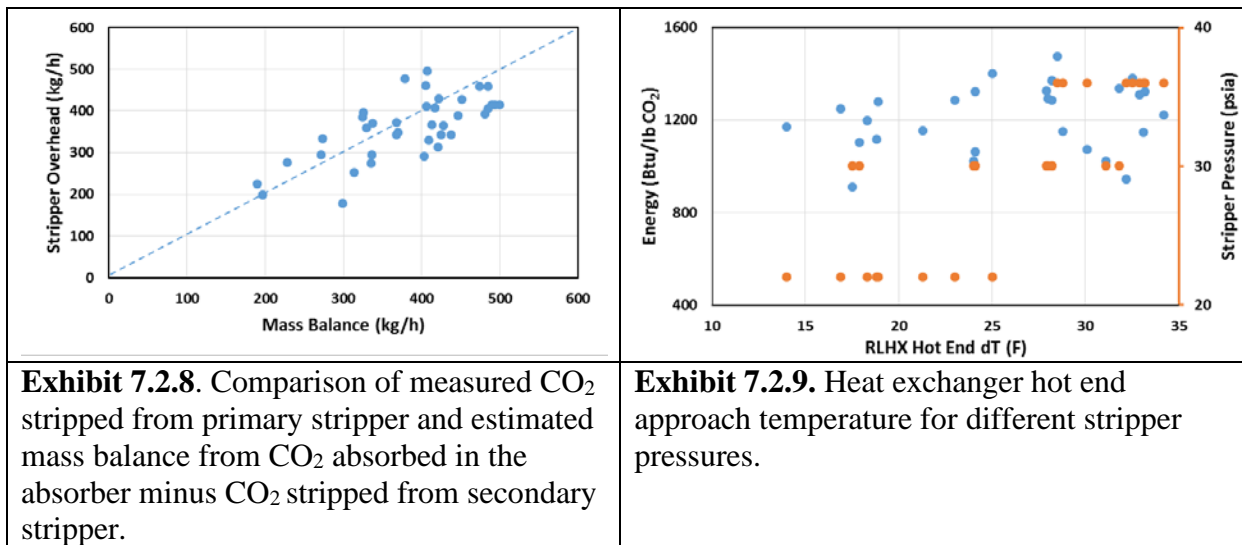
Run	Inlet CO ₂ Concentration (vol%)	Absorber L/G (wt/wt)	Stripper Pressure (psia)	Extra Lean Return to Absorber (mol C/mol N)	Rich Loading in Absorber (mol C/mol N)	Lean Loading from Primary Stripper (mol C/mol N)
1	12	3.1	30	0.30	0.46	0.36
2	16	3.1	30	0.24	0.45	0.28
3	12.5	3.7	30	0.31	0.44	0.35
4	16	3.7	30	0.29	0.49	0.33
5	12.4	3.7	36	0.31	0.51	0.39
6	16	3.7	36	0.29	0.48	0.34
7	14	4	36	0.32	0.48	0.39
8	16	4	36	0.31	0.48	0.36
9	12	4	22	0.35	0.50	0.41
10	14	4	22	0.34	0.48	0.40
11	16	4	22	0.30	0.50	0.42
12	12	4	36	0.35	0.51	0.42
13	14	4	36	0.33	0.50	0.38
14	16	4	36	0.29	0.50	0.34

Exhibit 7.2.5 shows results of the liquid analyses for the tests performed for different inlet CO₂ concentrations presented above in **Exhibit 7.2.4**. After the rich solvent is stripped in the primary stripper, extra CO₂ is stripped in the secondary stripper and returned to the absorber as the extra lean solvent. The results show that the secondary stripper helps in lowering the lean loading of the solvent returned to the absorber. Generally, as the inlet CO₂ concentration was increased, the loading of the lean solvent to the absorber was lowered to enable the solvent to absorb the extra CO₂ gas. The rich loading at the bottom of the absorber, however, did not show any significant increases. Thus, the expected mass transfer enhancement at the bottom of the absorber with the increased driving force from the increase in CO₂ inlet concentration was minimal. Though an increase in cyclic capacity is obtained for the same liquid circulation rates with the inlet CO₂ concentration increase, the leaner solvents that were required for the corresponding increase in inlet CO₂ concentration was at an energy cost and hence the general energy increase with increased inlet CO₂ concentrations.



In **Exhibit 7.2.6**, the impact of the stripper pressure on energy of regeneration did not follow a particular trend. In some cases, increased stripper pressure resulted in a corresponding increase whereas the reverse was seen in some. Generally, there was a reduction in energy by increasing the stripper pressure from 22 to 30 psia, however when this was increased to 36 psia, an energy increase was observed. It is expected that operating the stripper at a higher pressure (at tolerable stripper bottom temperatures that will not accelerate solvent degradation), due to increased partial pressure of CO₂ in the stripper, the enthalpy of vaporization for water could be significantly reduced to lower the reboiler duty for the regeneration.

Exhibit 7.2.7 highlights a low error margin for most of the repeat runs. The difference in L/G ratios of 3.7 and 4 are from the gas flow of 1400 and 1300 acfm used respectively. All the other conditions were mostly maintained.



The energy of regeneration was estimated based on the stripped CO₂ measured from the overhead of the primary stripper. The amount of CO₂ stripped was also estimated from the difference of CO₂ absorbed in the absorber and the amount stripped from the secondary stripper. The parity plot in **Exhibit 7.2.8** shows the variation in the CO₂ stripped from the primary stripper from the two approaches. With a few outliers, reasonable balance is obtained between the measured CO₂ stripped from the primary stripper and the calculated estimates from the absorber and secondary stripper.

The hot end temperature approach is shown for various conditions and the stripper pressure. The energy of regeneration (corrected for heat exchanger design approach temperature) does not show any specific correlation with hot end L/R HXER approach temperature as shown in **Exhibit 7.2.9**. Due to the higher stripper temperature for the high stripper pressure runs, higher approach temperatures were generally obtained.

7.3 Corrosion

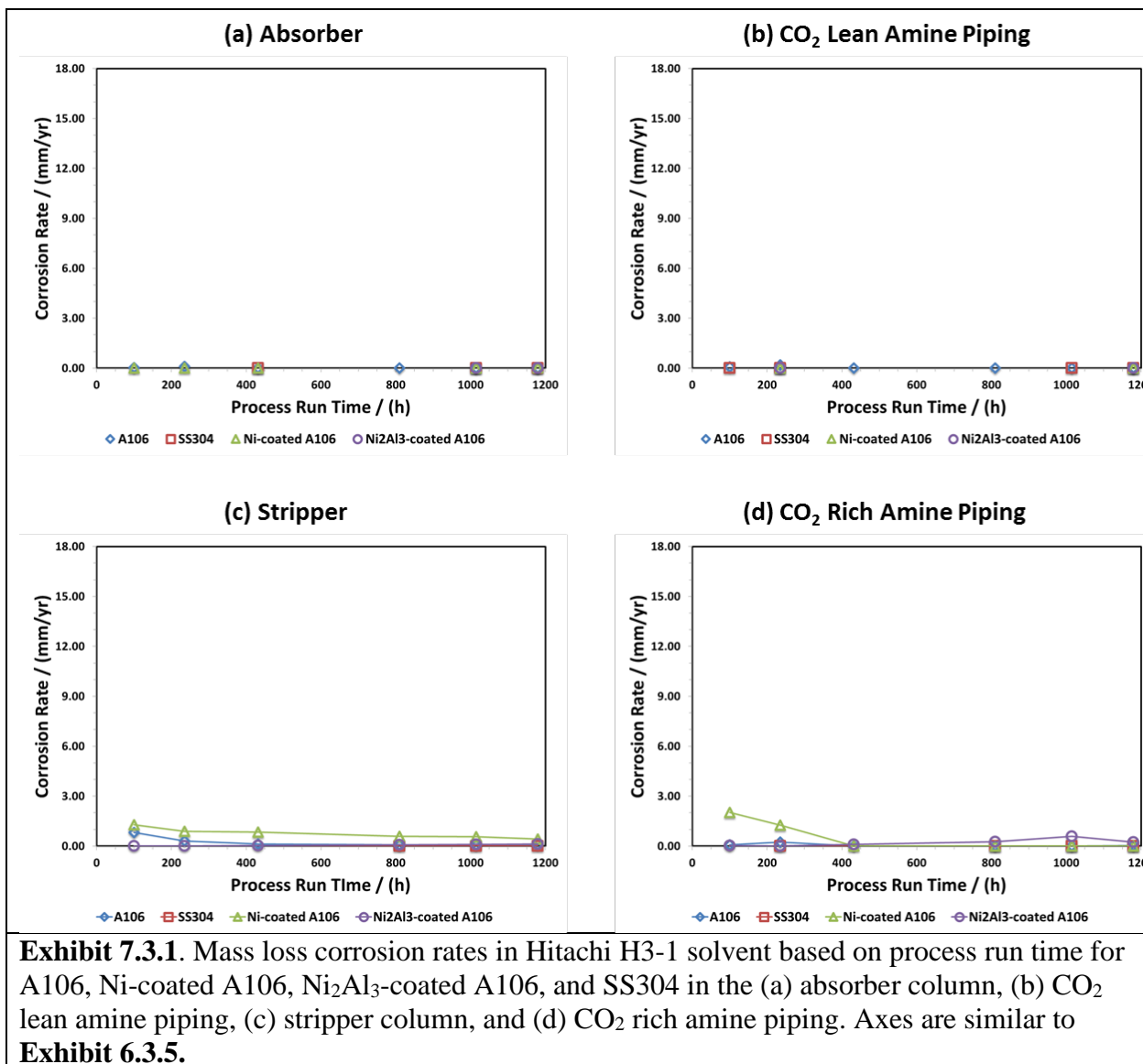
A similar study to that carried out in Section 6.3 was used for the Hitachi H3-1 campaign. Corrosion coupons were placed in the same four locations shown in Exhibit 6.3.1. The same four coupon types were chosen (A106 carbon steel, stainless steel 304, Ni-coated A106 carbon steel, and Ni₂Al₃-coated A106 carbon steel possessing a surface layer of Al₂O₃). The corrosion rate was tracked for approximately 1180 process run hours with nearly 1900 exposure hours in the system.

Corrosion Rates

Exhibit 7.3.1 shows the corrosion rates as measured by the mass loss method for all specimens in the four locations of the process (see **Exhibit 6.3.1**) after approximately 125, 250, 500, 750, 1000, and 1200 hours of process run time. As seen in **Exhibit 7.3.1**, the corrosion rate for all of these coupons is markedly lower than that seen during the MEA campaign (**Exhibit 6.3.5**). Corrosion rates never exceeded 3 mm/yr, and even those corrosion rates were short-lived. The axes in **Exhibit 7.3.1** are the same as those used in **Exhibit 6.3.5** for ease of comparison.

Negligible corrosion was found in the absorber and in the CO₂ lean amine piping prior to entering the absorber for all of the corrosion coupons. In the stripper and the CO₂ rich amine piping prior to entering the stripper, some corrosion is shown for the A106 carbon steel and Ni-coated A106 coupons. Specifically, Ni-coated A106 shows the highest corrosion rate of any of the coupons during the H3-1 campaign, but again, these rates are still far lower than those seen during the MEA campaign. Ni₂Al₃-coated carbon steel showed negligible corrosion, similar to the SS304 coupons.

Exhibit 7.3.2 shows representative pictures of each specimen at all four sampling locations after approximately 500 hours of process run time. While all coupons appear to retain significant thickness and mass, there is the appearance of a deposition or corrosion product on the A106 carbon steel in the stripper and Ni-coated A106 carbon steel in the stripper and CO₂ rich amine piping prior to the stripper. While these products did not lead to appreciable corrosion rates, they were further examined through XRD studies.



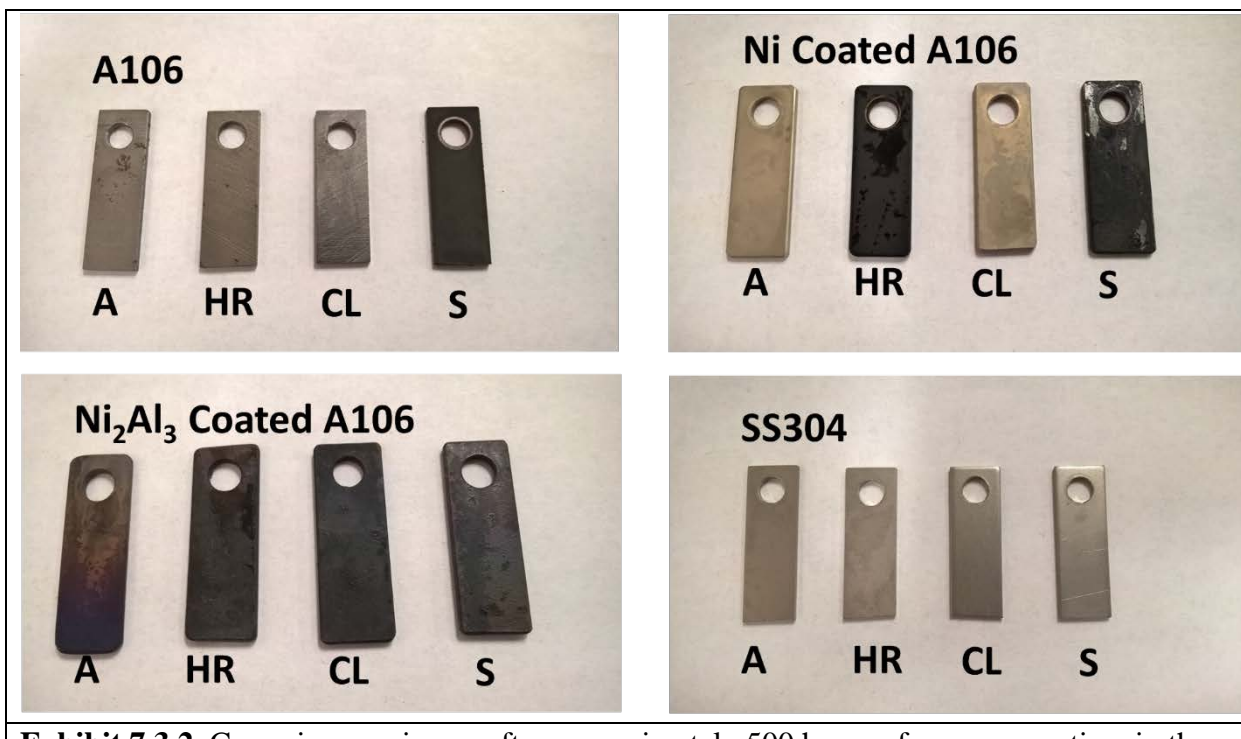
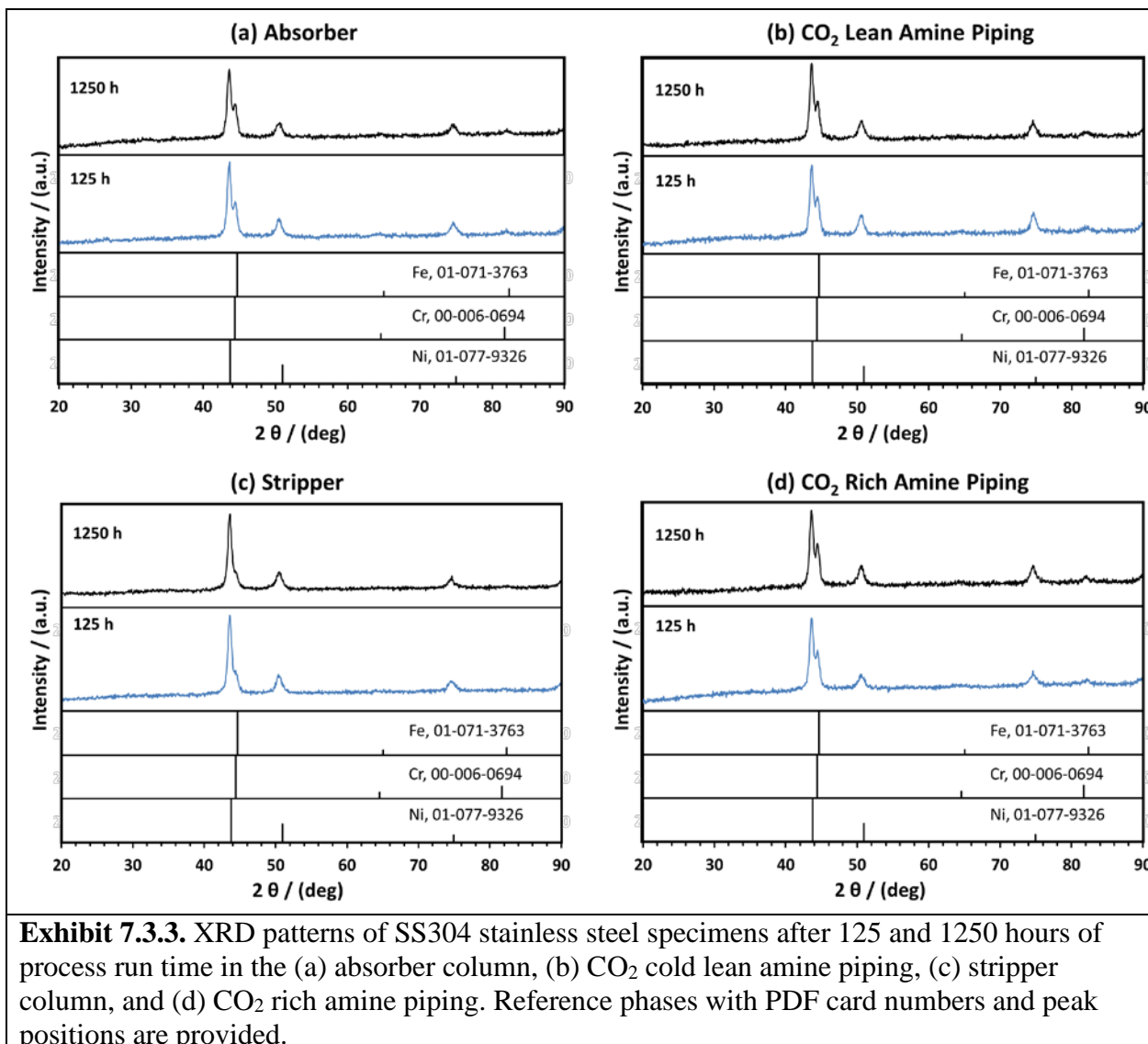
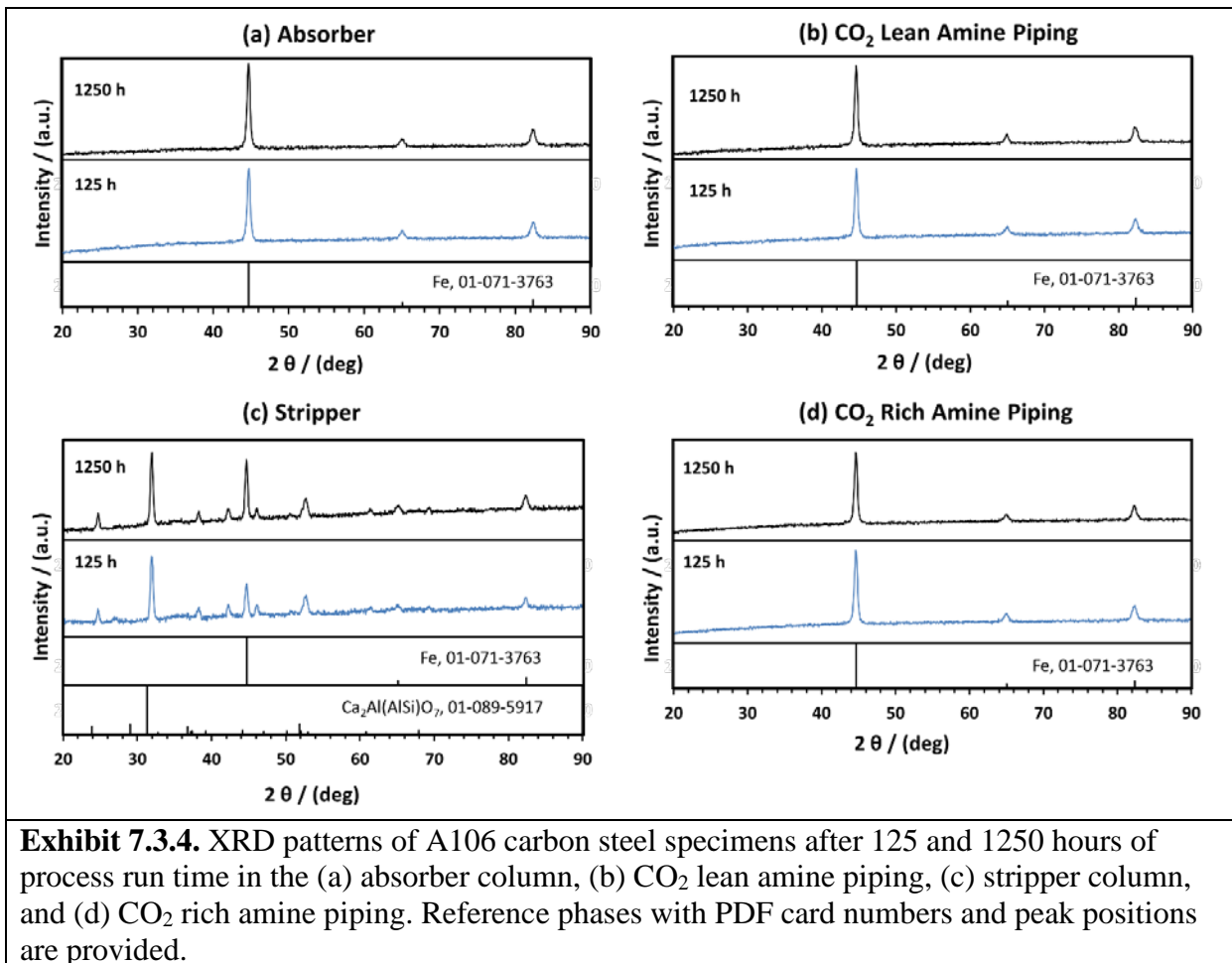


Exhibit 7.3.2. Corrosion specimens after approximately 500 hours of process run time in the carbon capture unit in the absorber column (A), CO₂ rich amine piping prior to the stripper (HR), CO₂ lean amine piping prior to the absorber (CL), and stripper column (S).

XRD analysis was carried out to determine the presence and type of corrosion products for each of the corrosion specimens at each sampling location. Phases were identified by matching the measured peaks to reference phases in the International Centre for Diffraction Data (ICDD) – Powder Diffraction File (PDF) database. XRD analysis was carried out after 125 and 1250 process run hours. Shown in **Exhibit 7.3.3** are the XRD spectra for stainless steel (SS304) at all four sampling locations at 125 and 1250 hours of process run time. The only peaks present in these spectra correspond to the major chemical constituents of stainless steel such as iron, chromium and nickel, and the characteristic peak positions are similar to those of SS304 reported in the literature. These results were anticipated as the corrosion rate of SS304 was zero, and corrosion specimens appeared unaffected at all sampling locations.

A106 carbon steel did show some differences in phases present depending on the process location. Shown in **Exhibit 7.3.4** are the XRD spectra for A106 at all 4 sample locations. In the absorber, the CO₂ lean amine piping, and the CO₂ rich amine piping, only the steel substrate (iron) was identified. On the other hand, a corrosion product was found on specimens within the stripper. An additional phase, probably Ca₂Al(AlSi)O₇ (Gehlenite), was found for A106 carbon steel coupons in the stripper after 125 and 1250 process run hours. As in the MEA campaign, the source of the calcium was most likely related to the water used in this CO₂ capture process or entrainment from the limestone-based WFGD unit deployed for SO_x control. Additional additives found in the H3-1 solvent may have contributed to this product as well.





Overall, the corrosion coupons were found to be far more stable in the Hitachi H3-1 campaign than in the MEA campaign. This result is most likely due to the presence of both corrosion inhibitors and a difference in the amine composition of the solvent. Soluble corrosion inhibitors have been found to be quite effective in a variety of chemical processes, and their presence here may stabilize a variety of metallic coatings intended to protect unit lifetimes. UK CAER has also investigated the use of environmentally-friendly inhibitors for conventional and blended amine solvents, and this area is certainly worthy of future study.

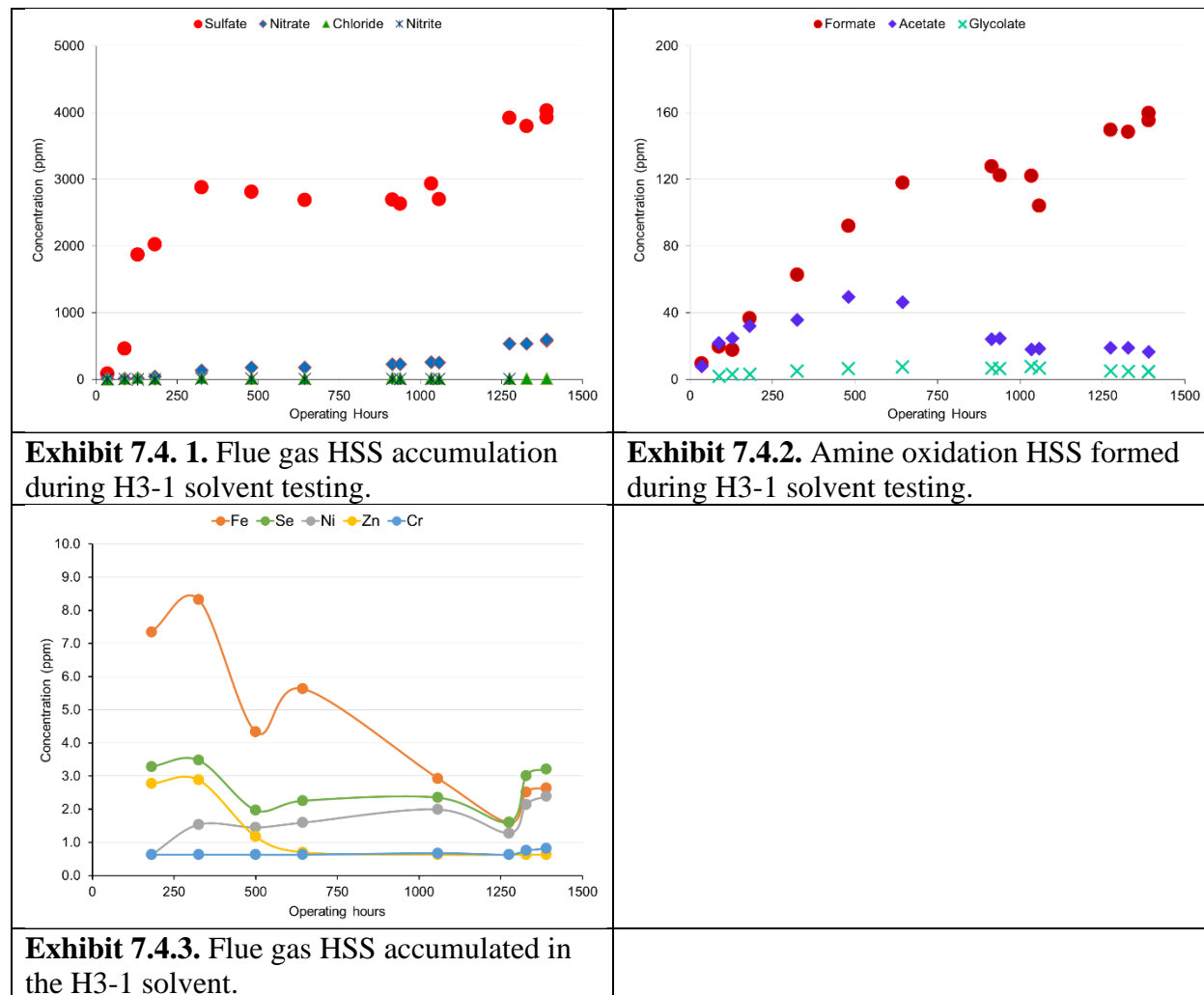
7.4 Degradation

The Hitachi's H3-1 solvent used was diluted to the target operating concentration using service water provided by the plant from a nearby lake with minimal pretreatment. The H3-1 solvent testing operating hours refer only to periods when flue gas was contacting the solvent and steam was used for regeneration. A total of 1390 operating hours were achieved with the H3-1 solvent from combined parametric and long-term testing. The solvent was not reclaimed until after completion of the entire testing program.

Analysis of the H3-1 solvent was performed on samples collected after the absorber (CO₂ rich) in certified metal and inorganic analyte free high density polyethylene (HDPE) bottles. Detection and

quantitation of HSS was performed with a Dionex ICS-3000 IC system. Aldehydes were analyzed as 2,4-dinitrophenylhydrazine (2,4-DNPH) derivatives in a similar fashion to the methodology described in US EPA Method 8315A (1996). Elemental concentrations in the solvent were examined after acidic microwave digestion using ICP-MS (Agilent).

Results



The accumulation of the individual flue gas HSS species is presented in **Exhibit 7.4.1** through a total of 1390 operating hours. The major species observed in the H3-1 solvent was sulfate. Even at less than 5ppm in the flue gas after SO₂ polishing, the high solubility of SO₂ in the solvent lead to high sulfate levels (approximately 0.38 wt. %). Nitrate was also observed at significant quantities from exposure to NO_x in the flue gas. Minor amounts (< 25 ppm) of chloride and nitrite were also observed.

Amine oxidation species were also observed in the H3-1 solvent (**Exhibit 7.4.2**). Formate was the major species reaching near 160 ppm. Formate is commonly used as an indication of overall amine oxidative degradation (Chandan et al., 2014). Acetate and glycolate were also seen in the H3-1

solvent, but at relatively low concentration levels. The overall oxidation level of the H3-1 solvent appears to be very low with only 0.02 wt % oxidative degradation species present in the solvent after 1390 operating hours. At the end of the testing campaign a total of approximately 4800 ppm of HSS were found in the solvent, which equated to approximately 0.45 wt %.

Element concentrations were monitored throughout H3-1 testing campaign and remained relatively low. The concentrations of seven elements (Cr, Fe, Ni, Zn, Cu, As, and Se) were detected in the H3-1 solvent. The results for five elements in the H3-1 solvent are presented in **Exhibit 7.4.3**. Two elements, Cu and As were detected in the solvent but remained near their limit of quantitation of 0.63 ppm during the entire campaign. Zn was initially detected at 2.7 ppm, but then decreased and was not detected after 650 operating hours. Fe also started at its highest level (7.35 ppm) then decreased during the campaign before a final small increase at the very end of testing. Ni showed a slight increase during the campaign from 1.5 to 2.4 ppm. Se started relatively high at 3.3 ppm, followed by a drop in concentration during the middle of the campaign and ended near its starting level at 3.2 ppm.

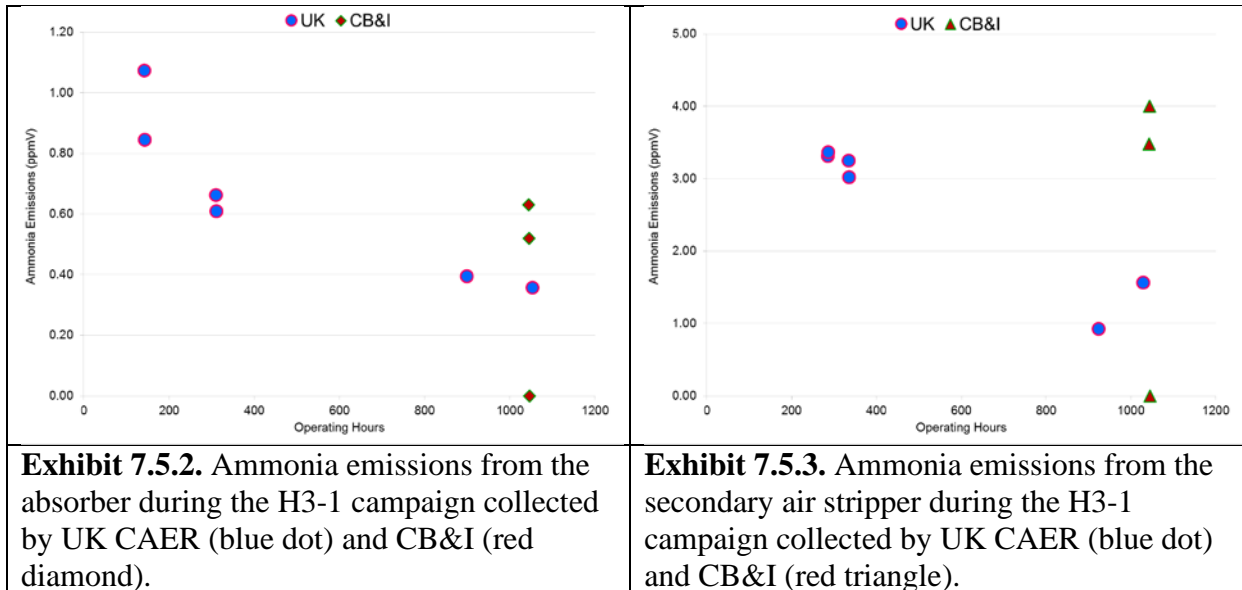
7.5 Emissions

Same as for the MEA gaseous emission study, samples were collected using sampling methodology adapted from U.S. EPA Methods 1 and 5, and individual methods including EPA SW-846 Test Method 0011 for aldehydes, and CTM-027 for ammonia. Nitrosamine emission samples were collected by UK CAER with an impinger train containing a dilute sulfamic acid solution. An aliquot of the collected nitrosamine samples were placed in transfer bottles and packaged for shipment to Hitachi in Japan for analysis. The analysis was conducted by Hitachi using a TEA analyzer that give a total nitrosamine value. **Exhibit 7.5.1** summarizes the samples collected and the associated quality control measures undertaken.

Exhibit 7.5.1. Nitrosamine emission samples collected during the H3-1 testing campaign.			
	Date	Location	Quality Control
1	5/3/2016	Absorber Outlet	Field Blank, Lab Spike
2	5/3/2016	Absorber Outlet	Field Blank, Lab Spike
3	5/6/2016	Absorber Outlet	Field Blank, Lab Spike
4	5/10/2016	Absorber Outlet	Lab Spike
5	5/10/2016	Absorber Outlet	
6	5/11/2016	Secondary Stripper Outlet	Matrix Spike
7	5/11/2016	Secondary Stripper Outlet	
8	6/8/2016	Absorber Outlet	Duplicate

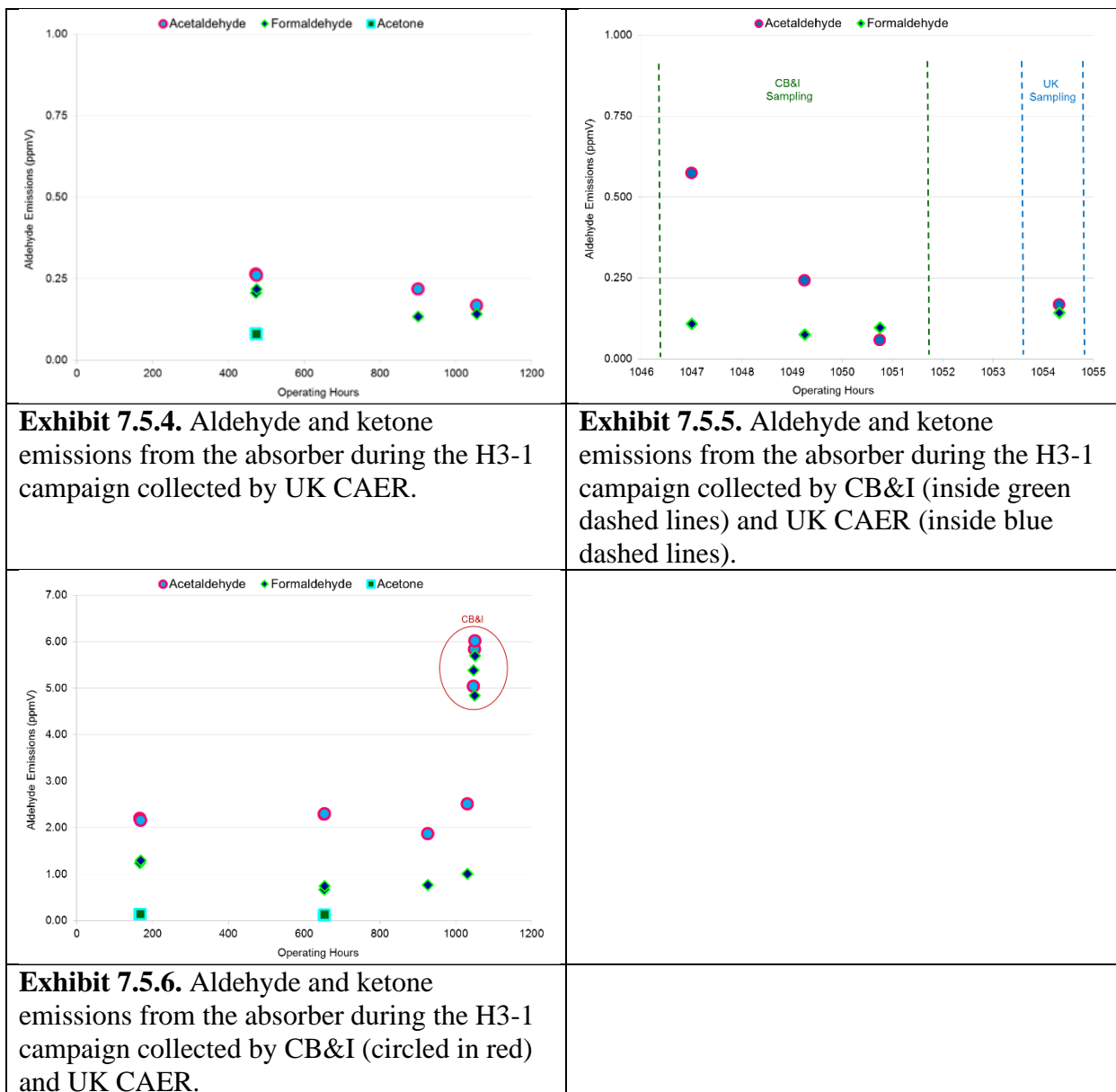
Emission sampling was also conducted by EPRI and its subcontractor, CB&I Environmental and Infrastructure, Inc. (Cincinnati, OH), as third-party verification (QA/QC data check) for a period of one week during the H3-1 testing campaign (at around 1050 operating hours). CB&I used the procedures outlined in EPA CTM-027 to collect samples for ammonia. Aldehyde and ketone compounds were collected and analyzed using the procedures found in EPA SW 846 Method 0011. The ammonia and aldehyde emissions data collected by EPRI/CB&I was used to validate the methodology and emission values obtained separately by UK CAER during the same testing period.

Results



Ammonia emissions from the absorber exit during the H3-1 testing campaign are presented in **Exhibit 7.5.2**. Ammonia emissions range from 0.4 ppmV to 1.1 ppmV over the course of the testing period and showed a decrease over time that corresponded with a drop in the amine concentration in the solvent, as measured through alkalinity. CB&I reported an average ammonia emission level of 0.4 ppmV, including the one data point that was reported as below the detection limit. When compared to the data from CB&I, the UK CAER results appear to be very similar; 0.4 ppmV (CB&I) vs 0.36 ppmV (UK CAER).

The ammonia emissions from the secondary stripper exit are presented in **Exhibit 7.5.3**. Ammonia emissions ranged from a little less than 1 ppmV to a high of 3.5 ppmV over the course of the testing campaign. Again, the ammonia emissions level showed a slight decrease over time that also corresponded with a drop in the amine concentration in the solvent. The ammonia emission levels at the secondary air stripper are slightly higher than at the absorber, but on an absolute basis these emissions levels are very low. The ammonia emission values from CB&I are also shown in **Exhibit 7.5.3**. The CB&I average gas phase ammonia concentration was 2.51 ppmV, again this is very close to the UK CAER emission value collected during the same testing period of 1.56 ppmV.



Aldehyde emissions, composed of formaldehyde, acetaldehyde and acetone, from the absorber exit are presented in **Exhibit 7.5.4**. The overall aldehyde/ketone emission levels at the absorber exit are very low ranging from 0.08 to 0.26 ppmV over the course of the testing campaign. The emission levels showed a decrease over time that again appears to correspond with a drop in the amine concentration in the solvent, as measured through alkalinity. Acetone was only observed in the first set of samples collected from the absorber and may be from contamination of the sampling equipment or UK CAER laboratory where acetone is commonly used.

Exhibit 7.5.5 shows a direct comparison of absorber exit aldehyde emission samples collected on June 6th 2016 by CB&I and UK CAER using similar sampling procedures. CB&I collected 3 sequential samples from 9am-3pm, while UK collected a single sample 3 hours later at 6pm. The emission levels are very comparable between these two separate sample sets; average

formaldehyde 0.093 ppmV (CB&I) vs. 0.143 ppmV (UK CAER), and acetaldehyde 0.291 ppmV (CB&I) vs 0.168 ppmV (UK CAER). The very similar values reported here helps to give confidence and validity to the method modifications undertaken by UK CAER.

The aldehyde emissions from the secondary stripper exit during the H3-1 testing campaign are presented in **Exhibit 7.5.6**. The overall aldehyde emission levels at the secondary stripper exit are again very low, with an average formaldehyde level of 0.95 ppmV and an average acetaldehyde level of 2.22 ppmV. Acetone was observed in 2 of the 4 sets at a consistent value of 0.1 ppmV, again this may be from contamination of the sampling equipment or UK CAER laboratory where acetone is commonly used. **Exhibit 7.5.6** also shows the comparison between the results from aldehyde emission sampling conducted by CB&I (circled) and UK CAER on June 7th, 2016. The emission values from CB&I were higher than the values obtained by UK CAER. It should be noted that the sampling port used by CB&I on the secondary stripper exit gas is located before E-113 (Secondary Heat Recovery exchanger) while the UK CAER sample port is located after E-113. The sampling port located before E-113 is better situated to collect gas flow rate measurements exiting the secondary stripper, however the water content in the gas at this location can make emissions sampling difficult which is why UK CAER collected emission samples after E-113 where the water content in the gas is lower and where the measurements would better reflect the actual gas concentration exiting the CCS process. In this case, the CB&I results are slightly higher than the comparable UK sample collected on the same day. The difference can likely be attributed to the different sampling locations. Overall, the absolute emission levels measured by both CB&I and UK CAER are very low and likely insignificant from a solvent degradation perspective.

Nitrosamine gas sampling was conducted by UK CAER during the H3-1 testing campaign, however due to the proprietary H3-1 solvent, analysis of the collected gas samples was performed by Hitachi in Japan. **Exhibit 7.5.7** show the results of the 8 samples and QA/QC samples collected with each set, along with the average flue gas NO_x levels in the 12-hour period before and during sample collection. Starting with the samples collected on 5/3/16 from the absorber exit, the nitrosamine emissions were calculated at 13.45 and 9.18 $\mu\text{mol}/\text{Nm}^3$. The lab spike recovery was very good at 88.4%, and the field blank did not show any ambient nitrosamines during sampling or contamination during sampling or analysis.

Exhibit 7.5.7. Nitrosamine Emissions Summary from H3-1 Testing Campaign.

Sampling Date	^a Arrival Date	ID	Location	Average NOx (ppm)	Nitrosamine Emissions ($\mu\text{mol}/\text{Nm}^3$)	Blank Amount	Spike Amount (nmol ^b NA)	Hitachi Analysis (nmol/NA)	Spike Recovery
5/3/16	5/9/16	Set #1	Absorber	29.5	13.45				
		Set #2	Absorber	29.5	9.18				
		Field Blank	-			^c ND			
		Lab Spike	-				1.418	1.253	88.4%
5/6/16	5/9/16	Set #1	Absorber	21.9	0.0543				
		Field Blank	-			ND			
		Lab Spike	-				1.418	1.395	98.4%
5/10/16	5/16/16	Set #1	Absorber	25.7	8.15				
		Set #2	Absorber	25.7	17.34				
		Lab Spike	-				2.837	0.377	13.3%
5/11/16	5/16/16	Set #1	Secondary Stripper	-	0.354				
		Set #2	Secondary Stripper	-	0.393				
		Matrix Spike	-				1.310	0.172	10.2%
6/8/16	6/13/16	Set #1	Absorber	136	51.8				
		Duplicate	Absorber	136	54.1				

^aArrival at Hitachi in Japan for analysis. ^bNA – Nitrosamine. ^cND - Not detected (LOD values for Hitachi analysis not provided)

A single sample was collected at the absorber exit on 5/6/16 due to an operational issue that moved the system away from steady state not allowing a second duplicate sample to be collected. The nitrosamine emission level on this sample was very low at 0.05 $\mu\text{mol}/\text{Nm}^3$. Again, the lab spike recovery was very good at 98.4% and the field blank did not show any ambient nitrosamines.

Another set of samples was collected on 5/10/16 at the absorber exit that yielded nitrosamine emission levels of 8.15 and 17.34 $\mu\text{mol}/\text{Nm}^3$ respectively. While these values are in line with the samples collected on 5/3/16, these results are suspect due to the poor recovery of the lab spike at only 13.3%. Poor recovery (10.2%) was also observed with the matrix spike that accompanied the samples collected on 5/11/16 from the secondary stripper exit. Hitachi was contacted to reconcile the poor spike recoveries and potentially re-run these samples, however UK CAER was informed that the TEA analyzer that performed the analysis was no longer operating correctly and had been returned to the manufacturer for repairs. Repair of the analyzer was not complete in a timely fashion to allow re-analysis of the samples. Finally, the single sample was also collected on 6/8/16 and split into 2 bottles to serve as a duplicate. The two samples show very good agreement, but at the highest observed emission levels of 51.8 and 54.1 $\mu\text{mol}/\text{Nm}^3$.

8) CAER SOLVENT CAMPAIGN

A solvent campaign was conducted with the CAER solvent from 8/4/16 – 10/6/17 with an accumulation of 976 operating hours. The campaign was carried out in phases, not continuously and consisted of an initial parametric study followed by a long-term study during which the solvent stability, degradation, and emissions were examined. During the parametric studies, operational parameters were varied as in previous campaigns to determine their impacts on the solvent performance and particularly on the energy of regeneration. The main parameters varied and the ranges tested are shown in **Exhibit 8.0.1**. For a given test condition, the experiment was conducted to achieve target 90% CO_2 capture by mainly adjusting the steam flow rate to the reboiler. After reaching steady state, conditions were maintained for 2 hours and liquid samples were collected in the middle of the duration from SP-1, SP-2 and SP-3 (shown in **Exhibit 6.0.2**). The solvent performance (CO_2 capture efficiency and solvent regeneration energy) was analyzed by averaging process parameters over the steady state period.

Exhibit 8.0.4. CAER Solvent Parametric Campaign Operating Conditions.		
Absorber Liquid/Gas Flow Rate Ratio, L/G (kg/kg)	Primary Stripper Pressure (psia)	Inlet CO_2 Concentration (vol%)
3.5-5	30 and 36	14 and 16

8.1 Parametric Impacts on Solvent Regeneration Energy

During the parametric tests, the L/G, the inlet CO_2 concentration to the absorber and the stripper pressure were varied to determine their impacts on the solvent regeneration energy. These effects are shown in **Exhibits 8.1.1 - 8.1.3**. As shown in **Exhibit 8.1.1**, increasing the L/G ratio increased the energy of regeneration at the various conditions as highlighted with the blue arrows. Reducing the L/G ratio from 5 to 4, resulted in about 12% energy savings. **Exhibit 8.1.2** shows that increasing the inlet CO_2 concentration from 14% to 16 % generally resulted in a reduction of the

regeneration energy as indicated by the downward red arrows. The effect is clearly observed in both cases at the lower stripper pressure run at 30 psia and seem to be diminished at the higher stripper pressure run at 36 psia.

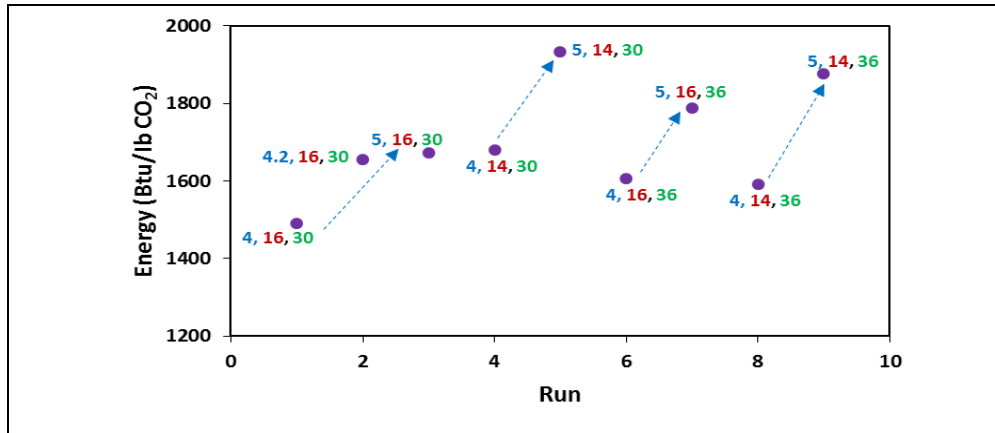


Exhibit 8.1.1. Effect of L/G ratio energy of regeneration. 3 numbers in exhibit for the different run conditions are L/G (blue), inlet CO₂ concentration (vol% - red), and stripper pressure (psia – green) respectively.

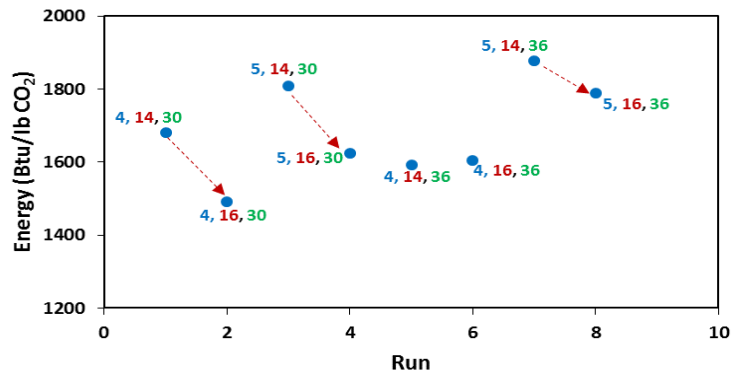


Exhibit 8.1.2. Effect of inlet CO₂ concentration on energy of regeneration.

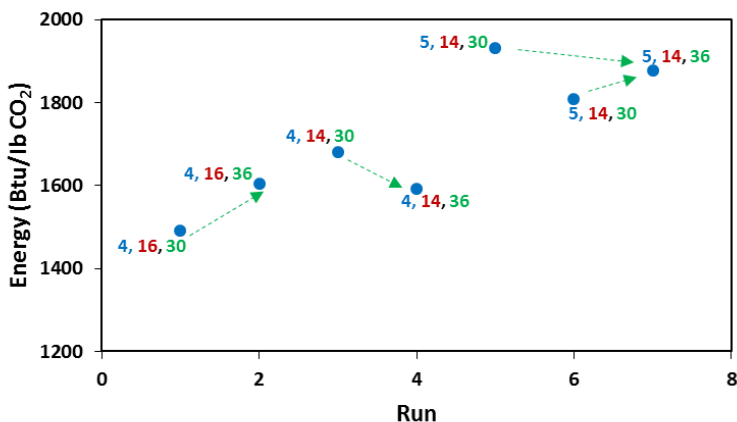
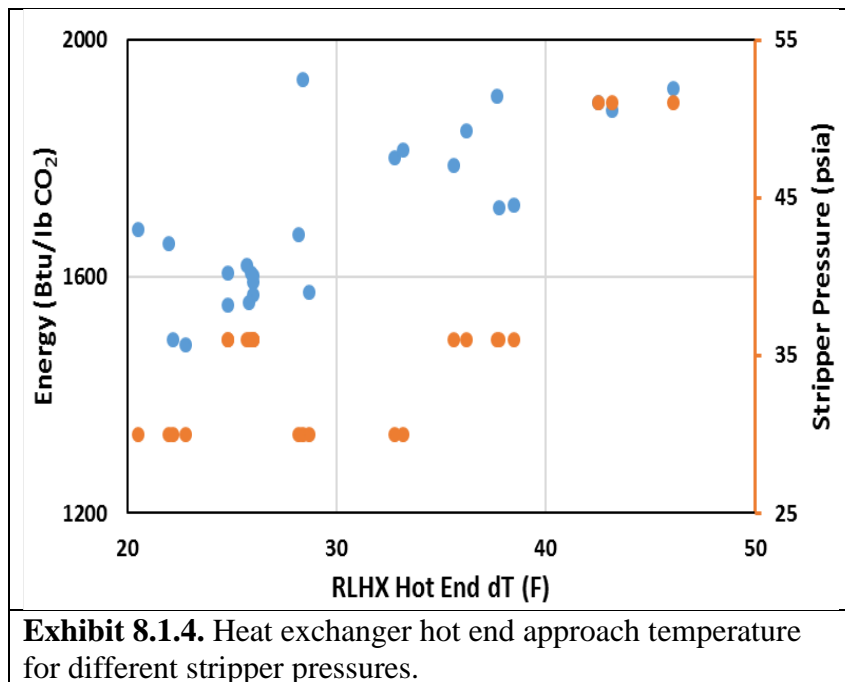


Exhibit 8.1.3. Effect of stripper pressure on energy of regeneration.

The impact of the stripper pressure on energy of regeneration did not follow a particular trend as shown in **Exhibit 8.1.3**. The hot end approach temperature for the L/R HXER increased with increased stripper pressure as shown in **Exhibit 8.1.4**. The increased stripper pressure resulted in higher stripper bottom temperatures which results generally in a higher approach temperature for the fixed size of the L/R HXER. For a given stripper pressure, this increase in approach temperature corresponds to an increased energy of regeneration. The effect of the stripper pressure could therefore be appropriately assessed if comparable approach temperatures in the L/R HXER were obtained as noted by Frimpong et al.(2019).



It must be noted that the trend observed for the impact of the stripper pressure was also not as definitive in the H3-1 campaign due to the observed variation in the approach temperature. While increasing the inlet CO₂ concentration resulted in energy reduction for the CAER solvent (see **Exhibit 8.1.2**), for H3-1, an increase in energy was rather observed. To absorb the additional CO₂ from the inlet concentration increase for a given L/G, leaner solvents have to be returned to the top of the absorber which is achieved through a balance of providing extra heat in the reboiler and the extent of additional stripping obtained from the secondary stripper. An energy benefit is realized where the increased concentration results in a mass transfer enhancement for rich solutions at the bottom of the absorber which require minimal additional heat input to the reboiler. Since multiple process factors have to be considered, the one-factor analyses as presented here is inherently limited in establishing definitive trends and a more holistic approach capable of examining multiple parametric effects is necessary (Frimpong et al., 2019).

8.2 Multi-Parametric Impact on Regeneration Energy and Loading

The parametric studies of the solvent were done by fixing process parameters such as L/G, inlet CO₂ concentration, stripper pressure, solvent temperature to secondary stripper at pre-determined set points to assess their impacts on solvent performance. Other parameters which can also impact operations are ambient temperature dependent (e.g., cooling water temperature, secondary stripper air temperature) and therefore vary during the course of the runs. Approach temperatures in heat exchangers and heat rejection for example, in the heat-integrated process can vary as a result, affecting many process parameters and solvent performance as a whole. Performing the one-parameter effect analysis, such as determining impact on stripper pressure on energy of regeneration with uncontrollable variations in other process parameters can be challenging. A statistical approach was therefore adopted that allowed multiple parameters to be examined simultaneously.

The statistical evaluation was done by defining a response variable Y, (e.g., regeneration energy or solvent loading) and assessing the impacts of parameters of choice, the predictor variables, X_i, (for i = 1...n, n being the number of variables) to determine those that have a real effect on Y. The effect is determined using a null hypothesis testing where based on a multi-regression analysis a relation of the form $Y = \beta_i X_i + C$ is obtained; C is a constant and the β_i are parameter estimates based on which a *p-value* is assigned for how significant each X could be on predicting Y. The analyses were performed at a significance level of 5% using the JMP statistical software. For a *p-value* of 0.05 or less, the independent variable was considered to have a significant impact on the response. This approach was used solely to screen multiple parameters to determine their impacts and not for any quantitative prediction.

The analysis was performed for the CAER parametric campaign to determine process parameters that had a significant impact on regeneration energy and rich carbon loading. **Exhibit 8.2.1** shows the process parameters that were screened in each case to determine their effects. As shown in **Exhibit 8.2.2.**, the liquid circulation rate, the inlet CO₂ concentration and the stripper bottom temperature had an impact on the regeneration energy of the solvent. The liquid circulation rate impacts the sensible heat of the solvent which correlates with the energy of regeneration. The inlet CO₂ concentration as discussed in Section 8.1 influences how lean the solvent returned to the absorber must be stripped to attain target 90% capture and therefore affects the heat required for regeneration. The stripper bottom temperature is a function of the operating pressure and steam supplied to the reboiler to regenerate the solvent. **Exhibit 8.2.3** indicates the main predictors for the rich loading of the solvent are the lean alkalinity, lean loading and the inlet CO₂ concentration which all reflect the extent of CO₂ uptake by the solvent and hence the correlation with the rich loading. It is worth noting that the relative significance of these predictor variables on impacting regeneration energy or rich loading may vary for different solvent campaigns. However, approach has proven useful in providing insights into understanding differences in solvent behavior, performance and process effects like intercooling (Frimpong et al., 2019).

Exhibit 8.2.1. Screening process variables for impact on regeneration energy and rich loading.

Response	Predictor Variables
1. Regeneration Energy	Stripper bottom temperature Stripper overhead temperature Absorber bottom temperature Intercool dT Lean loading to absorber Rich loading to absorber Liquid circulation rate Inlet CO ₂ concentration
2. Rich Loading	Lean alkalinity Lean loading to absorber Lean inlet temperature Flue gas temperature Intercool return temperature Inlet CO ₂ concentration Liquid circulation rate

Exhibit 8.2.2. Impact of process variables on regeneration energy of solvent.

Source (Variable)	p-value
Liquid circulation rate	0.0009
Inlet CO ₂ concentration	0.0285
Stripper bottom temperature	0.0285
Intercool dT	0.2389
Lean loading	0.3575
Rich loading	0.6752
Stripper overhead temperature	0.7905
Absorber bottom temperature	0.7938

Exhibit 8.2.3. Impact of process variables on rich loading of solvent.

Source (Variable)	p-value
Lean alkalinity	<0.00001
Lean Loading	0.0076
Inlet CO ₂ concentration	0.0206
Intercool return temperature	0.2614
Lean inlet temperature	0.6075
Flue gas inlet temperature	0.6405
Liquid circulation rates	0.9056

8.3 Varying CO₂ Capture Efficiency and Impacts on Regeneration Energy

During the CAER Solvent campaign, experiments were performed to determine how varying the capture efficiency for CO₂ impacts the energy of regeneration. This is in attempt to address the question of the whether the energy penalty of the capture process could be reduced, and to what extent, if 90% capture is not the target. A one-variable approach was used in the experiments performed; that is varying lean solvent carbon loading via managing heat input to reboiler to vary the capture duty without changing any other process conditions. It must be pointed out that, minimizing the energy of regeneration requires optimizing different process conditions as in using appropriate liquid to gas ratios for a given capture efficiency for example. Therefore, the tests done were by no means exhaustive but meant to provide some general insights into what could be expected.

Experiments were done at fixed conditions for stripper pressure, inlet CO₂ concentration, L/G ratio, secondary air and desiccant flow rates etc. The steam flow to the reboiler was initially set to obtain desired capture. After steady state was obtained at test conditions liquid samples for the rich sample from absorber (SP1), lean from the primary stripper (SP2) and extra lean from the secondary stripper (SP3) were taken. To vary the CO₂ capture efficiency, the quantity of steam input to the reboiler was changed while maintaining all other operating conditions constant. Two L/G ratios and inlet CO₂ concentration were tested. A summary of test conditions is shown in **Exhibit 8.3.1**.

Exhibit 8.3.1. Test Conditions for Varying CO ₂ Capture.	
Parameter	Value/Range
Lean inlet temperature	81-85 °F
L/G ratio	3.5, 4
Inlet CO ₂ concentration	14, 16 vol%
Stripper pressure	30 psia
Secondary stripper air flow	300 acfm
Liquid desiccant flow	40-45 gpm

Results

The effect of varied CO₂ capture duty on energy of regeneration was done at two L/G ratios and inlet CO₂ concentrations. As shown in **Exhibit 8.3.2**, the energy of regeneration was lowered for a capture efficiency close to 80% for the conditions tested. The same trend was observed for the different L/G ratios and inlet CO₂ concentrations with energy increasing with L/G ratio and reduced inlet CO₂ concentration. As reported in the previous section, liquid circulation rate and inlet CO₂ concentration were shown to significantly impact the energy of regeneration, **Exhibit 8.3.3**, and effects are similarly observed in the graph.

	<table border="1"> <thead> <tr> <th>Source (Variable)</th><th>P-value</th></tr> </thead> <tbody> <tr> <td>Liquid circulation rate</td><td>0.00002</td></tr> <tr> <td>Inlet CO₂ concentration</td><td>0.00114</td></tr> <tr> <td>Stripper bottom temperature</td><td>0.03341</td></tr> <tr> <td>Lean loading</td><td>0.30845</td></tr> <tr> <td>Rich Loading</td><td>0.48286</td></tr> <tr> <td>Stripper overhead temperature</td><td>0.84842</td></tr> </tbody> </table>	Source (Variable)	P-value	Liquid circulation rate	0.00002	Inlet CO ₂ concentration	0.00114	Stripper bottom temperature	0.03341	Lean loading	0.30845	Rich Loading	0.48286	Stripper overhead temperature	0.84842
Source (Variable)	P-value														
Liquid circulation rate	0.00002														
Inlet CO ₂ concentration	0.00114														
Stripper bottom temperature	0.03341														
Lean loading	0.30845														
Rich Loading	0.48286														
Stripper overhead temperature	0.84842														
Exhibit 8.3.2. Energy of Regeneration of CAER Solvent for Varying Capture Efficiency.	Exhibit 8.3.3. Variable Impact on Energy of Regeneration of Solvent.														

The energy of regeneration is comprised of the three components: the sensible heat, the heat of vaporization, and the heat of reaction of the solvent. The L/G ratio (liquid circulation rate) contributes directly to the sensible heat in the regeneration of the solvent. For a given L/G ratio, at higher than 80% capture, the solvent has to be stripped leaner to provide the capacity for the solvent to absorb at that higher efficiency requiring increased steam input and consequently contributing to the higher energy. At the lower capture efficiencies, the increase in energy observed is due to the greater sensible heat loss from the low carbon cyclic capacity of the solvent. Though the lower capture efficiencies were obtained from a reduction of steam to the reboiler, the same L/G ratio used and the resultant increase in heat rejection contributed to higher energy per the amount of CO₂ captured. By appropriately tuning the L/G ratio for each desired capture (specifically at the lower capture efficiencies with lower L/G ratios), the observed energy of regeneration could be further reduced.

8.4 Degradation

Exhibit 8.4.1. MBT Inhibitor concentration present in the CAER solvent.	Exhibit 8.4.2. Events during CAER-B3 ~1000 run hour campaign.

Solvent degradation was studied and monitored during the testing campaign after the initial charging of the CAER solvent into the system. Amine make-up was added periodically to maintain the operational concentration near a total amine concentration of 35 wt % (5.2 mol/kg alkalinity). For this report, the HSS accumulation rates and organic degradation products were monitored through the end of the CAER testing campaign, a total of 976 operating hours (8/4/16 - 10/6/17). Operating hours are based on solvent flue gas contact time (when the flue gas blower was running and CO₂ was captured), and do not take into account process downtime. During the first 400 hours of the testing campaign, the solvent contained an oxidative degradation inhibitor, 2-Mercaptobenzothiazole (MBT). MBT is an oxygen radical scavenger and is therefore consumed over time. **Exhibit 8.4.1** shows the concentration of the inhibitor during the campaign. The inhibitor was consumed for 200 hours at which point more inhibitor was added to the solvent. The inhibitor was completely consumed around 400 hours; no more inhibitor was added after this point. Reclaiming also occurred periodically between 146-730 operational hours for a total of 73 hours. A slipstream of the solvent was also passed through the activated carbon filter for short period of time (46 hours). All the significant events related to solvent degradation that occurred during the 976 hour CAER campaign are represented in **Exhibit 8.4.2**.

Degradation analysis was performed on solvent samples collected after the absorber (CO₂ rich) in certified metal and inorganic analyte free HDPE bottles. Detection and quantitation of HSS was performed with a Dionex ICS-3000 IC system. Solvent samples were analyzed to identify and quantify polymeric degradation products with an Agilent 1260 Infinity HPLC system coupled with an Agilent 6224 TOF-MS. Elemental concentrations in the solvent were examined after acidic microwave digestion using ICP-MS (Agilent).

Detailed IC, LC-MS analysis conditions including IC-QC data and isotope masses from ICP-MS analysis are listed in the Appendix.

Results

The primary goal of this study was to understand the impact of flue gas contaminants on the CAER solvent and determine its stability during pilot testing of coal combustion flue gas. Due to the winter weather and other maintenance services the system was not ran continuously during this campaign. Overall, an increase in total HSS concentration was observed during periods of significant downtime when the solvent level was decreased to minimum circulation levels. The system volume reduction concentrated the amine loop during these outages, artificially raising the contaminant concentrations during these periods. When normal operation restarted, the solvent levels were returned to normal with the addition of water, thereby returning the contaminant levels close to their initial concentration. This concentration/dilution effect can be seen during short periods, but the overall trends are a better reflection of the total solvent degradation.

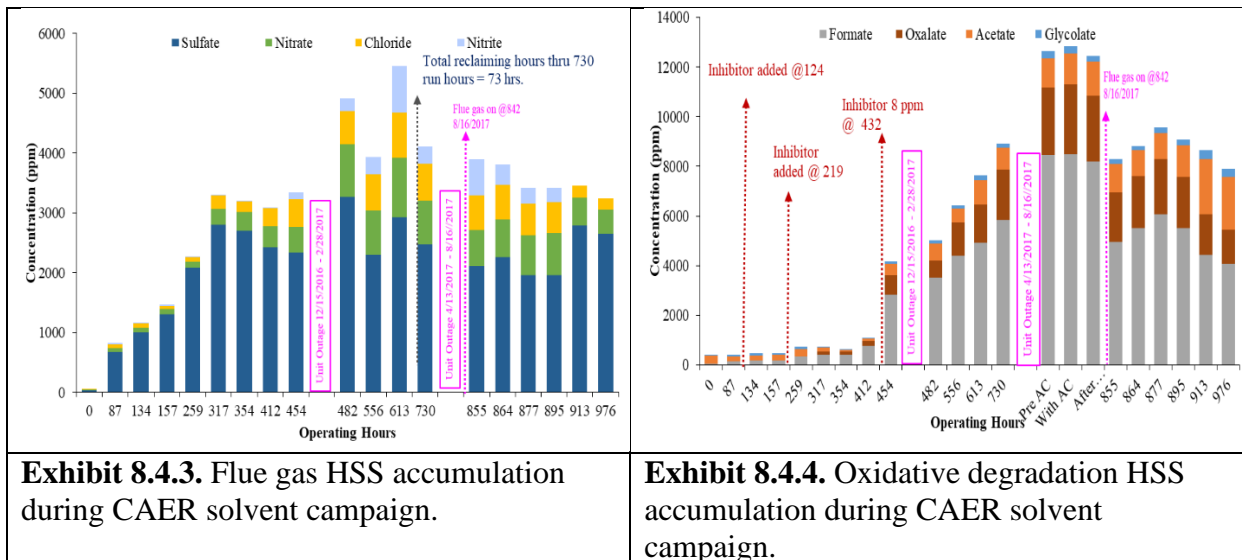


Exhibit 8.4.3. Flue gas HSS accumulation during CAER solvent campaign.

Exhibit 8.4.4. Oxidative degradation HSS accumulation during CAER solvent campaign.

Heat stable salts formed in the solvent and produced from coal flue gas is primarily a function of the flue gas composition, including residual SO₂ and NO_x. The flue gas from KU's Brown Station was treated of NO_x and SO₂ before being supplied to the small pilot CCS. The accumulation of the flue gas derived HSS during this CAER testing campaign is presented in **Exhibit 8.4.3** as concentration in the solvent (ppm) against operating hours. The flue gas SO₂ concentration entering the absorber was normally maintained below 5 ppm by polishing with soda ash in the pretreatment tower of the small pilot scale CCS. As expected, sulfate was the major HSS species observed. Even with the additional SO₂ polishing, sulfate had a steady accumulation rate and reached a maximum of 2646 mg/mL at the end of this monitoring period. The sulfate concentration was gradually increasing during this campaign till 317 operating hours when, due to some reclaiming, it decreased by approximately 500 ppm before the first unit outage. A closer examination of the HSS results requires splitting them into separate groups; HSS from flue gas and HSS from solvent oxidation. Chloride levels reached 182 mg/L, while nitrate concentration reached 410 mg/L. Interestingly, there was no nitrite detected at the end of campaign. This may be related to a change of the IC column which caused several peaks to shift, including nitrite, or a sign of nitrite oxidation to nitrate or consumption through some other side reaction such as nitrosamine formation.

Formation of oxidative HSS species from CAER solvent were examined and are shown in **Exhibit 8.4.4**. The major oxidative HSS is formate, which was expected and is used as an indication for overall solvent oxidative degradation. The total oxidative HSS at the end of the campaign reached 7908 ppm or approximately 0.71 wt. %. During this campaign, a higher oxidative HSS formation rate (28 ppm/hour) was observed after 412 hours due to depletion of MBT (oxidation inhibitor) in the solvent, versus a formation rate of 3 ppm/hr when the inhibitor was present. The optimum concentration of this inhibitor which would be required to sufficiently minimize amine oxidation, or the working/critical concentration, was calculated at < 60 ppm. Additionally, there was no clear reduction in oxidative HSS from application of the activated carbon filter.

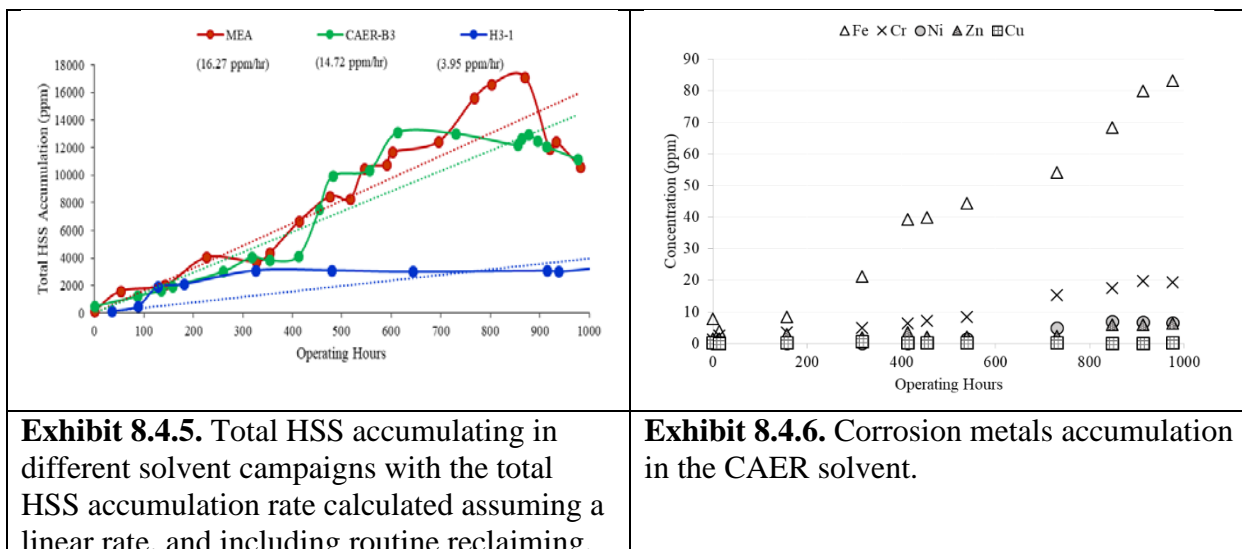


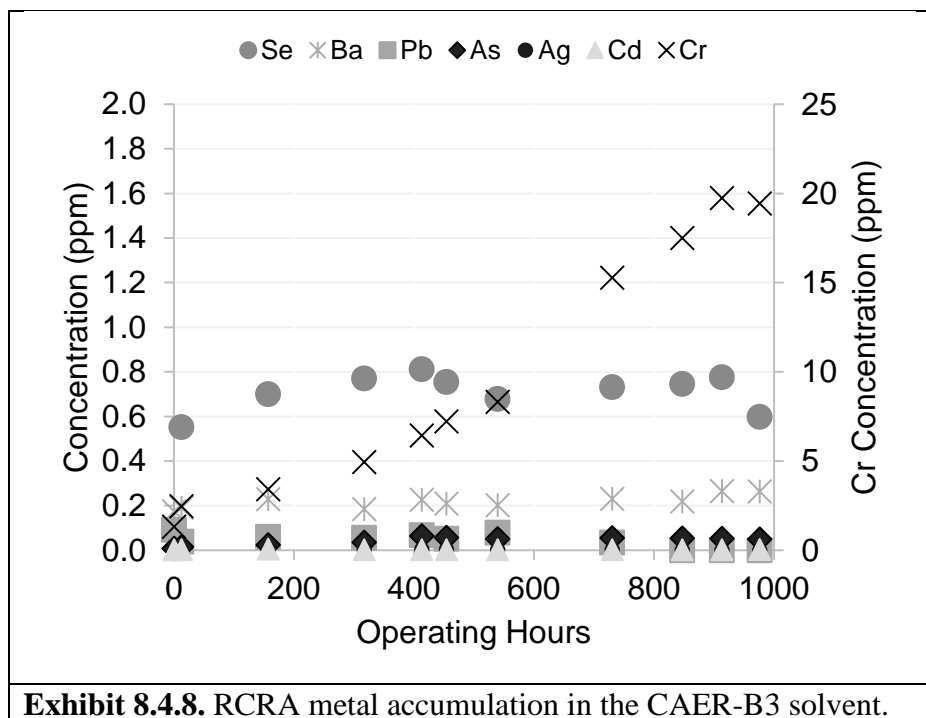
Exhibit 8.4.5 compares HSS level from the different solvent campaigns at comparable run time (~1000 hours). Total accumulation was only slightly higher during the MEA campaign compared to CAER solvent. As a reminder, the MEA solvent did not contain any inhibitor to reduce oxidation, whereas the CAER solvent contained an inhibitor, and the H3-1 likely also contained some type of oxidation/corrosion inhibitor. Metals can accumulate in process solvents from coal-combustion flue gas and by corrosion of structural components. Metal accumulation in the solvent can catalyze and accelerate amine degradation. Metals accumulations could also impact the cost of treating or disposing of spent solvent by exceeding hazardous waste characterization limits.

The metal accumulation from corrosion during the CAER solvent campaign are presented in **Exhibit 8.4.6**. The corrosion metals observed in the solvent were Fe, Ni, Cu, Zn and Cr. Fe and Cr accumulated at much higher concentrations than Ni, Zn and Cu. All the corrosion metals showed an increase in accumulation over the course of the testing campaign with the exception of Cu. The Cu was most likely carry over from previous campaigns where Cu was observed in the solvent. Fe had the highest accumulation rate of 0.08 ppm/hr suggesting that some component in the amine loop is corroding. Cr had the next highest accumulation rate at 0.018 ppm/hr. Ni and Zn did not show any significant accumulation, and neither reached levels above 7 ppm over the course of the campaign. One thing to note is that not all metals started with an initial concentration of 0 ppm. When the amine solvent as received was analyzed it showed low ppm levels of Fe, Zn and Cr, **Exhibit 8.4.7**. This could explain the initial concentrations of the corrosion metals.

Exhibit 8.4.7. Metals found in the solvent as received.

Purchased Amine	Cr (ppm)	Fe (ppm)	Zn (ppm)	Ba (ppm)	Pb (ppm)
Amine 1	0.73	1.23	0.25	0.08	0.02
Amine 2	1.00	1.04	3.33	0.10	0.03
Amine 3	0.80	4.19	1.40	0.17	0.05

The RCRA-8 (Cr, As, Se, Ba, Pb, Ag, Cd) minus mercury (RCRA 1976) were detected in the CAER solvent, **Exhibit 8.4.8**. The Cr concentration can be found on the secondary y-axis due to its high accumulation over the course of the campaign. As, Se, Ba, Pb, Ag, and Cd were all observed in the solvent, however in very low concentrations. None showed any significant accumulation over the course of the campaign, rather their concentrations remained relatively constant. Ag and Cd were observed always around the detection limits. Ba and Pb were found in the amine as received so they likely come from amine contamination. All the metals were observed below their RCRA limits with the exception of Cr.

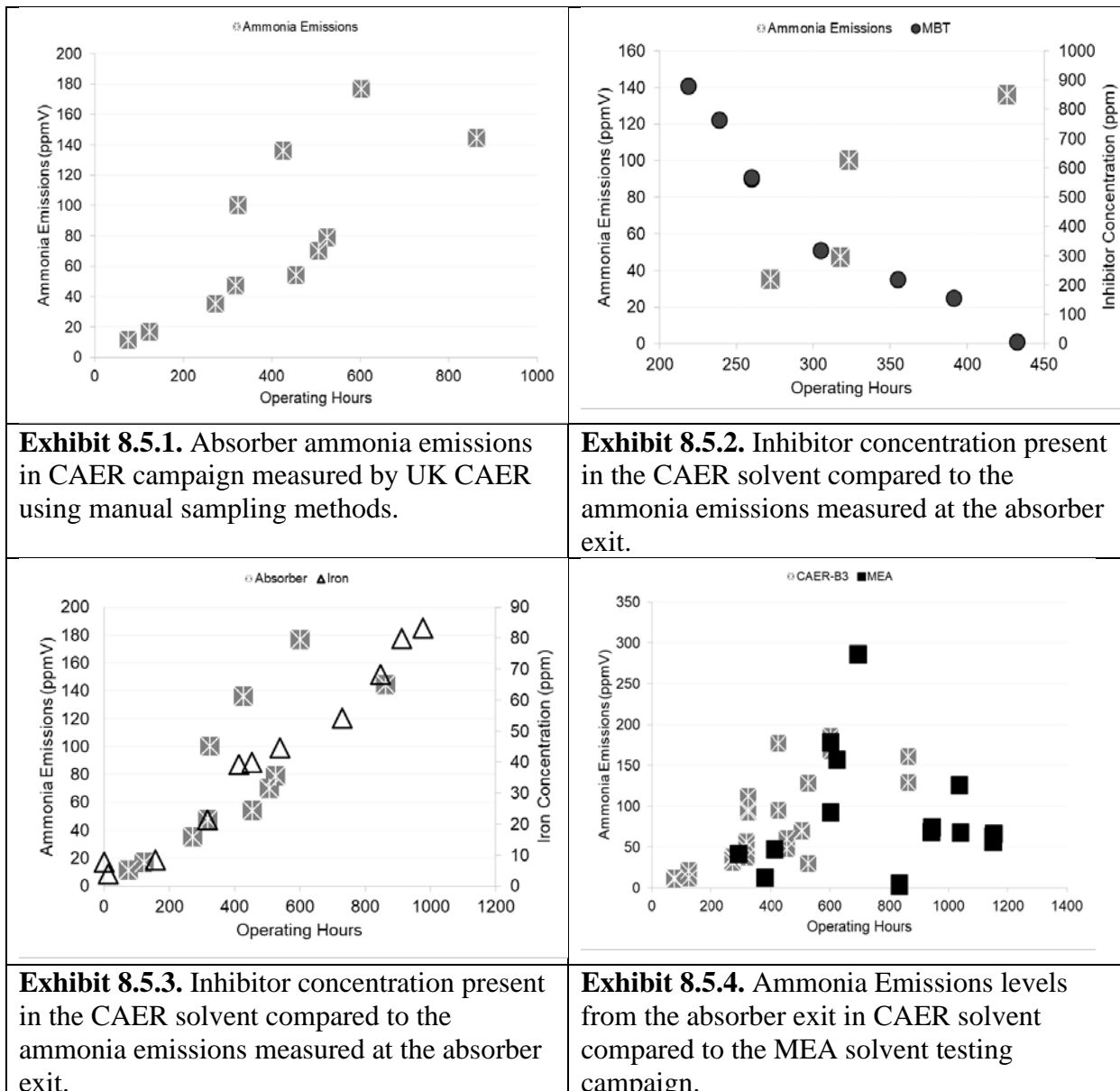


8.5 Emissions

Same as MEA and H3-1 campaigns, gas phase degradation products and amine emissions were collected using sampling methodology adapted from U.S. EPA Methods 1 and 5, and individual methods including EPA SW-846 Test Method 0011 for aldehydes, and CTM-027 for ammonia. Detection and quantitation of ammonia and amine samples were performed with a Dionex ICS-3000 IC system. Aldehydes were analyzed as 2,4-dinitrophenylhydrazine (2,4-DNPH) derivatives in a similar fashion to the methodology described in US EPA Method 8315A (1996) using an Agilent 1260 Infinity HPLC. Nitrosamine emission samples were collected with an impinger train containing a dilute sulfamic acid solution. Nitrosamines emissions samples were concentrated from the sample using SPE cartridges and analyzed using an Agilent Technologies 7890A GC with 7693 auto sampler and 5975C EI/MSD.

Results

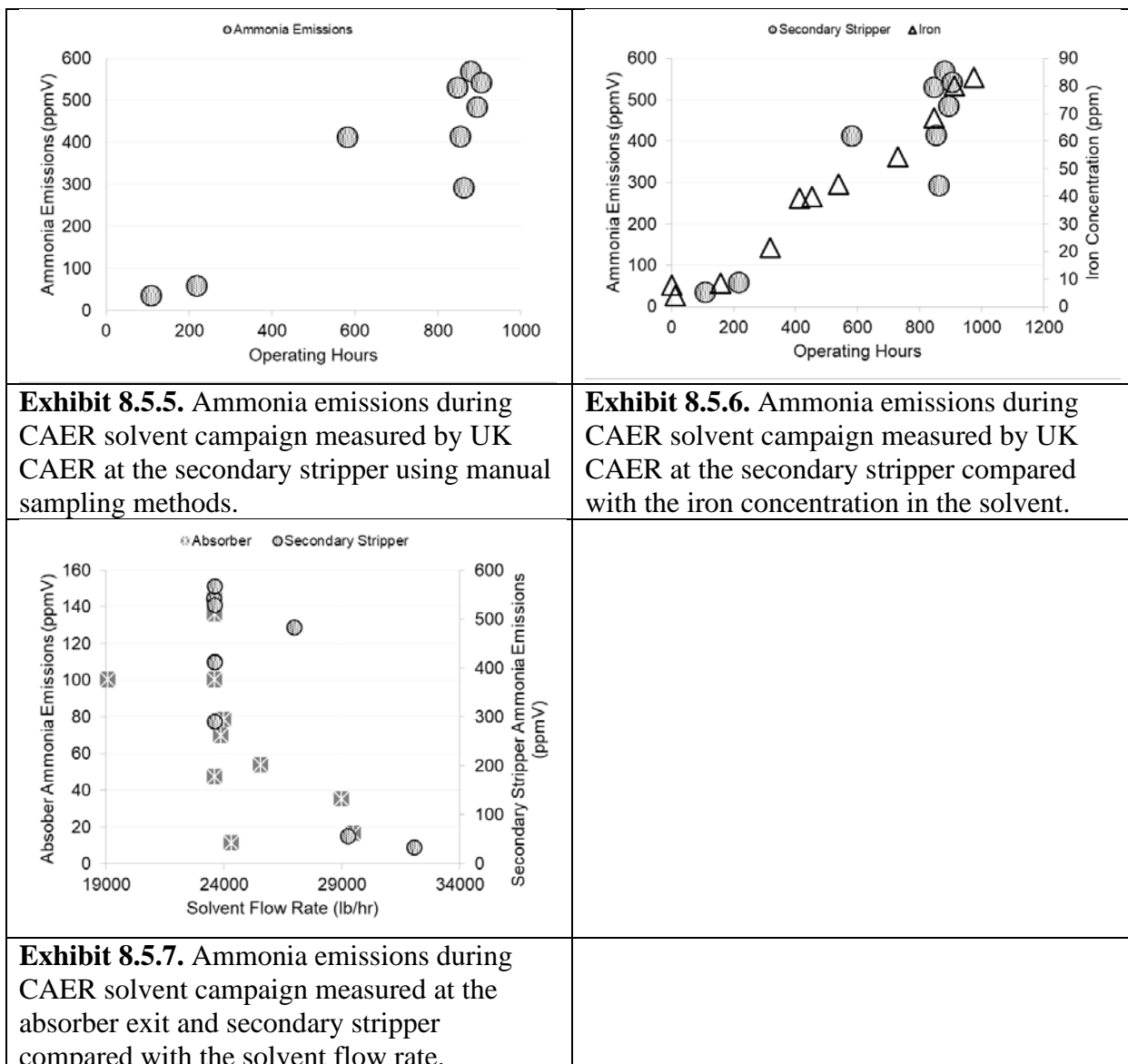
Emission samples were collected in this study during a variety of operation conditions including; (1) parametric testing conditions where major operating changes were intentionally imposed on the capture system, (2) daily operating changes during long-term testing when changes were related to power plant load following, local weather conditions, and miscellaneous system testing and (3) with and without the inhibitor present in the solvent.



Ammonia emissions from the absorber exit are presented in **Exhibit 8.5.1** in ppmV units. Ammonia emissions ranged from 10 ppmV to 180 ppmV over the course of the testing campaign. The ammonia emissions showed an increase in time throughout the campaign due to oxidative degradation. During the first 400 hours of the testing campaign the solvent contained an oxidative degradation inhibitor, MBT. During the time the inhibitor was present in the solvent we had relatively low ammonia emissions, and as the inhibitor was being consumed the ammonia emissions was increasing, **Exhibit 8.5.2**. This shows that inhibitor was effective in reducing oxidative degradation which leads to increased ammonia emissions.

In addition to oxidative degradation, the increase in ammonia emissions could be due to the accumulation of metals in the solvent. The impact of dissolved metals, specifically iron and copper, on oxidative degradation has been previously reported (Thompson et al., 2017), which has been shown to increase NH_3 production. The ammonia emission levels versus the iron concentration in the CAER solvent is shown in **Exhibit 8.5.3**, where a clear relationship between these two parameters can be seen. This trend is similar to those reported by Khakharia (2015) where ammonia emissions increased along with Fe accumulation in the solvent. There was no significant copper accumulation in the solvent during the campaign, therefore emissions levels were not impacted by copper.

The absorber exit ammonia emission were very similar to those observed during the MEA campaign, **Exhibit 8.5.4**. The inhibitor helped control ammonia levels up until 400 hours during the CAER campaign compared to MEA. From 400 to 800 operating hours the emissions levels for the two campaigns showed very similar trends. After 800 operating hours the MEA solvent was reclaimed, decreasing ammonia emissions, whereas the CAER solvent was not reclaimed during this time.

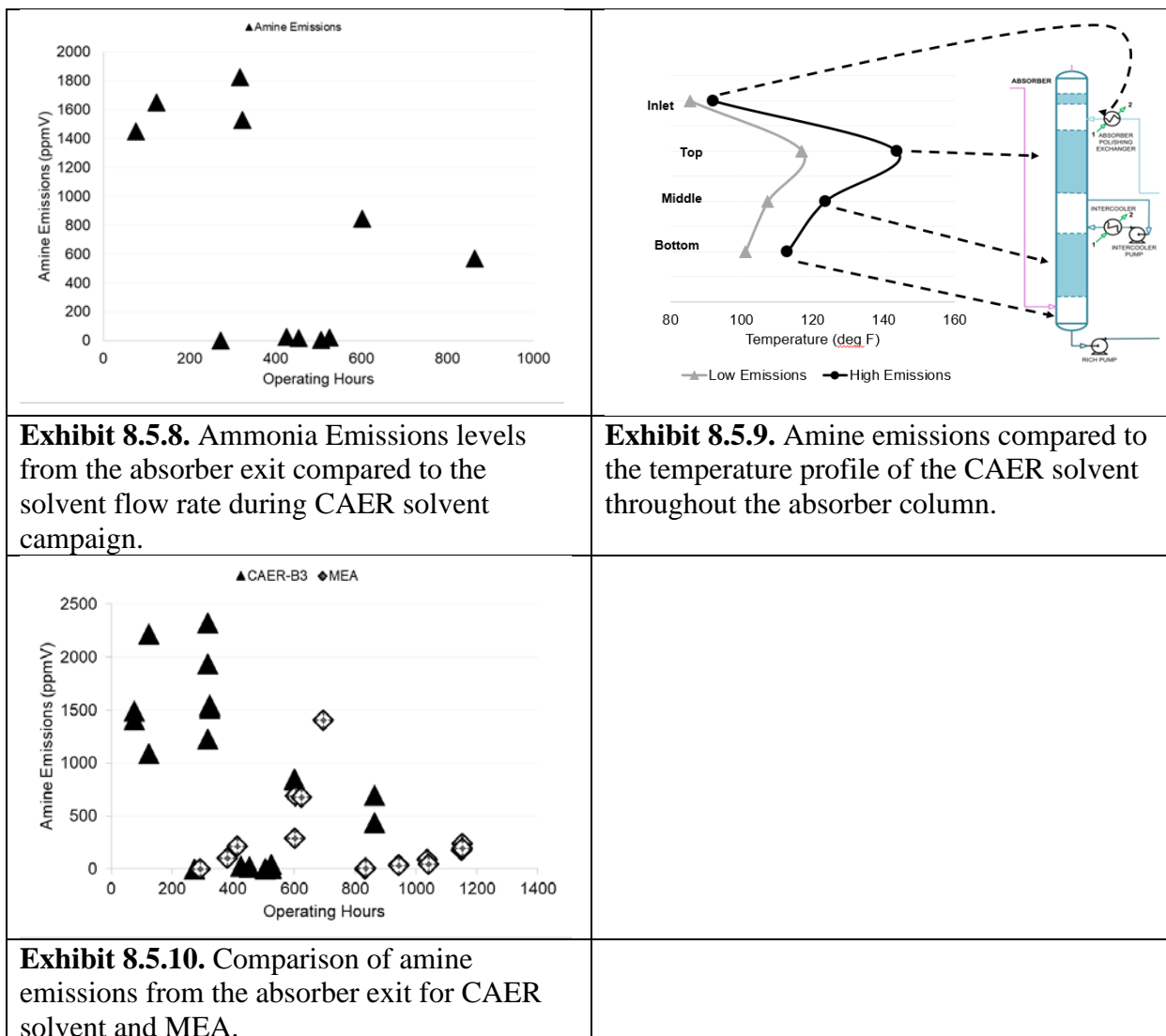


The secondary stripper is another location in our process where ammonia emissions can be observed. **Exhibit 8.5.5** shows the ammonia emissions levels collected at the secondary stripper. Ammonia emissions from the secondary stripper also show an increase over the course of the campaign ranging from 33 to 541 ppmV. Just as seen with absorber exit emissions, secondary stripper ammonia emissions have a strong relationship with the increasing iron concentration in the solvent, **Exhibit 8.5.6**.

In addition to solvent degradation and metals accumulation, some process conditions were found to have an impact on ammonia emissions levels. Process conditions that can have an impact on emissions include, solvent flow rates and solvent temperatures. A linear pairwise correlation (Pearson product moment correlation) analysis was completed, using the JMP 11.1.1 statistical software, with the process variables and emissions values. Averages of the process variables were calculated using values from times before and during emissions sampling to get a single value for each sampling day. Any process variables that were not stable during this time were excluded. The

values that are outputted from this correlation analysis are tabulated, **Exhibit 8.5.13**. The closer the value is to 1 the more associated together the variables are in the positive or negative direction.

One process condition that has an impact on the ammonia levels emitted from the absorber and secondary stripper was the solvent flow rate. **Exhibit 8.5.7** shows the relationship of the absorber (1° y-axis) and secondary stripper (2° y-axis) ammonia emissions with the solvent flow rate (x-axis). As the solvent flow rate increases, the ammonia emissions from the absorber decrease. This relationship has a strong negative correlation analysis value, -0.5796 for the absorber and -0.8207 for the secondary stripper (**Exhibit 8.5.13**). This relationship between can likely be explained by residence time, meaning that the slower the solvent is flowing the longer ammonia has to partition from the liquid to the gas phase leading to higher detected emissions levels. A correlation analysis was also done with the ammonia emissions levels from the absorber and the secondary stripper and the iron concentration of the solvent to verify the relationship. The correlation values can be found in **Exhibit 8.5.13**.



Amine emissions from the absorber exit are presented in **Exhibit 8.5.8**. Amine emissions ranged from 0.3 to 1827 ppmV throughout the course of the campaign. Unlike the ammonia emissions from the same location, the amine emissions did not show any clear trend. This is a case where the variation in emissions can likely be explained by the system conditions. The system condition that has the greatest impact on amine emissions at the absorber exit is the solvent temperature profile throughout the column. **Exhibit 8.5.9** is a representation of this observation. The solvent (liquid) temperature is measured at the inlet of the absorber, at the top of the packing, middle of the packing and at the sump as the solvent flows down the absorber giving a temperature profile. When our amine emissions are low this temperature profile is lower compared to when our emissions are higher. One explanation for this could be the formation of aerosols. Aerosols can be formed in the absorber column in carbon capture processes. When the temperatures in the absorber are high there is more amine in the vapor phase. This amine can then condense onto these aerosol particles and are emitted from the absorber, leading to increased amine emissions

When compared with the MEA campaign, **Exhibit 8.5.10**, amine emissions levels from the CAER solvent are generally within the same range. The only time this is not the case is during the first 200 hours of the CAER campaign where the high emissions levels can be explained by the high temperatures. Amine losses can occur from the secondary stripper as well. Since there should be a low concentration of aerosol nuclei in the ambient air used by the secondary stripper, amine emissions as aerosols from this location should be negligible. The observed amine emissions are most likely due to amine volatility. The condensate spray at the top secondary stripper will remove some of the vapor emissions, while the heat recovery exchanger on the exhaust will further cool the air and condense more water that will also help capture more of the amine vapor. Therefore, the total amine emissions from the air stripper should be much lower than those from the absorber.

Emission samples collected after the heat exchanger in **Exhibit 8.5.11** show amine emissions from this location. The emissions levels from this location ranged from 7-58 ppmV and do show that they are generally lower than emissions from the absorber. Just as seen from the absorber, these amine emissions values show some variability due to system conditions. In this case the system condition that had an impact on amine emissions levels was the lean solvent temperature entering the secondary stripper. This impact can be seen in **Exhibit 8.5.12** where amine emissions from the secondary stripper (y-axis) increases with increasing lean solvent temperature (x-axis). The correlations analysis had a strong positive value (**Exhibit 8.5.13**) indicating a good relationship between the two variables. This relationship was also verified by doing a correlation analysis with the amine emissions and the rich amine temperature entering the primary stripper. The amine temperatures in our system are related to one another therefore both temperatures should show the same trend with amine emissions. The correlation values for both temperatures were similar, **Exhibit 8.5.13**, which verifies the trend.

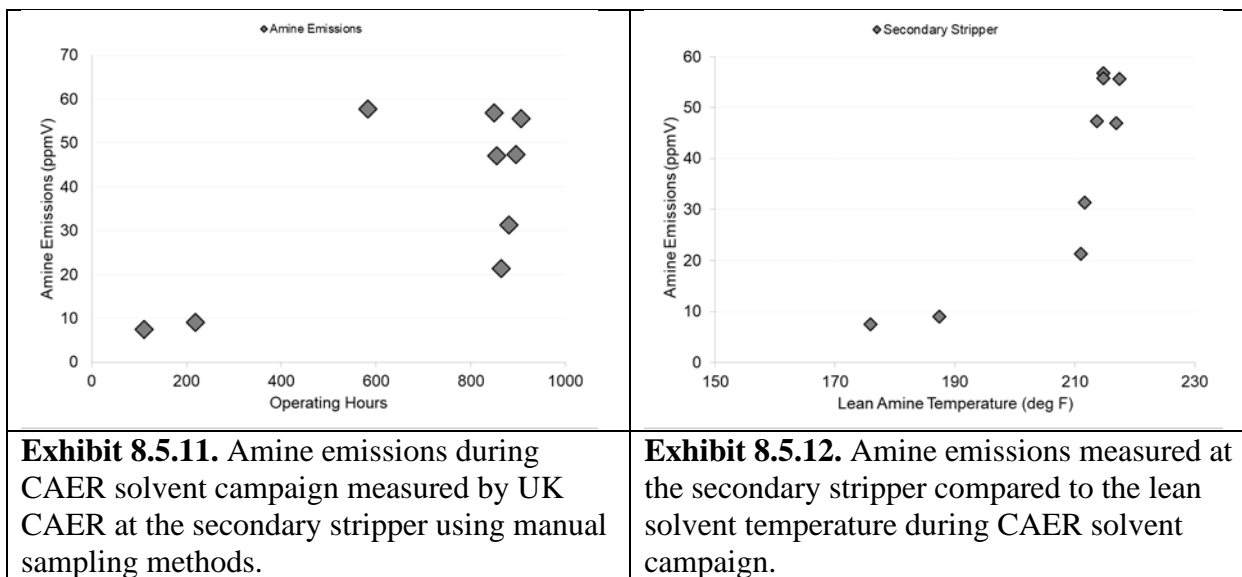


Exhibit 8.5.13. Pairwise correlation analysis values.

	Absorber Exit Ammonia Emissions	Absorber Exit Amine Emissions	Secondary Stripper Ammonia Emissions	Secondary Stripper Ammonia Emissions
Iron Concentration	0.7609	-	0.9202	-
Solvent Flow Rate	-0.5796	-	-0.8207	-
Lean Amine Temperature	-	-	-	0.8553
Rich Amine Temperature	-	-	-	0.8320

In addition to ammonia and amine emissions, aldehyde and nitrosamine emissions are also measured from the absorber exit and secondary stripper. The main aldehydes of interest are formaldehyde and acetaldehyde as they have been reported as degradation products. **Exhibit 8.5.14** shows the ranges of the observed aldehydes from each location in ppmV. The formaldehyde and acetaldehyde emissions values from the absorber are similar to those observed during the MEA campaign. Propionaldehyde emissions from the absorber were observed for the first time during this solvent testing campaign, however in very low quantities. Secondary stripper aldehyde emissions cannot be compared with the MEA campaign since no significant sampling was done from that location during the MEA campaign. However, the emissions result from the secondary stripper are higher than those from the absorber and propionaldehyde is observed above our limit of detection in all the samples taken.

Exhibit 8.5.14. Aldehyde emissions collected from the absorber exit and the secondary stripper.		
	Absorber Exit (ppmV)	Secondary Stripper (ppmV)
Formaldehyde	0.040 – 0.775	0.380 – 0.760
Acetaldehyde	0.752 – 2.303	17.109 - 18.612
Propionaldehyde	<0.011 – 0.039	0.185 – 0.247

A total of ten nitrosamine emission samples were collected from the absorber exit and two were collected from the secondary stripper. Eight distinct nitrosamines were examined in detail. In all the collected samples, no nitrosamines were identified above the calculated limits of quantitation (LOQ). **Exhibit 8.5.15** shows the limit of quantitation ranges, in the high parts per trillion (pptV) to low parts per billion (ppbV), for the individual nitrosamines calculated from the combined sampling, sample preparation and analysis procedures.

The same sulfamic acid used for sampling was spiked with a known amount of nitrosamines and worked up in the same manner as the samples. This was for quality control and assurance purposes as well as to test the validity of the analysis method. The lab spike recoveries were good and ranged from 82% to 120%. The field blanks did not show any ambient nitrosamines during sampling or contamination during sampling or analysis.

Exhibit 8.5.15. Nitrosamine emissions collected from the absorber exit and the secondary stripper.		
Nitrosamine	Absorber Exit	Secondary Stripper
N-nitrosopiperidine (NPIP)	0.054 - 0.112	0.047 - 0.055
N-nitrosodimethylamine (NDMA)	0.083 - 0.125	0.073 - 0.086
N-nitrosomethylethylamine (NMEA)	0.070 - 0.227	0.061 - 0.072
N-nitrosodiethylamine (NDEA)	0.060 - 0.105	0.053 - 0.062
N-nitrosodipropylamine (NDPA)	0.047 - 0.115	0.041 - 0.049
N-nitrosomorpholine (NMOR)	0.211 - 0.382	0.273 - 0.233
N-nitrosopyrrolidine (NPY)	0.062 - 0.089	0.054 - 0.063
N-nitrosodibutylamine (NDBA)	0.039 - 0.149	0.034 - 0.040

Conclusion

The overall solvent emissions from the CAER solvent testing campaign were comparable to those of the MEA solvent testing campaign. Ammonia emissions increased with time due to solvent degradation and the degradation inhibitor in the solvent helped at the beginning of the campaign. The ammonia emissions were also strongly correlated with the accumulated concentrations of dissolved iron in the solvent as well as a process conditions. The variability in amine emissions were as a result of process conditions and aerosols. Process conditions will need to be monitored to manage amine emission. Solvent oxidation in the form of aldehyde emissions levels were low and observed at both sampling locations. Nitrosamine emissions were not observed above the low ppbV detection limits calculated during this testing campaign.

9) POST MODIFICATION – PROPRIETARY SOLVENT C CAMPAIGN

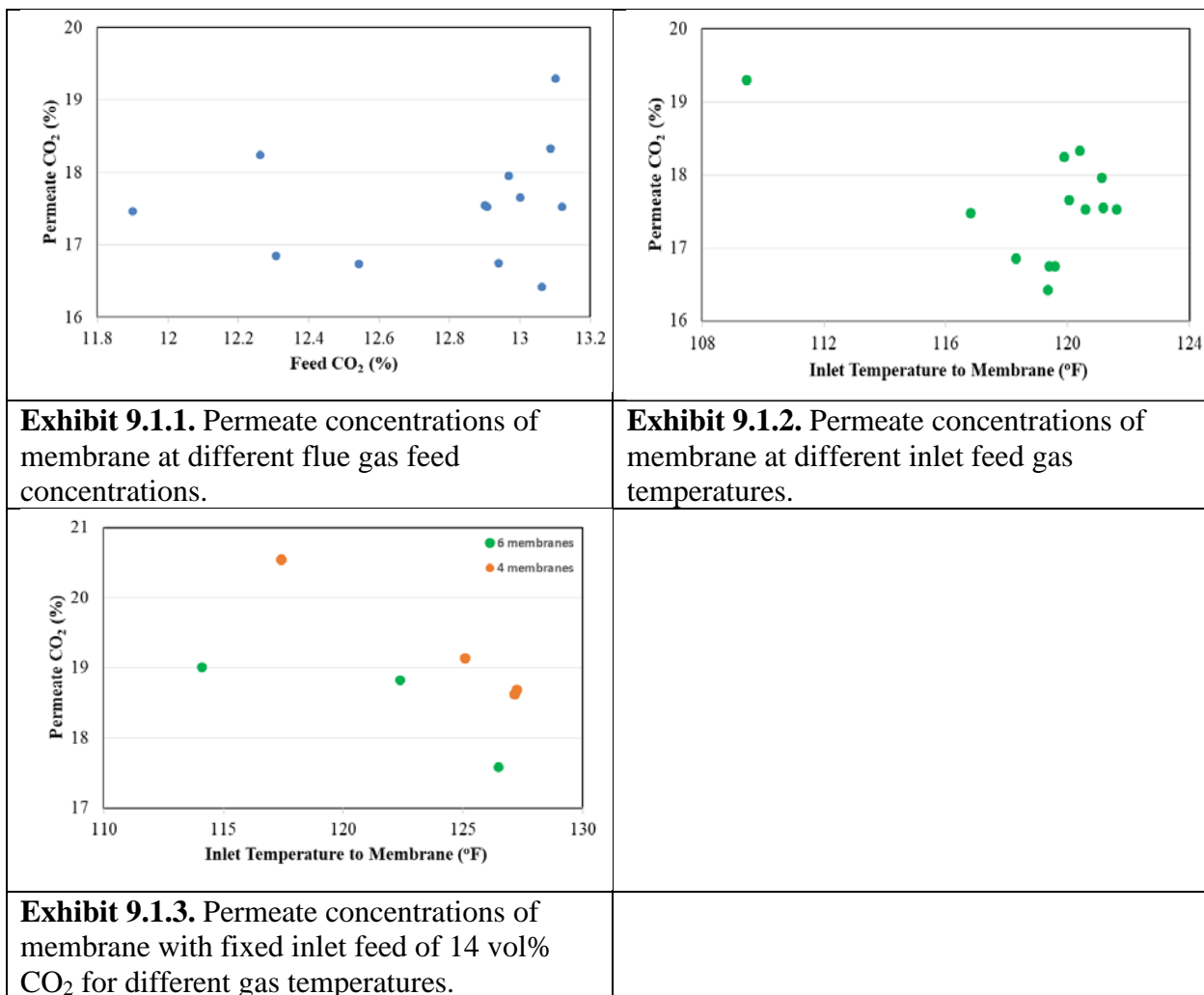
After the addition of the membrane separation unit and water wash system, their impacts on process performance were evaluated with Proprietary Solvent C. The membrane was used in a hybrid process to pre-concentrate CO₂ in the flue gas to a higher concentration permeate stream fed to the bottom of the absorber to enhance mass transfer in the absorption of the gas by the solvent. The residue stream from the membrane was fed to the lower section of the top packing of the column. The process was evaluated for the performance of the membrane and the comparative performance of the solvent with respect to solvent rich loading and the energy of regeneration with and without the membrane. The effectiveness of water wash system was assessed from experiments that monitored solvent emissions from the outlet of the absorber compared to the water wash column.

9.1 Membrane Performance

Tests were performed with flue gas fed to the membrane at the desired flow rate with two blowers in series. The first blower (B-100) feeds flue gas to the pre-treatment tower after which it is fed to the membrane with the additional blower (B-200). The vacuum pump on the permeate stream of the membrane provides needed driving force across the membrane, and the pre-concentrated CO₂ permeate is fed to bottom of the lower section packing of the absorber. The residue stream, with a lower CO₂ concentration, was fed at the bottom of the high section of packing of the absorber column which is at a higher stage with respect to the permeate stream. During the tests, the feed gas temperature, feed pressure to the membrane and the vacuum pressure were recorded. The feed CO₂ to the membrane and resultant permeate CO₂ concentrations were also measured using gas analyzers. Experiments were also done where two out of the six membranes in the module were shut off (off-line) to reduce available surface area and increase the vacuum by reducing the membrane permeance as a means to improve the permeate purity and increase the CO₂ concentration.

Results

For varying inlet flue gas feed CO₂ concentration to the membrane, the permeate CO₂ concentrations ranged from ~16.5-19 vol% (**Exhibit 9.1.1**). For these tests with varying inlet feed CO₂ concentrations as received from the plant (without CO₂ doping), the graph shows averages for the inlet and permeate CO₂ concentrations over a duration of 3-4 hours. The temperature of the inlet feed gas to the membrane impacts the permeance and selectivity of the membrane. The permeate CO₂ concentration is shown for the different inlet feed temperatures to the membrane in **Exhibit 9.1.2**. The highest permeate concentration observed was for a test condition where ambient conditions cooled the flue gas significantly.



For a steady operation for performance testing of the solvent, a fixed inlet feed concentration of 14 vol% was fed to the membrane after doping the flue gas from the plant with recycled stripped CO₂. To improve the permeate purity, 4 sets of membranes were used instead of the total 6 by closing valves to a pair. **Exhibit 9.1.3** shows typical permeate concentrations of ~19-20 vol% could be obtained with the fixed inlet feed of 14 vol%. It should be noted that at a given inlet feed condition, with 4 membranes (reduced permeance of gas), a slight increase (within a percentage point) could be obtained relative to when all membranes are used. As noted previously, lower inlet gas feed temperatures result in higher permeate CO₂ concentration as similarly observed in the graph for both scenarios of testing. Ambient conditions reduce inlet feed temperatures to 114 and 117 °F compared to the typical test conditions at 122-127 °F. **Exhibit 9.1.4** shows representative feed gas conditions to the membrane, the product streams and the vacuum. With 4 membranes, a greater vacuum was obtained and similar at reduced inlet gas inlet temperatures. The improved driving force contributed to increase the permeate purity.

Exhibit 9.1.4. Representative membrane test conditions with 14 vol% CO₂ feed.

	Inlet gas temp. (°F)	Permeate CO ₂ conc. (%)	Reject CO ₂ conc. (%)	Feed pressure (psia)	Vacuum pressure (psia)
6 membrane Units	114	19.0	10.7	16	5.3
	122	18.8	11.0	15.9	5.7
	126	17.6	-	-	6.0
4 membrane Units	125	19.2	-	-	4.6
	127	18.7	10.9	16.7	4.7
	127	18.6	10.9	16.7	4.6
	117	20.6	10.2	16.6	4.1

9.2 Proprietary Solvent C Tests with Hybrid Process

Tests were performed at L/G of 2.5 and 3.2 and at stripper pressures of 24 and 30 psia. The tests were mostly conducted with a fixed inlet CO₂ concentration of 14 vol% to the membrane achieved by doping the flue gas from the plant with recycled CO₂ from the primary stripper. A few experiments were also done with varying inlet gas concentrations. The target capture was set at 90% and steady state was maintained for 2 hours with liquid samples taken for the extra lean from the bottom of the secondary stripper (SP1), lean from the bottom of the primary stripper (SP2) and rich sample from the bottom of the absorber (SP3) in the middle of the steady period. The process data was analyzed over the steady state period to determine the solvent regeneration energy. This was compared with runs without the membrane at similar conditions, some of which were done prior to the process modification to include the membrane.

Results

The specific reboiler duty of the solvent for L/G = 2.5 and stripper pressure of 30 psia with 14 vol% CO₂ inlet feed is shown in **Exhibit 9.2.1** and compared with runs without the membrane at similar conditions. **Exhibit 9.2.2** is a summary of corresponding test conditions and show some of the process variables such as inlet lean return temperature. The highlighted last run for the non-membrane experiment (6L) is a run after process modification while the others were runs prior to modifications during cold days. Run 9BmL (not included in graph for direct comparison) was at a lower feed CO₂ concentration (no doping). Generally, the ambient conditions and extent of heat recovery in heat exchangers and different sections of the process from flow rate changes of cooling water and liquid desiccants all contribute to the overall heat duty of the solvent, in particular rich solvent temperature at the absorber bottom accounting for some of the observed energy differences. Generally 10-15 °F higher rich solvent leaving the absorber was observed with the membrane operations, which could counteract driving force gained from increased CO₂ concentration resulting from membrane pre-concentrating.

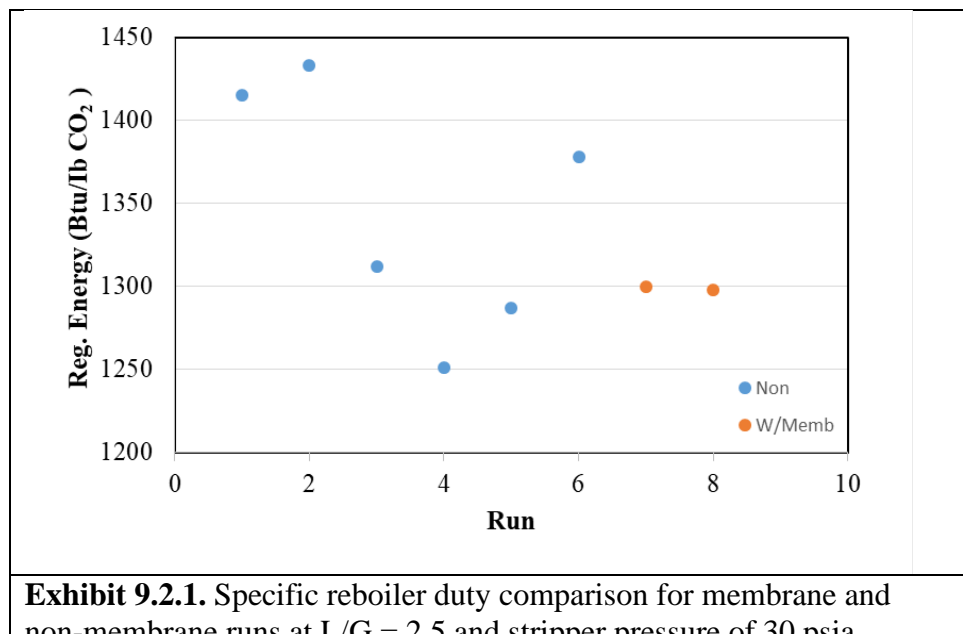


Exhibit 9.2.1. Specific reboiler duty comparison for membrane and non-membrane runs at L/G = 2.5 and stripper pressure of 30 psia.

Exhibit 9.2.2. Test conditions comparison for Proprietary Solvent C solvent at L/G = 2.5, stripper pressure = 30 psia.

	Run	Inlet CO ₂ (%)	Absorber Inlet Temp (°F)	Absorber Bottom Temp (°F)	Stripper Bottom Temp (°F)	Stripper Top Temp (°F)	Ambient Temp (°F)	% Capture	Energy (Btu/lb CO ₂)
Without Membrane	1B	14	93	109	248	205	33	92	1415
	2B	14	94	108	248	206	34	93	1433
	3B	14	94	111	246	207	38	92	1312
	4B	14	94	110	248	206	44	90	1251
	5B	14	92	110	247	206	44	90	1287
	6B	14	99	112	249	212	80	92	1378
Memb rane	7Bm	14	96	117	245	208	87	89	1300
	8Bm	14	102	119	247	210	87	91	1298
	9BmL	13	99	118	245	211	87	88	1338

Exhibit 9.2.3 also compares similar test conditions for the same L/G of 2.5 at a lower stripper pressure. At this circulation rate and these test conditions, as observed in **Exhibit 9.2.1**, there is marginal improvement in the specific reboiler duty from the pre-concentrating membrane. Run 5CmL is a membrane experiment at a lower inlet CO₂ feed concentration.

Exhibit 9.2.3. Test conditions comparison at L/G = 2.5, Stripper pressure = 24 psia.

	Run	Inlet CO ₂ (%)	Absorber Inlet Temp (°F)	Absorber Bottom Temp (°F)	Stripper Bottom Temp (°F)	Stripper Top (°F)	Ambient Temp (°F)	% Capture	Energy (Btu/lb CO ₂)
No Membrane	1C	14	69	102	237	196	45	90	1331
	2C	14	96	111	239	200	32	93	1410
	3C	14	95	109	238	202	76	92	1378
Membrane	4Cm	14	102	120	237	202	78	92	1312
	5CmL	13	99	119	235	203	87	89	1345

The graph in **Exhibit 9.2.4** is a comparison at a higher liquid circulation rate, (L/G = 3.2) at a stripper pressure of 30 psia with test conditions shown in **Exhibit 9.2.5**. It must be noted that for this higher liquid circulation rate, the temperature at the bottom of the absorber was significantly higher for the membrane runs as a result of reduced intercooling and could limit gas absorption in the bottom section of the absorber. This is discussed further when the temperature profiles are compared subsequently.

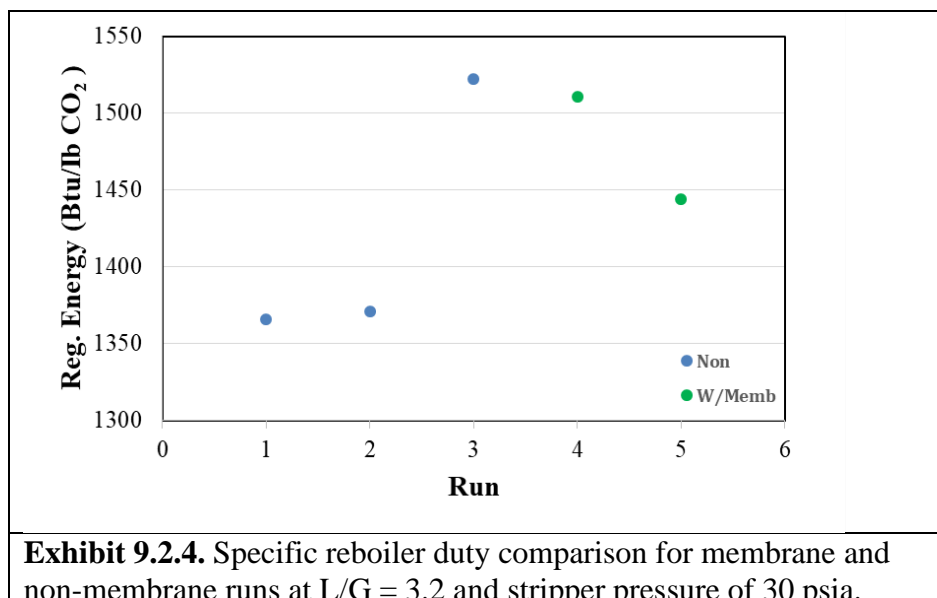


Exhibit 9.2.5. Test conditions comparison for Proprietary Solvent C at L/G = 3.2, Stripper pressure = 30 psia.

	Run	Inlet CO ₂ (%)	Absorber Inlet Temp (°F)	Absorber Bottom Temp (°F)	Stripper Bottom Temp (°F)	Stripper Top (°F)	Ambient Temp (°F)	% Capture	Energy (Btu/lb CO ₂)
No Membrane	1H	14	80	111	241	205	59	90	1366
	2H	14	94	112	246	210	28	91	1371
	3H	14	102	117	247	212	85	91	1522
Membrane	4Hm	14	105	134	244	214	96	90	1511
	5Hm	14	98	126	243	210	86	92	1444

Representative Liquid Sample Analysis

The liquid analyses shown in **Exhibit 9.2.6** indicate that for the same solvent circulation, similar operating range for the extra lean and rich loadings were obtained. No further enrichment with the membrane is seen for the rich loading obtained at the bottom of the absorber.

	Exhibit 9.2.6. Comparison of liquid analysis for membrane and non-membrane runs.									
		SP1 - Rich from Absorber Bottom			SP2 – Lean from Primary Stripper			SP3 – Lean Return to Absorber		
	Run	Alkalinity (mol/kg)	Carbon Loading (mol/kg)	C/N (mol/mol)	Alkalinity (mol/kg)	Carbon Loading (mol/kg)	C/N (mol/mol)	Alkalinity (mol/kg)	Carbon Loading (mol/kg)	C/N (mol/mol)
L/G = 2.5, 30 psia stripping										
No Memb	1B	5.61	2.24	0.40	6.22	1.31	0.21	6.52	1.24	0.19
	2B	5.38	2.18	0.41	5.84	1.26	0.22	5.98	1.19	0.20
	3B	5.36	2.43	0.45	5.77	1.41	0.24	6.18	1.36	0.22
	4B	5.23	2.43	0.46	5.64	1.33	0.24	6.35	1.31	0.21
	5B	5.15	2.38	0.46	5.52	1.39	0.25	6.21	1.37	0.22
	6B	5.46	2.11	0.39	5.96	1.19	0.20	6.06	1.09	0.18
Memb	7Bm	5.22	2.43	0.47	5.63	1.35	0.24	5.82	1.28	0.22
	8Bm	4.85	2.27	0.47	5.27	1.34	0.25	5.53	1.23	0.22
	9BmL	4.78	2.09	0.44	5.17	1.15	0.22	5.51	1.07	0.19
L/G = 2.5, 24 psia stripping										
No Memb	1C	5.25	2.22	0.42	5.74	1.22	0.21	5.93	1.14	0.20
	2C	5.72	2.28	0.40	6.19	1.33	0.21	6.40	1.27	0.20
	3C	5.46	2.11	0.39	5.96	1.19	0.20	6.06	1.09	0.18
Memb	4Cm	5.44	2.28	0.42	5.54	1.18	0.21	5.97	1.14	0.19
	5CmL	4.81	2.02	0.42	5.12	1.18	0.23	5.37	1.14	0.21
L/G = 3.2, 30 psia stripping										
No Memb	1H	5.00	2.18	0.44	5.52	1.35	0.24	5.73	1.27	0.22
	2H	4.98	2.20	0.44	5.32	1.38	0.26	5.97	1.31	0.22
	3H	5.46	2.08	0.39	5.82	1.29	0.22	6.01	1.27	0.21
Memb	4Hm	5.39	2.29	0.42	5.90	1.54	0.26	6.04	1.47	0.24
	5Hm	5.12	2.13	0.42	5.36	1.45	0.27	5.64	1.35	0.24

Absorber Temperature Profile

It was observed that the absorber bottom temperature was higher for the membrane runs compared to non-membrane runs. A comparison of the temperature profile in the absorber in **Exhibit 9.2.7** shows similar behavior in the top section of the absorber prior to intercooling after which higher temperatures were seen in the membrane runs. The extent of cooling could be reduced from additional cooling requirements with the modified process. The temperature difference at the bottom of the absorber between the membrane and non-membrane runs increased with higher liquid circulation rates (**Exhibit 9.2.5**). The higher CO₂ concentration in the permeate stream fed to the bottom of the absorber could potentially generate more heat from the reaction of the solvent and therefore requires effective cooling to maximize solvent performance.

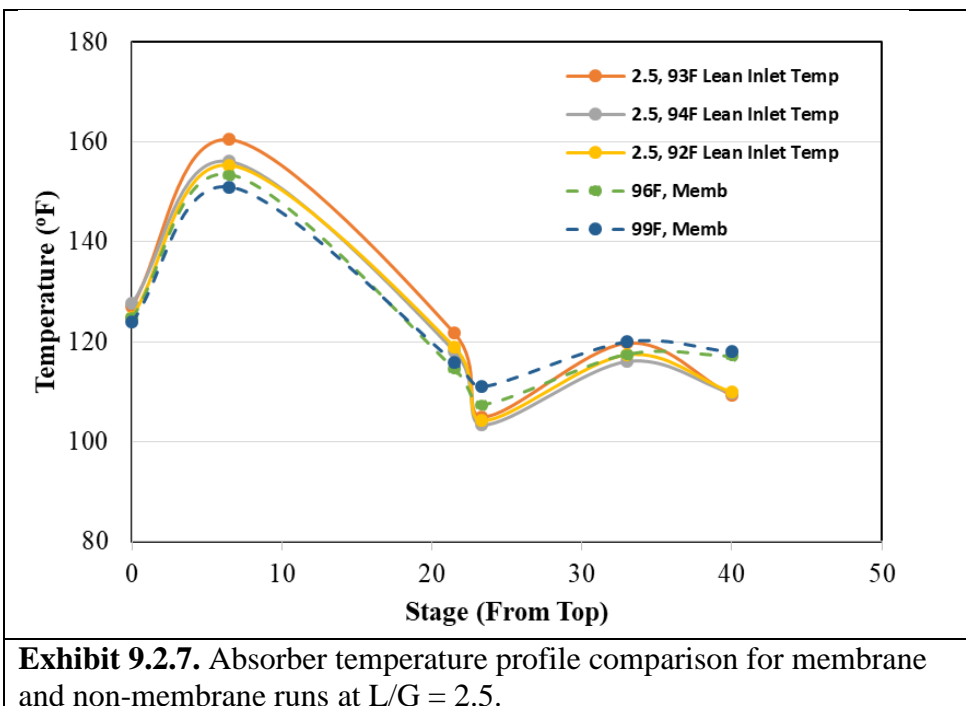


Exhibit 9.2.7. Absorber temperature profile comparison for membrane and non-membrane runs at L/G = 2.5.

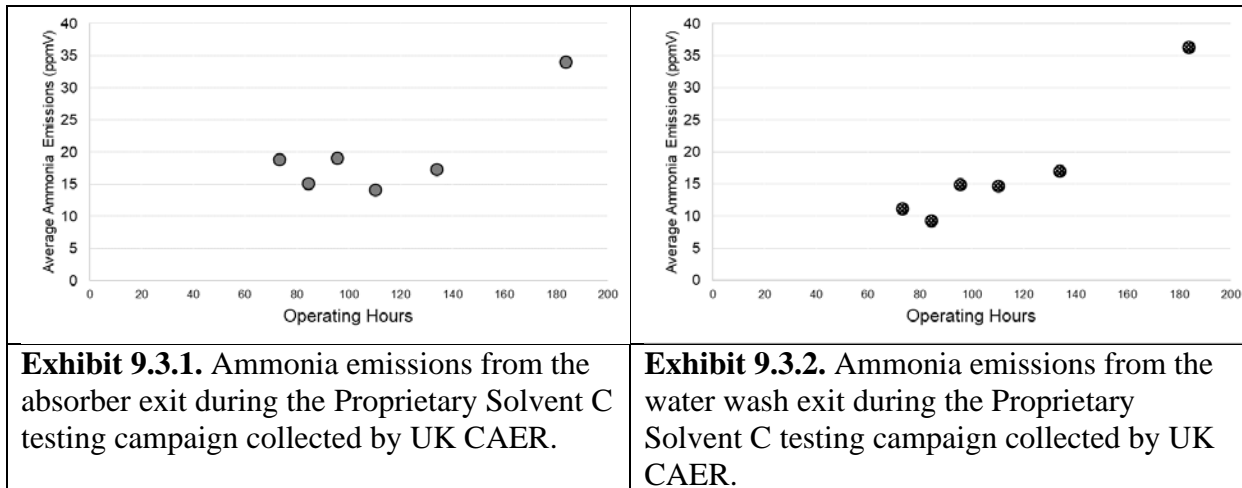
9.3 Emissions and Solvent Recovery with Water Wash System

Gaseous samples were collected using a stainless steel gas sampling impinger train with 0.05 M sulfuric acid. In a set of four impingers, the first three impingers contained 150 mL of sulfuric acid solution, and the fourth impinger contained up to 200g silica beads. The impinger train was connected to a 3/8 in. tube fitting at the secondary stripper (extractive gas sampling). A field blank of sulfuric acid was measured for quality control and ambient levels of ammonia during sampling. The collected samples were transferred to plastic containers and labeled by date, sample port ID, barcode number, volume, and analyte sampled. Two to three samples were collected each day to calculate an average emissions value. Samples were stored at 4°C until analyzed at the UK CAER analytical laboratory. Samples were diluted 10 fold with MilliQ water, and an aliquot of the diluted sample was transferred to 2 mL vials and analyzed using Ion Chromatography. A standard curve for ammonium and amines were used to quantify sample concentrations and calibration check standards were analyzed concurrently with samples to validate calibration.

Results

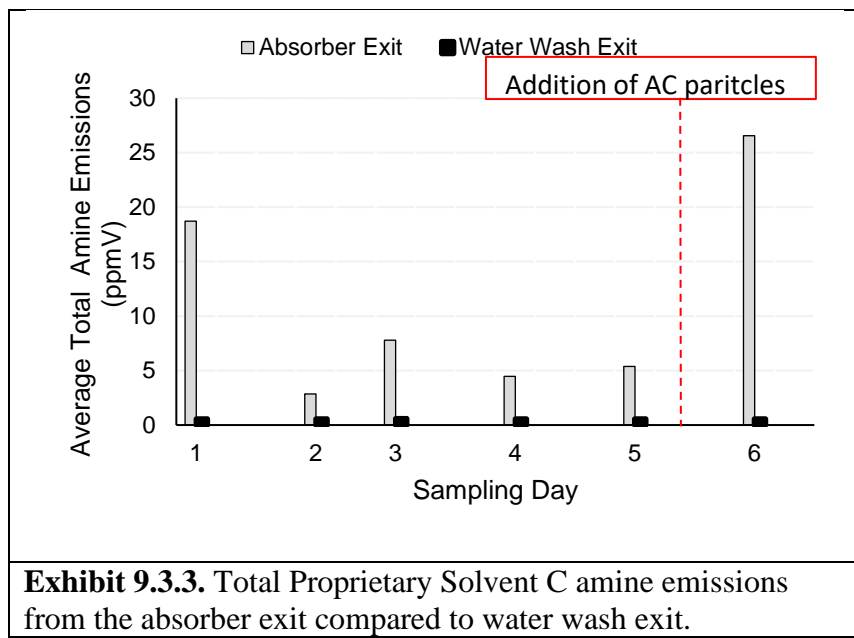
Ammonia Emissions

Ammonia emissions from the absorber exit are presented in **Exhibit 9.3.1**. Ammonia emissions ranged from 14 ppmV to 34 ppmV during this testing period. Ammonia emissions increased over the course of the testing campaign. This is likely due to solvent degradation, as similar increases in ammonia emissions have been correlated to solvent degradation in all previous solvent testing campaigns. Ammonia emissions from the water wash exit are presented in **Exhibit 9.3.2**. As expected, ammonia emission here is very close to its inlet concentration, ranging from 13 to 37 ppmV during this time due to its high volatility.



Amine Emissions

Amine emissions from the absorber exit ranged from 2.8 to 26.5 ppmV. Amine emissions vary somewhat on a day to day basis depending on absorber gas exhaust temperatures, which is similar to trends observed in the past solvent campaigns, due to changes to atmospheric conditions. Amine emissions from the water wash exit for amines were below our instrument (GC-MS) detection levels of <0.8 ppmV. In order to understand the effectiveness of the water wash to reduce amine emissions, a comparison of the total amine emissions from both locations (entering and exiting the water wash) is needed (**Exhibit 9.3.3**). The comparison shows that the water wash column is very effective in reducing amine emissions with an average reduction of 91% to levels less than 1 ppmV.

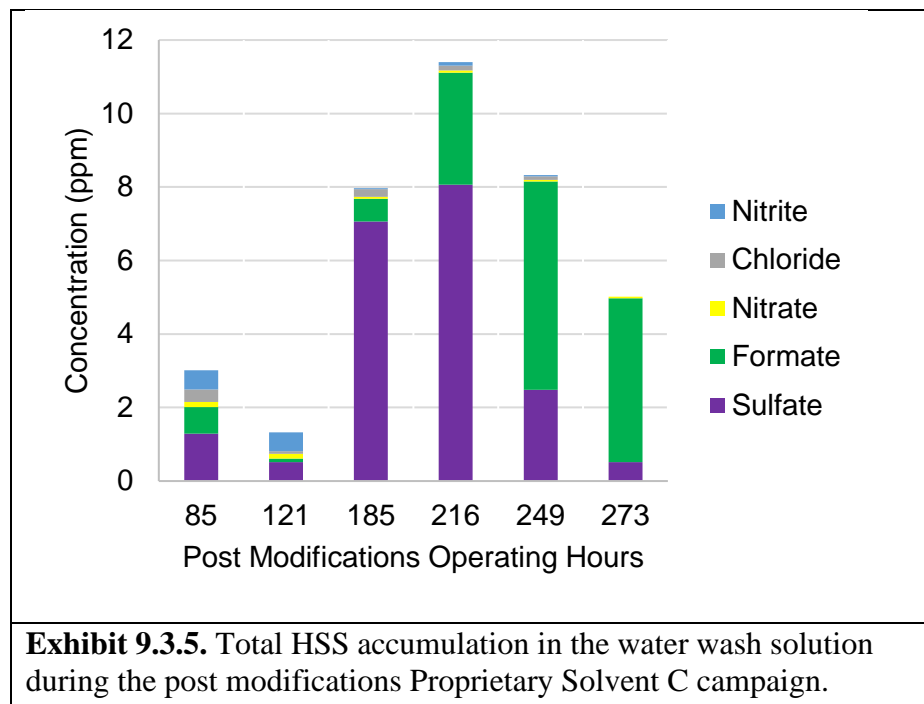


Water Wash Solution Characterization

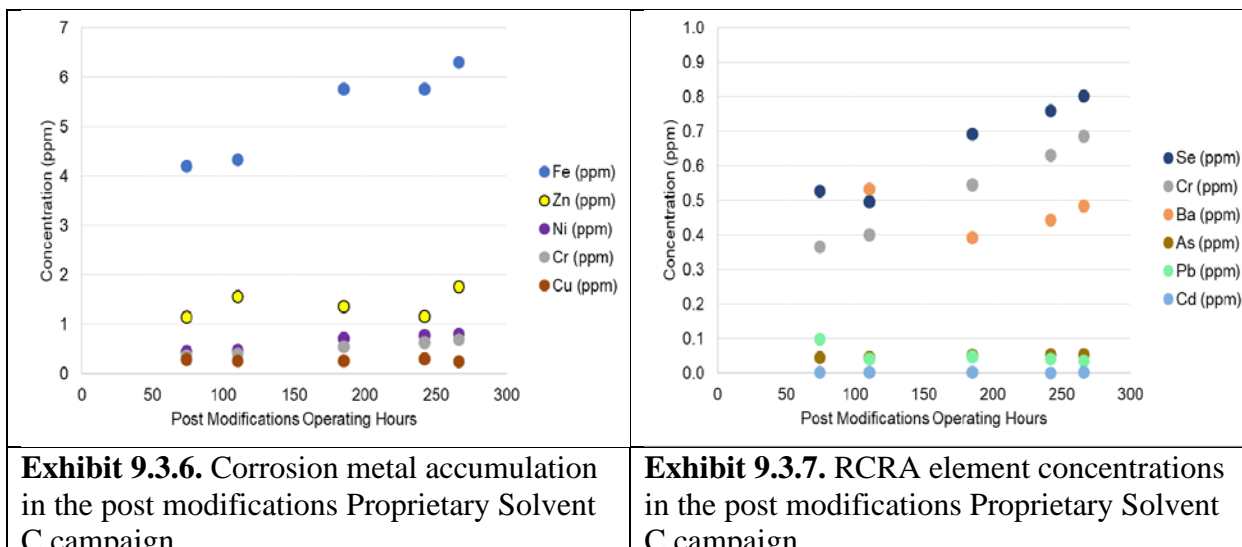
Water wash solutions were analyzed for amine and ammonia content to monitor their fate. The total ammonia and amine content in these samples are presented in **Exhibit 9.3.4**. The concentration of both compounds remain relatively constant, which is to be expected due to the constant blow down of water wash solution back to the amine loop throughout the campaign. **Exhibit 9.3.5** presents the HSS species detected in the water wash solution. The variable nature of the species is due to the different conditions in the column, amine content and could come from the water itself. Sulfate is found in this solution at a higher concentration than the other compounds which is to be expected since sulfate has the highest concentration in the amine solution.

Exhibit 9.3.4. Ammonia and Amine concentration in the Water Wash solution during the advanced solvent post modifications campaign.

Date	Operating Hours	Ammonia (ppm)	Total Amine (ppm)
8/6/2019	74	61.102	2815.35
8/7/2019	85	61.206	3033.68
8/8/2019	96	88.062	2846.53
8/13/2019	110	87.874	2701.41
8/14/2019	121	88.017	2765.06
8/15/2019	133	86.707	2626.88
9/13/2019	185	124.220	1921.44
9/23/2019	216	179.852	1815.77
9/30/2019	249	98.732	2482.05
10/4/2019	273	231.814	2155.42



Metals Accumulation in Solvent



All the monitored elements were observed in the amine solvent at varying concentrations. **Exhibit 9.3.6** shows accumulation over the course of the campaign of the metals most associated with corrosion, including iron, zinc, chromium, copper and nickel. Iron increased over the course of the campaign and was the metal with the highest accumulation at a rate of 0.023 ppm/hr post modification. The accumulation rate of iron is much lower than previous solvent testing campaigns (MEA and CAER through 350 operating hours). Although chromium, zinc, copper and nickel were detected in the solvent, their concentrations remained relatively constant throughout the campaign and showed minimal accumulation. These metals may be residuals from previous testing

campaigns. The as received solvent was not analyzed, nor were any solvent samples collected prior to the modifications.

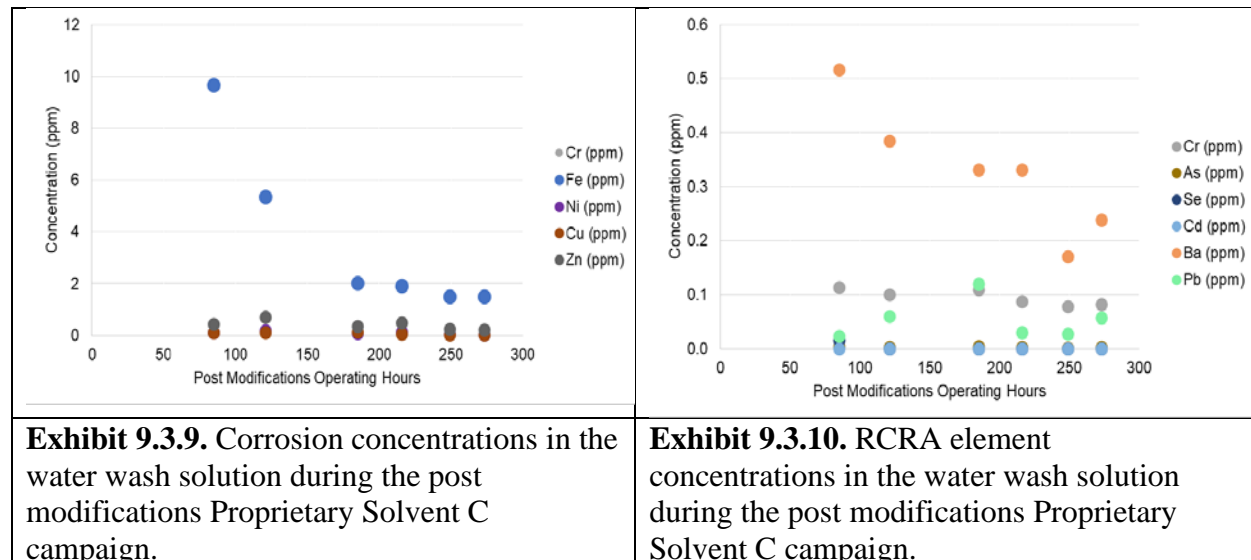
The RCRA regulated metals present in the advanced solvent are shown in **Exhibit 9.3.7**. These regulated metals include selenium, chromium, barium, lead, arsenic, and cadmium. All the observed regulated metals were below their RCRA waste limits throughout the entire campaign. Chromium and selenium were the only RCRA metals that showed any accumulation during the campaign. All other metals remained stable indicating that the concentration is likely residuals from previous solvent testing campaigns, or are present in the as-received solvent.

Beryllium, vanadium, manganese, and molybdenum were all observed in the solvent above the limit of detection during the testing campaign, **Exhibit 9.3.8**. However, these metals were not observed at any significant level, all remaining below 1 ppm.

Exhibit 9.3.8. Be, V, Mn, and Mo concentrations in the post modifications Proprietary Solvent C campaign.

Sample	Run Hours	Be (ppm)	V (ppm)	Mn (ppm)	Mo (ppm)
8-6-19 SP-1	74	0.004	0.084	0.706	0.170
8-13-19 SP-1	110	0.003	0.081	0.710	0.171
9-13-19 SP-1	185	0.001	0.090	0.751	0.198
9-27-19 SP-1	242	0.000	0.090	0.780	0.219
10-3-19 SP-1	266	0.001	0.093	0.793	0.227

Metals Accumulation in Water Wash Solution



The corrosion metals present in the water wash solution are presented in **Exhibit 9.3.9**. The high initial iron concentration can likely be associated to the fact that this was a brand new column and piping with some residual grease, metal filings, etc. left behind during fabrication and installation. The decrease in iron is likely from the solution blowdown during operation. All other corrosion metals (chromium, zinc, copper and nickel) were detected at very low concentrations and show no significant accumulations. The RCRA regulated metals present in the water wash solutions are shown in **Exhibit 9.3.10**. They are all observed much below their concentration detected in the amine solution.

10) RECLAIMING AND MASS BALANCE

Reclaiming

During the baseline MEA solvent testing campaign, the solvent was purified by thermal reclaiming with soda ash caustic in a batch mode type process for a period of approximately 66 hours during a 90 hour operating period. The visual schematic of the UK CAER kettle-type reclamer is shown in **Exhibit 10.1**.

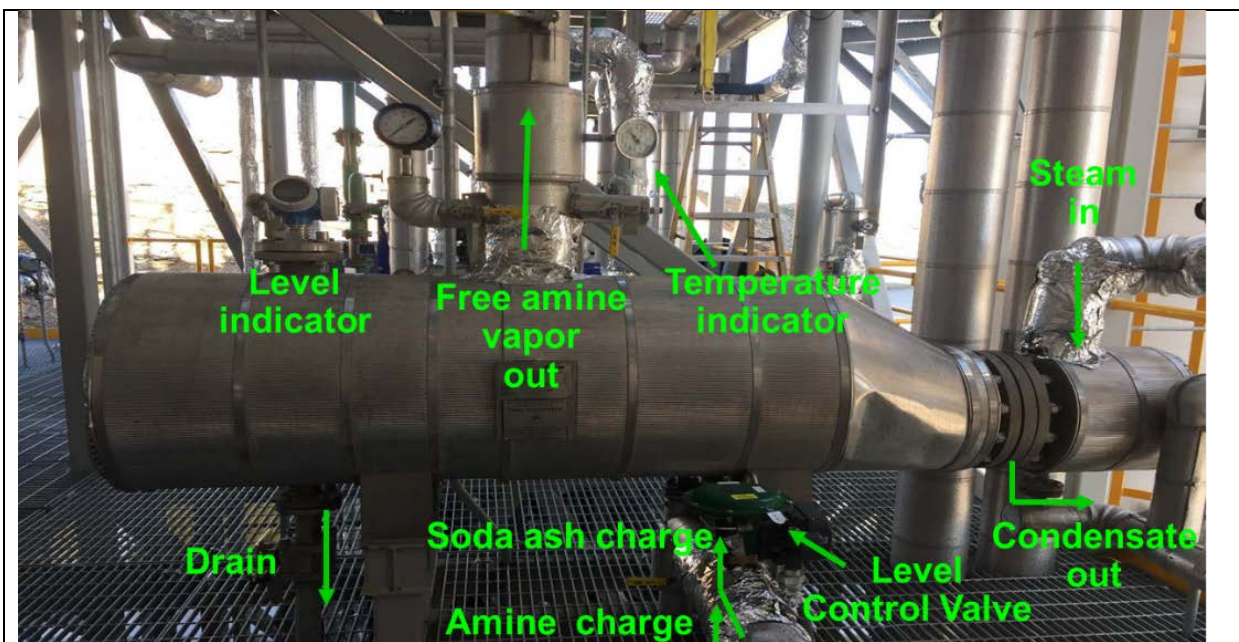


Exhibit 10.1. Kettle-type tube and shell thermal reclamer with a combined soda ash and amine charge line, temperature and level indicators, and drain for removing reclamer sludge.

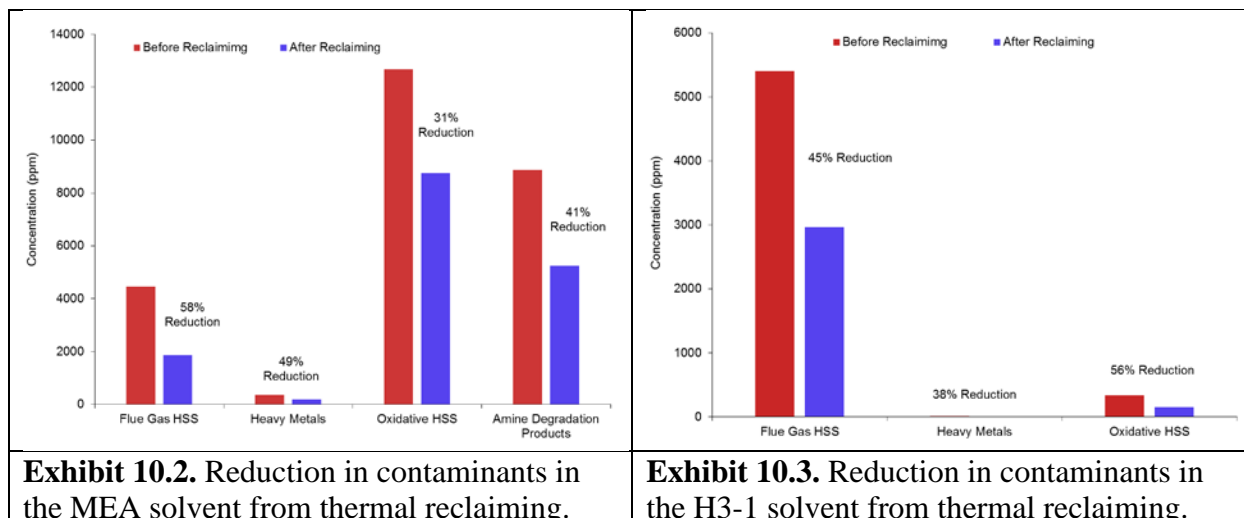


Exhibit 10.2. Reduction in contaminants in the MEA solvent from thermal reclaiming.

Exhibit 10.3. Reduction in contaminants in the H3-1 solvent from thermal reclaiming.

Analysis of the solvent was performed before, during and after this period to determine the % removal of contaminant species including flue gas HSS (sulfate, nitrate, nitrite), amine oxidation HSS (formate, acetate, glycolate and oxalate), metals and other amine degradation products from the main solvent loop. Analysis of the reclaimer “sludge” was also completed for waste characterization and disposal purposes. **Exhibit 10.2** shows the relative decrease in each contaminant group as a result of thermal reclaiming in the MEA solvent. Thermal reclaiming was most effective at reducing the level of flue gas HSS species from the solvent. A 58% reduction was observed due in part to the addition of the caustic soda ash. The soda ash is used to increase the solution pH and provide a positively charged ion to replace the protonated-amine in the charge balance with the negatively charged HSS anion species. This charge transfer process will also free the protonated amine, which will subsequently be deprotonated due to the high pH in the reclaimer. The now neutral amine will have sufficient vapor pressure to be volatilized in the steam stripping reclaiming process and returned to the amine loop.

Metals and polymeric amine degradation products were also significantly reduced as a result of thermal reclaiming, with reduction of 49% and 41% respectively. The least impacted contaminant was the oxidative HSS species (formate, acetate, glycolate and oxalate), where only a 31% reduction was observed. It is possible that during the reclaiming period the amount of these compounds continued to increase in the solvent as the system continued to capture CO₂ and therefore the actual impact by thermal reclaiming may indeed be somewhat higher, but overall impact will still be lowest among the contaminant groups examined based on observed accumulation rates.

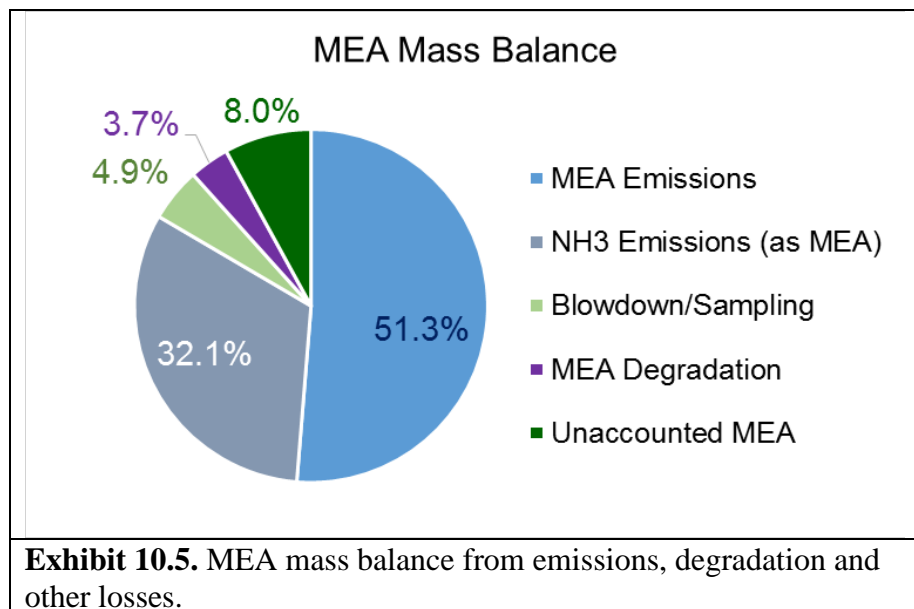
Similar contaminant removal was also observed during the H3-1 campaign. **Exhibit 10.3** shows the relative decrease in each contaminant group as a result of thermal reclaiming in the H3-1 solvent. Here the highest removal was observed with the oxidative HSS species at 58%. Significant removal of the flue gas HSS species was also observed. Percentage of metal removal in the H3-1 solvent was lower, however the absolute magnitude of metals in this solvent was also lower suggesting that there is a diminishing return on thermal reclaiming at lower concentrations.

Exhibit 10.4 summarizes the relative energy (as steam) requirements to remove each class of contaminant; heat stable salts (HSS), amine degradation compounds and metals (from flue gas and corrosion). When the concentration of impurities is very low, such as with the corrosion and RCRA metals, a significantly higher energy input is required.

Exhibit 10.4. Relative energy (as stream) required to remove solvent contaminants by thermal reclaiming.					
Solvent	Contaminant class	Amine loop concentration before reclaiming (Kg)	Amine loop concentration after reclaiming (Kg)	Amount removed from amine loop (Kg)	Steam required per Kg removed (KWth/Kg)
MEA	Total HSS	90	52	38	10.53
	Total Metals	1.9	1.0	0.9	427.08
	Corrosion Metals	1.73	0.89	0.84	474.50
	RCRA Metals	0.19	0.09	0.10	4016.07
	MEA Degradation Compounds	47.02	27.79	19.23	20.80
H3-1	Total HSS	30.45	16.54	13.91	16.18
	Total Metals	0.06	0.04	0.02	9868.42
	Corrosion Metals	0.03	0.02	0.01	21844.66
	RCRA Metals	0.03	0.02	0.01	19911.5

Amine Mass Balance

During this project, solvent losses resulted from direct amine emissions, amine degradation, blowdown, sampling and other unaccounted losses. Total amine loss during each testing campaign was calculated from the total amount of amine loaded into the system minus the amount removed at the end of the testing campaign and other losses as described above. A mass balance around the MEA of 92% was achieved during the baseline testing (**Exhibit 10.5**). Comparable mass balance around the H3-1 solvent was also observed during its testing campaign. Solvent loss during the baseline MEA testing campaign was calculated at 7.1 lbs/1000 lbs CO₂ captured. Loss of the H3-1 solvent was calculated in the same manner at 5.6 lbs/1000 lbs CO₂ captured, an improvement of 20% compared to the baseline MEA.



11) CONSTRUCTION AND DESIGN CHALLENGES

	
<p>Exhibit 11.1. P-109 Connecting Pipe Section Did Not Fit Correctly, 9/30/2014.</p>	<p>Exhibit 11.2. Example of Two Problems with the Cross-over Grating, 1) Lack of Support at Edges and 2) Gap Too Large Between Adjacent Pieces, 9/19/2014.</p>

For future projects of this nature, attention should be paid to the zero elevation definition. This is important when shipped-loose equipment is mounted on foundation pedestals, as shown in **Exhibit 11.1**. Loose-shipped pump foundations needed to be altered.

Grating was also shipped loose by KMPS and installed after the modules were erected. In many places the grating between modules was not long enough to securely span the distance, **Exhibit 11.2**. Several sections of grating needed to be replaced. Additionally, host site requirements are that every piece of grating must be mechanically secured to the structure. Many such securing clips needed to be added.

12) STATE POINT DATA TABLE AND SYSTEM OPERATING CONDITIONS

In accordance with the Project PMP, the State Point Data Table has been updated in **Exhibit 12.1** for the MHPSC H3-1 advanced solvent.

Exhibit 12.1. Updated State Point Data Table.		
	Units	H3-1 From UK CAER 0.7 MWe CCS Performance
Molecular Weight	mol ⁻¹	<120g
Normal Boiling Point	°C	169
Normal Freezing Point	°C	-8.8
Vapor Pressure	bar	5.38×10 ⁻⁴
Concentration	kg/kg	0.45/1.00
Specific Gravity	g/mL	0.982 ^a
Specific Heat Capacity	kJ/kg·K	0.924 ^b
Viscosity (fresh solvent)	cP	7.04 ^a
Surface Tension fresh solvent)	dyn/cm	45 ^c
Pressure	bar	1.01
Temperature	°C	47-68
Equilibrium CO ₂ Loading	mol CO ₂ /kg	2.2
Heat of Absorption	kJ/mol CO ₂	< 70
Solution Viscosity	cP	14.2 ^a
Pressure	bar	2.5
Temperature	°C	119
Equilibrium CO ₂ Loading	mol CO ₂ /kg	1.2
Heat of Desorption	kJ/mol CO ₂	< 75

^a Measured at 25 °C

^b Calculated at 40 °C

Also in accordance with the Project PMP, the recommended system operating conditions, pressures (in units of bar), temperatures (in units of °C) and working capacity (in units of kg CO₂ per kg solvent), for the H3-1 advanced solvent are given in **Exhibit 12.2**.

Exhibit 12.2. Recommended System Operating Conditions and Solvent Working Capacity.			
Equipment Name	Parameters	Units	MHPSA H3-1 Advanced Solvent
Absorber	Pressure	psia (bar)	14.7-14.9 (1.014-1.027)
	Bottom Temperature	°F (°C)	110-130 (43-54)
	Top Temperature	°F (°C)	95-105 (35-41)
	L/G	mass/mass	4-5
Primary Stripper	Pressure	psia (bar)	30-40 (2.07-2.76)
	Bottom Temperature	°F (°C)	230-245 (110-118)
	Top Temperature	°F (°C)	210-225 (99-107)
Secondary Air Stripper	Pressure	Psia (bar)	14.7-14.9 (1.014-1.027)
	Bottom Temperature	°F (°C)	130-140 (54-60)
	Top Temperature	°F (°C)	170-180 (77-82)
	Solvent Working Capacity	Mol CO ₂ /kg solvent (kg CO ₂ /kg solvent)	1.3 (0.057)

13) SUMMARY OF TEA

The TEA was conducted in accordance with U.S. DOE NETL guidelines. RC 9, a subcritical pulverized coal combustion case, and RC 10, the same combustion case with CCS, were used for comparison with the UK CAER CCS. The final TEA was issued by the EPRI and submitted as a Project Topical Report to U.S. DOE NETL in May 2020.

13.1 TEA Methodology

A team from EPRI, led by Abhoyjit Bhowm, working independently from the UK CAER team, constructed a rate based Aspen Plus® model of a complete power plant with the UK CAER CCS and completed the simulation portion of the preliminary EA, generating the heat and mass balance stream table and sizing major equipment such as columns and heat exchangers, with input from Hitachi and UK CAER.

Two equations of state (ELECNRTL and NRTL-RK) were used throughout the model to closely match expected results for the design based on published data. As the model results were produced, they were checked by EPRI and UK CAER against published data to ensure that they fell within the expected range. This includes estimation of secondary stripper performance, which is one innovation included in the design offered by UK CAER. The CO₂ capture system was modeled in a stand-alone

model with the overall results merged into a power plant model to ensure overall process results convergence. Some manual iteration was required to ensure accuracy.

During power plant performance modeling, an adjustment was made to boiler performance due to the recycle of non-combustible gas into the secondary set of burners. The estimated reduction in boiler efficiency is 0.7% (HHV basis) and is based on results observed during a related study on membrane separation of CO₂ from flue gas that has a recycle to the boiler.

The base case is retrofit with a CO₂ capture system using MEA solvent with a 30 wt% concentration to remove 90% of the CO₂ present in the flue gas. The process lineup includes:

- Flue gas desulfurization unit to remove greater than 95% of the sulfur.
- Direct contact cooler that uses water and soda ash (Na₂CO₃) with a pH less than 7.0 to further reduce sulfur content to less than 10 ppmv and the temperature to less than 100 °F.
- Fan to pressurize flue gas in order to overcome the pressure drop of downstream CO₂ capture equipment
- Reactive absorption distillation column to remove 90% of the CO₂. The column includes a pump-around and intercooler to help reduce solvent flowrate.
- Primary stripper using pressure drop and low pressure steam to drive off the majority of CO₂ from the rich solvent. The primary stripper overhead is cooled by preheating solvent and other process streams
- Secondary stripper using air to remove remainder of CO₂ from semi-rich solvent, which is then cooled and returned to the secondary air rans upstream of the boiler

A team from WorleyParsons completed the capital cost estimation. Capital costs were developed using a combination of commercial capital cost estimating software, factored equipment estimates, and WorleyParsons in-house parametric models supplemented by WorleyParsons' extensive in-house equipment cost database.

Aspen In-Plant Cost Estimator software was used to develop costs for most of the major equipment in the UK CAER CO₂ removal process. This includes reactor vessels, absorbers, and other specialized process equipment. The associated capital costs for bulk materials and installation were developed by applying a factor to the established equipment cost to derive a total installed cost. Factors vary by type of equipment, metallurgy, and complexity, and conform to WorleyParsons standards.

13.2 TEA Findings

Two cases utilizing the UKy process are compared, using different approach temperatures and solvent, against the DOE/NETL RC 10. The results are shown comparing the energy demand for post-combustion CO₂ capture and the net HHV efficiency of the power plant integrated with the post-combustion CO₂ capture process. A LCOE assessment was performed showing the costs of the options presented in the study. The key factors contributing to the reduction of LCOE were identified as CO₂ partial pressure increase at the flue gas inlet, thermal integration of the process, and performance of the Hitachi H3-1 solvent.

UK CAER process pilot-scale testing data and process simulation data showed that the packing heights of absorber and stripper columns were significantly oversized in the preliminary TEA

(Task 2 of this project) and thus updated in this final TEA. In addition, the solvent make-up cost for H3-1 was updated based on latest test results. Finally, a heat integration with the main power plant was applied in this final TEA to increase overall energy efficiency.

The net efficiency of the UK CAER integrated PC power plant with CO₂ capture changes from 26.2% for the RC 10 plant in 2010 revised DOE/NETL baseline report to 27.6% for the MEA options considered, and 29.1% for the options utilizing the Hitachi advanced solvent. The UK CAER Process + Hitachi case also produces an extra 30.9 MW of generation compared to the UK CAER Process + MEA case and total 60.9 MW more than DOE RC 10. LCOE (\$/MWh) values are \$172.08/MWh for the MEA option and \$157.65/MWh for the Hitachi H3-1 solvent cases considered in comparison to \$189.59/MWh in January 2012 dollar for RC 10.

The UK CAER CCS process MEA case lowers energy consumption for CO₂ capture to 1340 Btu/lb-CO₂ captured as compared to 1540 Btu/lb-CO₂ in RC 10. The UK CAER CCS process with H3-1 case further lowers energy consumption for CO₂ capture to 973 Btu/lb-CO₂ captured, for an advantage of 36.8% less energy consumption than RC 10. The study also shows 38.1% less heat rejection associated with the carbon capture system from 3398 MBtu/hr (RC10) to 2104 MBtu/hr for the UK CAER + MEA system. Heat rejection is reduced to 2464 MBtu/hr in the UK CAER + H3-1 case, for a 27.5 % decrease compared to RC 10. Modeling outputs show that in the UK CAER process, cooling water 2-5°C cooler than conventional cooling tower water can be achieved for ambient conditions common to the midwest and other regions. The results from the TEA show that the proposed technology can be investigated further as a viable alternative to conventional CO₂ capture technology.

The evaluation also shows the effect of the critical parameters on the LCOE, with the main variables being the approach temperature and CO₂ partial pressure increase at the flue gas inlet. A summary of the key advantages of the UK CAER Process + H3-1 case for LCOE and other economic factors compared to the DOE RC 10 is as follows:

- A lower variable operating cost by \$1.56/MWh (\$1.08MWh less than UK CAER Process + MEA case), a 11.7% reduction compared to the DOE RC 10
- A lower COE by \$25.32MWh (\$13.94/MWh lower than UK CAER Process + MEA case), a 16.9% reduction compared to the DOE RC 10
- A lower LCOE by \$31.94/MWh (\$17.51/MWh lower than UK CAER Process + MEA case), a 16.9% reduction compared to the DOE RC 10
- A lower cost of CO₂ captured by \$18.65/tonne CO₂ (\$9.44/tonne CO₂ lower than UK CAER Process + MEA case), a 30.4% reduction compared to the DOE RC 10
- A lower cost of CO₂ avoided by \$34.95/tonne CO₂ (\$18.53 tonne CO₂ lower than UK CAER Process + MEA case), a 38.7% reduction compared to the DOE RC 10

14) SUMMARY OF EH&S ASSESSMENT

This EH&S assessment was conducted by Smith Management Group (SMG) and submitted as a Project Topical Report to U.S. DOE NETL in May 2020.

The scope of the assessment was limited to evaluating process design plans, process operation and testing information provided by UK CAER and MHPS as well as a literature review. The literature review was performed to identify EH&S hazards of raw materials used in the process as well as information available for similar operations to evaluate potential air emissions, wastes and wastewater generated. Additionally, chemical constituent evaluation was conducted for substances known or anticipated to be generated by the process. Process design and operation information included: process flow diagrams; operating parameters; raw material storage and consumption rates; air emissions testing; solvent testing; quantification and characterization of wastes generated and wastewater discharged.

The pilot plant was designed to operate at a 0.7 MWe (2 MWth) scale (~13.7 tonnes per day CO₂) receiving a slipstream flow of approximately 2340 SCMH (1400 cfm) from the E.W. Brown Generating Station combined exhaust stream, after the WFGD. The pilot plant was approximately 24.5 meters (80 ft.) tall and had a footprint of about 93 m² (1000 ft²), excluding associated lab/control center and auxiliary facilities. The initial EH&S assessment covered the first 1.5 years of operation when the performance of a conventional CO₂ scrubbing solvent (monoethanolamine or MEA) and the advanced Hitachi H3-1 solvent were evaluated. The EH&S assessment was updated

The methodology used to conduct this quantitative evaluation is consistent with the Risk Assessment Guidance for Superfund (RAGS) developed by the U.S. EPA. The evaluation focused primarily on potential health risks related to possible exposures to nitrosamines which may result from degradation of the CO₂ capture solvents. The assessment was based on potential exposures during the 0.7 MWe-scale post-combustion CCS study at E.W. Brown Generating Station and analytical results obtained during the study. Analytical results were obtained from several sources. CB&I Environmental & Infrastructure, Inc. performed system exhaust stack testing on two separate occasions, once each during the MEA and H3-1 solvent testing campaigns. The results for the MEA testing represent results for samples collected between September 29 and October 2, 2015, while the results for the second testing represented results from the H3-1 campaign collected between June 5 and 7, 2016. Additional analytical results, including gas phase emissions, solvent degradation, nitrosamines assessment and waste characterization for MEA and H3-1 testing campaigns were provided by UK CAER. MHPSA provided nitrosamine data for the H3-1 testing campaign.

Prior qualitative and quantitative health risk assessments were prepared for the proposed operation of the post-combustion CCS using amine based solvents (MEA and Hitachi H3-1) in a 0.7 MWe pilot plant at the E.W. Brown Generating Station (SMG, 2012; ENRISQ and SMG, 2013). These preliminary evaluations concluded that MEA, H3-1 and their likely degradation products and other materials used at the pilot plant pose little human health or ecological risk when proper safety, handling, and industrial hygiene procedures are followed.

Air emission test data and calculated potential emissions exceeded estimates determined in the Initial Environmental, Health and Safety Assessment (SMG, 2012). Although actual air emissions were higher than estimated, operation of the pilot plant for limited hours as a research and development facility would still qualify as an Insignificant Activity (IA).

MEA with associated degradation compounds were the largest contributors to actual air emissions during the MEA campaign. Refer to **Section 6.5** of this report for details pertaining to the MEA campaign emissions. The highest emitting degradation compound was ammonia. Although actual air emissions were higher than estimated, the relatively small amount of emissions would not adversely impact surrounding terrestrial or water resources, since they were readily diluted and dispersed from the main exhaust stack at the E.W. Brown Generating Station.

A toxicity assessment of the solvents, other raw materials and potential solvent degradation products was completed in the initial EH&S assessment completed in 2012 (SMG, 2012). The primary health concern identified for the unused CO₂ capture solvents is the corrosive nature of the materials. An additional health concern identified in the initial EH&S assessment was the potential cancer risk from exposure to nitrosamines derived from solvent use and degradation. Materials such as MEA, Hitachi H3-1, piperazine isomers and other secondary and tertiary amines may be nitrosated during the solvent capture process and generate nitrosamines. While direct exposures to the solvents may be prevented, and low-level exposures through ambient air inhalation to pure solvents have not been identified as posing a cancer risk, inhalation exposures to nitrosamines in ambient air or during process sampling may pose a cancer risk to study workers. The primary health concern related to nitrosamines is cancer risk, even at relatively low levels of exposure. The industrial (workplace) ambient air screening levels (RSLs) for the individual nitrosamines at a cancer risk level of 1E-6 (one-in-a million) is based on workplace exposures occurring 8 hours per day, 250 days per year for 25 years. This is a total of 50,000 hours of exposure through inhalation, which is substantially greater than likely exposures during the pilot test, but may be considered for full-scale operations. Due to uncertainties in general exposure scenarios and data generated, extrapolating to operations at a large scale post-combustion CCS may not accurately identify potential risks of nitrosamine exposure by site workers or the surrounding community. However, it is reasonable to presume that a larger scale facility will consume greater amounts of solvent. Depending upon the solvent formulation, a larger scale facility may generate relatively larger amounts of nitrosamines, albeit at similar concentrations due to increased air flow, that could result in greater risk of exposure and harmful health effects without additional emission control measures.

Additionally, elevated concentrations of ammonia, MEA and possibly formaldehyde detected at the secondary stripper using MEA or a similar solvent and extrapolated to a large-scale facility warrants additional evaluation and possibly consideration of additional emission control measures, if this exhaust stream will not be diverted to a power plant's boiler.

Extrapolated air emissions from a large scale post-combustion CCS suggest ammonia, process solvent and other solvent degradation products will likely be emitted in quantities requiring emission controls. While the extrapolation methods used in this assessment are useful to estimate order-of-magnitude impacts, specific process data for: gas flow rates, solvent liquid flow rates, stack parameters (height, diameter, gas velocity), and flue gas composition are needed before accurately quantifying risks/impacts to human health or the environment. The extrapolated data obtained from the pilot plant testing suggests that a larger scale (550 MWe) post-combustion CCS located at an existing coal-fired steam electric plant would trigger a Prevention of Significant Deterioration (PSD) review, likely requiring installation of best available control technology (BACT) for VOC emissions. If the system were installed within a Nonattainment Area for VOCs,

the project would also be subject to the Nonattainment New Source Review (NA-NSR) program that requires application of the lowest achievable emission rate (LAER) technology. BACT or LAER control measures for VOC emissions can add significant costs to the installation and operation of a 550 MWe post-combustion CCS and the plausible permitting procedure could require a minimum of 1.5–2.5 years for approval prior to commencing construction.

Process wastewater volumes were relatively minor and primarily generated from the SO₂ pretreatment tower and cooling tower blowdown. Wastewaters were pumped to a WFGD unit on site as a supplement water source and were not discharged or disposed on site. Due to the wastewater volumes, contaminant concentrations and ultimate disposal method, wastewater management was not a significant environmental concern. Increased wastewater volumes and constituent concentrations for a larger scale facility will need further evaluation to determine appropriate disposal methods. Recent changes in steam electric power generating effluent guidelines published by the EPA (40 CFR Part 423) will need to be considered to determine any required treatment and associated implementation needs for surface water discharges.

Waste quantities and constituent concentrations estimated in the initial EH&S Assessment (SMG, 2012) were generally consistent with actual wastes generated. In many cases, volume of waste was less than anticipated. A few unanticipated wastes were generated from periodic maintenance and cleaning activities that were not a hazardous waste. Unexpectedly, used H3-1 solvent was characterized as a hazardous waste due to its higher than expected selenium concentration. A larger scale facility will generate relatively greater waste volumes, although there should be some economy of scale that will prevent a directly proportional increase in waste generated. Management of a larger volume of wastes not regulated as a hazardous waste should be manageable for a typical steam electric power generating facility. Increased quantities of hazardous solvent waste would need to be considered in future operating plans, registered, and managed appropriately.

15) PROJECT MILESTONES AND LESSONS LEARED

Also from the Project PMP, the project Milestones are listed below with the completion dates.

Exhibit 15.1. Project Milestones.							
Budget Period	ID	Task Number	Title	Description	Planned Completion Date	Actual Completion Date	Verification Method
1	1	2	Preliminary Technical and Economic Analysis - Topical Report submitted	Details viable technical merit of UK CAER CCS process for slipstream scale study	12/31/12	12/18/12	Preliminary TEA Topical Report file
1	2	3	Initial EH&S report submitted	Details environmental implications of slipstream operation and proposes mitigation for anticipated environmental safety obstacles to operation, if any	12/31/12	11/27/12	Initial EH&S Topical Report file
1	3	4	Design Base Report submitted	Provides foundation for finalization of pilot unit design in BP2, Task 7	12/31/12	11/20/12	Design Basis Topical Report file
2	4	6	Identification of Flue Gas Clean-up Requirements at EW Brown test site	Identification of Flue Gas Clean-up Requirements specific to slipstream operation at E.W. Brown Station, which is applicable to finalization of pilot unit design in Task 7	3/29/13	4/8/13	Written report submitted as part of Quarterly report Q2FY14
2	5	7	Finalize Project Design Package (PDP) for slipstream pilot unit fabrication	Finalize PDP for pilot unit fabrication to take place in BP 3, Task 9	5/17/13	5/16/13	Written verification after Process Design Package

							Engineering Review Meeting held at KMPS
2	6	8	UK CAER Finalize Test Plan for slipstream campaigns	UK Finalize Test Plan with completed P&ID specifications from Task 7	5/31/13	5/15/13	Sampling and Test Plan Topical Report file
3	7	11	Documented Safety Training for test site procedures/ protocols	Safety training for slipstream onsite procedures/ protocols will be conducted for CAER and MHPSC representatives	7/31/14	8/26/14	Quarterly report Q4FY14
3	8	12	Pouring of foundations for platform for slipstream pilot unit setup	Platform for slipstream module setup which meets engineering load/ specifications of module design	7/1/14	9/11/14	Quarterly report Q4FY14
3	9	13	Fabrication of slipstream unit modules completed	KMPS will fabricate modules offsite and deliver to E.W. Brown Station by this date for installation, Task 16	8/18/14	8/28/14	Quarterly report Q4FY14
3	10	14.3	Control Room/ Field Lab Trailer Assembled and Setup	Completed assembly and set up of the control room/ field lab trailer	10/31/14	11/14/14	Quarterly report Q1FY15
3	11	14.5	Site Water and Electric Utility Tie Ins in place for slipstream pilot unit and control room/ field lab trailer	Water and electric utility tie ins in place for control room/ field lab trailer, and slipstream modules. Predecessor for commissioning and startup of the unit, Task 16	4/30/14	4/30/14	Quarterly report Q3FY14
3	12	15	Corrosion test rack and pretreated metal coupons ready for use in test campaign	Corrosion rack set up ready with prepared metal coupons for corrosion testing to take place in BP 4, Task 18	12/31/14	12/15/14	Quarterly report Q1FY15

3	13	16.1	Slipstream pilot unit ready for start-up and commissioning	Slipstream pilot unit tied into utilities and power plant flue gas, steam and exhaust	2/26/15	3/31/15	Written verification
3	14	16.3	Slipstream pilot unit commissioning complete	Slipstream unit ready for testing to take place in BP 4, Task 18	3/31/15	3/31/15	Written verification
4	15	18.1	Test Campaign: Parametric study using 30% wt MEA complete	Completion of 27 experiments chosen to evaluate 4 independent variables using 30% wt MEA.	8/6/15	8/10/15	Quarterly report Q4FY15
4	16	18.4	Test Campaign: MEA Long term study complete	Completion of 1000 hour load-following campaign using 30% wt MEA while maintaining a daily average of > 90% CO ₂ capture efficiency. Calculate the reference energy consumption, corrosion data and emissions data for comparison with H3-1.	2/5/16	1/15/16	Quarterly report Q2FY16
4	17	18.2	Test Campaign: Parametric study using H3-1 complete	Completion of 27 experiments chosen to evaluate 4 independent variables using H3-1	3/4/16	4/25/2016	Quarterly report Q3FY16
4	18	18.4	Test Campaign: H3-1 Long term Study complete	Completion of 1000 hour load-following campaign using H3-1 while maintaining a daily average of > 90% CO ₂ capture efficiency. Calculate the reference energy consumption, corrosion data and emissions data for comparison with 30% wt MEA.	7/11/16	7/1/2016	Quarterly report Q3FY16
4	19	19	Report 500 hour baseline performance of 30% MEA in slipstream pilot unit	An intermediate report that provides an update to the preliminary technical and economic analysis and	11/16/15	1/15/16	Quarterly report Q2FY16

				incorporates data from the 30% MEA continuous verification run			
4	20	19	Issue Final Update of Techno-Economic Analysis (TRL Level 6)	Issue Topical Report	6/23/2020		Topical Report file
4	21	19	Issue Final EH&S Assessment	Issue Topical Report	6/23/2020		Topical Report file
4	22	17	Issue Project Final Scientific Report	Final Report	6/25/2020		Final Report file

16) LESSONS LEARNED

UK CAER has learned much during the course of this project, during which the UK CAER CCS was advanced to TRL 6. The 0.7 MWe UK CAER CCS has been in regular operation by UK CAER staff since May 2015, has accrued about 4880 operational hours, and has certainly been demonstrated in an operating power generation environment at KU's E.W. Brown Generating Station in Harrodsburg, KY. During this time, 24 hour per day, 7 days per week operations were conducted in addition to operating with daily process start-up and shutdowns, both in the summer and winter, with specific requirements associated with each scenario being documented in the Standard Operating Procedures.

1. *Large pilot scale CCSs (equivalent 10-25 MWe scale) will be large quantity hazardous waste generators and will need to make accommodations for meeting all related regulations.* Most amine solvents have a high propensity to degrade due to interactions with flue gas components such as limestone/fly ash, SO₂ and NO₂ or from thermal effects. Some degradation products must be removed from the solvent via a reclaimer. Based on operational experiences of 0.7 MWe carbon capture pilot units, it is almost certain that the waste from reclaiming solvent will be considered hazardous waste. This designation requires specific accommodations for storage, handling, disposal and notifications, which need to be included from the beginning of the design phase to ensure proper compliance. It should be noted here that disposal of hazardous material can add a considerable expense to the overall project budget.
2. *Frequent reclaiming may be necessary to keep the working solvent categorized as non-hazardous.* In the field of water treatment, amines have been widely used to remove metallic elements such as selenium, arsenic, and others. Accumulation of such elements, especially selenium and arsenic, has been reported in solvents from post combustion aqueous CO₂ capture processes at levels over RCRA limits, for instance 1 ppm for Se. To minimize the complications of accidental chemical spills from CO₂ capture systems, the host site power plant could require the working solution to be maintained as a non-hazardous material. This can be achieved with continuous or frequent batch operation of a thermal reclaimer to remove these metallic elements from the solvent.
3. *Costs of the advanced solvent need to be balanced with the savings from energy consumption.* During the solvent sensitivity and TEA study conducted by UK CAER, it was realized that advanced solvents are expensive and any economy of scale savings in production may not be realized due to high raw material costs. Therefore, when evaluating advanced solvents for use in large pilot scale systems (or bigger), a cost/benefit analysis is needed to verify that the expected energy savings more than offsets the additional cost to using a more standard solvent.
4. *Utilization of Engineering Procurement and Construction (EPC) services are important and they must satisfy the requirements of the host site and the technology developer (project prime) in a triangular relationship.* In order to ensure the design and construction of a pilot plant occurs on time and on budget, utilization of an EPC firm is vital. The EPC, while under contract to provide the technology developer's engineering design, procurement, and construction services, also must work with the host utility to meet host site requirements including established best practices that often exceed OSHA and other lawful requirements and

guidelines. In order to mitigate any potential delay and cost overruns, the scope and boundaries must be clearly defined at the beginning of the project and clearly understood by all parties. A representative from the host site must be included and integrated into the team from the beginning of the design/integration phase. This allows the host site to make sure all applicable site requirements are included up front, prior to construction phase.

5. *Utilities (electricity, water, and steam) supplied to large pilot scale CCS may generate complications for a utility in a regulated state.* The host site will need an approval from the governing agency for cost of power/steam supplied to the pilot scale CCS, if the host site is considering recouping costs associated with providing this steam and/or electricity to the project as cost share. Secondarily, established boundaries of electricity service territories may require the pilot scale CCS to tie-in to electrical power outside the host power plant, rather than utilizing a direct tie-in to the host auxiliary power panel.
6. *Advancing through the TRLs in small steps is necessary and jumps from the bench scale, plus modeling to the pilot scale is not recommended.* From UK CAER's extensive work in the CCS field over the last 10+ years, it has become evident that scale-ups should occur gradually for a number of reasons. First, at each scale new issues and solutions become apparent that were unknown at the previous scale. Second, each scale-up should build upon the lessons learned at the previous scale. Finally, following the TRL development plan provides good risk management for any technology. Specifically in the CCS field, there are many instances where attempting to jump from the model to a large pilot scale unit would produce a system that was significantly over built (columns much taller than would be required based on actual operational data). One specific example is based on UK CAER's own recent experience. Based on simulation/modeling work performed at UK CAER it is well known that the sizing of the packed columns is quite sensitive to three parameters: kinetic data, the flow model and packing selection including correlations for mass transfer and interfacial area. Using only the modeling data mentioned above, commercial scale systems similar in size to the large pilot would have very tall columns, over 100 ft. (30 m). However, based on actual operation data, it has been proven that columns much shorter than this are sufficient. Thus reducing the capital costs of the CO₂ capture system while simultaneously proving that good risk management through the gradual progression through the TRLs is ideal.
7. *A mutually beneficial partnership between the CCS operations team and the host site is critical.* In general, the host site volunteers to assume risk associated with operations of an experimental pilot scale unit on their property for the benefit of advancing the technology, which has the potential to benefit society. Finding a utility that is forward looking to partner with on pilot scale CCS units of significant scale is a necessity. UK CAER has been fortunate to have a strong business relationship with LGE/KU for over a decade, including almost 6 years of small pilot scale CCS operation on their property. As a guest on the Utility's property, it is essential that pilot scale CCS operations impact the host utility as little as possible in order to maintain an effective relationship.
8. *The integration of a large pilot scale CCS project into a coal-fired unit with capacity of less than 25MWe or equivalent base load rating, may put the unit over the current Clean Air Act (CAA) thresholds to be recognized as an electricity generating unit (EGU).* Due to the

extensive steam requirement for solvent regeneration, and MWe-scale electricity requirement to run the auxiliary pumps/blowers of a CCS unit, extra coal will need to be burned if the unit nameplate net output is maintained to meet the external load demand. In this case retrofitting the unit with desulfurization, denitration, and mercury removal shall be required on top of the CCS installation.

9. *The integration of a CCS project to a commercial coal-fired unit with an existing air permit may require permit modification to reflect the conventional pollutant concentration changes due to massive amounts of CO₂ being removed from the flue gas.* The change in the flue gas conditions without CO₂ going to the stack is significant, including a reduction in volumetric flow, gas velocity, and gas temperature. This may affect the design of a future stack and CEMS and the performance of an existing stack and CEMS. This may also impact the plume exiting the stack. The pollutant concentration calculations may also need to be altered taking into account the new flue gas conditions. All of these variables will need to be considered and evaluated by the host site before and during CCS design.

17) TECHNOLOGY BENEFITS AND SHORTCOMINGS

The overall benefits of the technology have been captured in the cost savings of the technology relative to DOE RC10 as summarized in the TEA (**Section 13**) and demonstrated experimentally for the different advanced solvents tested. The uniqueness of solvents notwithstanding, the versatility of technology allowed for tuning process parameters to optimize energy benefits as well as controlling secondary emissions. The benefits are derived from the process heat integration and approaches adopted to enhance the mass transfer of CO₂ from the flue gas into the solvents to maximize solvent performance and reduce the energy penalty to the plant. Specific benefits realized relate to:

- (i) the two-staged stripping process which reduces lean solvent loading to the absorber with the simultaneous enrichment of the CO₂ in the flue gas from recycled stripped CO₂ to increase the driving force for high rich carbon loading at the bottom of the absorber; resulting in reduced energy penalty of the CCS system.
- (ii) the heat integrated cooling tower recovers low quality energy which is typically rejected to the environment; contributing to the energy savings from the process.
- (iii) the additional water wash recovery column reduces solvent emissions significantly at the absorber outlet; the recovered solvent is used for solvent make-up resulting in operational cost savings from minimized solvent make-up and losses.
- (iv) the water balance of solvents is effectively managed from water recovered from the air used in the secondary stripper to ensure minimal water-up to maintain desired solvent concentrations.

Some shortcomings identified relate to handling of solvent waste in the process. Interaction of flue gas contaminants with the solvent and process conditions contribute to solvent degradation; resulting in the formation of degradation products and accumulation of some RCRA metals in the solvent. Functionality of the solvent is sustained for longer term operation by reclaiming which

can result in the concentration of RCRA metals higher than permissible levels and render solvent hazardous with stringent disposal requirements. Approach to mitigate this concern together with other technical gaps that need to be addressed to advance the technology are discussed in the next section.

18) RECOMMENDATIONS FOR FUTURE R&D ADDRESSING SHORTCOMINGS

The pilot scale demonstration of the CCS in this work tested new concepts which have proven beneficial in meeting cost and energy savings targets per DOE's performance goals and guidelines for the application of the technology to mitigate CO₂ emissions from coal-fired power plants. Knowledge and experience gained from the design, construction and operation of the pilot plant have provided opportunities to identify key technological areas that need to be further explored as well as short-comings that have to be addressed as the technology is advanced eventually to the commercial scale. UK CAER leveraging its experience from lab-, bench- and pilot-scale work in CO₂ capture presented a technical gap analysis in a project report (DE-FE0026497) to DOE (Liu, 2016) with more comprehensive details for near and long-term recommendations for the advancement of the technology. Some of the pertinent recommendations are highlighted here with proposed approaches for addressing shortcomings where identified.

1. Heat Integration

As previously noted, a major benefit realized with the UK CAER technology is from the heat integration schemes that resulted in energy savings for the process. New and innovative process schemes and heat integration techniques need to be employed. Various heat integration schemes have been proposed and the energy benefits to the process have been demonstrated from simulations and require to be tested at scale. Examples of this include rich solvent splitting to the absorber, water vapor compression produced from lean solution flashing at the stripper bottom exit, and multi-effect strippers. UK CAER will explore the benefits of rich-solvent splitting as this technology is scaled up in a 10 MWe large pilot project (DE-FE0031583). With this heat integration, a portion of the rich stream from the bottom of the absorber is by-passed around the lean/rich heat exchanger and introduced to the top of the stripper and the heated rich stream is sent to suitable lower point in the stripping column to optimize heat recovery from the hot lean solvent and the stripper overhead section.

2. Cost-effective solvents with high stability, high cyclic capacity and fast kinetics

Advanced solvents tested in the pilot unit showed higher stability, faster kinetics and cyclic capacity relative to MEA resulting in varying degrees of energy savings as well as lower emissions, make-up and corrosion rates. The lower solvent circulation rates used due to the high cyclic capacities is an advantage for capital cost savings as reduced column sizes can be used. The alternative solvents with these desirable properties for CO₂ capture however, are generally more costly than MEA and therefore the design of cost-effective advanced solvents can further contribute to lowering the operating cost of the process.

3. Process Intensification

In the conventional carbon capture system, the absorber and stripper constitute a major portion of ~55% and 17% respectively of the total cost (Yu et al., 2012). While the use of high capacity

solvents contribute to size reduction in columns, process intensification is also expected to reduce column sizes with significant reduction in the overall capital costs. Process intensification to the lean/rich heat exchanger is also proposed as an area for further development for efficient heat recovery in the capture process to improve system operation and capital costs.

Analysis of solvent performance in the pilot unit showed that the absorber column was tall enough for solvents to attain close to the equilibrium loading at the bottom of the absorber with appropriate process conditions. The greater part of the reaction of the solvent with CO₂ takes part in a few stages from the top of the absorber column with lower stages conditioning the solvent to enrich its loading. UK CAER using results from the pilot tests to validate simulations has shown that the size of the absorber column can be further reduced by optimizing the stages required for the desired equilibrium loading to be attained. This will be implemented in the 10 MWe scaled-up process to reduce capital costs.

4. Materials of Construction

The corrosive tendencies of amines as demonstrated in the pilot campaign particularly in areas of process where amine is high in CO₂ loading with high temperature or both, require construction material resistant to corrosion as this presents operating and equipment replacement challenges. Corrosion in the capture process is addressed by using corrosion inhibitors in addition to using stainless steel in locations where wetter surfaces are expected. Materials such as concrete, with plastic/polymer or ceramic liners are used for the CO₂ absorber constituting a high capital expense. It is recommended that low cost material be used in certain locations such as the CO₂ absorber and the lean polisher prior to the solvent return to the absorber. Suitable coatings or liners would also allow the construction of reaction columns with non-metal materials.

5. Waste Management

The degradation of solvents from flue-gas contaminants and process conditions results in the formation of heat stable salts (HSS) and concentration of degradation products. These products have to be minimized to maintain solvent activity and reduce the negative impacts for corrosion. Minimizing the formation of degradation by-products is necessary as large quantity disposal can significantly increase operating costs. Thermal reclaiming, which is energy intensive, is a way of reducing HSS and other heavy metals from the flue gas that could be present in the solvent. The pilot campaign showed that thermal reclamation cannot effectively remove oxidative degradation products. There is therefore a need for other solvent purification techniques, less energy intensive and non-distillation based as thermal reclaiming. Advanced reclaiming techniques for heavy metal separation from the amine capture solvents are also desired.

6. Aerosol Emissions Handling

Aerosol formations in the capture process result in loss of solvent from the top of the absorber with its associated operational cost of solvent make-up. Mechanisms relied upon by the state-of-the-art aerosol treatment technologies such as demisters and cyclone eliminators are based on the principle of contacting the aerosols with another surface to condense. The added complexities of these additional components lead to increased capital and operational costs.

UK CAER's proposed strategy is predicated on being able to eliminate aerosol formation to preclude the need for additional expensive equipment. An approach previously developed by UK CAER involved the use of charged colloidal gas aphrons (CGA) which combine electrostatic effects with physical contact in a cyclone type eliminator. The CGA tested on UK CAER's large bench unit showed 60% reduction of total emission by aerosol agglomeration (Li et al., 2015). There still exists opportunities for addressing aerosol emissions and the water wash system developed more recently by CAER and tested on the pilot unit with over 90% reduction in solvent emissions from the top of the absorber is recommended.

7. Gas-Liquid Distribution and Prevention of Channel Flow

Dramatic changes in operational guidelines for coal-fired power plants will make it a common practice to balance load changes from intermittent renewable generation with that of large-scale PC units. Thus, PC units will not be operated at traditional constant base loads. The considerable dynamic load changes are expected to pose significant challenges for the operation of the carbon capture systems. Adjusting to these load changes lead to changes in liquid and gas flow rates with resultant pressure drop changes in the absorber impacting flow patterns. Flow channeling and flooding can occur as a result. Flow stability issues therefore necessitate the careful selection of packing during the design to optimize gas-liquid distribution to accommodate potential operational scenarios due to the dynamic changes to prevent/minimize channeling and flooding. The development and utilization of advanced gas and liquid distributors with relatively low gas-side pressure drop is recommended.

Addressing or narrowing the identified technical gaps from the successful demonstration of proposed technologies will continue to be necessary to the advancement of capture technology prior to scaling-up and commercialization.

19) LIST OF EXHIBITS

Exhibit 1.1.1. Three Aspects of the UK CAER CCS.....	10
Exhibit 2.1.1. Project Goal and Objectives.....	20
Exhibit 2.2.1. UK CAER 0.7 MWe Post-Combustion CO ₂ Capture System at E.W. Brown Generating Station, Harrodsburg, KY.....	21
Exhibit 2.2.2. Detailed Integration of the Proposed UK CAER Technology into an Existing Commercial Scale Power Plant.....	22
Exhibit 3.0.1. Division of the Design Scope of Work.....	24
Exhibit 3.1.1. Pretreatment Tower Block PFD.....	28
Exhibit 3.1.2. Absorber and Stripping Columns Block PFD.....	28
Exhibit 3.1.3. Cooling Tower Block PFD.....	28
Exhibit 3.1.4. UK CAER 0.7 MWe Small-pilot Scale CCS Pretreatment Step P&ID.....	29
Exhibit 3.1.5. 0.7 MWe Small Pilot Scale CCS Module Anchor Bolt Location Detail Prepared by KMPS.....	30
Exhibit 3.1.6. UK CAER 0.7 MWe Small-pilot Scale CCS Piping Tie In List Prepared by KMPS.....	31
Exhibit 3.1.7. 0.7 MWe Small Pilot Scale CCS Equipment List Prepared by KMPS.....	32
Exhibit 3.1.8. UK CAER 0.7 MWe Small Pilot Scale CCS System Volumes Prepared by KMPS.....	35

Exhibit 3.1.9. Navisworks® Freedom 3-D Model of the Entire 0.7 MWe Small Pilot Scale CCS Created by KMPS.....	36
Exhibit 3.1.10. Navisworks® Freedom 3-D Model Closeups From the 0.7 MWe Small Pilot Scale CCS Created by KMPS.....	36
Exhibit 3.1.11. Spectrum Systems, Inc. Continuous Emissions Monitoring System.....	37
Exhibit 3.1.12. Spectrum Systems, Inc. Continuous Emissions Monitoring System.....	37
Exhibit 3.1.13. The Controlling Computers with Delta V Supplied by KMPS.....	38
Exhibit 3.1.14. Delta V Control System Operations Screenshot.....	38
Exhibit 3.1.15. Shipping Modules Required a Crane to Lift the Back when Going Around this Corner, Very Near E.W. Brown Generating Station, 8/20/2014.....	38
Exhibit 3.1.16. Another Tight Corner Very Near E.W. Brown Generating Station, 8/20/2014... Exhibit 3.1.17. Modules Stages Along the E.W. Brown Generating Station Entrance for Organized Placement the Following Day, 8/20/2014.....	38
Exhibit 3.1.18. Moving Modules into Place for Erection at Process Site, 8/21/2014.....	39
Exhibit 3.2.1. Process Foundation Design by B+K.....	40
Exhibit 3.2.2. Reinforcing Steel Inspection by B+K During the Construction Phase.....	40
Exhibit 3.3.1. A Portion of the Steam Supply and Condensate Return Piping System Design Completed by Black and Veatch (B&V).	41
Exhibit 4.1.1. Division of Construction.....	42
Exhibit 4.2.1. Removed Existing Electrical Duct Bank, 6/2/2014.....	42
Exhibit 4.2.2. Drilling Foundation Pier A, 4, 6/13/2014.....	42
Exhibit 4.3.1. Slab reinforcement, 07/17/2014.....	43
Exhibit 4.3.2. Modular Structure Anchor Bolt Dimension Check, 7/17/2014.....	43
Exhibit 4.3.3. Main Slab Concrete Pour, 7/22/2014.....	43
Exhibit 4.3.4. Main Slab with Completed Anchor Bolt Pedestals, 8/8/2014.....	43
Exhibit 4.4.1. Erection of Module 2, 8/21/2014.....	44
Exhibit 4.4.2. Erection of Module 6, 8/29/2014.....	44
Exhibit 4.4.3. Erection of Cooling Tower, 9/17/2014.....	44
Exhibit 4.4.4. Cooling Tower Blower (B-103) is Set, 10/15/2014.....	44
Exhibit 4.5.1. Off-module Piping Installation, 10/15/2014.....	45
Exhibit 4.5.2. Secondary Egress Ladder Installation, 10/15/2014.....	45
Exhibit 4.6.1. Flue Gas Supply Lines Installed at Top of Stack Duct, 4/7/2015.....	46
Exhibit 4.6.2. Vertical Sections of Flue Gas Supply and Return Lines, 4/7/2015.....	46
Exhibit 4.6.3. Construction of the Steam Supply Line, 12/3/2014.....	46
Exhibit 4.6.4. Steam Supply and Condensate Return Lines Installed on Pipe Roller Support, 12/3/2014.....	46
Exhibit 4.7.1. Process Grounding Ring Trench, 6/25/2014.....	47
Exhibit 4.7.2. Electrical Shed Set, 10/8/2014.....	47
Exhibit 4.8.1. Mobile Control Room and Field Laboratory is Set, 11/13/2014.....	48
Exhibit 4.8.2. Automatic Liquid Sample Analysis Instrument, 5/6/2015.....	48
Exhibit 4.8.3. Field Laboratory, 5/6/2015.....	48
Exhibit 4.8.4. Mobile Control Room Identification Sign, 4/8/2016.....	48
Exhibit 4.9.1. Cooling Tower Level Gauge (LT-C106-01), 5/7/2015.....	50
Exhibit 4.9.2. Soda Ash Loop pH Probes, 1/23/2015.....	50
Exhibit 4.9.3. Column Liquid/Gas Sample Collection Port.	50
Exhibit 4.9.4. Controls Wiring Installed by UK CAER, 2/11/2015.	50

Exhibit 4.10.1. 3D model of the UK CAER process including planned MSU related piping.....	51
Exhibit 4.10.2. The vacuum pump installed within Module 2.....	52
Exhibit 4.10.3. The solvent recovery column (C-200) installed within Module 1.....	52
Exhibit 4.10.4. The MSU and B-200 blower installed on the newly constructed floor atop Module 2.....	52
Exhibit 4.10.5. Heat exchanger (E-200) installation within Module 1.....	52
Exhibit 6.0.1. MEA Parametric Campaign Operating Conditions.....	55
Exhibit 6.0.2. 0.7 MWe Small Pilot Scale UK CAER CCS Location of Liquid Sample Collection Points.....	55
Exhibit 6.1.1. Most Pertinent Process Parameters from One Steady State Condition from the MEA Campaign: 9/30/2015 from 21:15 to 23:15.....	56
Exhibit 6.1.2. Solvent Alkalinity from the Parametric Portion of the MEA Campaign.....	58
Exhibit 6.1.3. MEA Parametric Campaign CO ₂ Capture Efficiency and Solvent Regeneration Energy.....	58
Exhibit 6.1.4. Effect of Absorber L/G on Solvent Regeneration Energy, Labels – L/G shown in blue, CO ₂ Concentration (vol %, dry) shown in red, Primary Stripper Pressure (psia) shown in green.....	59
Exhibit 6.1.5. Effect of Absorber Inlet CO ₂ Concentration on Solvent Regeneration Energy, Labels – L/G shown in blue, CO ₂ Concentration (vol %, dry) shown in red, Primary Stripper Pressure (psia) shown in green	59
Exhibit 6.1.6. Effect of Primary Stripper Pressure on Solvent Regeneration Energy, Labels – L/G shown in blue, CO ₂ Concentration (vol %, dry) shown in red, Primary Stripper Pressure (psia) shown in green	59
Exhibit 6.1.7. Experimental Repeatability in MEA campaign, Labels – L/G shown in blue, CO ₂ Concentration (vol %, dry) shown in red, Primary Stripper Pressure (psia) shown in green.....	59
Exhibit 6.3.1. The four corrosion sampling points (marked by dash lines) in the 0.7 MWe CO ₂ capture unit at KU’s E.W. Brown Station. Within the absorber column (A), in the CO ₂ lean amine piping (CL), within the stripper column (S), and in the CO ₂ rich amine piping (HR).	60
Exhibit 6.3.2. Chemical composition of A106 carbon steel and 304 stainless steel (wt.%).....	61
Exhibit 6.3.3. Corrosion sample rod containing six specimens.....	61
Exhibit 6.3.4. Typical operating conditions in the pilot-scale CO ₂ capture process.	63
Exhibit 6.3.5. Mass loss corrosion rates in 30 wt.% monoethanolamine based on process run time for A106, Ni-coated A106, Ni ₂ Al ₃ -coated A106, and SS304 in the (a) absorber column, (b) CO ₂ lean amine piping, (c) stripper column, and (d) CO ₂ rich amine piping. For the stripper (c), corrosion rates for carbon steels after 500 process run hours are calculated values (dash lines), assuming a final specimen mass of zero.	65
Exhibit 6.3.6. Corrosion specimens after approximately 500 hours of process run time in the carbon capture unit in the absorber column (A), CO ₂ rich amine piping prior to the stripper (HR), CO ₂ lean amine piping prior to the absorber (CL), and stripper column (S).....	66
Exhibit 6.3.7. Corrosion specimens after approximately 1000 hours of process run time in the carbon capture unit in the absorber column (A), CO ₂ rich amine piping prior to the stripper (HR), CO ₂ lean amine piping prior to the absorber (CL), and stripper column (S). A106 specimens in the stripper column are not shown due to loss of specimen after 500 hours.	66
Exhibit 6.3.8. SEM images of corrosion specimens after 500 hours of process run time in the stripper column: (a) A106 carbon steel, (b) Ni-coated A106, (c) Ni ₂ Al ₃ -coated A106, and (d) SS304 stainless steel.	67

Exhibit 6.3.9. Cross-sectional SEM images of corrosion specimens with EDS line scan results from within the stripper column: (a) Ni-coated A106 after 250 hours, (b) Ni ₂ Al ₃ -coated A106 after 250 hours. EDS scans follow the yellow lines.	68
Exhibit 6.3.10. Cross-sectional SEM images of corrosion specimens with EDS line scan results from within the stripper column: (a) Ni-coated A106 after 500 hours, (b) Ni ₂ Al ₃ -coated A106 after 500 hours. EDS scans follow the yellow lines.	69
Exhibit 6.4.1. Flue gas HSS accumulation during MEA solvent testing (the gap and vertical dashed line represent the period when the solvent was thermally reclaimed).	71
Exhibit 6.4.2. Oxidative degradation product formation during MEA solvent testing (the gap and vertical dashed line represent the period when the solvent was thermally reclaimed).	71
Exhibit 6.4.3. MEA degradation (polymerization) products formed during this MEA solvent testing campaign (the gap and vertical dashed line represent the period when the solvent was thermally reclaimed).	72
Exhibit 6.4.4. Formation pathway of MEA thermal degradation compounds observed (in bold) in this solvent testing campaign; (1) HEEDA, (2) HEIA and (3) HEAEIA.	73
Exhibit 6.4.5. Formation pathway of MEA oxidative degradation compounds HEI and HEMI, as reported by Vavelstad et al. (2013), from (a) formaldehyde and (b) acetaldehyde.	73
Exhibit 6.4.6. Aldehydes observed in 30% MEA solvent during pilot testing campaign.	73
Exhibit 6.4.7. Metal accumulation from coal flue gas during MEA solvent testing (the dashed line represent the period when the solvent was thermally reclaimed; the light gray line represents when the analysis method was changed from ICP-OES to ICP-MS).	75
Exhibit 6.4.8. Metal accumulation from corrosion during MEA solvent testing (the dashed line represent the period when the solvent was thermally reclaimed; the light gray line represents when the analysis method was changed from ICP-OES to ICP-MS).	75
Exhibit 6.4.9. Corroding amine strainer fabricated materials not specified for amine service that was removed after the conclusion of the MEA solvent testing campaign.	75
Exhibit 6.5.1. Absorber ammonia emissions measured by UK CAER (dark X) and EPRI (grey square) using manual sampling methods.	79
Exhibit 6.5.2. Absorber ammonia emissions (in ppmV) compared with the Fe concentration (ppm) in the solvent (vertical dashed line represents period of thermal solvent reclaiming).	79
Exhibit 6.5.3. Absorber ammonia emissions (in ppmV) compared to the Cu concentration (ppm) in the solvent (vertical dashed line represents period of thermal solvent reclaiming).	80
Exhibit 6.5.4. Absorber MEA emissions measured by UK CAER (dark X) and EPRI (grey square) using manual sampling methods.	80
Exhibit 6.5.5. Aldehyde and ketone emissions measured during pilot MEA testing.	81
Exhibit 6.5.6. Calculated nitrosamine emissions limits of quantitation (LOQ) during MEA pilot testing.	82
Exhibit 6.5.7. MEA emissions (in ppmV) from the secondary air stripper.	83
Exhibit 6.6.1. 6M MEA Parametric Test Conditions.	84
Exhibit 6.6.2. Experimental conditions and results for 6M MEA at 36 psia.	84
Exhibit 6.6.3. Regeneration energy for 6M MEA at 36 psia for different L/G. Designation (% capture, stripper bottom temp., absorber inlet temp.)	85
Exhibit 6.6.4. Rich and lean carbon loadings of 6M MEA solution for experiments at 36 psia.	85
Exhibit 6.6.5. Alkalinity and solvent loadings for 6M MEA solvent.	85
Exhibit 6.6.6. Temperature in absorber for 6M MEA for different tests.	85
Exhibit 6.6.7. Energy of regeneration for ~36 wt% MEA for different stripper pressures.	86

Exhibit 6.6.8. Comparison of energy of regeneration for different concentrations of MEA.....	86
Exhibit 7.0.1. H3-1 Parametric Campaign Operating Conditions.	87
Exhibit 7.0.2. Mass Balance Between CO ₂ stripped from Primary Stripper and that from CO ₂ Removed in the Absorber minus CO ₂ Stripped in Secondary Stripper.	87
Exhibit 7.1.1. Most Pertinent Process Parameters from one steady state condition from the H3-1 Campaign: 4/26/2016 from 13:00 to 15:00.....	88
Exhibit 7.1.2. Process Performance Temperatures During Entire H3-1 Campaign.	90
Exhibit 7.1.3. Stripper Pressure During Entire H3-1 Campaign.....	90
Exhibit 7.1.4. Gas and Liquid Flow Rates During Entire H3-1 Campaign.	90
Exhibit 7.1.5. Gas CO ₂ Composition During Entire H3-1 Campaign.	90
Exhibit 7.1.6. Amine Stream C-Loading During Entire H3-1 Campaign.	90
Exhibit 7.1.7. Absorber Liquid/Gas Flow Rate Ratio and Absorber Gas Velocity During Entire H3-1 Campaign.....	90
Exhibit 7.1.8. System Temperatures at one Steady State Condition, 4/26/2016 from 13:00 to 15:00.	91
Exhibit 7.1.9. Stripper Pressure at one Steady State Condition, 4/26/2016 from 13:00 to 15:00.	91
Exhibit 7.1.10. Gas and Liquid Flow Rates at one Steady State Condition, 4/26/2016 from 13:00 to 15:00.	91
Exhibit 7.1.11. Gas CO ₂ Composition at one Steady State Condition, 4/26/2016 from 13:00 to 15:00.	91
Exhibit 7.1.12. Amine Stream C-Loading at one Steady State Condition, 4/26/2016 from 13:00 to 15:00.	91
Exhibit 7.1.13. Absorber Liquid/Gas Ratio and Absorber Gas Velocity at same Condition, 4/26/2016 from 13:00 to 15:00.	91
Exhibit 7.1.14. Solvent Concentrations for H3-1 Campaign.	92
Exhibit 7.2.1. Solvent Alkalinity and CO ₂ Capture Efficiency from the Entire H3-1 Campaign.	93
Exhibit 7.2.2. Solvent Alkalinity, Energy Consumption and Absorber L/G Flow Rate Ratio from the Entire H3-1 Campaign.	93
Exhibit 7.2.3. Effect of L/G ratio energy of regeneration, Labels – L/G shown in blue, CO ₂ Concentration (vol %, dry) shown in red, Primary Stripper Pressure (psia) shown in green.....	93
Exhibit 7.2.4. Effect of inlet CO ₂ concentration on energy of regeneration, Labels – L/G shown in blue, CO ₂ Concentration (vol %, dry) shown in red, Primary Stripper Pressure (psia) shown in green.....	93
Exhibit 7.2.5. Liquid analyses comparison for different inlet CO ₂ concentrations.	94
Exhibit 7.2.6. Effect of stripper pressure on energy of regeneration, Labels – L/G shown in blue, CO ₂ Concentration (vol %, dry) shown in red, Primary Stripper Pressure (psia) shown in green.	95
Exhibit 7.2.7. Repeatability of experiments. All conditions were maintained except for the different gas flow rates of 1400 acfm (L/G = 3.7) and 1300 acfm (L/G = 4), Labels – L/G shown in blue, CO ₂ Concentration (vol %, dry) shown in red, Primary Stripper Pressure (psia) shown in green.....	95
Exhibit 7.2.8. Comparison of measured CO ₂ stripped from primary stripper and estimated mass balance from CO ₂ absorbed in the absorber minus CO ₂ stripped from secondary stripper.	95
Exhibit 7.2.9. Heat exchanger hot end approach temperature for different stripper pressures....	95
Exhibit 7.3.1. Mass loss corrosion rates in Hitachi H3-1 solvent based on process run time for A106, Ni-coated A106, Ni ₂ Al ₃ -coated A106, and SS304 in the (a) absorber column, (b) CO ₂ lean	

amine piping, (c) stripper column, and (d) CO ₂ rich amine piping. Axes are similar to Exhibit 6.3.5.....	97
Exhibit 7.3.2. Corrosion specimens after approximately 500 hours of process run time in the carbon capture unit in the absorber column (A), CO ₂ rich amine piping prior to the stripper (HR), CO ₂ lean amine piping prior to the absorber (CL), and stripper column (S).....	98
Exhibit 7.3.3. XRD patterns of SS304 stainless steel specimens after 125 and 1250 hours of process run time in the (a) absorber column, (b) CO ₂ cold lean amine piping, (c) stripper column, and (d) CO ₂ rich amine piping. Reference phases with PDF card numbers and peak positions are provided.	99
Exhibit 7.3.4. XRD patterns of A106 carbon steel specimens after 125 and 1250 hours of process run time in the (a) absorber column, (b) CO ₂ lean amine piping, (c) stripper column, and (d) CO ₂ rich amine piping. Reference phases with PDF card numbers and peak positions are provided.	100
Exhibit 7.4. 1. Flue gas HSS accumulation during H3-1 solvent testing.....	101
Exhibit 7.4.2. Amine oxidation HSS formed during H3-1 solvent testing.....	101
Exhibit 7.4.3. Flue gas HSS accumulated in the H3-1 solvent.....	101
Exhibit 7.5.1. Nitrosamine emission samples collected during the H3-1 testing campaign.....	102
Exhibit 7.5.2. Ammonia emissions from the absorber during the H3-1 campaign collected by UK CAER (blue dot) and CB&I (red diamond).....	103
Exhibit 7.5.3. Ammonia emissions from the secondary air stripper during the H3-1 campaign collected by UK CAER (blue dot) and CB&I (red triangle).....	103
Exhibit 7.5.4. Aldehyde and ketone emissions from the absorber during the H3-1 campaign collected by UK CAER.....	104
Exhibit 7.5.5. Aldehyde and ketone emissions from the absorber during the H3-1 campaign collected by CB&I (inside green dashed lines) and UK CAER (inside blue dashed lines).....	104
Exhibit 7.5.6. Aldehyde and ketone emissions from the absorber during the H3-1 campaign collected by CB&I (circled in red) and UK CAER.....	104
Exhibit 7.5.7. Nitrosamine Emissions Summary from H3-1 Testing Campaign.....	106
Exhibit 8.0.1. CAER Solvent Parametric Campaign Operating Conditions.....	107
Exhibit 8.1.1. Effect of L/G ratio energy of regeneration. 3 numbers in exhibit for the different run conditions are L/G (blue), inlet CO ₂ concentration (vol% - red), and stripper pressure (psia – green) respectively.....	108
Exhibit 8.1.2. Effect of inlet CO ₂ concentration on energy of regeneration.....	108
Exhibit 8.1.3. Effect of stripper pressure on energy of regeneration.....	108
Exhibit 8.1.4. Heat exchanger hot end approach temperature for different stripper pressures... 109	109
Exhibit 8.2.1. Screening process variables for impact on regeneration energy and rich loading.	111
Exhibit 8.2.2. Impact of process variables on regeneration energy of solvent.....	111
Exhibit 8.2.3. Impact of process variables on rich loading of solvent.....	111
Exhibit 8.3.1. Test Conditions for Varying CO ₂ Capture.....	112
Exhibit 8.3.2. Energy of Regeneration of CAER Solvent for Varying Capture Efficiency.....	113
Exhibit 8.3.3. Variable Impact on Energy of Regeneration of Solvent.....	113
Exhibit 8.4.1. MBT Inhibitor concentration present in the CAER solvent.....	113
Exhibit 8.4.2. Events during CAER-B3 ~1000 run hour campaign.....	113
Exhibit 8.4.3. Flue gas HSS accumulation during CAER solvent campaign.....	115
Exhibit 8.4.4. Oxidative degradation HSS accumulation during CAER solvent campaign.....	115

Exhibit 8.4.5. Total HSS accumulating in different solvent campaigns with the total HSS accumulation rate calculated assuming a linear rate, and including routine reclaiming.	116
Exhibit 8.4.6. Corrosion metals accumulation in the CAER solvent.....	116
Exhibit 8.4.7. Metals found in the solvent as received.	116
Exhibit 8.4.8. RCRA metal accumulation in the CAER-B3 solvent.	117
Exhibit 8.5.1. Absorber ammonia emissions in CAER campaign measured by UK CAER using manual sampling methods.....	118
Exhibit 8.5.2. Inhibitor concentration present in the CAER solvent compared to the ammonia emissions measured at the absorber exit.	118
Exhibit 8.5.3. Inhibitor concentration present in the CAER solvent compared to the ammonia emissions measured at the absorber exit.	118
Exhibit 8.5.4. Ammonia Emissions levels from the absorber exit in CAER solvent compared to the MEA solvent testing campaign.	118
Exhibit 8.5.5. Ammonia emissions during CAER solvent campaign measured by UK CAER at the secondary stripper using manual sampling methods.....	120
Exhibit 8.5.6. Ammonia emissions during CAER solvent campaign measured by UK CAER at the secondary stripper compared with the iron concentration in the solvent.	120
Exhibit 8.5.7. Ammonia emissions during CAER solvent campaign measured at the absorber exit and secondary stripper compared with the solvent flow rate.....	120
Exhibit 8.5.8. Ammonia Emissions levels from the absorber exit compared to the solvent flow rate during CAER solvent campaign.	121
Exhibit 8.5.9. Amine emissions compared to the temperature profile of the CAER solvent throughout the absorber column.	121
Exhibit 8.5.10. Comparison of amine emissions from the absorber exit for CAER solvent and MEA.....	121
Exhibit 8.5.11. Amine emissions during CAER solvent campaign measured by UK CAER at the secondary stripper using manual sampling methods.	123
Exhibit 8.5.12. Amine emissions measured at the secondary stripper compared to the lean solvent temperature during CAER solvent campaign.	123
Exhibit 8.5.13. Pairwise correlation analysis values.....	123
Exhibit 8.5.14. Aldehyde Emissions collected from the absorber exit and the secondary stripper.	124
Exhibit 8.5.15. Nitrosamine Emissions collected from the absorber exit and the secondary stripper.	124
Exhibit 9.1.1. Permeate concentrations of membrane at different flue gas feed concentrations.	126
Exhibit 9.1.2. Permeate concentrations of membrane at different inlet feed gas temperatures..	126
Exhibit 9.1.3. Permeate concentrations of membrane with fixed inlet feed of 14 vol% CO ₂ for different gas temperatures.....	126
Exhibit 9.1.4. Representative membrane test conditions with 14 vol% CO ₂ feed.....	127
Exhibit 9.2.1. Specific reboiler duty comparison for membrane and non-membrane runs at L/G = 2.5 and stripper pressure of 30 psia.	128
Exhibit 9.2.2. Test conditions comparison for Proprietary Solvent C solvent at L/G = 2.5, stripper pressure = 30 psia.	128
Exhibit 9.2.3. Test conditions comparison at L/G = 2.5, Stripper pressure = 24 psia.	129
Exhibit 9.2.4. Specific reboiler duty comparison for membrane and non-membrane runs at L/G = 3.2 and stripper pressure of 30 psia.	129

Exhibit 9.2.5. Test conditions comparison for Proprietary Solvent C at L/G = 3.2, Stripper pressure = 30 psia.	130
Exhibit 9.2.7. Absorber temperature profile comparison for membrane and non-membrane runs at L/G = 2.5.	132
Exhibit 9.3.1. Ammonia emissions from the absorber exit during the Proprietary Solvent C testing campaign collected by UK CAER.	133
Exhibit 9.3.2. Ammonia emissions from the water wash exit during the Proprietary Solvent C testing campaign collected by UK CAER.	133
Exhibit 9.3.3. Total Proprietary Solvent C amine emissions from the absorber exit compared to water wash exit.	134
Exhibit 9.3.4. Ammonia and Amine concentration in the Water Wash solution during the advanced solvent post modifications campaign.	134
Exhibit 9.3.5. Total HSS accumulation in the water wash solution during the post modifications Proprietary Solvent C campaign.	135
Exhibit 9.3.6. Corrosion metal accumulation in the post modifications Proprietary Solvent C campaign.	135
Exhibit 9.3.7. RCRA element concentrations in the post modifications Proprietary Solvent C campaign.	135
Exhibit 9.3.8. Be, V, Mn, and Mo concentrations in the post modifications Proprietary Solvent C campaign.	136
Exhibit 9.3.9. Corrosion concentrations in the water wash solution during the post modifications Proprietary Solvent C campaign.	136
Exhibit 9.3.10. RCRA element concentrations in the water wash solution during the post modifications Proprietary Solvent C campaign.	136
Exhibit 10.1. Kettle-type tube and shell thermal reclaimer with a combined soda ash and amine charge line, temperature and level indicators, and drain for removing reclaimer sludge.	137
Exhibit 10.2. Reduction in contaminants in the MEA solvent from thermal reclaiming.	138
Exhibit 10.3. Reduction in contaminants in the H3-1 solvent from thermal reclaiming.	138
Exhibit 10.4. Relative energy (as stream) required to remove solvent contaminants by thermal reclaiming.	139
Exhibit 10.5. MEA mass balance from emissions, degradation and other losses.	140
Exhibit 11.1. P-109 Connecting Pipe Section Did Not Fit Correctly, 9/30/2014.	140
Exhibit 11.2. Example of Two Problems with the Cross-over Grating, 1) Lack of Support at Edges and 2) Gap Too Large Between Adjacent Pieces, 9/19/2014.	140
Exhibit 12.1. Updated State Point Data Table.	141
Exhibit 12.2. Recommended System Operating Conditions and Solvent Working Capacity.	142
Exhibit 15.1. Project Milestones.	148

20) REFERENCES

1. Aspen Technology, Inc., Aspen One – Process Optimization Software for Engineering, Manufacturing, and Supply Chain. 2012-2015, Houston, Texas.
2. Bhow, Abhoyjit S. Electric Power Research Institute. “Implementation of a Rate-based Model to Analyze the Application of a Heat Integrated Post-combustion CO₂ Capture System with Hitachi Advanced Solvent into Existing Coal-fired Power Plant.” Submitted to U.S. Department of Energy National Energy Technology Laboratory. March 2015.

3. Bhowm, Abhoyjit S. Electric Power Research Institute. "Preliminary Technical and Economic Feasibility Study on the Application of a Heat Integrated Post-combustion CO₂ Capture System with Hitachi Advanced Solvent into Existing Coal-fired Power Plant." Submitted to U.S. Department of Energy National Energy Technology Laboratory. December 2012.
4. Bhowm, Abhoyjit S. Electric Power Research Institute. "Technical and Economic Feasibility Study on the Application of a Heat Integrated Post-combustion CO₂ Capture System with Hitachi Advanced Solvent into Existing Coal-fired Power Plant." Submitted to U.S. Department of Energy National Energy Technology Laboratory. May 2020.
5. Carter, T. 2012. National Carbon Capture Center: Post-Combustion. Presented at the NETL CO₂ Capture Technology Meeting, 9-12 July, Pittsburgh, PA, USA.
6. Chahen, L., Huard, T., Cuccia, L., Cuzuel, V., Dugay, J., Pichon, V., Vial, J., Gouedard, C., Bonnard, L., Cellier, N., Carrette, P-L. 2016. Comprehensive monitoring of MEA degradation in a post-combustion CO₂ capture pilot plant with identification of novel degradation products in gaseous effluents. *Int. J. Greenh. Gas Control* 51, 305-316. DOI: 10.1016/j.ijggc.2016.05.020.
7. Chandan, P., Richburg, L., Bhatnagar, S., Remias, J. E., Liu, K. 2014. Impact of fly ash on monoethanolamine degradation during CO₂ capture. *Int. J. Greenh. Gas Control* 25, 102-108.
8. da Silva, E., Lepaumier, H., Grimstvedt, A., Vevelstad, S. J., Einbu, A., Vernstad, K., Svendsen, H. F., Zahlsen, K. 2012. Understanding 2-ethanolamine degradation in postcombustion CO₂ capture. *Ind. Eng. Chem. Res.* 51, 13329-13338.
9. Dai, N., Shah, A. D., Hu, L., Plewa, M. J., McKague, B., Mitch, W. A. 2012. Measurement of nitrosamine and nitramine formation from NO_x reactions with amines during amine-based carbon dioxide capture for postcombustion carbon sequestration. *Environ. Sci. Technol.* 46, 9793-9801. DOI: 10.1021/es301867b.
10. ENRISQ, LLC and Smith Management Group (SMG). 2013. Preliminary Quantitative Risk Evaluation Potential Nitrosamine Exposure During a Pilot Test of a Post-Combustion CO₂ Capture System Using Hitachi H3-1 Solvent and Monoethanolamine at the E.W. Brown Coal-Fired Power Plant, Harrodsburg, KY. Prepared for the University of Kentucky, Center for Applied Energy Research under a grant from the U.S. Department of Energy, National Energy Technology Laboratory. DOE/NETL Project DE-FE007395. February 2013.
11. ENRISQ, LLC and Smith Management Group (SMG). 2020. "Supplemental Environmental Health and Safety Assessment Application of a Heat Integrated Post-combustion CO₂ Capture System with Additional Air Emission Control Using a Proprietary Amine Solvent at the E.W. Brown Coal-fired Power Plant, Harrodsburg, KY." Submitted to U.S. Department of Energy National Energy Technology Laboratory. DOE/NETL Project DE-FE007395.
12. Fan, Zhen and Nikolic, Heather. "Applicability of the Liquid Desiccant Air Drying System on Power Plant Performance for the Application of a Heat-Integrated Post-Combustion CO₂ Capture System with Hitachi Advanced Solvent into Existing Coal-Fired Power Plant. Submitted to U.S. Department of Energy National Energy Technology Laboratory. September 2014.
13. Farren, N. J., Ramirez, N., Lee, J. D., Finessi, E., Lewis, A. C., Hamilton, J. F. 2015. Estimated exposure risks from carcinogenic nitrosamines in urban airborne particulate matter. *Environ. Sci. Technol.* 49, 9648-9656.
14. Fisher-Rosemount Systems, Inc, Emerson Process Management-Process Systems and Solutions, DeltaV. Version 12.3, Round Rock, Texas.

15. Fraboulet, I., Chahen, L., Lestremau, F., Grimstvedt, A., Schallert, B., Moeller, B. C., Järvinen, E. 2016. Round robin tests on nitrosamines analysis in the effluents of a CO₂ capture pilot plant. Proceeding of the 8th Trondheim Conference on CO₂ Capture, Transport and Storage (TCCS8), 16-18 June 2015, Trondheim, Norway. Energy Procedia 86, 252-261. DOI: 10.1016/j.egypro.2016.01.026.
16. Frimpong, R.A., Nikolic, H., Pelgen, J., Ghorbanian, M., Figueroa, J.D., Liu, K. 2019 Evaluation of different solvent performance in a 0.7 MWe pilot scale CO₂ capture unit. Chem. Eng. Res. Des. 148, 11-20.
17. Fulk, S. M., Rochelle, G. T. 2014. Quantification of gas and aerosol-phase piperazine emissions by FTIR under variable bench-scale absorber conditions. Proceeding of the 12th International Conference on Greenhouse Gas Control Technologies (GHT-12), 5-9 October 2014, Austin, Texas. Energy Procedia 63, 871-883. DOI: 10.1016/j.egypro.2014.11.097.
18. Goff, G. S., Rochelle, G. T. 2004. Monoethanolamine degradation: O₂ mass transfer effects under CO₂ capture conditions. Ind. Eng. Chem. Res. 43, 6400-6408.
19. Goff, G. S., Rochelle, G. T. 2006. Oxidation inhibitors for copper and iron catalyzed degradation of monoethanolamine in CO₂ capture processes. Ind. Eng. Chem. Res. 45, 2513-2521.
20. Huang, Q., Thompson, J., Bhatnagar, S., Chandan, P., Remias, J. E., Selegue, J. P., Liu, K. 2014. Impact of flue gas contaminants on monoethanolamine thermal degradation. Ind. Eng. Chem. Res. 53, 553-563.
21. Khakharia, P., Mertens, J., Huizinga, A., De Vroey, S., Fernandez, E. S., Srinivasan, S., Vlugt, T. J. H., Goetheer, E. 2015. Online corrosion monitoring in a postcombustion CO₂ capture pilot plant and its relation to solvent degradation and ammonia emissions. Ind. Eng. Chem. Res. 54, 5336-5344. DOI: 10.1021/acs.iecr.5b00729.
22. Léonard, G., Voice, A., Toye, D., Heyen, G. 2014. Influence of dissolved metals and oxidative degradation inhibitors on the oxidative and thermal degradation of monoethanolamine in postcombustion CO₂ capture. Ind. Eng. Chem. Res. 53, 18121-18129.
23. Lepaumier, H., Picq, D., Carrette, P.L. 2009. Degradation study of new solvents for CO₂ capture in post combustion. Energy Procedia, 01, 893-900.
24. Li, X., Thompson, J.G., Liu, K. 2015. Reduction of amine mist emissions from a pilot-scale CO₂ capture process using charged colloidal gas aaphrons. Sep. Sci. Technol. 1-8.
25. Liu, K., Placido, A., Richburg, L., Fan, Z., Nikolic, H., Thompson, J., Landon, J., Lippert, C., Widger, L., Bryant, J. A technical gap analysis report for Large Pilot CAER Heat Integrated Post-combustion CO₂ Capture Technology for Reducing the Cost of Electricity under a grant from the U.S. Department of Energy, National Energy Technology Laboratory. DOE/NETL Project DE-FE0026497, March 2016.
26. Mertens, J., Lepaumier, H., Desagher, D., Thielen, M. 2013. Understanding ethanolamine (MEA) and ammonia emissions from amine based post combustion carbon capture: Lessons learned from field tests. Int. J. Greenh. Gas Control 13, 72-77. DOI: 10.1016/j.ijggc.2012.12.013.
27. Moser, P., Schmidt, S., Stahl, K., 2011. Investigation of trace elements in the inlet and outlet streams of a MEA-based post-combustion capture process results from the test programme at the Niederaussem pilot plant. Proceeding of the 10th International Conference on Greenhouse Gas Control Technologies (GHT-10), 19-23 September 2010, Amsterdam, The Netherlands. Energy Procedia 4, 473-479. DOI: 10.1016/j.egypro.2011.01.077.

28. Nikolic, H., Frimpong, R., Liu, K. 2015. Trace metals accumulation in a coal-fired post combustion CO₂ capture process with amine-based solvents. *Int. J. Greenh. Gas Control* 42, 59-65.

29. Placido, Andy, Nikolic, Heather. University of Kentucky. "Design Basis for the Application of a Heat-integrated Post-combustion CO₂ Capture System with Hitachi Advanced Solvent into Existing Coal-fired Power Plant." Submitted to U.S. Department of Energy National Energy Technology Laboratory. November 2012.

30. Resource Conservation and Recovery Act (RCRA) 42 U.S.C. §6901 et seq. 1976.

31. Reynolds, A. J., Verheyen, T. V., Adelaju, S. B., Chaffee, A. L. Meuleman, E. 2015. Monoethanolamine Degradation during Pilot-Scale Post-combustion Capture of CO₂ from a Brown Coal-Fired Power Station. *Energy Fuels*, 29, 11, 7441-7455.

32. Sexton A. J., Rochelle, G. T. 2011. Reaction products from the oxidative degradation of monoethanolamine. *Ind. Eng. Chem. Res.* 50, 667-673.

33. Smith Management Group (SMG). 2012. "Initial Environmental, Health and Safety Assessment – Application of a Heat Integrated, Post-Combustion CO₂ Capture System Using Monoethanolamine and Hitachi H3-1 Solvent at the E. W. Brown Coal-Fired Plant – Harrodsburg, Kentucky. Prepared for the University of Kentucky, Center for Applied Energy Research under a grant from the U.S. Department of Energy, National Energy Technology Laboratory. DOE/NETL Project DE-FE007395. November 2012.

34. Strazisar, B. R., Anderson, R. R., White, C. M. 2003. Degradation pathways for monoethanolamine in a CO₂ capture facility. *Energy Fuels* 17, 1034-1039.

35. Thompson, Jesse. University of Kentucky. "Sampling and Test Plan." Submitted to U.S. Department of Energy National Energy Technology Laboratory. April 2013.

36. U.S. DOE NETL. Cost and Performance Baseline for Fossil Energy Plants Volume 1: Bituminous Coal and Natural Gas to Electricity Revision 2a. National Energy Technology Laboratory: Washington, DC, USA, 2013.

37. U.S. DOE NETL. Cost and Performance Baseline for Fossil Energy Plants Volume 1a: Bituminous Coal (PC) and Natural Gas to Electricity Revision 3. National Energy Technology Laboratory: Washington, DC, USA, 2015.

38. Varghese, E., Pinkerton, L.L., Woods, M. Updated Costs (June 2011 Basis) for Selected Bituminous Baseline Cases. United States Department of Energy (DOE), National Energy Technology Laboratory (NETL), 2012. (DOE/NETL-341/082312) Pittsburgh, Pennsylvania.

39. Venkatesan, A. K., Pycke, B. F., Halden R. U. 2015. Detection and occurrence of N-nitrosamines in archived biosolids from the targeted national sewage sludge survey of the U.S. Environmental Protection Agency. *Environ. Sci. Technol.* 48, 5085-5092.

40. Vevelstad, S. J., Grimstvedt, A., Elnan, J., da Silva, E. F., Svendsen, H. F. 2013. Oxidative degradation of 2-ethanolamine: The effect of oxygen concentration and temperature on product formation. *Int. J. Greenh. Gas Control* 18, 88-100.

41. Voice A. K., Rochelle G. T., 2013. Products and process variables in oxidation of monoethanolamine for CO₂ capture. *Int. J. Greenh. Gas Control* 12, 472-477.

42. Wheeldon, J., 2013. National Carbon Capture Center: Post-Combustion CO₂ Capture Program. Presented at the NETL CO₂ Capture Technology Meeting, 8-11 July 2013, Pittsburgh, PA, USA.

43. Yu, C.-H., Huang, C.-H, Tan, C.-S. 2012. A review of CO₂ capture by absorption and desorption. *Aerosol Air Qual. Res.* 12 (5), 745-769.

44. Zhen Fan, Kun Liu, Guojie Qi, Reynolds Frimpong, Heather Nikolic, Kunlei Liu. 2015. Aspen modeling for MEA–CO₂ loop: Dynamic gridding for accurate column profile. *Int. J. Greenh. Gas Control* 37, 318-324.

45. Zhu, L., Schade, G. W., Nielsen, C. J. 2013. Real-time monitoring of emissions from monoethanolamine-based industrial scale carbon capture facilities. *Environ. Sci. Technol.* 47, 14306-14314. DOI: 10.1021/es4035045.

21) LIST OF ACRONYMS AND ABBREVIATIONS

3-D – Three-dimensional
 AISI - American Iron and Steel Institute
 ASME - American Society of Mechanical Engineers
 ASTM - American Society for Testing and Materials
 B&V - Black & Veatch
 B+K – Brown + Kubican
 BACT – Best Available Control Technology
 BOP – Balance of Plant
 BP – Budget Period
 C/N – Carbon to nitrogen Molar Ratio
 CAA – Clean Air Act
 CAER – Center for Applied Energy Research
 CCS – CO₂ Capture System
 CEMS - Continuous Emissions Monitoring System
 CGA – Charged Colloidal Gas Aphrons
 CPR - Cardiopulmonary Resuscitation
 CPVC – Chlorinated Polyvinyl Chloride
 CS – Carbon Steel
 DCC – Direct Contact Cooler
 DI – deionized
 DM – Demineralized
 DOE – U.S. Department of Energy
 EDS - Energy Dispersive X-ray Spectroscopy
 EGU – Electricity Generating Unit
 EH&S – Environmental, Health and Safety
 EPA - Environmental Protection Agency
 EPRI – Electric Power Research Institute
 FRP – Fiber Reinforced Plastic
 GA – General Arrangement
 HDPE – High Density Polyethylene
 HHV – Higher Heating Value
 HPLC - High Performance Liquid Chromatography
 HSS – Heat Stable Salt (HEIA, HEMI, HEGly, HEAEIA, HEEDA, HEDETA, HEAEIA, HEI, HEMI)
 HSS – Heat Stable Salts
 HVAC – Heating, Ventilation, Air Conditioning
 HXER – Heat Exchanger

I/O – Input/Output
IA - Insignificant Activity
IC - Ion Chromatography
ICDD - International Centre for Diffraction Data
ICP-MS - ICP Mass Spectrometry
ICP-OES - Inductively Coupled Plasma-Optical Emission Spectrometry
ISBL – Inside Boundary Limits
KMPS – Koch Modular Process Systems
L/G – Liquid to Gas Mass Flow Ratio
L/R – Lean/Rich
LAER – Lowest Achievable Emission Rate
LCOE – Levelized Cost of Electricity
LG&E and KU - Louisville Gas & Electric and Kentucky Utilities
LO/TO – Lock Out/Tag Out
LOQ - Limits of Quantitation
MBT – 2-mercaptobenzothiazole
MEA – Monoethanolamine
MHPS – Mitsubishi Hitachi Power Systems
MSU – Membrane Separation Unit
MTR – Membrane Technology Research
NA-NSR - Nonattainment New Source Review
NEPA – National Environmental Policy Act
NETL – National Energy Technology Laboratory
NSC - National Safety Council
OSBL – Outside Boundary Limits
OSHA - Occupational Safety and Health Administration
P&ID – Piping and Instrumentation Diagram
PC – Pulverized Coal
PCC – Post-combustion Capture
PDF – Powder Diffraction File
PDP – Process Design Package
PFD – Process Flow Diagram
PMP – Project Management Plan
PO – Purchase Order
PPE – Personal Protective Equipment
PSD - Prevention of Significant Deterioration
PTFE – Polytetrafluoroethylene
QA/QC – Quality Assurance/Quality Control
RAGS - Risk Assessment Guidance for Superfund
RC – Reference Case
RCRA - Resource Conservation and Recovery Act
RFP – Request for Proposal
RTD – Resistance Temperature Device
SDS – Safety Data Sheet
SEM - Scanning Electron Microscopy
SMG – Smith Management Group

SOP – Standard Operating Procedures
SOPO – Statement of Project Objectives
SPE - Solid Phase Extraction
SS – Stainless Steel
SS/EW – Safety Shower/Eye Wash
TEA – Techno-economic Analysis
TOF-MS - Time of Flight Mass Spectrometer
UK – University of Kentucky
UV – Ultraviolet
VFD – Variable Frequency Drive
VLE – Vapor-Liquid Equilibrium
VOC – Volatile Organic Compounds
WFGD – Wed Flue Gas Desulfurization
WWS – Water Wash System
XRD – X-ray diffraction